

**EXPLORATION OF MISCELLANEOUS INTERFACES OF SOME
IONIC SOLIDS AND IONIC LIQUIDS PREVAILING IN VARIOUS
SOLVENT SYSTEMS BY THE PROCESS OF PHYSICOCHEMICAL
CONTRIVANCE**

A Thesis Submitted to the
UNIVERSITY OF NORTH BENGAL

For the Award of
Degree of Doctor of Philosophy (Ph. D.)
in
CHEMISTRY

By
Biswajit Datta, M.Sc. in Chemistry

Guided and Supervised by
DR. MAHENDRA NATH ROY
PROFESSOR OF CHEMISTRY

DEPARTMENT OF CHEMISTRY
UNIVERSITY OF NORTH BENGAL
DARJEELING, PIN-734013, WB, INDIA

April 2017



*This Thesis is
Dedicated to
My Beloved Parents
For Their Loving Care
& Irreparable Indebtedness*



DECLARATION

I declare that the thesis entitled "EXPLORATION OF MISCELLANEOUS INTERFACES OF SOME IONIC SOLIDS AND IONIC LIQUIDS PREVAILING IN VARIOUS SOLVENT SYSTEMS BY THE PROCESS OF PHYSICOCHEMICAL CONTRIVANCE" has been prepared by me under the guidance of Dr. Mahendra Nath Roy, Head and Professor, Department of Chemistry, University of North Bengal. No part of this thesis has formed the basis for the award of any degree or fellowship previously.

Mr. Biswajit Datta,

*Department of Chemistry,
University of North Bengal,
Dist: Darjeeling, Pin-734013,
West Bengal, INDIA*

Date:

UNIVERSITY OF NORTH BENGAL

Prof. (Dr.) M. N. Roy, UGC one
time Grant Awardee (BSR) Head
and Programme Coordinator, SAP
DRS-III

Department of Chemistry

Email: mahendraroy2002@yahoo.co.in



Phone : 0353 2776381
Mobile: 094344 96154
Fax: +91 353 2699001
Darjeeling-734 013, West
Bengal, INDIA.

April, 2017

CERTIFICATE

I certify that *Mr. Biswajit Datta* has prepared the thesis entitled "**EXPLORATION OF MISCELLANEOUS INTERFACES OF SOME IONIC SOLIDS AND IONIC LIQUIDS PREVAILING IN VARIOUS SOLVENT SYSTEMS BY THE PROCESS OF PHYSICOCHEMICAL CONTRIVANCE**", for the award of **Ph. D. Degree (*Doctor of Philosophy*)** of the University of North Bengal, under my guidance. He has carried out the work at the **Department of Chemistry, University of North Bengal.**

DR. MAHENDRA NATH ROY,

*Department of Chemistry,
University of North Bengal,
Dist: Darjeeling, Pin: 734013,
West Bengal, INDIA*

DATE:

Acknowledgment

Open My Eyes...

That I May See...

One of the most cherished dreams of my life right from the early days of my education life was the accomplishment of Ph. D. degree. At the moment of this signpost attainment, I would like to express my heartfelt appreciation to everyone who believed in me and to whom I am really indebted to their assist, sustain and motivation in all my accomplishments.

Firstly, I would like to express my appreciation and internal stance to my esteemed teacher, guide and scientific supervisor Dr. Mahendra Nath Roy, Professor in Chemistry, Department of Chemistry, University of North Bengal, Darjeeling, India. Throughout my research period, I received regular guidance, priceless suggestions, ceaseless inspirations and beneficial criticism from him. I am deeply obliged to him for his enthusiastic interest, constant keenness, deep knowledge, confidence and sympathetic consideration. The trust, support and ‘the freedom to create’ that he has provided throughout the work is very much appreciated. The good advice, support and encouragement that I have received from him has been priceless on both an academic and a personal life, for which I shall ever remain extremely obliged.

I also express my insightful keenness of gratification to the honourable faculty members of Department of Chemistry, University of North Bengal for their untiring assistance, academic, technical support and continual inspiration during the course of my research work. I am gaily thanked to the non-teaching staff of our Department for their assist and help.

The inspiration, encouragement and whole-hearted cooperation



PREFACE

The endeavor in this thesis entitled “EXPLORATION OF MISCELLANEOUS INTERFACES OF SOME IONIC SOLIDS AND IONIC LIQUIDS PREVAILING IN VARIOUS SOLVENT SYSTEMS BY THE PROCESS OF PHYSICOCHEMICAL CONTRIVANCE” was ongoing in December 2012 under the supervision of Dr. M. N. Roy, Professor of Physical Chemistry, Department of Chemistry, University of North Bengal, Darjeeling. This research becomes conscious within the scaffold of the Programme in the field of “Ionic Liquids, Solution Thermodynamics & Host-Guest Inclusion Complex Formation”.

The work is an effort to investigate molecular as well as ionic level interfaces of IONIC LIQUIDS and IONIC SOLIDS in various aqueous/non-aqueous solution systems by studying their thermophysical, thermodynamic, transport, acoustic, surface, optical and spectroscopic properties.

I was extremely motivated by my listening, interrelating and cooperating with famous researchers, experts, reviewers and scientists during my research work course with the involvement in a number of meets and attaining/presenting in seminars/symposiums/conferences athwart the country. I was even enough auspicious to publish my original research works as article enclosed in the thesis in various reputed National and International Journals.

In custody with broad achieve of reporting scientific surveillance, owed acknowledgement has been made whenever the work described was based on the finding of other investigators. I must obtain the liability of any involuntary omissions and mistakes, which might have slinked notwithstanding defenses.

I anticipate that the knowledge that I have earned during my work specified more challenges in my future life so that can be devote to a better accomplishment.



ABSTRACT

Ionic solids may be defined as a customary salt in solid state having symmetric cation and anion. Ionic solids are mainly made up by the chemical combination of **metallic** and **non-metallic** elements. "Salt"- a broad chemical expression refers to ionic compounds (ionic solids) created when a reaction between acid and base occurs. The unique properties of ionic solids signify strong forces between the particles and it takes a lot of energy to move them all relative to each other. In case of ionic solid the three dimensional lattice is held together strongly by electrostatic forces of attraction between positive and negative ions. At present, salt extends to be of leading monetary corollary, with thousands of uses in accumulation to senescing and conserving food.

Ionic Liquids (ILs) are liquid salts that consist of combinations of organic/organic or organic/inorganic cation/anions are found a variety of industrial applications, as in chemical industry, pharmaceuticals, cellulose processing, gas handling, gas treatment, solar thermal energy, nuclear fuel processing, food and biproducts, waste recycling, batteries etc. *Amino acids* serve as the building blocks of proteins, peptides, polypeptides, essential for human body, they are used in nutrition supplements, fertilizers, food technology, industry, include the production of biodegradable plastics, drugs, and chiral catalysts.

'*Solution Chemistry*' is an imperative branch of the physical chemistry, which deal the change in properties that arise when one substance dissolves in another substance. The investigation have been done for the solubility of substances and studied how it is affected in both the physical and chemical nature for the solute and solvent. There are three types of approach have been made to estimate the extent of salvation in physical chemistry. The first one is involves the studies of transport properties as viscosity, conductance, diffusion coefficient, ionic mobility etc., of the electrolytes in aqueous and non-aqueous solvents and the derivation of various factors associated with ionic salvation; the second one is the thermodynamic approach by measuring the free energies, enthalpies and entropies of solvation of ions from which factors associated

with solvation can be explain; and the third one is to use spectroscopic study where the spectral line shifts or the chemical shifts of the functional group of electrolytes or non-electrolytes in solvents has been resolved qualitatively and quantitatively with their nature/mode of interactions.

'*Host-guest chemistry*' majorly describes complexes that are composed of two or more molecules which are held together in unique structural relationships by non covalent interactions. Yet as its innovation, the notion of supramolecular chemistry has concerned plenty of interest from chemists, biologists, and material scientists, where they exploit the noncovalent interactions, together with hydrogen-bonding communication, π - π stacking interface, electrostatic interface, van der Waals force and hydrophobic/hydrophilic attraction. In an emblematic host-guest inclusion complex, a host molecule affords a cavity to encapsulate a guest molecule through noncovalent communications. Due to having a variety of noncovalent interfaces in host-guest complexation, host-guest interaction based on macrocyclic molecules is an extremely imperative incident that has been widely explored. Two or more chemical moieties can be incorporated together during such host-guest inclusion, in a facile and reversible manner which provides immense potential for the edifice of new-fangled supramolecular structures.

In the modern era, there have been increasing interests in the interacting behaviour of electrolytes in aqueous/non-aqueous and mixed solvent systems with the outlook to examining ion-ion or solute-solute and ion-solvent or solute-solvent interactions in various conditions. However, unlike succession of solubility, variation in solvating power and possibilities of physical, chemical or electrochemical reactions, are foreign in aqueous chemistry, have open vistas for physical chemists and interests in these organic solvents transcend the traditional boundaries of physical, inorganic, organic, analytical and electrochemistry etc.

Studies of thermodynamic properties of ionic solids and ionic liquids, based on the considered parameters from physicochemical as well as spectroscopic study, provides valuable information about molecular interactions occurring in solution systems. The

Abstract

influence of the ion-solvent interactions is amply huge to reason dramatic changes in chemical reactions involving ions. The changes in ionic solvation by the solvent molecules have vast application in miscellaneous areas, for example organic and inorganic synthesis, studies of reaction mechanisms, non-aqueous battery technology and extraction etc.

Knowledge of various types of interactions in aqueous, non-aqueous solutions and mixed solvents used in industries is very important in many practical problems concerning energy transport, heat transport, mass transport and fluid flow. Besides finding applications in engineering branch, the study is important from practical and theoretical point of view in understanding liquid theory. The non-aqueous systems have been of immense importance to the technologist and theoretician as many chemical processes occur in these systems. This is helpful for scientists in optimal choice of solvents as well as solutes used in industries. Even though solvents studied during the course of my research work have drawn much focus in recent years as solvents for thermophysical investigations, still a lot remains to be explored.

Using mixed solvents in these studies enable the variation of thermophysical properties such as dielectric constant, viscosity, and therefore the ion-ion and ion-solvent interactions could be better studied. Furthermore, the quantities strongly influenced by solvent properties could be derived from concentration dependence of the electrolyte conductivity. Accordingly, a number of conductometric and related studies of different electrolytes in aqueous/nonaqueous solvents, especially mixed organic solvents, have been made for their optimal use in high-energy batteries and for understanding organic reaction mechanisms. Ionic association of electrolytes in solution systems depends upon the mode of solvation, charge distribution, dipole moment, columbic force and electrostriction of its respective ions; which in turn depends on the nature of the solvents/solvent mixtures. The solvent properties such as viscosity and the relative permittivity have been taken into account as these properties helpful in determining the degree of ion-association and the solvent-solvent interactions. Hence, extensive studies on electrical conductance in mixed organic solvents have been

performed to examine the manner and magnitude of ion-ion and ion-solvent interactions.

SUMMARY OF THE WORKS EMPHASIZE IN THE THESIS

CHAPTER-I

This chapter contains the *objective, utility and applications of the research work*, the important solutes and solvents used and methods of investigation. This also occupies the summary of the works done allied with the thesis.

CHAPTER-II

The chapter encloses *the general introduction* of the thesis and forms the strong background of the work embodied in the thesis. A brief review of noteworthy works in the field of molecular as well as ionic interaction has been given. The discussion includes ion-solvent/solute-solvent, ion-ion/solute-solute and solvent-solvent interactions in binary, ternary mixed solvent systems and of electrolytes in pure and non-aqueous solvent systems at various temperatures in terms of various derived parameters, estimated from the experimentally observed thermodynamic properties viz., *density, viscosity, ultrasonic speed, refractive index, conductance and another important properties such as Surface Tension, FTIR Spectroscopy and NMR Spectroscopy*. Several semi-empirical models to estimate dynamic viscosity of binary liquid mixtures have been discussed. Ionic association and its dependence on ion-size parameters as well as relation between solution viscosity and limiting conductance of an ion has been discussed using Stokes' law and Walden rule. Crucial assessment of different methods on the relative merits and demerits on the basis of various assumption employed from time to time of acquiring the single ion values (viscosity *B*-coefficient and limiting equivalent conductance) and their implications have been discussed. The molecular interactions are interpreted based on various derived parameters.

CHAPTER-III

The chapter comprises *the experimental section* which principally involves the basic information, structure, source, purification and uses of the ionic solids, ionic liquids and solvents have been used throughout the entire research work. It also restrains the details of the instruments, procedure, working principle and equations that are employed to understand the thermodynamic, transport, acoustic, optical and spectroscopic properties.

CHAPTER-IV

The chapter deals precise measurements on electrolytic conductivities, densities and viscosities of lithium salts (LiI, LiClO₄ and LiAsF₆) in (0.25, 0.50 and 0.75) mass fraction of acetonitrile (AN) in diethyl carbonate (DEC) at 298.15K. The limiting molar conductivities (Λ^0), association constants (K_A) and the distance of closest approach of the ions (R) have been evaluated using the Fuoss conductance equation (1978). The Walden product are obtained and discussed. However, the deviation of the conductometric curves (Λ versus \sqrt{c}) from linearity for the electrolytes in 0.25 mass fraction of acetonitrile (AN) in diethyl carbonate (DEC) indicated triple-ion formation, and therefore the corresponding conductance data have been analysed by the Fuoss-Kraus theory of triple ions. The observed molar conductivities were explained by the ion-pair ($M^+ + X^- \leftrightarrow MX$) and triple-ion ($2M^+ + X^- \leftrightarrow M_2X^+$, $M^+ + 2X^- \leftrightarrow MX_2^-$) formation. The limiting apparent molar volumes (ϕ_V^0), experimental slopes (S_V^*) derived from the Masson equation and viscosity A and B-coefficients using the Jones-Dole equation have been interpreted in terms of ion-ion and ion-solvent interactions respectively.

CHAPTER-V

In this chapter, we present conductivities (Λ), densities (ρ) and viscosities (η) of Hept₄NI in o-Toluidine, o-Xylene and 2-Nitrotoluene at 298.15 K. Limiting molar conductivity (Λ^0), association constant (K_A), distance of closest approach of the ions (R),

for Hept₄NI in 2-Nitrotoluene have been evaluated using the Fuoss conductance equation (1978). The Walden product and Gibb's energy change are obtained and discussed. Deviation of the conductometric curves (Λ versus \sqrt{c}) from linearity for Hept₄NI in o-Toluidine and o-Xylene indicates triple-ion formation, therefore the corresponding conductance data have been analysed by the Fuoss-Kraus theory of triple-ions. Observed molar conductivities have been explained by the ion-pair ($M^+ + X^- \leftrightarrow MX$) and triple-ion ($2M^+ + X^- \leftrightarrow M_2X^+$, $M^+ + 2X^- \leftrightarrow MX_2^-$) formation. Limiting apparent molar volumes (ϕ_V^0), experimental slopes (S_V^*) derived from the Masson equation and viscosity A and B -coefficients using the Jones-Dole equation have been interpreted in terms of ion-ion and ion-solvent interactions respectively.

CHAPTER-VI

The chapter embraces Interface properties of an IL, 1-butyl-1-methylpyrrolidinium chloride ([bmp]Cl) in different concentrations of aqueous carbohydrate solutions at diverse temperatures. In spite of having "green solvent" property toxicity of ILs has been revealed. So the interface of ILs with biomolecules is a progressive research topic. Gibbs free energy (ΔG_A^0), enthalpy (ΔH_A^0), entropy (ΔS_A^0) of ion-pair formation, limiting partial molal transfer volumes, $\Delta_v \phi_V^0$ and dB/dT have been determined. Through ¹H NMR study, changes in terms of size and structure of carbohydrates and IL by means of the interaction between IL and biomolecules, the potential toxicity of ILs originate.

CHAPTER-VII

In this chapter precise measurements on electrical conductance of solutions of 1-butyl-1-methylpyrrolidinium bromide in formamide, N, N-dimethyl formamide and N, N-dimethyl acetamide have been studied at 298.15 K. The conductance data have been analyzed by the Fuoss conductance equation (1978) in terms of limiting molar conductance, association constant, and association diameter for ion-pair formation. The

apparent molar volume, viscosity B -coefficient, molar refraction and adiabatic compressibility have also been studied, supplemented from the values of density, viscosity, refractive index and ultrasonic speed respectively, to interpret the ion-ion and ion-solvent interactions. Limiting apparent molar volumes, experimental slopes have been obtained from the Masson equation. The viscosity data have been analyzed using Jones-Dole equation to derive A and B coefficients. Molar refractions have been determined with the help of Lorentz-Lorenz equation and limiting apparent molar adiabatic compressibilities in all three solvents at infinite dilution have been evaluated and discussed. IR study of the functional group of solvents in presence and absence of IL has also been taken into account for interpretation.

CHAPTER-VIII

This chapter involves host-guest inclusion complex construction of an ionic solid (*viz.*, tetrabutyl ammonium iodide) with α and β -cyclodextrins by various physicochemical and spectroscopic methods. Which act as preservative, transporter and regulatory releaser of the guest molecules. Surface tension and conductivity studies proposed 1:1 stoichiometry of the inclusion complexes and ^1H NMR and FT-IR studies substantiate the inclusion phenomenon. Density, viscosity and refractive index studies characterize the interactions of cyclodextrin with ionic salt which also indicates greater extent of encapsulation in case of β -cyclodextrin than that in α -cyclodextrin. Hydrophobic effect, structural effect, electrostatic force and H-bonding interfaces were mainly exploited to explicate the development of inclusion complex.

CHAPTER-IX

In this chapter self assembly of inclusion complexes and interfaces phenomenon of a surface active ionic liquid (SAIL) *n*-dodecyl-*n*, *n*-dimethyl-3-ammonio-1-propanesulfonate (DDAPS) as a guest insight into the favorably fitted host cavity of hollow cylinder oligosaccharides such as α - and β -cyclodextrins in aqueous media, have been characterized and explored on recent research gaining far achievement outcome.

Abstract

The interfacial inclusion complex formation have been established with the manifested by surface tension and conductance measurements. These two experimentally determined parameters have been revealed that the formation of 1:1(CD/IL) stoichiometric inclusion complex is suggested itself by IL with α - and β -CDs. The variation of the thermodynamic parameters with guest size and state are used to draw inferences about contributions to the overall binding from the driving forces, viz., hydrophobic and hydrophilic interfaces, van der Waals force, H-bonding, electrostatic force, structural effect and configurational theory.

CHAPTER-X

This chapter presents Electrolytic conductivity, density, viscosity and FTIR study of an ionic liquid, 1-butyl-4-methylpyridinium hexafluorophosphate ([bmpy]PF₆) have been measured in diverse industrially significant solvents viz. acetonitrile, tetrahydrofuran and 1,3 dioxolane at various temperatures. In acetonitrile, the ion-pair formation of the IL was analyzed by Fuoss conductance equation. In Tetrahydrofuran and 1,3 Dioxolane systems, triple-ion formation analyzed by the Fuoss-Kraus theory. Ion-solvent interactions have been inferred in terms of limiting apparent molal volumes and viscosity *B*-coefficients. The results obtained from the experimental study, have been conferred in terms of ion-dipole interactions, structural aspect, configurational theory and solvatochromic effect.

CHAPTER-XI

This chapter contains the concluding remarks of the works related or detailed described in the thesis.

TABLE OF CONTENTS

TOPIC	PAGE NO.
<i>Declaration</i>	<i>iii</i>
<i>Certificate</i>	<i>iv</i>
<i>Abstract</i>	<i>v-xii</i>
<i>Preface</i>	<i>xiii</i>
<i>Acknowledgement</i>	<i>xiv-xv</i>

List of Tables	1-9
List of Figures	11-14
List of Schemes	15-16
List of Appendices	
<i>Appendix A: List of Publications</i>	
<i>Appendix B: List of Seminars/Symposiums/Conferences Attended</i>	

CHAPTER I	23-32
Necessity of the Research Work	

- I. 1. Object, Scope and Application of the Research Work
- I. 2. Assortment of Solvents and Solutes Used
- I. 3. Methods of Exploration

CHAPTER II	33-120
General Introduction (Review of the Earlier Works)	

- II. 1. Ionic Solids

TABLE OF CONTENTS

- II. 2.** Ionic Liquids
- II. 3.** Solution Chemistry
- II. 4.** Density
- II. 5.** Viscosity
- II. 6.** Ultrasonic Speed
- II. 7.** Conductance
- II. 8.** Refractive Index
- II. 9.** Surface Tension
- II. 10.** FTIR Spectroscopy
- II. 11.** Nuclear Magnetic Resonance Spectroscopy

CHAPTER III

121-158

Experimental Section

- III. 1.** Name, Structure, Physical properties, Purification and Applications of the Solvents and Solutes Used in the Research Work
- III. 2.** Experimental Methods

CHAPTER IV

159-180

Ionic interplay of lithium salts in binary mixtures of acetonitrile and diethyl carbonate probed by physicochemical approach

- IV. 1.** Introduction
- IV. 2.** Experimental Methods
- IV. 3.** Results and Discussion
- IV. 4.** Conclusion
 - Tables
 - Figures
 - Schemes

***Published in *Fluid Phase Equilibria* 358 (2013) 233-240**

TABLE OF CONTENTS

CHAPTER V	181-198
Essential foundation of triple-ion and ion-pair formation of tetraheptylammonium iodide (Hept₄NI) salt in organic solvents investigated by physicochemical approach	

- V. 1. Introduction
- V. 2. Experimental Section
- V. 3. Results and Discussion
- V. 4. Conclusion

Tables

Figures

* **Published in *Physics and Chemistry of Liquids* 53 (2015) 574–586**

CHAPTER VI	199-232
A study of NMR, density, viscosity and conductance vis-à-vis interactions of 1-butyl-1-methylpyrrolidinium chloride with oligosaccharides in aqueous environments	

- VI. 1. Introduction
- VI. 2. Experimental Section
- VI. 3. Results and Discussion
- VI. 4. Conclusion

Tables

Figures

Schemes

* **Communicated**

TABLE OF CONTENTS

CHAPTER VII **233-252**

Exploration of Miscellaneous Interfaces of a Green Liquid in Diverse Solvent Systems by the Process of Physicochemical Contrivances

VII.1. Introduction

VII.2. Experiments

VII.3. Results and Discussion

VII.4. Conclusion

Tables

Figures

Schemes

**Published in Indian Journal of Advances in Chemical Science 2(4)(2014) 253-263*

CHAPTER VIII **253-270**

Inclusion complexation of tetrabutylammonium iodide by cyclodextrins

VIII. 1. Introduction

VIII. 2. Experimental

VIII. 3. Results and Discussion

VIII. 4. Conclusion

Tables

Figures

Schemes

** Accepted for Publication in Journal of Chemical Sciences*

CHAPTER IX **271-284**

Self assembly inclusion of ionic liquid into hollow cylinder oligosaccharides

TABLE OF CONTENTS

- IX. 1.** Introduction
- IX. 2.** Experimental Section
- IX. 3.** Results and Discussion
- IX. 4.** Conclusion
 - Tables
 - Figures
 - Schemes

**Published in Journal of Molecular Liquids 214 (2016) 264–269*

CHAPTER X	285-312
Physicochemical Study of Solution Behavior of Ionic Liquid Prevalent in Diverse Solvent Systems at Different Temperatures	

- X. 1.** Introduction
- X. 2.** Experimental Section
- X. 3.** Results and Discussion
- X. 4.** Conclusion
 - Tables
 - Figures
 - Schemes

**Published in Chemical Physics Letters 665 (2016) 85–94*

CHAPTER XI	313-318
Concluding Remarks	

BIBLIOGRAPHY	319-350
INDEX	351-354

LIST OF TABLES

<i>CHAPTERS</i>	<i>TABLES</i>	<i>PAGE NO.</i>
Chapter IV	<p>Table IV.1: Density (ρ), viscosity (η) and relative permittivity (ϵ) of the different mass fraction (w_1) of AN in DEC at 298.15K</p> <p>Table IV.2: The concentration (c) and molar conductance (Λ) of LiI, LiClO₄ and LiAsF₆ in different mass fraction of (w_1) of AN in DEC at 298.15 K.</p> <p>Table IV.3: The calculated limiting molar conductance of ion-pair (Λ_0), limiting molar conductances of triple ion Λ_0^T, experimental slope and intercept obtained from Fuoss-Kraus Equation for LiI, LiClO₄ and LiAsF₆ in 0.025 mass fraction of (w_1) of AN in DEC at 298.15 K.</p> <p>Table IV.4: Salt concentration at the minimum conductivity (C_{\min}) along with the ion-pair formation constant (K_P), triple ion formation constant (K_T) for LiI, LiClO₄ and LiAsF₆ in 0.025 mass fraction of (w_1) of AN in DEC at 298.15 K.</p> <p>Table IV.5: Salt concentration at the minimum conductivity (c_{\min}), the ion pair fraction (α), triple ion fraction (α_T), ion pair concentration (c_P) and triple-ion concentration (c_T) for LiI, LiClO₄ and LiAsF₆ in 0.025 mass fraction of (w_1) of AN in DEC at 298.15 K.</p> <p>Table IV.6: Limiting molar conductance (Λ_0), association constant (K_A), co-sphere diameter (R)</p>	162-171

	<p>and standard deviations of experimental Λ (δ) obtained from Fuoss conductance equation for LiI, LiClO₄ and LiAsF₆ in 0.025 mass fraction of (w_1) of AN in DEC at 298.15 K.</p> <p>Table IV.7: Walden product ($\Lambda_0 \cdot \eta$) and Gibb's energy change (ΔG°) of LiI, LiClO₄ and LiAsF₆ in 0.025 mass fraction of (w_1) of AN in DEC at 298.15 K.</p> <p>Table IV.8: Concentration, c, density, ρ, apparent molar volume, ϕ_v, limiting apparent molar volume ϕ_v^0 and experimental slope for LiI, LiClO₄ and LiAsF₆ in 0.025 mass fraction of (w_1) of AN in DEC at 298.15 K.</p> <p>Table IV.9: Concentration, c, viscosity, η, $\frac{(\eta_r - 1)}{\sqrt{c}}$, viscosity A and B coefficients for LiI, LiClO₄ and LiAsF₆ in 0.025 mass fraction of (w_1) of AN in DEC at 298.15 K.</p>	
Chapter V	<p>Table V.1 Density (ρ), viscosity (η) and relative permittivity (ϵ) of the different solvents o-Toluidine, o-Xylene and 2-Nitrotoluene.</p> <p>Table V.2. The concentration (c) and molar conductance (Λ) of o-Toluidine, o-Xylene and 2-Nitrotoluene at 298.15 K.</p> <p>Table V.3. The calculated limiting molar conductance of ion-pair (Λ_0), limiting molar conductances of triple ion Λ_0^T, experimental slope and intercept obtained from Fuoss-Kraus Equation for Hept₄NI in o-Toluidine and o-Xylene at 298.15 K.</p> <p>Table V.4. Salt concentration at the minimum conductivity (C_{\min}) along with the ion-pair formation</p>	184-189

	<p>constant (K_P), triple ion formation constant (K_T) for Hept₄NI in o-Toluidine and o-Xylene at 298.15 K.</p> <p>Table V.5. Salt concentration at the minimum conductivity (c_{\min}), the ion pair fraction (α), triple ion fraction (α_T), ion pair concentration (c_P) and triple-ion concentration (c_T) for Hept₄NI in o-Toluidine and o-Xylene at 298.15 K.</p> <p>Table V.6. Limiting molar conductance (Λ_0), association constant (K_A), co-sphere diameter (R) and standard deviations of experimental Λ (δ) obtained from Fuoss conductance equation for Hept₄NI in 2-Nitrotoluene at 298.15 K.</p> <p>Table V.7. Walden product ($\Lambda_0 \cdot \eta$) and Gibb's energy change (ΔG°) of Hept₄NI in 2-Nitrotoluene at 298.15 K.</p> <p>Table V.8. Limiting Ionic Conductance (λ_0^\pm), Ionic Walden Product ($\lambda_0^\pm \eta$), Stokes' Radii (r_s), and Crystallographic Radii (r_c) of Hept₄NI in 2-Nitrotoluene at 298.15 K.</p> <p>Table V.9. Concentration, c, density, ρ, apparent molar volume, ϕ_V, limiting apparent molar volume ϕ_V^0 and experimental slope for Hept₄NI in o-Xylene, o-Toluidine and 2-Nitrotoluene at 298.15 K.</p> <p>Table V.10. Concentration, c, viscosity, η, $\frac{(\eta_r - 1)}{\sqrt{c}}$, viscosity A and B coefficients for Hept₄NI in o-Xylene, o-Toluidine and 2-Nitrotoluene at 298.15 K.</p>	
--	---	--

Chapter VI	<p>Table VI.1. Density (ρ), viscosity (η) and relative permittivity (ϵ) of the different concentration (m) of aqueous D(-)fructose and D(+)galactose at 298.15, 303.15 and 308.15 K^a respectively.</p> <p>Table VI.2. Molar conductivities (Λ) of [bmp]Cl in aqueous D(-)fructose solutions as a function of ionic liquid molality (m) at different temperatures.</p> <p>Table VI.3. Molar conductivities (Λ) of [bmp]Cl in aqueous D(+)galactose solutions as a function of ionic liquid molality (m) at different temperatures.</p> <p>Table VI.4. Ion association constants (K_A), limiting molar conductivities (Λ_0), distance parameters (R), Walden product ($\Lambda_0 \cdot \eta$) and standard deviations of experimental Λ (δ) obtained from Fuoss conductance equation of IL in aqueous D(-)fructose and D(+)galactose solutions as a function of ionic liquid molality (m) at different temperatures^a.</p> <p>Table VI.5. The values of coefficients in Eq. (11) A_0, A_1 and A_2 at different solvent compositions.</p> <p>Table VI.6. Thermodynamic functions ($\Delta G_A^0, \Delta S_A^0, \Delta H_A^0$) of IL in aqueous d(-)fructose and d(+)galactose solutions as a function of ionic liquid molality (m) at different temperatures^a.</p> <p>Table VI.7. Limiting apparent molar volume (ϕ_V^0), experimental slope (S_V^*), viscosity-B and A co-</p>	207-218
-------------------	--	----------------

	<p>efficients of IL in aqueous d(-)fructose and d(+)galactose solutions at different temperatures.</p> <p>Table VI.8. Values of $\phi_V^0(\text{aq})$, $\Delta\phi_{V\text{tr}}^0$, $B(\text{aqueous})$, ΔB for IL in different solvent systems at different temperatures.</p> <p>Table VI.9. Values of empirical coefficients (a_0, a_1, and a_2) of eqn (17) for IL in different solvent systems.</p> <p>Table VI.10. Limiting apparent molal expansibilities (ϕ_E^0) and $(\delta\phi_E^0/\delta T)_p$ for IL in different solvent systems at different temperatures.</p> <p>Table VI.11. Values of dB/dT, A_1 and A_2 coefficient of equation (22) for the IL in different solvent systems.</p> <p>Table VI.12. ^1H NMR data of [BMP]Cl, D(-)fructose, D(+)galactose and IL- carbohydrates mixture</p>	
Chapter VII	<p>Table VII.1: Density (ρ), viscosity (η), refractive index (n_D), ultrasonic speed (u) and relative permittivity (ϵ) of the different solvents FA, DMA and DMF.</p> <p>Table VII.2: Concentration (c) and molar conductance (Λ) of [BMP][Br] in Formamide, DMA and DMF at 298.15 K.</p> <p>Table VII.3: Limiting molar conductance (Λ_0), association constant (K_A), co-sphere diameter (R) and standard deviations of experimental Λ (δ) obtained from Fuoss conductance equation for [BMP][Br] in</p>	235-240

	<p>Formamide, DMA and DMF at 298.15 K.</p> <p>Table VII.4: Walden product ($\Lambda_o \cdot \eta$) and Gibb's energy change (ΔG°) of [BMP][Br] in Formamide, DMA and DMF at 298.15 K.</p> <p>Table VII.5: . Limiting Ionic Conductance (λ_o^\pm), Ionic Walden Product ($\lambda_o^\pm \eta$), Stokes' Radii (r_s), and Crystallographic Radii (r_c) of [BMP][Br] in Formamide, DMA and DMF at 298.15 K.</p> <p>Table VII.6: Concentration (c), density (ρ), apparent molar volume (ϕ_V), limiting apparent molar volume (ϕ_V^0) and experimental slope (S_V^*) for [BMP][Br] in Formamide, DMA and DMF at 298.15K and Experimental Pressure 0.1MPa.</p> <p>Table VII.7: Concentration (c) viscosity (η), $\frac{(\eta_r - 1)}{\sqrt{c}}$, viscosity A and B coefficients for [BMP][Br] in Formamide, DMA and DMF at 298.15K and Experimental Pressure 0.1MPa.</p> <p>Table VII.8: Refractive indices (n_D) and molar refractions (R_M) of [BMP][Br] in Formamide, DMA and DMF at Temperature ($^n T$) 298.15K and Experimental Pressure 0.1MPa.</p> <p>Table VII.9: Limiting partial adiabatic compressibility (ϕ_K^0) and experimental slope (S_K^*) of [BMP][Br] in Formamide, DMA and DMF at Temperature ($^n T$)</p>	
--	---	--

	298.15K and Experimental Pressure 0.1MPa. Table VII.10: Stretching frequencies of the functional groups present in the pure solvent and change of frequency after addition of 0.05(M) concentration of [BMP][Br] in Formamide, DMA and DMF.	
Chapter VIII	Table VIII.1: Values of surface tension (γ) at the break point with corresponding concentrations of cyclodextrins and but ₄ NI at 298.15 K ^a . Table VIII.2: Values of conductivity (κ) at the break point with corresponding concentrations of cyclodextrins and but ₄ NI at 298.15 K ^a . Table VIII.3: Formation constants of ionic solid-cyclodextrin inclusion complexes.	256
Chapter IX	Table IX.1: Values of surface tension at the break point (γ) with corresponding concentration of IL (n-dodecyl-n n-dimethyl-3-ammonio-1-propanesulfonate) in different mass fraction of aqueous α and β -cyclodextrin respectively at 298.15K ^a Table IX.2: Values of conductance at the break point (Λ) with corresponding concentration of IL (n-dodecyl-n n-dimethyl-3-ammonio-1-propanesulfonate) in different mass fraction of aqueous α and β -cyclodextrin respectively at 298.15K ^a .	272
Chapter X	Table X.1: Density (ρ), viscosity (η), relative	293-299

permittivity (ϵ) and Conductance (Λ) of the different solvents Acetonitrile, Tetrahydrofuran and 1,3 Dioxolane at different temperatures^a.

Table X.2: Limiting molar conductance (Λ_0), association constant (K_A), co-sphere diameter (R) and standard deviations of experimental Λ (δ) obtained from Fuoss conductance equation of [bmpy]PF₆ in Acetonitrile at 298.15 K, 303.15 K and 308.15 K respectively.

Table X.3: Walden product ($\Lambda_0 \cdot \eta$) and Gibb's energy change (ΔG°) of [bmpy]PF₆ in Acetonitrile at 298.15 K, 303.15 K and 308.15 K respectively.

Table X.4: Limiting Ionic Conductance (λ_0^\pm), Ionic Walden Product ($\lambda_0^\pm \eta$), Stokes' Radii (r_s), and Crystallographic Radii (r_c) of [bmpy]PF₆ in ACN at 298.15 K, 303.15 K and 308.15 K respectively.

Table X.5: Average computed thermodynamic parameters for [bmpy]PF₆ in Acetonitrile.

Table X.6: The calculated limiting molal conductance of ion-pair (Λ_0), limiting molar conductances of triple ion Λ_0^T , experimental slope and intercept obtained from Fuoss-Kraus Equation for [bmpy]PF₆ in THF and DO at 298.15 K, 303.15 K and 308.15 K respectively.

Table X.7: Salt concentration at the minimum conductivity (C_{\min}) along with the ion-pair formation constant (K_P), triple ion formation constant (K_T) for

	<p>[bmpy]PF₆ in THF and 1,3 DO at 298.15 K, 303.15 K and 308.15 K respectively.</p> <p>Table X.8: Salt concentration at the minimum conductivity (c_{\min}), the ion pair fraction (α), triple ion fraction (α_T), ion pair concentration (c_P) and triple-ion concentration (c_T) for [bmpy]PF₆ in THF and DO at 298.15 K, 303.15 K and 308.15 K respectively.</p> <p>Table X.9: Limiting apparent molal volume (ϕ_V^0), experimental slope (S_V^*), viscosity $-B$ and $-A$ coefficient for [bmpy]PF₆ in ACN, THF and DO at 298.15 K, 303.15 K and 308.15 K respectively.</p> <p>Table X.10: Values of empirical coefficients (a_0, a_1, and a_2) of Equation 4 for IL in ACN, THF and DO</p> <p>Table X.11: Limiting apparent molal expansibilities (ϕ_E^0) for IL in different solvents (ACN, THF and DO) at 298.15K to 308.15K respectively</p> <p>Table X.12: Stretching frequencies of the functional groups present in the pure solvent and change of frequency after addition of IL in the solvents.</p>	
--	--	--

LIST OF FIGURES

<i>CHAPTERS</i>	<i>FIGURES</i>	<i>PAGE NO.</i>
Chapter IV	<p>Figure IV.1: Plot of molar conductance (Λ) versus \sqrt{c} for LiI(-◆-), LiClO₄ (-■-) and LiAsF₆ (-▲ -) in 0.025 mass fraction of AN in DEC at 298.15</p> <p>Figure IV.2: Plot of limiting molar conductance (Λ_0) for LiI, LiClO₄ and LiAsF₆ in 0.50(-◆-) and 0.75 (-■-) mass fraction of AN in DEC at 298.15.</p> <p>Figure IV.3: Limiting apparent molar volume (ϕ_V^0) for LiI, LiClO₄ and LiAsF₆ in 0.25(-◆-), 0.50(-■-) and 0.75 (-▲ -) mass fraction of AN in DEC and experimental slope (S_V^*) for LiI, LiClO₄ and LiAsF₆ in 0.25 (-x-), 0.50(-*-) and 0.75 (-◇-) mass fraction of AN in DEC at 298.15 K</p> <p>Figure IV.4: Viscosity <i>B</i>-coefficient for LiI, LiClO₄ and LiAsF₆ in 0.25(-◆-), 0.50(-■-) and 0.75 (-▲ -) mass fraction of AN in DEC and viscosity <i>A</i>-coefficient for LiI, LiClO₄ and LiAsF₆ in 0.25 (-x-), 0.50(-*-) and 0.75 (-◇-) mass fraction of AN in DEC at 298.15 K</p>	172-173
Chapter V	<p>Figure 1. Plot of molar conductance (Λ) versus $C^{1/2}$ for Hept₄NI in o-Toluidine at 298.15 K.</p> <p>Figure 2. Plot of molar conductance (Λ) versus $C^{1/2}$ for Hept₄NI in o-Xylene at 298.15 K.</p> <p>Figure 3. Plot of molar conductance (Λ) versus $C^{1/2}$ for Hept₄NI in 2-Nitrotoluene at 298.15 K</p> <p>Figure 4. Plot of $C^{1/2}$ versus Limiting apparent molar volume (ϕ_V^0) for Hept₄NI in o-Toluidine (—■—), o-Xylene (—▲—) and 2-Nitrotoluene (—◆—) at 298.15 K.</p>	190-192

	<p>Figure 5. Plot of $C^{1/2}$ versus $\frac{(\eta_r - 1)}{\sqrt{c}}$ for Hept₄NI in o-Toluidine (—◆—), o-Xylene (—■—) and 2-Nitrotoluene (—▲—) at 298.15 K.</p>	
Chapter VI	<p>Figure VI.1: Plot of $T\Delta S_A^0$ of IL in different mass fractions of aqueous D(-)fructose and D(+)galactose solution respectively at different temperatures</p> <p>Figure VI.2: Plot of ΔH_A^0 of IL in different mass fractions of aqueous D(-)fructose and D(+)galactose solution respectively at 298.15 K (red), 303.15 K (blue) and 308.15 K (green) respectively</p> <p>Figure VI.3: Plot of ΔG_A^0 of IL in different mass fraction of aqueous D(-)fructose and D(+)galactose solution respectively at 298.15 K (red), 303.15 K (blue) and 308.15 K (green) respectively</p> <p>Figure VI.4: Plot of limiting molar volume (ϕ_r^0) of IL against mass fraction (w) of aqueous D(-)fructose and D(+)galactose at 298.15K (red), 303.15K (blue) and 308.15K (green) respectively</p> <p>Figure VI.5: Plot of viscosity B-coefficient of IL against mass fraction (w) of aqueous D(-)fructose and D(+)galactose at different temperatures</p> <p>Figure VI.6(a): ¹H NMR Spectra of D(-)Fructose, [BMP]Cl and 1:1 molar ratio of D(-)Fructose + [BMP]Cl in D₂O in 298.15 K.</p> <p>Figure VI.6(b): ¹H NMR Spectra of D(+)Galactose, [BMP]Cl and 1:1 molar ratio of D(+)Galactose + [BMP]Cl in D₂O in 298.15 K.</p>	219-222
Chapter VII	<p>Figure IV.1: Plot of \sqrt{c} versus molar conductance (Λ) for</p>	241-242

	<p>[BMP][Br] in Formamide (—◆—), DMA (—■—) and DMF (—▲—) at 298.15 K.</p> <p>Figure IV.2: Plot of \sqrt{c} versus Limiting apparent molar volume (ϕ_v^0) for [BMP][Br] in Formamide (—◆—), DMA (—■—) and DMF (—▲—) at 298.15 K.</p> <p>Figure IV.3: Plot of \sqrt{c} versus $\frac{(\eta_r - 1)}{\sqrt{c}}$ for [BMP][Br] in Formamide (—◆—), DMA(—■—) and DMF (—▲—) at 298.15 K.</p> <p>Figure IV.4: Plot of \sqrt{c} versus R_M for [BMP][Br] in Formamide (—◆—), DMA(—■—) and DMF (—▲—) at 298.15 K.</p>	
Chapter VIII	<p>Figure VIII.1(a). ^1H NMR Spectra of α-CD, Tetrabutyl ammonium iodide and 1:1 molar ratio of α-CD + Ionic Solid in D_2O in 298.15 K.</p> <p>Figure VIII.1(b). ^1H NMR Spectra of β-CD, Tetrabutyl ammonium iodide and 1:1 molar ratio of β-CD + Ionic Solid in D_2O in 298.15 K.</p> <p>Figure VIII.2. Variation of surface tension of aqueous (a) $\text{but}_4\text{NI}-\alpha$-CD and (b) $\text{but}_4\text{NI}-\beta$-CD systems respectively at 298.15 K.</p> <p>Figure VIII.3. Variation of conductivity of aqueous (a) $\text{but}_4\text{NI}-\alpha$-CD and (b) $\text{but}_4\text{NI}-\beta$-CD systems respectively at 298.15 K.</p> <p>Figure VIII.4. Plot of limiting molar volume (ϕ_v^0) against mass fraction (w) of aqueous α-CD (blue) and aqueous β-CD (purple) for but_4NI at 298.15 K.</p> <p>Figure VIII.5. Plot of viscosity B-coefficient against mass fraction (w) of aqueous α-CD (blue) and aqueous β-CD</p>	257-261

	<p>(purple) for but₄NI at 298.15 K.</p> <p>Figure VIII.6. Plot of limiting molar refraction (R^0_M) for but₄NI in different mass fractions (w) of aqueous α-CD (blue) and aqueous β-CD (purple) respectively at 298.15 K.</p> <p>Figure VIII.7(a). FTIR spectra of α-CD (top), but₄NI (middle) and but₄NI-α-CD inclusion complex (bottom).</p> <p>Figure VIII.7(b). FTIR spectra of β-CD (top), but₄NI (middle) and but₄NI-β-CD inclusion complex (bottom).</p>	
Chapter IX	<p>Figure 1. Plot of surface tension (γ) of ionic liquid corresponding to the added conc. of aq. β-CD (m) and aq. α-CD (m) in $w_1=0.001(\blacklozenge)$, $w_1=0.003(\blacktriangle)$, $w_1=0.005(\bullet)$ mass fraction of α-CD</p> <p>Figure 2. Plot of conductance of ionic liquid corresponding to the added conc of aq. α-CD (m) and aq. β-CD (m) in $w_1=0.001(\bullet)$, $w_1=0.003(\blacktriangle)$, $w_1=0.005(\blacksquare)$ mass fraction of β-CD respectively</p>	273
Chapter X	<p>Figure X.1. Plot of molal conductance (Λ) versus \sqrt{m} for [bmpy]PF₆ in ACN at 298.15 K (\blacklozenge), 303.15 K (\blacksquare) and 308.15 K (\blacktriangle).</p> <p>Figure X.2. Plot of molal conductance (Λ) versus \sqrt{m} for [bmpy]PF₆ in THF at 298.15 K (\blacklozenge), 303.15 K (\blacksquare), 308.15 K (\blacktriangle) and in DO at 298.15 K (\blacklozenge), 303.15 K (\square), 308.15 K (\triangle).</p> <p>Figure X.3: Plot of temperature versus limiting apparent molal volume (Φ_v^0) for [bmpy]PF₆ in ACN (red) , THF (blue) and 1,3 dioxolane (green).</p> <p>Figure X.4: Plot of temperature versus Viscosity B-Coefficient for [bmpy] PF₆ in ACN (red), THF (blue) and 1,3 dioxolane (green).</p>	300-301

LIST OF SCHEMES

<i>CHAPTERS</i>	<i>SCHEMES</i>	<i>PAGE NO.</i>
Chapter IV	Scheme IV.1. Trend in the ion solvent interaction.	172
Chapter VI	<p>Scheme VI.1: Plausible Interfaces between ionic liquid and diverse solvent systems.</p> <p>Scheme VI.2: Molecular structure of D(-)fructose, D(+)galactose, IL and Extent of ion-solvent interaction of ionic liquid in diverse solution systems.</p>	222-223
Chapter VII	<p>Scheme VII.1. Phase of interaction between [BMP]Br and Formamide, DMA and DMF respectively.</p> <p>Scheme VII.2. Trend of Ion-solvent interaction between [BMP]Br and Formamide, DMA and DMF respectively.</p>	221-222
Chapter VIII	Scheme VIII.1. Molecular structure of cyclodextrin molecules and tetrabutylammonium iodide.	260
Chapter IX	<p>Scheme IX.1: The molecular structure of chosen ionic liquid and α- and β-cyclodextrin (α- CD 6 membered and β- CD 7 membered sugar ring molecules).</p> <p>Scheme IX.2: The plausible stoichiometries inclusion ratio of host:guest molecule.</p> <p>Scheme IX.3: The feasible and restricted inclusion of host:guest molecule.</p>	272-274

	<p>Scheme IX.4: Schematic representation of convincing mechanism of 1:1 inclusion complexes insight into α- and β-cyclodextrin with the titled ionic liquid.</p> <p>Scheme IX.5: Extent of inclusion complex formation insight into α- and β- CD with the titled ionic liquid.</p>	
Chapter X	<p>Scheme X.1. Plausible interfaces between the ionic liquid and diverse solvent systems.</p> <p>Scheme X.2. Molecular structures of the IL and the solvents and pictorial representation of ion-pair and triple-ion formation for the electrolyte in diverse solvent systems.</p> <p>Scheme X.3. Electrostatic Forces of Attraction.</p> <hr/> <p>Scheme X.4. Extent of ion-solvent interaction of IL in miscellaneous solvent systems.</p>	300-302



LIST OF APPENDICES

APPENDIX A:

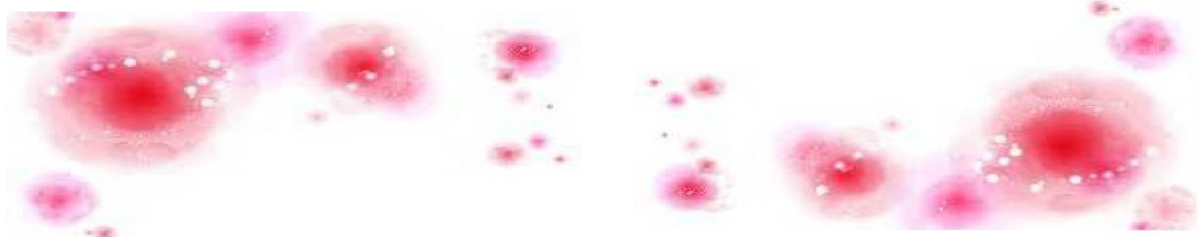
LIST OF PUBLICATION(S)

APPENDIX B:

LIST OF

SEMINARS/SYMPOSIUMS/CONVENTIONS

ATTENDED



CHAPTER: I

NECESSITY OF THE RESEARCH WORK

I.1. OBJECT, SCOPE AND APPLIANCES OF THE RESEARCH WORK

Ionic solid may be defined as a customary salt in solid state having symmetric cation and anion. Ionic solids are mainly made up by the chemical combination of *metallic* and *non-metallic* elements. "Salt"- a broad chemical expression refers to ionic compounds (ionic solids) created when a reaction between acid and base occurs. In case of ionic solid or salt, due to having strong forces between the particles, they are hard, brittle crystal and having high melting temperature. Since in solid state of ionic solids no free moving particles are present, they do not conduct electricity in solid state. Only in molten state or in solution having free moving particles ionic solids conduct electricity. Ionic salts are generally hard but brittle and having high melting and boiling temperatures. The unique properties of ionic solids signify strong forces between the particles and it takes a lot of energy to move them all relative to each other. In case of ionic solid the three dimensional lattice is held together strongly by electrostatic forces of attraction between positive and negative ions. This electrostatic force is called ionic bonding. At present, salt extends to be of leading monetary corollary, with thousands of uses in accumulation to senescing and conserving food. Sodium chloride (NaCl) occurs in nature as the mineral halide, generally known as rock salt, in great subversive deposits on each continent. Salts have so many uses such as Salt became an essential element of commercial dealings and was often used as money or trade. Ionic solids used as phase transfer catalyst, surface-active agents etc. In industrial usages ionic solids act as active ingredient for conditioners, antistatic agent, detergent sanitizers, softener for textiles and paper products etc. Due to low cost and low toxicity [1] of but₄NI in recent times it has appeared as a promising substitute as

a catalyst for functionalization of C-H bonds [2]. In medicinal field it uses as antimicrobials, algacide, slimicidal agents, disinfection agents and sanitizers etc.

Ionic Liquids (ILs), a new assemblage of resources existing as a salt in the liquid state attract very much attention in scientific and engineering investigate. ILs are the generic term for a class of materials, consisting entirely of ions and being liquid below 100°C. It is habitually defined as salts with low melting point, typically below 373K. [3] The straightforward combinatory investigation designates vis-à-vis 10^{18} ILs can perhaps be manufactured. These assortments unwrap broad occasions in the couture of ILs apposite for convenient appliances. The considerate of the performance of ILs and their properties is essential for any practical relevance.

Ionic liquids have achieved global awareness as green solvents in the preceding decade. These studies investigate the essential science and engineering of using ionic liquids as a novel cohort of solvents to reinstate the customary organic solvents. They are accessible as novel solvents for the alternative of organic solvents and the configuration of elegant liquids. The exploration also anticipated nano- and atom-scale structuring of ionic liquids, a characteristic that emerges to entirely buttress their unique behavioural features and assist exact prophecies of inclinations. Due to having various properties such as easy separation, very low vapor pressure, non-flammable substance, high thermally stable, high mechanically stable, electrochemically stable, low toxicity, non-volatility etc. properties ionic liquids have growing interest as **green solvent**. Ionic liquids are widely used as environmental-friendly reaction systems. An ionic liquid is mainly typified by a range of minimum specific conductivity in the mScm^{-1} , jointly with a molar conductivity [4,5] perhaps beyond $0.1 \text{ Scm}^2 \text{ mol}^{-1}$. In accumulation, the liquid ought to merely restrain ions with minor numbers of ion pairs or parent molecules. Ionic liquids are apt to have low dielectric constants, which signify they are not ionizing solvents [6,7]. With the extent of major issues we may assign ionicity [8] of an ionic liquid in terms of its conductivity values. From the above tête-à-tête one basic question may arise and thus in respond to the aperture issue, "What is an ionic liquid?" I desire the respond, "It be an appearance of liquid salt restraining ions and ion pairs in its current affirm." [9]

If at room temperature ionic liquids become liquid, we christen them as room temperature ionic liquids (RTILs). Information of the properties of the RTILs is essential for selecting an appropriate liquid for a piece of their trade employments.

The phrase '*solution*' is mainly employed in meticulous case of an assortment between diverse components, explicitly, when a little quantity of solid, liquid or gaseous substances disband to a firm limit in a liquid or solid substance (it may be pure, or a mixture itself), solvent.

An ionic solid is a conformist salt present in solid state having symmetric cation and anion. On the other hand an ionic liquid (IL) is a salt in the liquid state or phase having symmetric anion and asymmetric cation. Ionic Liquids (ILs) is the broad expression pro a set of resources, exclusively consisting ions and become liquid below 100°C. (Figure 1) IIs are a novel invention of chemicals having a great potential to contribute in the greenness of chemical procedures and developing new appliances such as in pharmaceutical industry. Green chemistry acts an extremely imperative function in the sustainable improvement, looking for reducing and averts effluence at its resource; reduce the vulnerability and exploit the effectiveness of the chemical procedures.

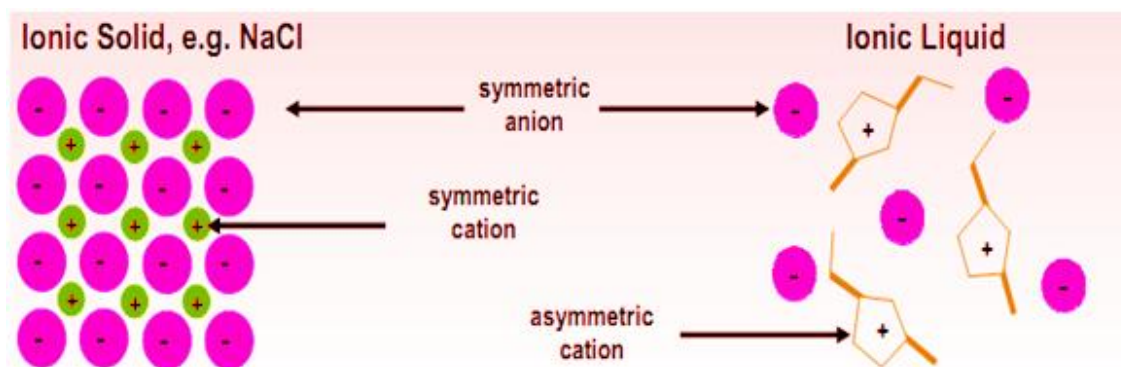


Figure 1: Basic structural differences between ionic solid and ionic liquid

HOST-GUEST INCLUSION CHEMISTRY

The greatest improvement of supramolecular chemistry was occurred from 1987 after the achievement of the Nobel Prize of Lehn, Cram, and Pedersen on explanation of their

important innovations about the host–guest systems. Host-guest chemistry majorly describes complexes that are composed of two or more molecules which are held together in unique structural relationships by non covalent interactions. Yet as its innovation, the notion of supramolecular chemistry has concerned plenty of interest from chemists, biologists, and material scientists, where they exploit the noncovalent interactions, together with hydrogen-bonding communication, π – π stacking interface, electrostatic interface, van der Waals force and hydrophobic/hydrophilic attraction [6–10]. Throughout the previous decades, substantial efforts have been remunerated to expand copious supramolecular systems and to inspect their appliances in catalysis, electronic devices, functional materials, nanomedicine, sensors and so on [7–10]. In virtue of the reversibility and adaptableness of host–guest communication, (Figure 2) supramolecular systems have been developed into diverse morphologies with diverse purposes to execute precise necessities in biomedical relevances.



Figure 2: Schematic Representation of Host-Guest Inclusion Complex Formation

In an emblematic host–guest inclusion complex, a host molecule affords a cavity to encapsulate a guest molecule through noncovalent communications. Due to having a variety of noncovalent interfaces in host-guest complexation, host–guest interaction

based on macrocyclic molecules is an extremely imperative incident that has been widely explored. Two or more chemical moieties can be incorporated together during such host-guest inclusion, in a facile and reversible manner which provides immense potential for the edifice of new-fangled supramolecular structures.

Major uses of host-guest chemistry are as follows

Pharmaceutical industry: Treatment of inflammation or throat infection (with iodine), coronary dilatation (with nitroglycerin), anti-ulcerate (with benexate), vectors for vitamins or hormones, decrease of side-effects and amplify in efficiency of anti-cancer drugs.

Cosmetics & Hygiene: Long-lasting perfume release deodoriser (with peppermint oil, i.e.), to remove dryness wrinkles (with seaweed compounds, vitamin A & E), anti-cellulitis compound, shampoo industry, teeth cleaning, anti-plaque compound, antibacterial in refrigerators.

Food industry: Emulsion stabiliser, taste-masking, long-lasting flavouring, removal of cholesterol from milk, butter, eggs etc.

Paint industry: Increase in compatibility of paint ingredients, enhance in stability of the paint, increase in the range of colours and in the quality of dyes.

Environmental protection: Reduction in oxidiser requirements in paper production, environmentally friendly oil-spill clean-up, treatment of tree-wounds (with auxin), mobilisation of toxins without leaving toxic residues behind (innovative technique), removal or detoxification of dissipate stuff, specially aromatic toxins, employ in agriculture for increasing the steadiness and the competence of herbicides, insecticides, repellents.

Chemical and biochemical appliances: Reaction catalyst in glue, apply in chromatography (separation of stereoisomers), enhance in speed of diagnostic test reaction.

In my present research study ionic solids and ionic liquids are taken as guest molecules and the major host molecules such as CDs and CBs are taken owing to their extensive appliances in the biomedical field.

Objective

The significance and exploits of chemical electrolytes (ionic solids and ionic liquids) in non-aqueous pure and mixed solvents have been abridged by very legendary scientists [11-23]. In recent times solute-solute/ion-ion and solute-solvent/ion-solvent communications have been focus of extensive attention.

The main aim of my present research work is to discuss and explain various interactions of some electrolytes especially ionic solids and ionic liquids in different industrially important solvent media through various physicochemical techniques. Elementary exploration on non-aqueous electrolyte solutions has catalysed their broad procedural appliance in a lot of grounds. Due to their elevated suppleness based on the variety of various solvents, additives and electrolytes with extensively varying properties, non-aqueous electrolyte solutions are essentially challenging with other ionic conductors. Prevalent achievement of non-aqueous electrolytic solutions are high energy primary and secondary batteries, photoelectrochemical cells, electro machining, etching, polishing, electrosynthesis, wet double layer capacitors, electro-deposition and electroplating.

Drug transport across biological cells and membranes is dependent on thermophysical properties of drugs. One of the well-organized approaches is the study of molecular interactions in fluids by thermodynamic methods as parameters are expedient for interpreting intermolecular interactions in solution. Also the study of thermodynamic properties of drug in a apposite medium can be correlated to its therapeutic effects [24,25].

Host-guest inclusion complexation studies majorly covered in biomedical relevances, chiefly addressing drug delivery, photodynamic cancer therapy, gene delivery as well as bioimaging.

The major aims of the research work are:

- ❖ To explore the physicochemical properties of ionic solids and ionic liquids in pure and mixed solvent systems.
- ❖ To comprehend the character and potency of diverse communications, their influence on structural and dynamic properties of ionic solids and ionic liquids in pure and mixed solvent systems.

- ❖ To study the transport properties of ionic solids and ionic liquids along with thermodynamic and acoustic ones to characterize molecular interactions in solutions.
- ❖ To survey the host-guest inclusion complex formation of some guest molecules (ionic solids and ionic liquids) with diverse host molecules.

Importance of Thermodynamic Parameters

The considered *thermophysical, thermodynamic, transport, optical, acoustic and spectroscopic properties* are of immense significance in illustrating the properties and structural features of solutions. The nature of intermolecular communications can be exposed from the interpretation of the derived properties through the thermophysical study.

Volumetric properties like apparent molar volume calculated from density measurement are of also enormous consequence in considered the properties and characteristic of solutions. The facts therefore hearten us to extent the study of binary or ternary solvent systems with several industrially imperative solvents (polar, weakly polar and non polar) and some solutes/electrolytes. The sign and magnitude of thermodynamic quantity such as partial molar volume (ϕ_r^0), affords information concerning the nature and extent of ion-solvent interaction whilst the experimental slope (S_v^*) affords information regarding ion-ion interactions.[xx] Furthermore, the derived parameters obtained from experimental density, viscosity and speeds of sound data and succeeding elucidation of the nature and strength of intermolecular interface assist in testing and improvement of various theories of solution. Thus the properties present imperative information regarding the nature and potency of intermolecular forces effective amongst assorted components also.

Precious information concerning the nature and strength of forces of electrolytes/non-electrolytes viz. viscosity B -coefficient, useful in solutions can be attained from viscosity data. Recently the use of computer simulation of molecular dynamics has led to major development in the direction of a unbeaten molecular theory of transport properties in fluids and a proper understanding of molecular motions and

interaction patterns in non-electrolytic solvent mixtures involving both hydrogen bonding and non-hydrogen bonding solvents has been established.[26,27]

The mode of communications akin to dissociation or association has accomplished an immense agreement which obtained from ultrasonic speed measurements and from the calculation of isentropic compressibility. It can also be used for the test of various solvent theories, statistical models and are fairly responsive for alteration in ionic concentration in addition to useful in illuminating the solute-solvent interactions.

Molar refraction obtained (R_M^0) from refractive index study using Lorenz-Lorentz relation is also an significant optical physical property of liquids and liquid mixtures persuade the solution of diverse problems in chemical engineering to facilitate the development of industrial processes. Knowledge of refractive index of multicomponent systems affords significant information vis-à-vis the molecular interactions happening in the solutions, [28-30] that is crucial for a lot of thermophysical calculations including the correlation of refractive index with density [31-33].

The study of thermophysical behaviours like dissociation or association from acoustic measurements and from the calculation of isentropic compressibility has achieved much significance. The acoustic measurements can also be used for the test of various solvent theories and statistical models and are quite sensitive to changes in ionic concentrations as well as useful in elucidating the solute-solvent interactions. Thermophysical properties involving excess thermodynamic functions have relevance in carrying out engineering applications in the industrial separation processes. The significance and use of the chemistry of electrolytes in non-aqueous and mixed solvents are well-recognised. However, the studies on properties of aqueous solutions have afforded adequate information on the thermodynamic properties of diverse electrolytes and non-electrolytes, the effects of variation in ionic structure, ionic mobility and common ions along with a multitude of other properties [34].

I. 2. ASSORTMENT OF SOLUTES AND SOLVENTS USED

Solvents: Industrially momentous solvents such as acetonitrile, diethyl carbonate, o-toluidine, o-xylene and 2-nitrotoluene, formamide, 2-methoxyethanol or methyl

cellosolve, N,N-dimethylformamide, N,N-dimethylacetamide, 1,3-dioxolane, tetrahydrofuran and widespread solvent water, have been preferred as main solvent in this research work.

Electrolytes: Ionic solids such as Lithium iodide, lithium perchlorate, lithium hexafluoroarsenate, tetrabutyl ammonium iodide, tetraheptyl ammonium iodide and ionic liquids such as 1-butyl-1-methylpyrrolidinium bromide, n-dodecyl, n-dimethyl-3-ammonio-1-propanesulfonate, 1-butyl-3-methylimidazolium chloride, 1-butyl-1-methylpyrrolidinium chloride, 1-butyl-2,3 dimethylimidazolium, tetrafluoroborate, 1-butyl-4-methylpyridinium hexafluorophosphate etc. are used as electrolytes.

Non-Electrolytes: The used non-electrolytes are α -cyclodextrin, β -cyclodextrin, D(-)fructose, D(+)galactose, cucurbit[6]uril etc.

I. 3. METHODS OF EXPLORATION

The subsistence of free ions, solvated ions, ion-pairs and triple-ions of electrolytes/non-electrolytes in aqueous and non-aqueous media depends upon the concentrations of the solution, size of ions, and intermolecular forces, such as, electronegativity of the atom, dipole-dipole forces, dipole-induced dipole forces, H-bonding, Van der Waal forces, columbic forces and electrostriction, Inductive effect, side chain effect etc. Therefore, the study of various communications and equilibrium of ions in miscellaneous concentration provinces are of enormous consequence to the technologist, theoretician, industrialist, researchers due to the occurrence of most of the chemical processes in these systems.

Fascinatingly the diverse experimental procedures have been engaged to find out a superior perceptive the occurrence of solvation and diverse communications established in solution. Hence, we have engaged the five considerable thermophysical methods, viz., conductometry, densitometry, viscometry, ultrasonic interferometry, and refractometry to investigate the solvation phenomena.

In most cases the transport properties are studied using the conductance data, especially the conductance at infinite dilution. Conductance data obtained as a function

of concentration can be used to study the ion-association with the help of appropriate equations. The limiting ionic conductance of the each ion has been anticipated from the “*reference electrolyte*” method using tetrabutylammonium tetraphenylborate. The ionic conductances also play the vital function to the elucidation of the ionic level of interface, association or ion-solvent interactions of ions as well as molecules. From conductometric study equivalent Conductance and Ion-Association Constant can be determined with the help of Fuoss conductance equation and Fuoss- Kraus conductance equation for Triple-Ion formation respectively. From density measurement with the help of Masson equation apparent molar volumes can be obtained, which are usually convenient parameters for interpreting ion-solvent/solute-solvent interfaces while, the experimental slopes afford ion-ion/solute-solute interactions in solution respectively. With the help of “*reference electrolyte*” method, ionic apparent molar volume for the individual ions has been acquired. From viscosity measurement with the help of Jones-Dole equation viscosity *B*- and *A*- co-efficients have been determined which imply ion-solvent and ion-ion interaction respectively. Moreover, the viscosity *B*-coefficient is alienated into ionic components by the ‘*reference electrolyte*’ method. From the temperature dependence of ionic values, a satisfactory elucidation of ion-solvent interactions such as the possessions of solvation, structure-breaking or structure-making, polarization, etc. has been prearranged. From refractometric measurements with the help of Lorentz-Lorenz relation molar refraction has been determined which implies the compactness of the solute in solution system. (Limiting apparent molar adiabatic compressibility) which implies solute-solvent interaction and (Experimental slope) which implies solute-solute interaction can be determined from experimental speed of sound measurements. Surface Tension measurement has also done to interpret correctly the host-guest phenomena.

The spectroscopic study has been ascertained by the exploration of FTIR, NMR spectroscopy. The study has been taking into explanation to qualitative interpreting the molecular as well as ionic association of the electrolytes in the solutions.

CHAPTER: II

GENERAL INTRODUCTION

(REVIEW OF THE EARLIER WORKS)

II. 1. IONIC SOLIDS

Ionic solids are made up by the chemical combination of *metallic* and *non-metallic* elements. Ionic solids have some unique properties such as, high melting temperature and hard, brittle crystals due to strong forces between the particles. Ionic solid does not conduct electricity in solid state due to absence of free electrons. Ionic solid conducts electricity in molten state or in solution due to presence of free moving electrons.

II. 1. 1. CLASSIFICATIONS OF IONIC SOLIDS

Classifications of ionic solids can be depicted by the following Table 1.

Table 1. Different types of ionic solids

Type	Built from	Examples
Amorphous	Covalently bonded network with limited ordering	Glass, plastics, polymers
Ionic	+ and - ions	NaCl, CsCl, $(\text{NH}_4)_2\text{SO}_4$
Metallic	Atoms or metallic ions in sea of e^-	
Molecular	Molecules with internal covalent bonds, and intramolecular attractions: dipole-dipole, H-bond. London dispersion	H_2 , ice, I_2 , CH_3OH
Network	Atoms held in network covalent bonds	Graphite, diamond, quartz

II. 1. 2. PROPERTIES OF IONIC SOLIDS

In case of ionic solids molecules, atoms or ions locked into a crystal lattice. The particles ionic solids are close together and attached with strong forces of attraction. So, ionic solids are rigid, highly ordered and incompressible regular three dimensional arrangements of equivalent lattice points in space. The lattice points define unit cells, the smallest repeating internal unit that has the symmetry characteristic of the solid. Chemists believe that when metallic and non-metallic atoms react to form ionic compounds the following steps occur:

- Metal atoms lose electrons to non-metallic atoms and become positively charged metal ions.
- Non-metal atoms achieve electrons from the metal atoms and so become negatively charged non-metal ions.
- Large numbers of positive and negative ions formed in this way then combine to form a three-dimensional lattice. The imperative properties of ionic solids can be interpreted more clearly with the help of Table 2.

Table 2: Physical Properties and inferred structural features of ionic solids

Properties of ionic solids	What these tell us about structure
High melting temperature	Forces between the particles are strong
Hard, brittle crystals	Forces between the particles are strong
Does not conduct electricity in the solid state	No free-moving charged particles present in solid ionic solid.
Conduct electricity in the molten state	Free-moving charged particles present in molten ionic solid.

The three dimensional lattice is held together strongly by electrostatic forces of attraction between positive and negative ions. This electrostatic force is called ionic bonding. The interesting properties of ionic solids can be depicted such as,

- Ever noticed that when we eat fish, chips and another foods which may become hot but the salt does not melt.

- This is because to melt an ionic solid energy must be provided to allow the ions to break free and move.
- NaCl has a high melting temp, this signifies a huge quantity of energy is required to decrease the electrostatic desirability between the oppositely charged ions and allow them to move freely.
- Unlike metals ionic compounds are not malleable. They rupture only for thumping.
- A force can disrupt the strong electrostatic forces holding the lattice in place.
- A sodium chloride crystal cannot be scratched easily but if a well-built strength (e.g. hammer blow) is given, it will explode.
- This is because the layers of ions will move relative to each other due to the force.
- During this movement, ions of like charge will become adjacent to each other. Resulting in repulsion. (Figure 1)

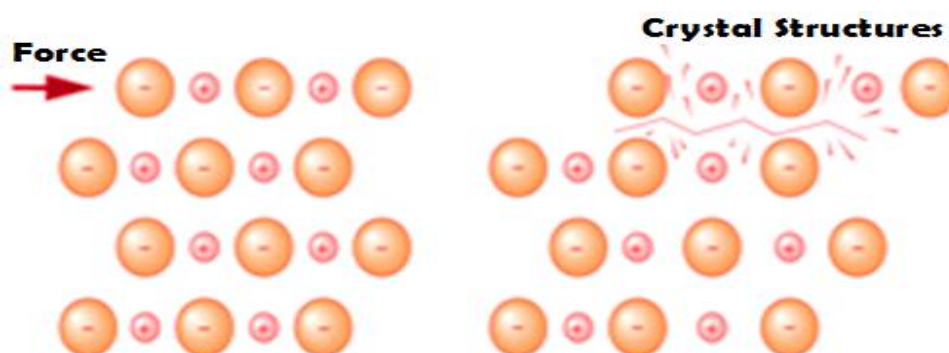


Figure 1. Repulsion between like charges causes this sodium chloride crystal to shatter when it is hit sharply

For the discussion of the reaction patterns of ionic solids can be discussed such as, metallic atoms have low ionisation energies and low electronegativities. Non-metallic atoms have low electronegativities and high ionisation energies. In other words metallic atoms misplace electrons easily and non-metallic atoms gain electrons easily. So, in case of ionic solids the metal atoms misplace an electron to the non-metal atoms. In doing so, both atoms will frequently accomplish the electronic configuration of the nearest noblest gas, which is particularly stable.

II. 2. IONIC LIQUIDS

Ionic liquids (ILs) are a salt in the liquid state/phase. In some contexts, the term has been classified to ionic species existing in liquid state, whose melting point is below some capricious temperature, for instance 100°C (212°F). Generally, Ionic Liquids (ILs) are liquid salts that consist of combinations of organic-organic or organic-inorganic cation or anions (Figure 2).

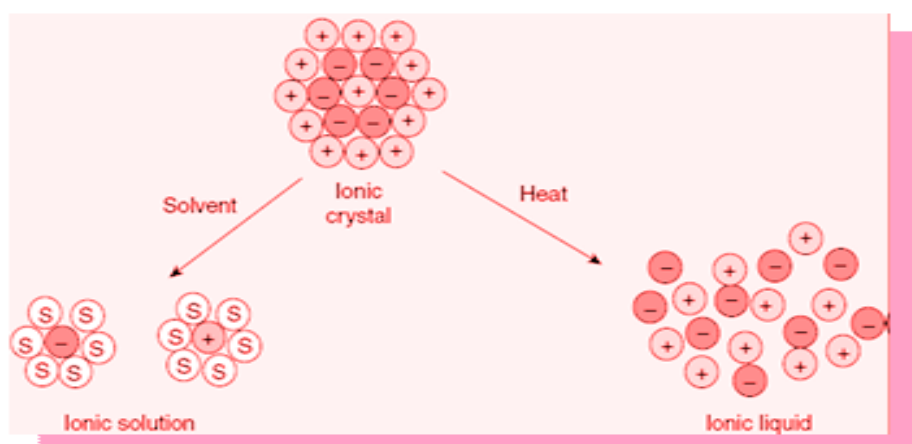


Figure 2: Difference between an ionic solution and an ionic liquid.

It is well acknowledged that it is possible to decrease the melting temperature, by increasing the size of the ions and making them asymmetric [1]. This is simply explained such that, given the nature of the ions in ionic liquids, they tend to attract each other due to electrostatic forces. If the ions are small and symmetric, as in the case of ionic solid such as sodium chloride (NaCl), the ions will be close to each other and interact strongly. Moreover, due to their symmetry, the development of crystals is favorable. If the size of the ions is increased, the distance between them will increase and as a result the electrostatic attractive force will reduce. Such manner the melting point of the ionic liquid can be guarded. Additionally, if the ions are asymmetric, the melting point can be diminished even more or eventually be suppressed. The flexibility of the ionic liquids lounges in that, it is possible to synthesize thousands of them by simply varying a functional group, and such variation will determine the final macroscopic characteristics of that ionic liquid. In the last years, ionic liquids have found different applications, e.g. as electroplating solvents, catalyzers, and electrolytes [2]. For the specific case of electrolytes, the attention in ionic liquid has significantly increased and some of the possible appliances are

originated in lithium-ion batteries, [3,4] fuel cells, [5] and solar cells [6,7]. In spite of the previously cited virtues of the ionic liquids, they are relatively new as electrolytes, and as such, there are some drawbacks, such as, toxicity, compatibility with the actual materials used, production cost, and all the problems that come with the introduction of a new technology. Now a days the large attention in ionic liquids was commenced because of its usefulness as eco-friendly “green” solvents [8,9]. Ionic liquids offer the advantage of both homogeneous and heterogeneous catalysts. This is because preferred ionic liquids can be immiscible with the reactants and products but can dissolve the catalysts. Enzymes are also stable in ionic liquids, opening the possibility for ionic liquids to be used in biological reactions, such as the synthesis of pharmaceuticals [10,11]. Ionizing radiation does not affect ionic liquids, so they could even be used to treat high-level nuclear waste. Ionic liquids can selectively dissolve and eliminate gases and could be used for air purification on submarines and spaceships. Ionic liquid used in the present widely used in solvent extraction, liquid-liquid extraction process, electrochemical studies, dye-sensitized solar cells [12-15]. Moreover, good thermal stability, variable viscosity, no effective vapor pressure, recyclability and conformist organic solvents have been replaced by ILs in organic synthesis is also great qualities of IL [16-18].

In the last decades a new class of compounds came into the focus of many research groups around the world: ionic liquids (IL). The count of publications with the topic “*ionic liquids*” grew steadily over the last ten years. But what are ionic liquids and why are they so interesting? The following section gives a short overview over this wide field. A much more exhaustive overview about the possible applications and properties of ionic liquids can be found in the recent book “*Ionic Liquids in Syntheses*”, edited by Peter Wasserscheid and Tom Welton [19]. The commonly accepted definition of ionic liquids is that they are “*ionic materials that are liquid below 373 K*” [20]. However, the opinions about the definition of “*ionic material*” are more scattered. Many alternatives to organic solvents have been proposed over the last two decades. Ideally solvent-free conditions or the use of water as the ultimate green solvent can be considered. However, many organic compounds do not dissolve in water, and especially solids cannot be processed without a solvent. Therefore suitable

alternatives have been sought and found in the classes of (i) ionic liquids; ionic liquids have gained a lot of attention as emerging environmentally benign solvents [21]. They can replace conventional organic solvents in several applications due to their unique features. Ionic liquids are salts with melting points below 373 K. They consist of an organic cation collective with an organic or inorganic anion [22]. Ionic liquids show, in general, a very interesting set of properties to be used for different applications in chemical industry. The melting points of these organic salts are frequently found below 150 °C and occasionally as low as -96 °C. Some ionic liquids are stable up to 500 K [23]. At room temperature they have no measurable vapor pressure due to their ionic nature [19]. They normally have high solvency power for polar and non-polar compounds. Billions of ionic liquids can be designed and synthesized by selecting different ion pair combinations, which enable them to possess specific properties. Furthermore, the ability to tune the solvent properties of the ionic liquids is one of their outstanding features, which makes them unique solvents for various reactions and separations [24,25]. Moreover ionic liquids are almost nonflammable, highly thermally and electro chemically stable and present a large liquid range. The main challenges to the large scale application of ionic liquids are their high costs, their high toxicity (many ionic liquids contain halogens), the unknown long term stability and their relatively high viscosity compared to most common molecular solvents. They are also exploiting as heat transfer fluids for processing biomass and as electrically conductive liquids in electrochemistry (batteries and solar cells) [26-28]. In the modern technology, the appliance of the salt is well understood by studying the ionic solvation or ion association. Ionic association of electrolytes in solution depends on the mode of solvation of its ions [29-32] which in turn depends on the nature of the solvent/solvent mixtures. Such solvent properties as viscosity and the relative permittivity have been taken into consideration as these properties help to determine the extent of ion association and the solvent-solvent interactions. The non-aqueous system has been of immense importance [33,34] to the technologist and theoretician as many chemical processes occur in these systems. The latter decreases the mass transfer rate during reaction and separation processes. However, the viscosity of ionic liquids can drop significantly by addition of co-solvents such as carbon

dioxide (CO₂). An overall comparison between ionic liquids and organic solvents is presented in Table 3 [35].

Table 3. Comparison between organic solvents and ionic liquids [36]

Property	Organic Solvents	Ionic Liquid
Number of solvents	>1000	>1,000,000
Applicability	Single function	Multifunction
Catalytic ability	Rare	Common and tuneable
Chirality	Rare	Common and tuneable
Vapour pressure	Obeys the Clausius–Clapeyron equation	Negligible vapour pressure under normal conditions
Flammability	Usually flammable	Usually nonflammable
Polarity	Conventional polarity concepts apply	Polarity concept questionable
Tuneability	Limited range of solvents available	Virtually unlimited range means “designer solvents”
Cost	Normally cheap	Typically between 2 and 100 times the cost of organic solvents
Recyclability	Green imperative	Economic imperative
Viscosity, cP	0.2–100	22–40,000
Density, g/cm ³	0.6–1.7	0.8–3.3
Refractive index	1.3–1.6	1.5–2.2

II. 2. 1. ROOM TEMPERATURE IONIC LIQUIDS (RTILs)

ILs which are liquid at room temperature are called room temperature ionic liquid (RTIL). In the older (and some current) literature, ionic liquids are occasionally called liquid organic salts, fused salts, molten salts, ionic melts, NAILs (non-aqueous ionic liquids), room-temperature molten salts, OILs (organic ionic liquids) and ionic fluids [37]. Heating normal salts, such as sodium chloride (NaCl, *mp* 801°C), to high temperature produces also a liquid, that consists entirely of ions, but this is a molten salt and not defined as an ionic liquid. In existing times Ionic liquids (IL) have appeared as room temperature ionic liquids (RTILs) and atmosphere responsive solvents for the development for the manufacturing accumulate of chemicals. Ionic liquids have been progressively more used for various commercial and potential applications such as organic synthesis, catalysis, electrochemical devices and solvent extraction of a assortment of compounds. Most of the cases of ILs the cations may be organic or inorganic while the anions are inorganic [38].

Usually ILs consist of a large hulking and asymmetric organic cations based on 1-alkyl-3-methylimidazolium (abbreviated $[C_n\text{mim}]^+$, where n = number of carbon atoms in a linear alkyl chain), N -alkylpyridinium (accordingly abbreviated $[C_n\text{py}]^+$), tetraalkylammonium (Bu_4N^+) or tetraalkylphosphonium (Bu_4P^+) cations, and many others; and inorganic anions such as hexafluorophosphate $[\text{PF}_6]^-$, tetrafluoroborate $[\text{BF}_4]^-$, alkylsulfates $[\text{RSO}_4]^-$, alkylsulfonates $[\text{RSO}_3]^-$, halides such as chloride $[\text{Cl}]^-$, bromide $[\text{Br}]^-$ or iodide $[\text{I}]^-$, nitrate $[\text{NO}_3]^-$, sulfate $[\text{SO}_4]^-$, aluminum chloride $[\text{AlCl}_4]^-$, triflate ($[\text{CF}_3\text{SO}_3]^- = [\text{TfO}]^-$), bis(trifluoromethylsulfonyl)imide ($[(\text{CF}_3\text{SO}_2)_2\text{N}]^- = [\text{Tf}_2\text{N}]^-$), etc. Recently very long alkyl, aryl or both are act as cationic part of the ionic liquids and that ionic liquids are called surface active ionic liquids (SAIL) [39]. Some commonly used ionic liquid systems are presented in Figure 3.

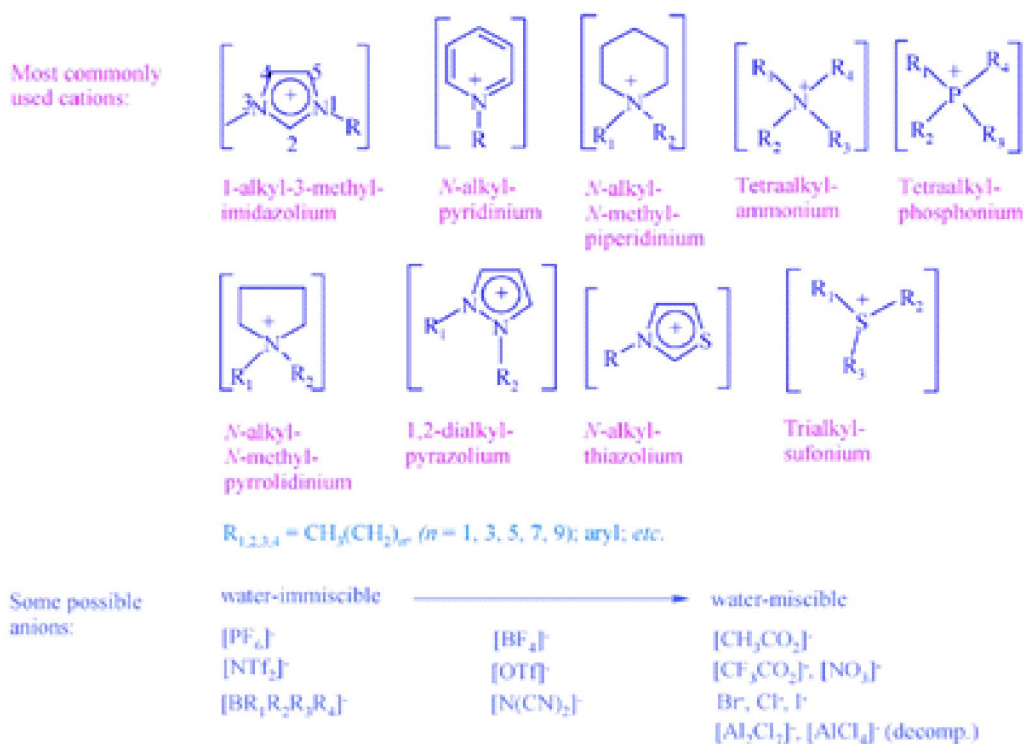


Figure 3: Some commonly used ionic liquid systems. The abbreviation $[C_n\text{pyr}]^+$ represents the 1-alkyl-1-methylpyrrolidinium cation, where the index n stands for the number of carbon atoms in the linear alkyl chain. $[\text{P}_{wxyz}]^+$, $[\text{N}_{wxyz}]^+$ and $[\text{S}_{xyz}]^+$ are normally used to represent tetraalkylphosphonium, trialkylsulfonium and tetraalkylammonium cations, respectively, where the indices w , x , y and z indicate the length of the corresponding linear alkyl chains.

Ionic liquids are eco-friendly as green solvents due to nonvolatility compared to conventional solvents, which are often volatile and contribute to air pollution and the green house effect. ILs also results in less solvent consumption because of being suitable for reuse. But the commonly used ILs are toxic in nature and are hardly biodegradable, which are characteristically not intrinsically green. In fact, ILs can be designed to be environmentally benign, which is the direction research and industry should steer towards.

II. 2. 2. PROPERTIES OF IONIC LIQUIDS:

Asymmetry of the cation is believed to be responsible for the little melting points of ionic liquids, while the nature of the anion is considered to be responsible for many of the physical properties of ionic liquids such as their miscibility with conventional solvents and hygroscopicity [40]. They are frequently referred to as “*Green Solvents*” due to their immeasurably low vapour pressure. A key feature of ionic liquids is that their physical properties such as melting point, viscosity, density, and hydrophobicity can be tailored to design different ionic liquids with a particular end use in mind by selection of different cation, anion, and substituents. Therefore ionic liquids are also described as “*Designer Solvent*” [41]. Ionic liquids have a number of advantages as solvents over molecular solvents such as negligible vapor pressure, high thermal stability, non-flammability, wide temperature range, Lewis acidity, hydrophobicity, gas solubility and hydrogen-bonding capability, therefore, these fluids have been proposed as an attractive alternative to volatile organic compounds (VOCs) for “*green processing*”. Replacement of conventional solvents with ionic liquids would prevent the emission of VOCs, a major source of environmental pollution [42].

II. 2. 3. GENERATION OF ILs

Ionic Liquids can be divided into three categories: First-generation; Second-generation; and Third-generation ionic liquids [43].

First-generation ionic liquids consist of bulky cations such as 1, 3-dialkylimidazolium (or *N, N'*-dialkylimidazolium) or 1-alkylpyridinium (or *N*-alkylpyridinium), and anions based mostly on haloaluminate (III); these have been studied extensively. The merit of

these ionic liquids is their tuneable Lewis acidity. The drawback of these systems is their great sensitivity towards water, which forms hydroxoaluminate(III) species with the aluminium(III) chloride and therefore decomposes the ionic liquid. The sensitivity towards water necessitates their handling in a dry-box.

The ionic liquids of the second category, the so-called *second-generation* ionic liquids, are usually air-stable and water-stable and can be used on the bench-top. However, it should be noted that water-stable does not imply that there is no interaction with water at all. Second-generation ionic liquids gradually absorb water from the atmosphere [44].

Recently, a *third generation* of “task-specific” ionic liquids have emerged [45]. These novel ionic liquids feature chemical functionalities which have been designed for specific applications. Very little is known to date about their physical properties, preparative methods, etc, and the future will show if they can bring about an ecological or economic benefit; but that future does look bright.

II. 2. 4. HISTORY AND NEW DEVELOPMENTS

Ionic liquids have been known for a long time, but their extensive use as solvents in chemical processes for synthesis, separation processes and catalysis has recently become significant. The first low melting salt (ionic liquid), ethylammonium nitrate ($[\text{EtNH}_3]^+[\text{NO}_3]^-$), with melting point of 12°C was synthesized by Paul Walden in 1914. During 1940s, aluminum chloride-based molten salts were utilized for electroplating at temperatures of hundreds of degrees Celsius. In 1951, low melting salts having chloroaluminate ions for low-temperature electroplating of aluminum were developed [45]. During the 1970s and 1980s, these liquids were studied mainly for electrochemical applications in nuclear warheads batteries [46]. In the early 1970s, Wilkes tried to develop better batteries for nuclear warheads and space probes which required molten salts to operate. These molten salts were hot enough for damaging the nearby materials. Therefore, the chemists searched for salts which remain liquid at lower temperatures and eventually they identified one which is liquid at room temperature. Wilkes and his colleagues continued to develop their ILs for use as battery electrolytes and then a small community of researchers began to make ILs and test their

properties [47,48]. In the mid 1980s, low melting point ionic liquids were proposed as solvents for organic synthesis [49,50]. In the late 1990s, ILs became one of the most promising chemicals as solvents. Initially, new ionic liquids such as organo-aluminate, have limited range of applications because they were unstable to air and water. Furthermore, these ILs were not inert towards various organic compounds. In 1992, after the first reports on the synthesis and applications of water and air stable ILs such as 1-butyl-1-methylpyrrolidinium bromide ([bmpy]Br) and 1-butyl-4-methylpyridinium hexafluorophosphate ([bmpy]PF₆), the number of air and water stable ILs have started to increase rapidly.

Interest in ionic liquids has now been grown dramatically in the scientific community (both in academia and industry) with over 8000 papers having been published in the last decade. There are about one million (10⁶) simple ionic liquids that can be easily prepared in the laboratory by combination of different cations and anions and this total are just for simple primary systems. If there are one million possible simple IL systems, then there are one billion (10¹²) possible binary combinations of these, and one trillion (10¹⁸) ternary possible IL systems that can be prepared from the combination of anions, cations, and substituents. At the moment only about 300 ionic liquids are commercialized, so one can imagine how many opportunities in this field are still undiscovered and why this field of chemistry is so tempting.

As the IL field grew in the 2000s, three distinct forces led to ILs becoming the victim of overgeneralizations that still plague the field today, including a plethora of new researchers in many diverse disciplines with little or no background in the IL field (or often not even chemistry), the rise in societal importance of green chemistry and sustainability, and the attractive new science and applications promised by study of ILs. The twin concepts of ILs as solvents and green chemistry propelled a dramatic augment in publications in this field (which is not yet slowing down) and initially an increase in the citations to Fuller et al [51].

II. 2. 5. POTENTIAL APPLICATIONS OF IONIC LIQUIDS

In recent years, ionic liquids have been used for a wide variety of applications at lab scale, such as the recovery of bio-fuels, desulfurization of diesel oil and supercritical

fluid extractions etc. Ionic liquids also have potential as lubricants, in solar cells, for heat storage, in nuclear fuel processing, in membrane technology, as sol-gel templates and in the dissolution of cellulose. Because of the unique physicochemical properties, the ionic liquids attract as innovative compound and their applications increases vastly in many fields (industrially as well as academic). The diverse application of ionic liquids is given in Figure 4, 5 and 6.

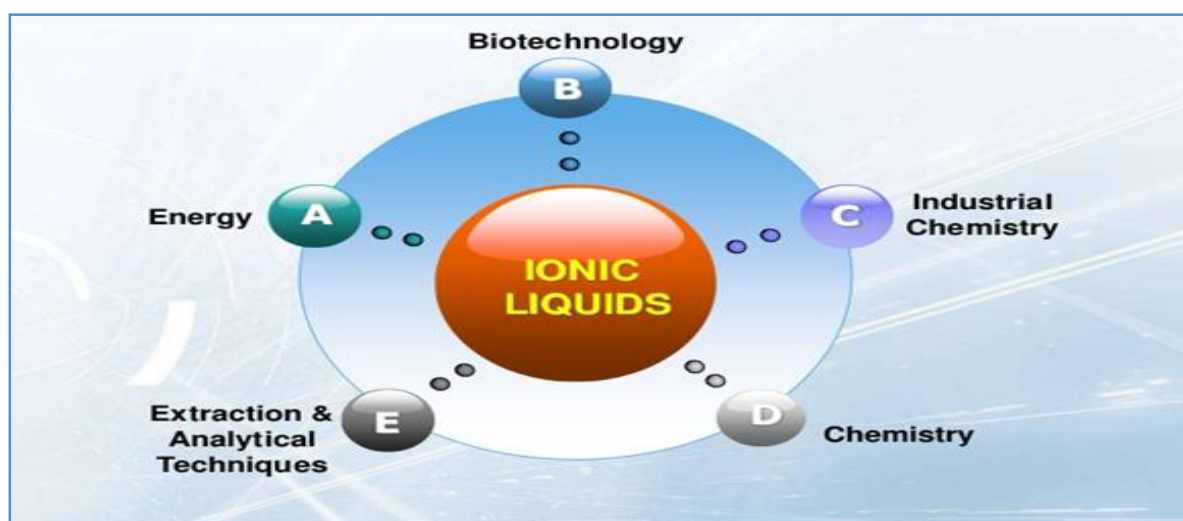


Figure 4: The diverse application areas of ionic liquids

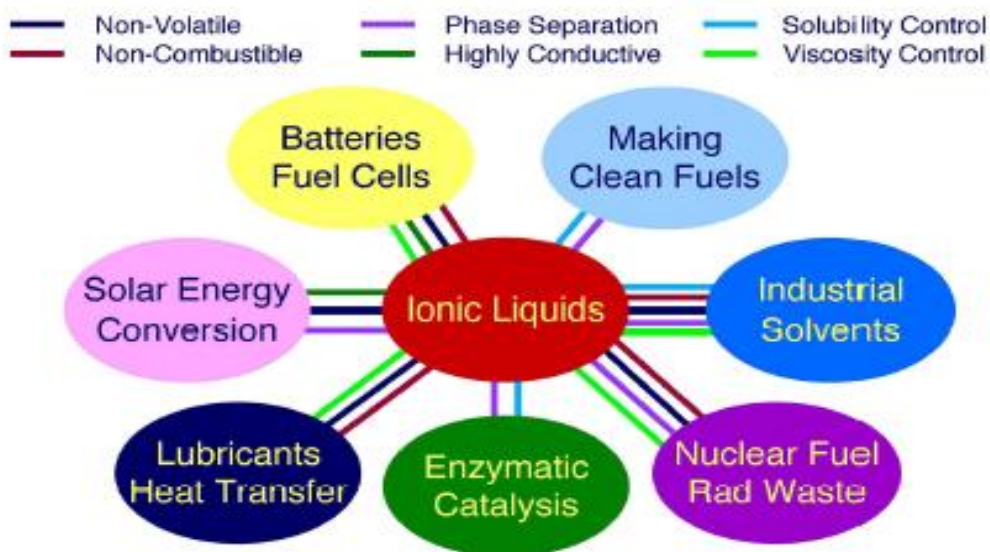


Figure 5: Miscellaneous applications of ionic liquids

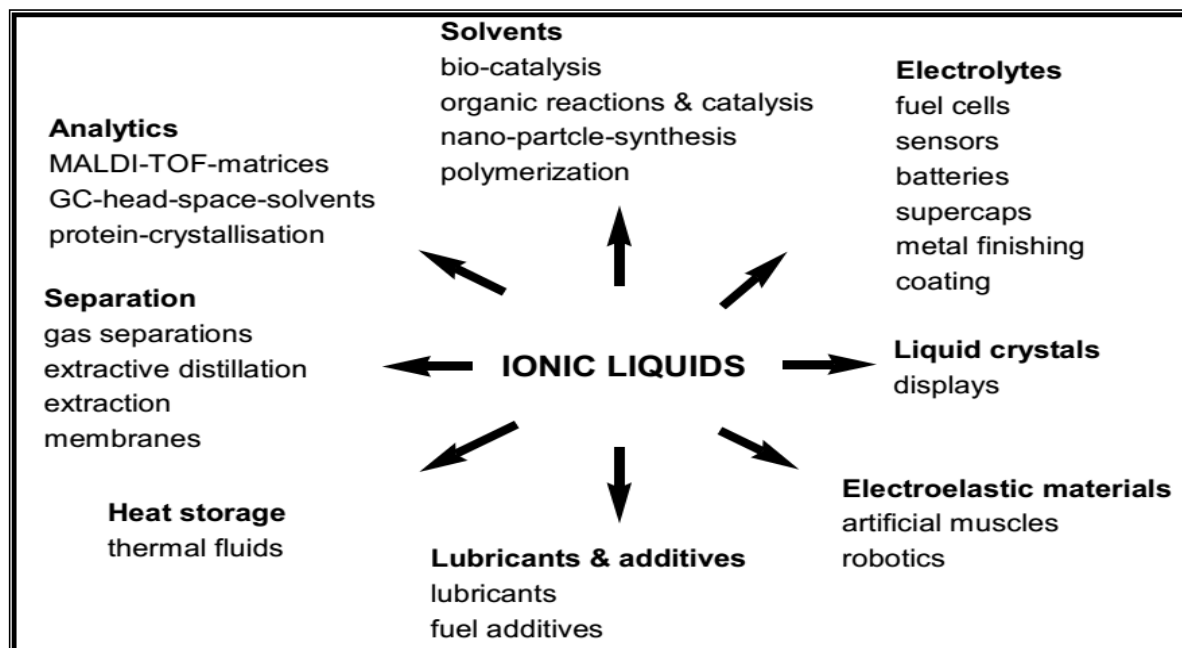


Figure 6: Selection of applications where ionic liquids have been used

II. 3. SOLUTION CHEMISTRY

The branch of physical chemistry that studies the change in properties that arise when one substance dissolves in another is called Solution chemistry. In ‘*Solution Chemistry*’ broadly three types of approaches have been made to estimate the extent of solvation. The first is the solvational approach involving the studies of viscosity, conductance, etc., of electrolytes and the derivation of various factors associated with ionic solvation, [52,53] the second is the thermodynamic approach by measuring the free energies, enthalpies and entropies of solvation of ions from which factors associated with solvation can be elucidated, [54] and the third is to use spectroscopic measurements where the spectral solvent shifts or the chemical shifts determine their qualitative and quantitative nature [55].

The mixing of diverse solute or solvent with another solvent/solvent mixtures gives rise to solutions that generally do not behave ideally. This deviation from ideality is expressed in terms of thermodynamic parameters, through excess properties in case of liquid-liquid mixtures and apparent molar properties in case of solid-liquid mixtures. These thermodynamic properties of solvent mixtures corresponds to the divergence between the actual property and the property if the system behaves ideally and thus are useful in the study of molecular interactions and arrangements. In particular, they

reflect the interface that take place between solute-solute, solute-solvent and solvent-solvent species. The addition of an ion or solute modifies the solvent structure to an extent whereas the solute molecules are also customized. The extent of ion-solvation is dependent upon the interactions taking place between solute-solute, solute-solvent, solvent-solvent species. The assesment of ion-pairing in these systems is imperative because of its effect on the ionic mobility and hence on the ionic conductivity of the ions in solution. These phenomenon thus paves the path for research in solution chemistry to elucidate the nature of interface through experimental studies involving densitometry, viscometry, interferrometry, refractometry and other suitable methods and to interpret the experimental data collected. Complete understanding of the phenomena of solution chemistry will become a reality only when solute-solute, solute-solvent and solvent-solvent interactions are elucidated and thus the present research work is intimately related to the studies of solute-solute, and solvent-solvent interactions in some industrially important liquid systems.

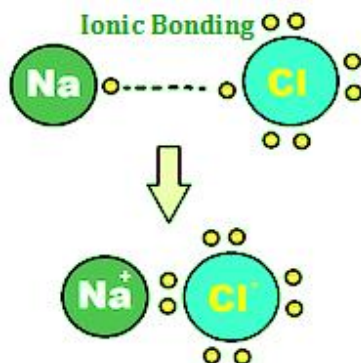
II. 3. 1. DIVERSE DRIVING FORCES OF INTERFACE

There are mainly attraction or repulsion two types of Intermolecular forces act between neighboring particles such as atoms, molecules or ions. In a molecule the binding forces of atoms are due to chemical bonding. The energy requisite to rupture a bond is termed as the bond-energy. The forces holding molecules collectively are usually called intermolecular forces. The energy essential to break molecules spaced out is much smaller than a typical bond-energy, but intermolecular forces play significant roles in determining the properties of substances. Intermolecular forces are particularly imperative in terms how molecules interact and form biological organisms or even life. These connections provide a superb introduction to the communications among molecules.

In general, intermolecular forces can be divided into several categories. The prominent types are:

- a. **Strong ionic interaction:** It is related to the properties of solids. The more ionic compound has the higher lattice energy. The following result can be

explained by way of ionic attraction: LiF, 1036; LiI, 737; KF, 821; MgF_2 , 2957 kJ/mol.



- b. **Intermediate dipole-dipole forces:** Substances, whose molecules have dipole moment have higher melting point or boiling point than those of similar molecular mass, having no dipole moment.



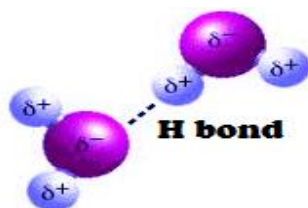
- c. **Weak London dispersion forces or van der Waal's force:** These forces always operate in any substance. The force arisen from induced dipole and the interaction is weaker than the dipole-dipole interface. In general, the heavier the molecule, the stronger the van der Waals force of interaction. For example, the boiling points of inert gases increase as their atomic masses increases due to stronger London dispersion interactions.



London dispersion force (I_2 bond)

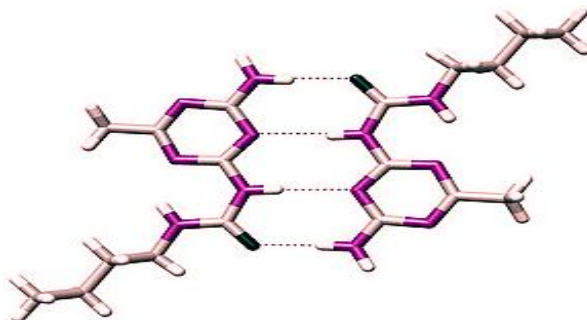
- d. **Hydrogen bonding:** Hydrogen bonding is the attractive interaction of a hydrogen atom with an electronegative atom, for example, nitrogen, oxygen or

fluorine (thus the name "hydrogen bonding," which should not be confused with a covalent bond to hydrogen). The hydrogen must be covalently bonded to another electronegative atom to construct the bond. These bonds can occur between molecules (*intermolecularly*), or within different parts of a single molecule (*intramolecularly*). The hydrogen bond (5 to 30 kJ/mole) is stronger than a van der Waals interface, but weaker than covalent or ionic bonds. This type of bond occurs in both inorganic molecules such as water and organic molecules such as DNA. Certain substances such as H₂O, HF, NH₃ form hydrogen bonds, and the formation of which affects properties (m.p, b.p, solubility) of substance.



Hydrogen bonding between water molecules

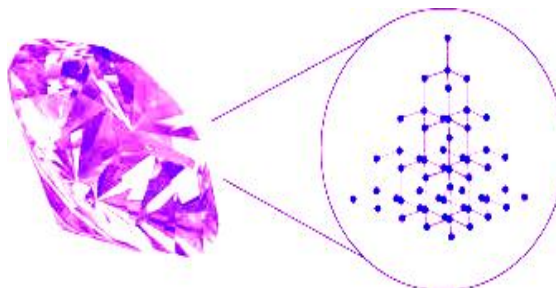
Other compounds containing OH and NH₂ groups also form hydrogen bonds. Molecules of several organic compounds such as alcohols, acids, amines, and amino acids contain these groups, and thus hydrogen bonding plays an important role in biological science.



Intermolecular hydrogen bonding in a self-assembled dimer complex

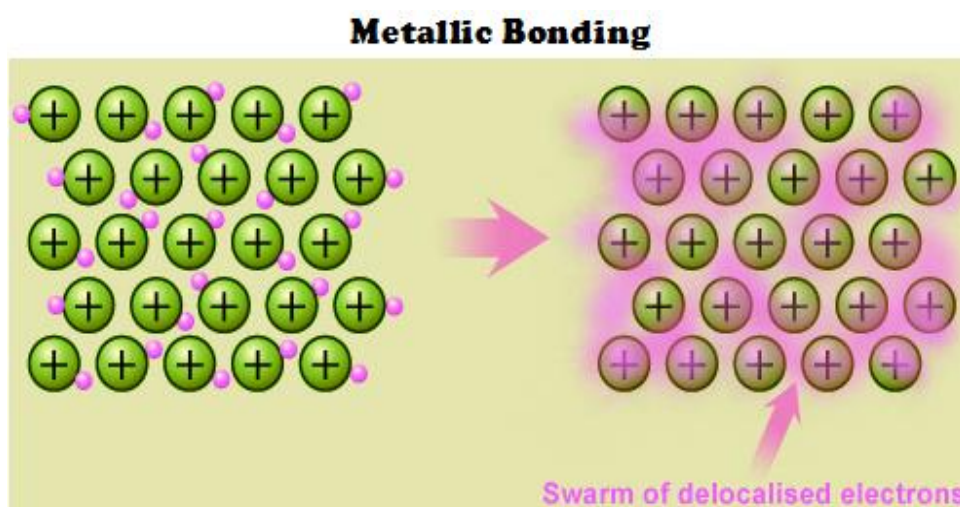
- e. **Covalent bonding:** Covalent is really intramolecular force rather than intermolecular force. It is revealed here, because some solids are formed due to covalent bonding. For example, in diamond, silicon, quartz etc., the all atoms in the entire crystal are linked together by covalent bonding. These solids are

hard, fragile, and have high melting points. Covalent bonding holds atoms tighter than ionic attraction.

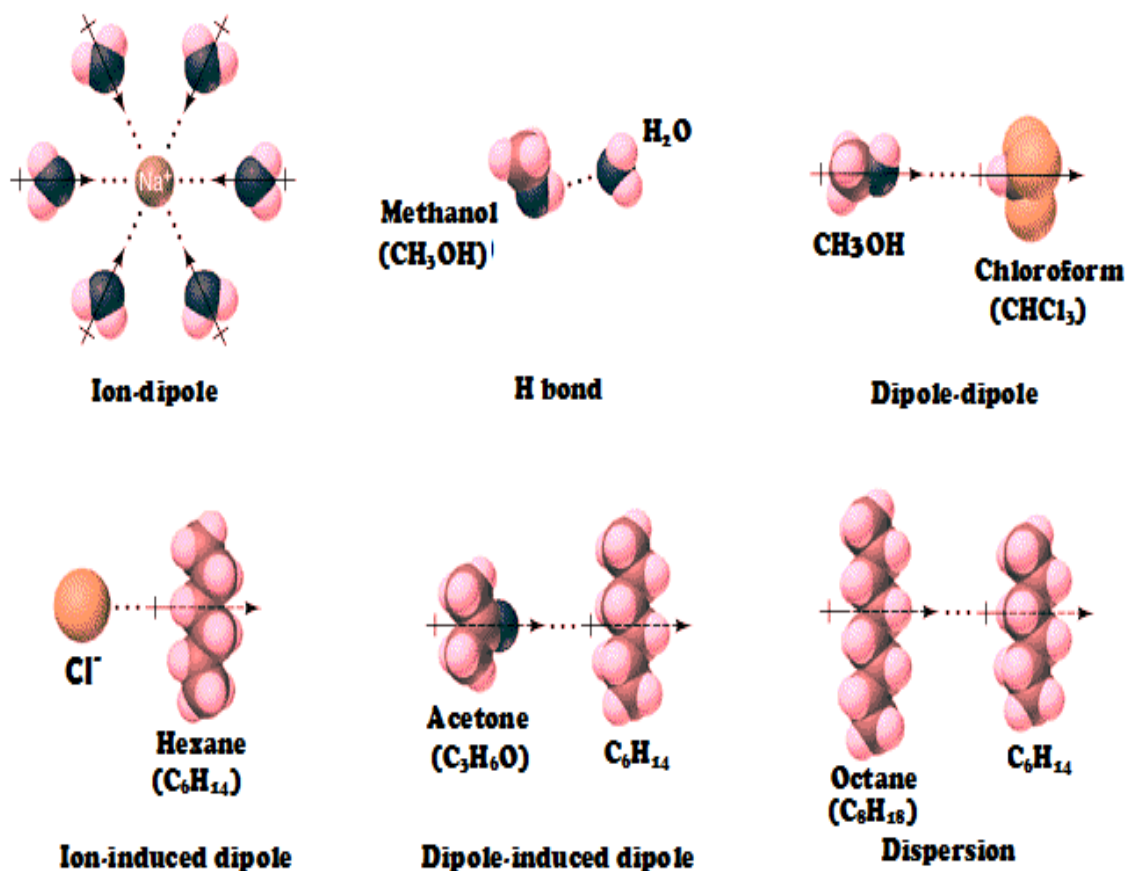


Covalent Bonding in Diamond

- f. **Metallic bonding:** Forces between atoms in metallic solids belong to another class. Valence electrons in metals are rampant. They are not restricted to certain atoms or bonds. Rather they run freely in the entire solid, providing good conductivity for heat and electric energy. These behaviours of electrons give special properties such as ductility and mechanical strength to metals.



All types can be present concurrently for many substances. Usually, intermolecular forces are discussed together with “*The States of Matter*”. Intermolecular forces also play important roles in solutions. A summary of the interactions is illustrated in the following diagram:



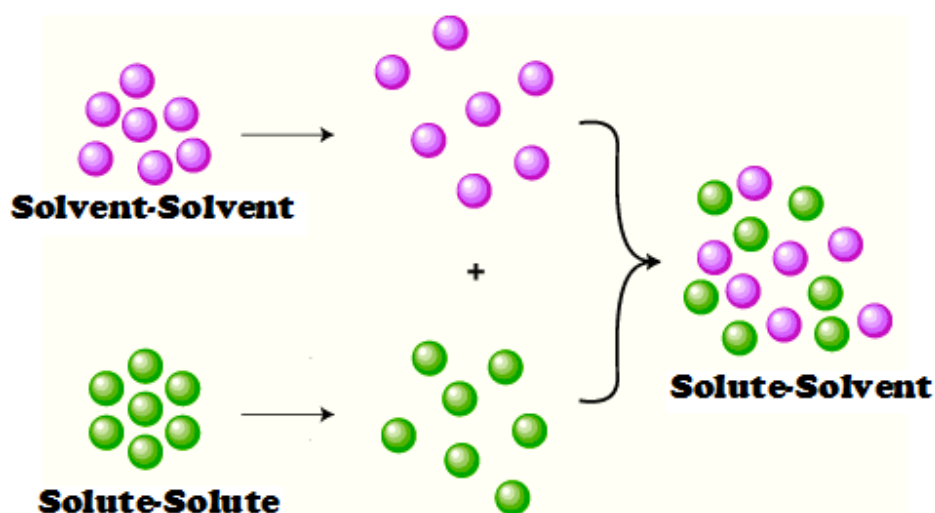
The majority of reactions occurring in solutions are of chemical or biological in nature. It was presumed previously that the solvent only afforded an inert medium for chemical reactions. The significance of ion-solvent interactions was realized after intensive studies in aqueous, non-aqueous and mixed solvents [56,57]. Intermolecular forces are also important in determining the solubility of a substance. "Like" intermolecular forces for solute and solvent will make the solute soluble in the solvent. In this regard ΔH_{soln} is sometimes negative and sometimes positive. Furthermore, solubility is affected by

- (i) Energy of attraction (due Ion-dipole force) affects the solubility.
- (ii) Lattice energy (energy holding the ions together in the lattice).
- (iii) Charge on ions: larger charge means higher lattice energy.
- (iv) Size of the ion: large ions mean smaller lattice energy.

II. 3. 2. INTERACTIONS IN SOLUTION SYSTEMS

There are three types of interactions in the solution systems:

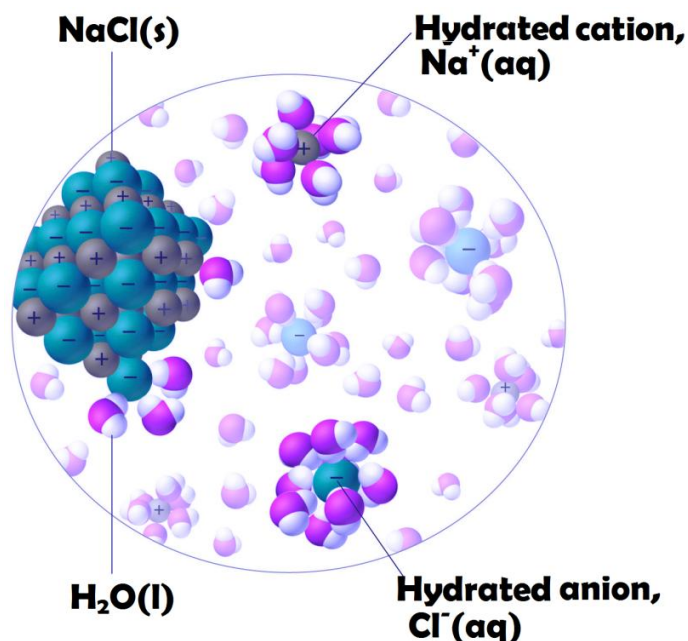
- Solvent-solvent interactions:** energy required to break weak bonds between solvent molecules.
- Solute-solute interactions:** energy required to break intermolecular bonds between the solute molecules.
- Solute-solvent interactions:** ΔH is negative since bonds are formed between them.



For liquid systems, the macroscopic properties are usually quite well known, whereas the microscopic structure is often much less studied. The liquid phase is characterized by local order along with long-range disorder, and to study processes in liquids, it is therefore valuable to use methods that probe the local surrounding of the constituent particles. The same is also correct for solvation processes: a local probe is important to obtain insight into the physical and chemical processes going on.

II. 3. 3. INVESTIGATION ON DIFFERENT KIND OF INTERACTIONS

When salt is dissolved in water, the ions present in the salt dissociate from each other and associate with the dipole of the water molecules. This result in a solution called an '*electrolyte*'.



This means that the forces of interaction (attraction or repulsion) depending on whether like or unlike charges are closer together. On average, dipoles in a liquid orient themselves to form attractive interactions with their neighbours, but thermal motion makes some instantaneous configurations unfavourable.

Therefore, if a crystal salt is put in water, the polar water molecules are attracted to ions on the crystal surfaces. The water molecules steadily surround and isolate the surface ions. The ions become hydrated. They gradually move away from the crystal into solution. This severance of ions from each other is called '*dissociation*'. The surrounding of solute particles by solvent particles is called '*solvation*'. When the ions are dissociated, each ionic species in the solution acts as though it were present alone. Thus, a solution of sodium chloride acts as a solution of sodium ions and chloride ions.

The determination of thermodynamic, transport, acoustic and optical properties of different electrolytes in various solvents would thus provide an important step in this direction. Naturally, in the development of theories, dealing with electrolyte solutions, much interest has been devoted to 'ion-solvent interactions' which are the controlling forces in infinitely dilute solutions where ion-ion interactions are absent. It is possible by separating these functions into ionic contributions to determine the contributions due to cations and anions in the solute-solvent interactions. Thus ion-

solvent interactions play a crucial role to understand the thermophysical, thermodynamic and physicochemical properties of solutions.

One of the causes for the intricacies in solution chemistry is that the structure of the solvent molecule is not known with certainty. The introduction of a solute also modifies the solvent structure to an uncertain magnitude whereas the solute molecule is also modified and the interplay of forces like solute-solute, solute-solvent and solvent-solvent interactions become predominant, though the isolated picture of any of the forces is still not known completely to the solution chemist.

The problems of ion-solvent interactions which are closely akin to ionic solvations can be studied from different angles using almost all the available thermophysical, thermodynamic and physicochemical techniques.

The ion-solvent interactions can also be studied from the thermophysical, and thermodynamic point of view, where the changes of free energy, enthalpy and entropy, etc. associated with a particular reaction. Qualitatively and quantitatively evaluated various thermophysical parameters, from which concluded regarding the factors associated with the ion-solvent interactions occurred in the studied solutions.

Similarly, the ion-solvent interactions can be studied using solvational approaches involving the studies of different properties such as, density, viscosity, ultrasonic speed, refractive index and conductance of electrolytes and various derived parameters, factors associated with ionic solvation.

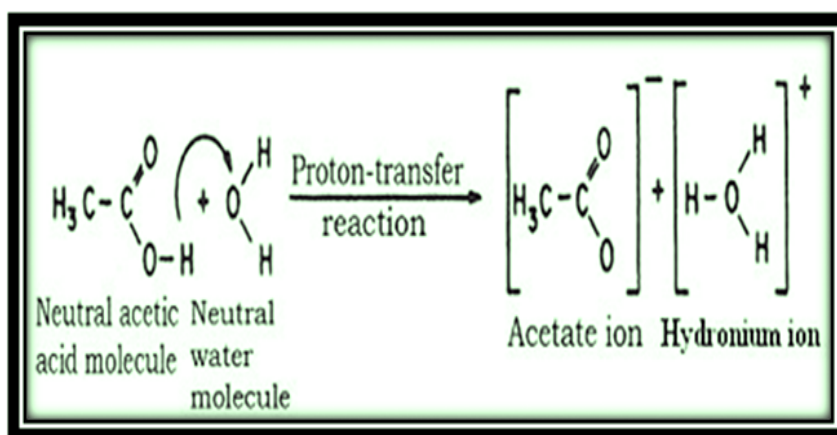
We shall particularly dwell upon the different aspects of these thermophysical, thermodynamic, transports, acoustic and optical properties as the present research work is warmly allied to the studies of ion-ion, ion-solvent and solvent-solvent interactions.

II. 3. 4. ION-SOLVENT INTERACTION

Ion-solvation is a phenomenon of primary interest in many milieu of chemistry because solvated ions are omnipresent on Earth. Hydrated ions occur in aqueous solution in many chemical and biological systems.[58] Solvated ions appear in high concentrations in living organisms, where their presence or absence can essentially alter the functions of life. Ions solvation in organic solvents, mixtures with water and

other organic solvents are awfully common [59]. The exchange of solvent molecules around ions in solutions is fundamental clue to the understanding of the reactivity of ions in solution [60]. Solvated ions also play a key function in electrochemical applications, where for instance the conductivity of electrolytes depends on ion-solvent interactions [61].

The formation of mobile ions in solution is a basic aspect to electrochemistry. There are two distinct ways that mobile ions form in solution to create ionically conducting phases. For example *first one* is illustrated for aqueous acetic acid below.



The chemical method of producing ionic solutions

The *second one* involves dissociation of a solid lattice of ions such as the lattice of sodium chloride. In the ion formation, the solvent colliding with the walls of the crystal gives the ions in the crystal lattice is energetically a better deal than they have within the lattice. It entices them out and into the solution. Thus there is a considerable energy of interaction between the ions and the solvent molecules. These interactions are collectively termed as *ion-solvent interactions*.

Ions orient dipoles. The spherically symmetrical electric field of the ion may tear solvent dipoles out of the solvent lattice and orient them with appropriate charged end toward the central ion. Thus, viewing the ion as a point charge and the solvent molecules as electric dipoles, ion-dipole forces become the principal source of ion-solvent interactions. The majority of reactions occurring in solutions are chemical or biological in nature. It was presumed earlier that the solvent only provides an inert

medium for chemical reactions. The significance of ion-solvent interactions was realized after extensive studies in aqueous, non-aqueous and mixed solvents [62-69].

Most chemical processes of individual and biological importance occur in solution. The role of solvent is so great that million fold rate changes take place in some reactions simply by changing the reaction medium. Our bodies contain 65 to 70% water, which acts as a lubricant, as an aid to digestion and more specifically as a stabilizing factor to the double helix conformations of DNA. With the exceptions of heterogeneous catalytic reactions most reactions in technical importance occur in solutions. In addition, molecules not only have to travel through a solvent to their reaction partner before reacting, but also need to present a sufficiently unsolvated rate for collision. The solvent governs the movement and energy of the reacting species to such an extent that a reaction undergoes a several-million fold change in rate when the solvent is changed. As water is the most abundant solvent in nature and its major importance to chemistry, biology, agriculture, geology, etc., water has been broadly used in kinetic and equilibrium studies. But still our knowledge of molecular interactions in water is extremely limited.

Moreover, the uniqueness of water as a solvent has been questioned [70,71] and it has been realized that the studies of other solvent media like non aqueous and mixed solvents would be of great help in understanding different molecular interactions and a host of complicated phenomena. The organic solvents have been classified on the basis of dielectric constants, organic group types, acid base properties, or association through hydrogen bonding [58] donor-acceptor properties [72,73] hard and soft acid-base principles [74] etc. As a result, the different solvents show a wide change in properties, ultimately influencing their thermophysical, thermodynamic, transport and acoustic properties qualitatively and quantitatively, in presence of electrolytes and non-electrolytes in these solvents. The determination of thermophysical, thermodynamic, transport and acoustic properties for various electrolytes or non-electrolytes in a variety of solvents would thus provide important information in this direction. Henceforth, in the development of theories of electrolytic solutions, much attention has been devoted to the controlling forces '*ion-solvent interactions*' in infinitely dilute solutions wherein ion-ion interactions are almost absent. By separating these functions

into ionic contributions, it is possible to determine the contributions of cations and anions in the ion-solvent interactions. One of the causes for the intricacies in solution chemistry is the uncertainty about the structure of the solvent molecules in solution. The introduction of a solute modifies the solvent structure to an uncertain magnitude, the solvent molecule and the interplay of forces like solute-solute, solute-solvent also modify the solute molecule and solvent-solvent interactions become predominant, though the isolated picture of any of the forces is still not known completely to the solution chemist.

Qualitative analysis of ion-solvent interactions can be studied by FTIR spectrometry [75,76]. The spectral solvent shifts or the chemical shifts can determine the qualitative and quantitative nature of ion-solvent interactions. But even qualitative or quantitative apportioning of the ion-solvent interactions into the various possible factors is still an uphill task. It is thus apparent that the real understanding of the ion-solvent interaction is a difficult task. The aspect embraces a wide range of topics but we concentrated only on the measurement of transport properties like viscosity, conductance etc; thermophysical, thermodynamic properties as apparent or partial molar volumes, apparent molar adiabatic compressibility, and spectral properties as FT-IR spectroscopy etc.

II. 3. 5. ION-ION INTERACTION:

Ion-solvent interactions are only a part of the story of an ion related to its environment. The surrounding of an ion sees only other ions, no solvent molecules. The mutual interactions between these ions represent the essential part '*ion-ion interactions*'. The degree of ion-ion interactions affects the properties of solution and depends on the nature of electrolyte under exploration. Ion-ion interactions, in general, are stronger than ion-solvent interactions. Ion-ion interaction in dilute electrolytic solutions is now theoretically well understood, but ion-solvent communications or ion-solvation still remains a complex process. While proton transfer reactions are particularly sensitive to the nature of the solvent, it has become cleared that the solvents extensively modify the majority of the solutes. Conversely, the nature of the strongly structured solvents, such as water, is substantially modified by the presence of

solutes. Comprehensive understanding of the phenomena of solution chemistry will become a reality only when solute-solute/ion-ion, solute-solvent/ ion-solvent and solvent-solvent interactions are elucidated. And thus the present thesis is affectionately related to the studies of solute-solute/ion-ion, solute-solvent/ ion-solvent and solvent-solvent interactions in some liquid systems.

II. 3. 6. SOLVENT-SOLVENT INTERACTIONS (THEORY OF MIXED SOLVENTS)

As the mixed and non-aqueous solvents are increasingly used in chromatography, solvent extraction, in the elucidation of reaction mechanism, in preparing high density batteries, etc. a number of molecular theories, based on either the radial distribution function or the choice of suitable physical model, have been developed for mixed solvents. L. Jones and Devonshire [77] were first to evaluate the thermodynamic functions for a single fluid in terms of interchange energy parameters. They used "Free volume" or "Cell model". Prigogine and Garikian [78] extended the above approach to solvent mixtures. Prigogine and Bellemans [79] developed a two fluid version of the cell model. They found that while excess molar volume (V^E) was negative for mixtures with molecules of almost same size, it was large positive for mixtures with molecules having small difference in their molecular sizes. Treszczanowicz *et. al.* [80] suggested that V^E is the result of several contributions from several opposing effects. These may be divided arbitrarily into three types, viz., physical, chemical and structural.

Physical contributions contribute a positive term to V^E . The chemical or specific intermolecular interactions result in a volume decrease and contribute negative values to V^E . The structural contributions are typically negative and arise from several effects, especially from interstitial accommodation and changes in the free volume. The actual volume change would therefore depend on the relative strength of these effects. However, it is generally assumed that when V^E is negative, viscosity deviation ($\Delta\eta$) may be positive and vice-versa. This assumption is not a concrete one, as evident from some studies [81,82]. Rastogi *et al.* [83] therefore suggested that the observed excess property is a combination of an interaction and non-interaction part. The non-

interaction part in the form of size effect can be comparable to the interface part and may be sufficient to reverse the trend set by the latter. Pitzer [84], L. Huggins [85] introduced a new approach in his theory of conformal solutions. Using a simple perturbation approach, he showed that the properties of mixtures could be obtained from the knowledge of intermolecular forces and thermophysical and thermodynamic properties of the pure components.

Rowlinson *et al.* [86-88] reformulated the average rules for Vander Waal's mixtures and their calculated values were in much better agreement with the experimental values even when one fluid theory was applied. The more recent independent effort is the perturbation theory of Baker and Henderson [89]. A more successful approach is due to Flory who made the use of certain features of cell theory [90-92] and developed a statistical theory for predicting the excess properties of binary mixtures by using the equation of state and the properties of pure components along with some adjustable parameters. This theory is applicable to mixtures containing components with molecules of different shapes and sizes. Patterson and Dilamas [93] combined both Prigogine and Flory theories to a unified one for rationalizing various contributions of free volume, internal pressure, etc. to the excess thermodynamic properties. Heintz [94-96] and coworkers suggested a theoretical model based on a statistical mechanical derivation and accounts for self-association and cross association in hydrogen bonded solvent mixtures is termed as Extended Real Associated Solution model (ERAS). It combines the effect of association with non-associative intermolecular interaction occurring in solvent mixtures based on equation of state developed originally by Flory. Subsequently the ERAS model has been successfully applied by many workers [97-99] to describe the excess thermodynamic properties of alkanol-amine mixtures. A new symmetrical reformation on the Extended Real Association (ERAS) model has been described in the literature [100]. The symmetrical-ERAS (S-ERAS) model makes it possible to describe excess molar enthalpies and excess molar volumes of binary mixtures containing very similar compounds described by extremely small mixing functions [101]. Gepert *et al.* [102] applied this model for studying some binary systems containing alcohols.

II. 4. DENSITY

The thermophysical properties of liquid mixtures have attracted much interest from both theoretical and engineering applications points of view. Many engineering applications require quantitative data on the density of liquid systems. They also provide information about the nature and molecular interactions between electrolyte or non-electrolyte and liquid components.

The volumetric property '*Density*' is a function of weight, volume and mole fraction and excess volumes of mixing. One of the well-recognized approaches to the study of molecular interactions in fluids is the use of thermophysical, thermodynamic methods. Thermophysical properties are generally convenient parameters for interpreting solute-solvent/ion-solvent and ion-ion/solute-solute interactions occurring in the solution phase. Fundamental properties such as enthalpy, entropy and Gibbs energy represent the macroscopic state of the system as an average of numerous microscopic states at a given temperature and pressure. An interpretation of these macroscopic properties in terms of molecular phenomena is generally difficult. Sometimes higher derivatives of these properties can be interpreted more effectively in terms of molecular interactions. The volumetric information may be of immense importance in this regard. Various concepts regarding molecular interaction in solutions is electrostriction, [103] hydrophobic hydration, [104] micellization, [105] and co-sphere overlap during ion-solvent/solute-solvent interactions [106] have been derived and interpreted from the partial molar volume data for electrolytes and non-electrolytes.

II. 4. 1. APPARENT AND PARTIAL MOLAR VOLUMES

Density data can be used for the calculation of molar volume of a pure substance. In complex multi-component systems such as solutions, it is easier to describe a system in terms of the intrinsic or molal properties rather than the extensive properties. Any extensive property of a system can be calculated as the sum of the respective partial molal properties if all components have a known concentration.

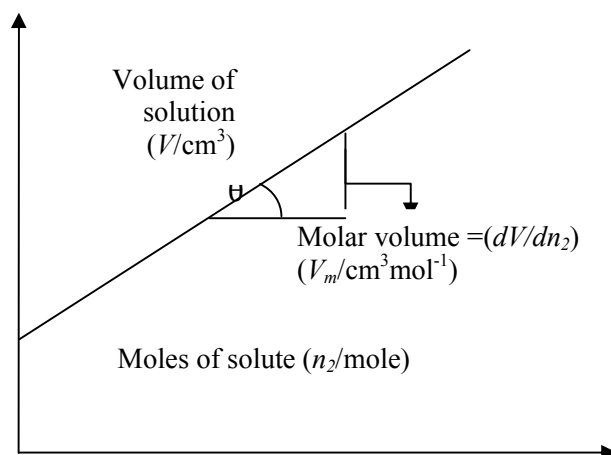


Figure 7: A diagram for the explanation of molal volume

The easiest way to explain this is in terms of the molal volume, V_m , shown in the Figure 7, where the volume increases with respect to the amount of solute added. A dissolved solute has its own property, referred to as partial molal property.

Therefore for a two component system, where one component is the solvent and the other is solute, the total volume of the system can be represented as the sum of the partial molal volumes of the solvent, \bar{V}_1 , and the solute, \bar{V}_2 :

$$V = n_1 \bar{V}_1 + n_2 \bar{V}_2 \quad (\text{II. 1c})$$

Dividing Eq. (II. 1c) by $n_1 + n_2$, the molal volume of the solution is obtained as:

$$V_m = x_1 \bar{V}_1 + x_2 \bar{V}_2 \quad (\text{II. 1d})$$

where, x_1 and x_2 represent the mole fraction of the solvent and the solute, respectively. The partial molal property of a solute is defined as the change in the total property of the system with respect to the change in the number of moles of solute added, with all other variables (T , P , and the amount of the solvent) are held constant. An alternative, widely used property of the solute is the apparent molal property. The apparent molal volume is the volume that should be attributed to the solute in solution if it is assumed that the solvent contributes the exact volume it would if it was in its pure state.

Under this assumption, the apparent molal volume of the solute, $\phi_{2,V}$, as defined by Harned and Owen, is the difference between the total volume (or the total molal volume) and the partial molal volume of the pure solvent (\bar{V}_1^0) divided by the number of moles (or the mole fraction) of the solute present:

$$\phi_{2,V} = \frac{V - n_1 \bar{V}_1^0}{n_2} \quad (\text{II. 1e})$$

$$\phi_{2,V} = \frac{V_m - x_1 \bar{V}_1^0}{x_2} \quad (\text{II. 1f})$$

In experimentation, \bar{V}_1^0 is generally considered to be constant over the range of solute concentration at constant temperature and pressure. Hence, $\phi_{2,V}$, can be easily calculated using Eq. (II. 1e) or (II. 1f) when the total volume or molal volume is known. Eq. (II. 1e) can be modified in order to find out the apparent molal volume of a solute using density of the solution containing the solute and the density of the pure solvent, ρ and ρ_0 , respectively. Assuming there is 1 kilogram (kg) of solvent:

$$n_1 = \frac{1}{M_1}, \quad \text{therefore,} \quad V = \frac{\bar{V}_1^0}{M_1} + m_2 \cdot \phi_{2,V} \quad (\text{II. 1g})$$

where, M_1 is the molal mass of the solvent.

Since $\rho_1 = \frac{\bar{V}_1^0}{M_1}$, Eq. (II. 1g) becomes:

$$V = \frac{1}{\rho_1} + m_2 \cdot \phi_{2,V} \quad (\text{II. 1h})$$

where, m_2 is the molality of the solute (which is equivalent to n_1 if 1kg of solvent is present). The entire mass of the solution will be composed of the mass of the solvent (1kg) and the mass of the solute ($m_2 \cdot M_2$). Since volume is the ratio of mass to density, the equation for V becomes:

$$\frac{1 + m_2 \cdot M_2}{\rho_1} = \frac{1}{\rho_1} + m_2 \cdot \phi_{2,V} \quad (\text{II. 1i})$$

By rearranging this Eq. (II. 1h) and solving for $\phi_{2,V}$, an equation for apparent molal volume for 1 kg of the solute is obtained:

$$\phi_{2,V} = \frac{\rho_2 - \rho_1}{m_2 \rho_1 \rho_2} + \frac{M_2}{\rho_2} \quad (\text{II. 1j})$$

However, the volume contributed to a solvent by the addition of one mole of an ion is difficult to determine. This is so because, upon entry into the solvent, the ions change the volume of the solution due to a breakup of the solvent structure near the

ions and the compression of the solvent under the influence of the ion's electric field, i.e., *electrostriction*. Electrostriction is a general phenomenon and whenever there are electric fields of the order of 10^9 - 10^{10} V·m⁻¹, the compression of ions and molecules is likely to be significant. The effective volume of an ion in solution, the partial molar volume, can be determined from a directly obtainable quantity apparent molar volume (ϕ_V). Thus the apparent molar volumes of the solutes can be calculated by using the following relation; [107]

$$\phi_V = \frac{M}{\rho_0} - \frac{1000(\rho - \rho_0)}{c\rho_0} \quad (\text{II.1k})$$

or

$$\phi_V = \frac{M}{\rho} - \frac{1000(\rho - \rho_0)}{m\rho\rho_0} \quad (\text{II.1l})$$

where M is the molar mass of the solute, c is the molarity, m is the molality of the solution; ρ_0 and ρ are the densities of the solvent and the solution respectively. The partial molar volumes, ϕ_{2V} can be obtained from the equation; [108]

$$\phi_{2V} = \phi_V + \frac{(1000 - c\phi_V)}{2000 + c^{3/2} \left(\frac{\partial \phi_V}{\partial \sqrt{c}} \right)} c^{1/2} \left(\frac{\partial \phi_V}{\partial \sqrt{c}} \right) \quad (\text{II. 2})$$

The extrapolation of the apparent molar volume of electrolyte to infinite dilution and the expression of the concentration dependence of the apparent molar volume have been made by four major equations over a period of years – the Masson equation, [109] the Redlich-Meyer equation, [110] the Owen-Brinkley equation, [111] and the Pitzer equation [81]. Masson found that the apparent molar volume of electrolyte, ϕ_V , vary with the square root of the molar concentration by the linear equation:

$$\phi_V = \phi_V^0 + S_V^* \sqrt{c} \quad (\text{II. 3a})$$

$$\phi_V = \phi_V^0 + S_V^* \sqrt{m} \quad (\text{II. 3b})$$

where, ϕ_V^0 is the apparent molar volume (equal to the partial molar volume) at infinite dilution and S_V^* the experimental slope. The majority of ϕ_V data in water [112] and nearly all ϕ_V data in non-aqueous [113-117] solvents have been extrapolated to infinite dilution through the use of equation (II. 3a) or (II.3b).

The temperature dependence of ϕ_V^0 or various investigated electrolytes in various solvents can be expressed by the general equation as follows:

$$\phi_V^0 = a_0 + a_1T + a_2T^2 + \dots \quad (\text{II. 4})$$

where a_0 , a_1 , a_2 are the coefficients of a particular electrolyte and T is the temperature in Kelvin.

The limiting apparent molar expansibilities (ϕ_E^0) can be obtained by the following equation:

$$\phi_E^0 = \left(\delta \phi_V^0 / \delta T \right)_P = a_1 + 2a_2T \quad (\text{II. 5})$$

The limiting apparent molar expansibilities (ϕ_E^0) change in magnitude with the change of temperature. During the past few years it has been emphasized by a number of workers that S_V^* is not the sole criterion for determining the structure-making or breaking tendency of any solute. Helper [118] developed a technique of examining the sign of $\left(\delta \phi_E^0 / \delta T \right)_P$ for the solute in terms of long-range structure-making and breaking capacity of the electrolytes in the mixed solvent systems. The general thermodynamic expression used is as follows:

$$\left(\delta \phi_E^0 / \delta T \right)_P = \left(\delta^2 \phi_V^0 / \delta T^2 \right)_P = 2a_2 \quad (\text{II. 6})$$

If the sign of $\left(\delta \phi_E^0 / \delta T \right)_P$ is positive or small negative the electrolyte is act as structure maker and when the sign of $\left(\delta \phi_E^0 / \delta T \right)_P$ is negative, it is a structure breaker. Redlich and Meyer [110] have shown that an equation (II. 3a) or (II. 3b) cannot be any more than a limiting law where for a given solvent and temperature, the slope S_V^* should depend only upon the valence type. They suggested the equation:

$$\phi_v = \phi_v^0 + S_v \sqrt{c} + b_v c \quad (\text{II. 7})$$

$$\text{where } S_v = Kw^{3/2} \quad (\text{II. 8})$$

S_v is the theoretical slope, based on molar concentration, including the valence factor where

$$w = 0.5 \sum_i^j Y_i Z_i^2 \quad (\text{II. 9})$$

$$\text{and } K = N^2 e^2 \left(\frac{8\pi}{1000 \epsilon^3 RT} \right)^{1/2} \left[\left(\frac{\partial \ln \epsilon}{\partial p} \right)_T - \frac{\beta}{3} \right] \quad (\text{II. 10})$$

In equation (II. 10), K is the compressibility of the solvent and the other terms have their usual significance.

The Redlich-Meyer's extrapolation equation [110] adequately represents the concentration dependence of many 1:1 and 2:1 electrolytes in dilute solutions; however, studies [110-122] on some 2:1, 3:1 and 4:1 electrolytes show deviations from this equation. Thus, for polyvalent electrolytes, the more appropriate Owen-Brinkley equation [111] can be used to aid in the extrapolation to infinite dilution and to adequately represent the concentration dependency of ϕ_v . The Owen-Brinkley equation [111] which includes the ion-size parameter, ' a ' (cm), is given by:

$$\phi_v = \phi_v^0 + S_v \tau (\kappa a) \sqrt{c} + 0.5 w_v \theta (\kappa a) c + 0.5 K_v c \quad (\text{II. 11})$$

where the symbols have their usual significance. However, this equation is not widely used for non-aqueous solutions.

Recently, the Pitzer formalism has been used by Pogue and Atkinson [124] to fit the apparent molal volume data. The Pitzer equation for the apparent molar volume of a single salt $M \gamma_X$ is :

$$\phi_v = \phi_v^0 + V |Z_M Z_X| A_v |2b \ln \left(I + bI^{1/2} \right) + 2\gamma_M \gamma_X RT \left[m B_{MX}^2 + m^2 (\gamma_M \gamma_X)^{1/2} C_{MX}^v \right] \quad (\text{II. 12})$$

where the symbols have their usual significance.

II. 4. 2. LIMITING IONIC PARTIAL MOLAR VOLUMES

The individual partial ionic volumes provide information relevant to the general question of the structure near the ion, i.e., its solvation. The calculation of the ionic limiting partial molar volumes in organic solvents is, however, a difficult one. At present, however, most of the existing ionic limiting partial molar volumes in organic solvents were obtained by the application of methods originally developed for aqueous solutions to non aqueous electrolyte solutions. In the last few years, the method suggested by Conway *et al.* [123] has been used more frequently. The authors used the method to determine the limiting partial molar volumes of the anion for a series of homologous tetra-alkyl ammonium chlorides, bromides and iodides in aqueous solution. They plotted the limiting partial molar volume ϕ_{V, R_4NX}^0 , for a series of these salts with a halide ion in common as a function of the formula weight of the cation, $M_{R_4N^+}$ and obtained straight-lines for each series. Therefore, they suggested the following equation:

$$\phi_{V, R_4NX}^0 = bM_{R_4N^+} + \phi_{V, X^-}^0 \quad (\text{II. 13})$$

The extrapolation to zero cationic formula weight gave the limiting partial molar volumes of the halide ions ϕ_{V, X^-}^0 . Uosaki *et al.* [124] used this method for the separation of some literature values and of their own ϕ_{V, R_4NX}^0 values into ionic contributions in organic electrolyte solutions. Krumgalz [125] applied the same method to a large number of partial molar volume data for non-aqueous electrolyte solutions in a wide temperature range.

II. 4. 3. EXCESS MOLAR VOLUMES

The excess molar volumes, V^E are calculated from the molar masses M_i and the densities of pure liquids and the mixtures according to the following equation; [126,127]

$$V^E = \sum_{i=1}^n x_i M_i \left(\frac{1}{\rho} - \frac{1}{\rho_i} \right) \quad (\text{II. 14})$$

where ρ_i and ρ are the density of the i^{th} component and density of the solution mixture respectively. V^E is the resultant of contributions from several

opposing effects. These may be divided arbitrarily into three types, viz. chemical, physical and structural. Physical contributions, which are nonspecific interactions between the real species present in the mixture, contribute a positive term to V^E . The chemical or specific intermolecular interactions result in a volume decrease, thereby contributing negative V^E values. The structural contributions are mostly negative and occur from several effects, especially from interstitial accommodation and changes of free volume [66]. These phenomena are the results of difference in energies of interface between molecules being in solutions and packing effects. Disruption of the ordered structure of pure constituent during formation of the mixture leads to a positive effect observed on excess volume while an order formation in the mixture leads to negative contribution.

II. 5. VISCOSITY

As fundamental and significant property of liquids is *viscosity*, provide a lot of information on the structures and molecular interactions in liquid systems. Viscosity and volume are different types of properties of one liquid, and there is a certain relationship between them. So by measuring and studying them together, relatively more realistic and comprehensive information could be expected to be gained. The viscometric information includes 'Viscosity' as a function of composition on the basis of weight, volume and mole fraction; comparison of experimental viscosities with those calculated with several equations and excess Gibbs free energy of viscous flow. Viscosity, one of the most important transport properties is used for the determination of ion-solvent interactions and studied extensively [128-129]. It is not a thermodynamic quantity, but of an electrolytic solution along with the thermophysical property, the partial molar volume $\phi_{v,2}^0$, gives a lot of information and insight regarding ion-solvent interactions and the nature of structures in the electrolytic solutions.

II. 5. 1. VISCOSITY OF PURE LIQUIDS AND LIQUID MIXTURES

Since the molecular motion in liquids is controlled by the influence of the neighbouring molecules, the transport of momentum in liquids takes place, in sharp contrast with gases at ordinary pressures, not by the actual movement of molecules but

by the intense influence of intermolecular force fields. It is this aspect of the mechanism of momentum transfer which forms the basis of the procedures for predicting the variations in the viscosity of liquids and liquid systems.

II. 5. 2. EARLY THEORETICAL CONSIDERATIONS ON LIQUID VISCOSITY

The theoretical development of liquid viscosity in early stages has been reviewed Andrade [130] and Frenkel [131]. By considering the forces of collision to be the only important factor and assuming that at the melting point, the frequency of vibration is equal to that in the solid state and that one-third of the molecules are vibrating along each of the three directions normal to one another. Andrade [130] developed equations which checked well against data on mono atomic metals at the melting point. Frenkel [131] considered the molecules of a liquid to be spheres moving with an average velocity with respect to the surrounding medium and using Stokes' law and Einstein's relation for self diffusion-coefficient, arrived at a complicated expression for liquid viscosity with only limited applicability. Furth [132] assumed the momentum transfer to take place by the irregular Brownian movement of the holes [133] which were linked to clusters in a gas and thus, in analogy with the gas theory of viscosity and with assumption of the equipartition law of energy, showed that for liquids:

$$\eta = 0.915 \frac{R_g T}{V} \left(\frac{M}{\sigma} \right) e^{\frac{A}{R_g T}} \quad (\text{II. 15})$$

where η , V and M are viscosity, volume and mass, respectively, T is the temperature, R_g is the universal gas constant, σ is the surface tension and A is the work function at the melting point. He compared his theory with experiment as well as with the theories of Andrade [131] and Ewell & Eyring, [134] Auluck, De & Kothari [135] further modified the theory and successfully explained the variations of the viscosity with pressure. A critical review of these simple theories and their abilities to explain momentum transport in liquids is given by Eisenschitz [136].

II. 5. 3. THE CELL LATTICE THEORY AND LIQUID VISCOSITY

A model related to in the literature by various names such as cell, lattice, cage, free volume or one particle model was introduced by Lennard- Jones and Devonshire

[137-138] and further expanded by Pople [139]. Eizenschitz employing this model developed a theory of viscosity by considering the motion of the representative molecules to be Brownian and their distribution according to the Smoluchowski equation. Even with certain assumptions, the final expression showed shortcomings most of which were later overcome in a subsequent publication [140].

II. 5. 4. STATISTICAL MECHANICAL APPROACH TO LIQUID VISCOSITY

The distribution functions for the liquid molecules were obtained on the basis of statistical mechanical theory mainly by the efforts of Kirkwood[141,142] Mayer and Montroll, [143] Mayer, [144] Born and Green [145] and the considerations on the basis of the general kinetic theory led Born and Green [145,146] to develop a viscosity equation which provided explanation for several empirical equations [129,130,132] proposed for liquid viscosity. In this connection the theoretical contributions of Kirkwood and coworkers [133,147-153] Zwanzig *et al.*, [154] Rice and coworkers [155-158] Longuet- Higgins and Valteau [159] and Davis and Coworkers [160-161] are worth mentioning.

II. 5. 5. PRINCIPLE OF CORRESPONDING STATES AND LIQUID VISCOSITY

The principle of the corresponding states has been applied to liquids in the same way as to gases [162] the basic assumption being that the intermolecular potential between two molecules is a universal function of the reduced intermolecular separation. This assumption is a good approximation for spherically symmetric mono atomic non-polar molecules. In general, more parameters are introduced in the corresponding state correlations on somewhat empirical grounds in the hope that such modification in some way compensates the shortcomings of the above stated assumption. In this connection the studies by Rogers and Brickwedde, [163] Boon and Thomaes [164-166] Boon, Legros and Thomaes, [167] and Hollman and Hijmans [168] are worth mentioning.

II. 5. 6. THE REACTION RATE THEORY FOR VISCOUS FLOW

Considering viscous flow as a chemical reaction in which a molecule moving in a plane occasionally acquires the activation energy necessary to slip over the potential barrier to the next equilibrium position in the same plane. Eyring [169] showed that the viscosity of the liquid is given by:

$$\eta = \frac{\lambda_1 h F_n}{\kappa \lambda^2 \lambda_2 \lambda_3 F_a^*} \exp \frac{\Delta E_{act}}{kT} \quad (\text{II. 16})$$

where λ is the average distance between the equilibrium positions in the direction of motion, λ_1 is the perpendicular distance between two neighbouring layers of molecules in relative motion, λ_2 is the distance between neighbouring molecules in the same direction and λ_3 is the distance from molecule to molecule in the plane normal to the direction of motion. The transmission coefficient (κ) is the measure of the chance that a molecule having once crossed the potential barrier will react and not recross in the reverse direction, F_n is the partition function of the normal molecules, F_a^* that of the activated molecule with a degree of freedom corresponding to flow, ΔE_{act} is the energy of activation for the flow process, h is Planck's constant and k is Boltzmann constant. Ewell and Eyring argued that for a molecule to flow into a hole, it is not necessary that the latter be of the same size as the molecule. Consequently they assume that ΔE_{act} is a function of ΔE_{vap} for viscous flow because ΔE_{vap} is the energy required to make a hole in the liquid of the size of a molecule. Utilizing the idea and criteria, certain relations [134,170] finally gets

$$\eta = \frac{N_A h (2\pi m kT)^{\frac{1}{2}}}{Vh} \frac{bRTV^{\frac{1}{3}}}{N_A^{\frac{1}{3}} \Delta E_{vap}} \exp \frac{\Delta E_{vap}}{nRT} \quad (\text{II. 17})$$

where n and b are constant. It was found that the theory could reproduce the trend in temperature dependence of η but the computed values are greater than the observed values by a factor of 2 or 3 for most liquids. Kincaid, Eyring and Stearn [171] have summarized all the working relations.

II. 5. 7. THE SIGNIFICANT STRUCTURAL THEORY AND LIQUID VISCOSITY

Eyring and coworkers [172-175] improved the “holes in solid” model theory [171-176] to picture the liquid state by identifying three significant structures. In brief, a molecule has solid like properties for the short time it vibrates about an equilibrium position and then it assumes instantly the gas like behaviour on jumping into the neighbouring vacancy. The above idea of significant structures leads to the following relation for the viscosity of liquid; [177,178]

$$\eta = \frac{V_s}{V} \eta_s + \frac{V - V_s}{V} \eta_g \quad (\text{II. 18})$$

where V_s is the molar volume of the solid at the melting point and V is the molar volume of the liquid at the temperature of interest while η_s and η_g are the viscosity contributions from the solid-like and gas-like degrees of freedom, respectively. The expressions for η_s and η_g are given by Carlson, Eyring and Ree. [178] Eyring and Ree [179] have discussed in detail the evaluation of η_s from the reaction rate theory of Eyring [179] assuming that a solid molecule can jump into all neighbouring empty sites. The expression for η_s takes the following form; [170]

$$\eta = \frac{N_A h}{Z_K} \left(\frac{V}{V_s} \right) \frac{6}{2^2} \left(\frac{1}{V - V_s} \right) \frac{1}{(1 - e)^{\frac{\theta}{T}}} \exp \left(\frac{a E_s V_s}{(V - V_s) RT} \right) \quad (\text{II. 19})$$

where N_A is Avogadro's number, Z is the number of nearest neighbours, θ is the Einstein characteristic temperature, E_s is the energy of sublimation and a' is the proportionality constant. On the other hand, the term η_g is obtained from the kinetic theory of gases [180] by the relation:

$$\eta_g = \frac{2}{3 d^2} \left(\frac{M k T}{\pi^3} \right)^{\frac{1}{2}} \quad (\text{II. 20})$$

where d is the molecular diameter and M is the molecular mass.

II. 5. 8. VISCOSITY OF ELECTROLYTIC SOLUTIONS

The viscosity relationships of electrolytic solutions are highly complicated. Because ion-ion and ion-solvent interactions are occurring in the solution and separation of the related forces is a difficult task. But, from careful analysis, vivid and valid conclusions can be drawn regarding the structure and the nature of the solvation of the particular system. As viscosity is a measure of the friction between adjacent, relatively moving parallel planes of the liquid, anything that increases or decreases the interaction between the planes will raise or lower the friction and thus, increase or decrease the viscosity. If large spheres are placed in the liquid, the planes will be keyed together in increasing the viscosity. Similarly, increase in the average degree of hydrogen bonding between the planes will increase the friction between the planes, thereby viscosity. An ion with a large rigid co-sphere for a structure-promoting ion will behave as a rigid sphere placed in the liquid and increase the inter-planar friction. Similarly, an ion increasing the degree of hydrogen bonding or the degree of correlation among the adjacent solvent molecules will increase the viscosity. Conversely, ions destroying correlation would decrease the viscosity. In 1905, Grüneisen [181] performed the first systematic measurement of viscosities of a number of electrolytic solutions over a wide range of concentrations. He noted non-linearity and negative curvature in the viscosity concentration curves irrespective of low or high concentrations. In 1929, Jones and Dole [182] suggested an empirical equation quantitatively correlating the relative viscosities of the electrolytes with molar concentrations (c):

$$\frac{\eta}{\eta_o} = \eta_r = 1 + A\sqrt{c} + Bc \quad (\text{II. 21})$$

The above equation can be rearranged as:

$$\frac{\eta_r - 1}{\sqrt{c}} = A + B\sqrt{c} \quad (\text{II. 22})$$

where A and B are constants specific to ion-ion and ion-solvent interactions. The equation is applicable equally to aqueous and non aqueous solvent systems where there is no ionic association and has been used extensively. The term $A\sqrt{c}$, originally ascribed to Grüneisen effect, arose from the long-range coulombic forces between the ions. The

significance of the term had since then been realized due to the development Debye-Hückel theory [183] of inter-ionic attractions in 1923. The A -coefficient depends on the ion-ion interactions and can be calculated from interionic attraction theory [184-186] and is given by the Falkenhagen Vernon [186] equation:

$$A_{Theo} = \frac{0.2577 A_o}{\eta_o (\epsilon T)^{0.5} \lambda_+^o \lambda_-^o} \left[1 - 0.6863 \left(\frac{\lambda_+^o \lambda_-^o}{A_o} \right)^2 \right] \quad (\text{II. 23})$$

where the symbols have their usual significance. In very accurate work on aqueous solutions, [187] A -coefficient has been obtained by fitting η_r to equation (II. 22) and compared with the values calculated from equation (II. 23), the agreement was excellent. The accuracy achieved with partially aqueous solutions was however poorer [188]. A -coefficient suggesting that should be calculated from conductivity measurements. Crudden *et al.* [189] suggested that if association of the ions occurs to form an ion pair, the viscosity should be changed and thus analysed by the equation:

$$\frac{\eta_r - 1 - A\sqrt{\alpha c}}{\alpha c} = B_i + B_p \left(\frac{1 - \alpha}{\alpha} \right) \quad (\text{II. 24})$$

where A , B_i and B_p are characteristic constants and α is the degree of dissociation of ion-pair. Thus, a plot of $\frac{\eta_r - 1 - A\sqrt{\alpha c}}{\alpha c}$ vs $\left(\frac{1 - \alpha}{\alpha} \right)$, when extrapolated to $\left(\frac{1 - \alpha}{\alpha} \right) = 0$ give the intercept B_i . However, for the most of the electrolytic solutions both aqueous and non-aqueous, the equation (II. 22) is valid up to 0.1 (M) [190-191] within experimental errors. At higher concentrations the extended Jones-Dole equation (II. 25), involving an additional coefficient D , originally used by Kaminsky, [192] has been used by several workers [193,194] and is given below:

$$\frac{\eta}{\eta_o} = \eta_r = 1 + A\sqrt{c} + Bc + Dc^2 \quad (\text{II. 25})$$

The coefficient D cannot be evaluated properly and the significance of the constant is also not always meaningful and therefore, equation (II. 22) is used by the most of the workers.

The plots of $\frac{(\eta/\eta_o - 1)}{\sqrt{c}}$ against \sqrt{c} for the electrolytes should give the value of A -coefficient. But sometimes, the values come out to be negative or considerably scatter

and also deviation from linearity occur [191,195,196]. Thus, instead of determining A -coefficient from the plots or by the least square method, the A -coefficient are generally calculated using Falkenhagen-Vernon equation (II. 23). A -coefficient should be zero for non-electrolytes. According to Jones and Dole, the A -coefficient probably represents the stiffening effect on the solution of the electric forces between the ions, which tend to maintain a space-lattice structure [182]. The B -coefficient may be either positive or negative and it is actually the ion-solvent interaction parameter. It is conditioned by the ions and the solvent and cannot be calculated a priori. The B -coefficients are obtained as slopes of the straight lines using the least square method and intercepts equal to the A -coefficient.

The factors influencing B -coefficients are: [197,198]

- (a) The effect of ionic solvation and the action of the field of the ion in producing long-range order in solvent molecules, increase η or B -value.
- (b) The destruction of the three dimensional structure of solvent molecules (i.e., structure breaking effect or depolymeriation effect) decreases η values.
- (c) High molal volume and low dielectric constant, which yield high B -values for similar solvents.
- (d) Reduced B -values are obtained when the primary solvation of ions is sterically hindered in high molal volume solvents or if either ion of a binary electrolyte cannot be specifically solvated.

II. 5. 9. VISCOSITIES AT HIGHER CONCENTRATION

It had been found that the viscosity at high concentrations (1 M to saturation) can be represented by the empirical formula suggested by Andrade:

$$\eta = A \exp \frac{b}{T} \quad (\text{II. 26})$$

The several alternative formulations have been proposed for representing the results of viscosity measurements in the high concentration range [197-204] and the equation suggested by Angell [205,206] based on an extension of the free volume theory of transport phenomena in liquids and fused salts to ionic solutions is particularly noteworthy. The equation is:

$$\frac{1}{\eta} = A \exp \left[-\frac{K_1}{N_o - N} \right] \quad (\text{II. 27})$$

where N represents the concentration of the salt in $\text{eqv}\cdot\text{litre}^{-1}$, A and K_1 are constants supposed to be independent of the salt composition and N_o is the hypothetical concentration at which the system becomes glass. The equation was recast by Majumder *et al.* [207-209] introducing the limiting condition, that is $N \rightarrow 0$, $\eta \rightarrow \eta_o$; which is the viscosity of the pure solvent. Thus, we have:

$$\ln \frac{\eta}{\eta_o} = \ln \eta_{Rel} = \left(\frac{K_1}{N_o} \right) \frac{N}{(N_o - N)} \quad (\text{II. 28})$$

Equation (II. 28) predicts a straight line passing through the origin for the plot of $\ln \eta_{Rel}$ vs. $N/(N_o - N)$ if a suitable choice for N_o is made. Majumder *et al.* tested the equation (II. 28) by using literature data as well as their own experimental data. The best choice for N_o and K_1 was selected by a trial and error methods. The set of K_1 and N_o producing minimum deviations between η_{Rel}^{Exp} and η_{Rel}^{Theo} was accepted.

In dilute solutions, $N \ll N_o$ and we have:

$$\eta_{Rel} = \exp \left(\frac{K_1 N}{N_o^2} \right) \cong 1 + \left(\frac{K_1}{N_o^2} \right) N \quad (\text{II. 29})$$

Equation (II. 29) is nothing but the Jones-Dole equation with the ion-solvent interaction term represented as $B = K_1/N_o^2$. The arrangement between B -values determined in this way and using Jones-Dole equation has been found to be good for several electrolytes.

Further, the equation (II. 28) can be written in the form:

$$\frac{N}{\ln \eta_{Rel}} = \frac{N_o^2}{K_1} - \left(\frac{N_o}{K_1} \right) N \quad (\text{II. 30})$$

It closely resembles the Vand's equation [202] for fluidity (reciprocal for viscosity):

$$\frac{2.5c}{2.3 \log \eta_{Rel}} = \frac{1}{V_h} - Qc \quad (\text{II. 31})$$

where c is the molar concentration of the solute and V_h is the effective rigid molar volume of the salt and Q is the interaction constant.

II. 5. 10. DIVISION OF B-COEFFICIENT INTO IONIC VALUES

The viscosity B -coefficients have been determined by a large number of workers in aqueous, mixed and non-aqueous solvents [210-240]. However, the B -coefficients as determined experimentally using the Jones-Dole equation, does not give any impression regarding ion-solvent interactions unless there is some way to identify the separate contribution of cations and anions to the total solute-solvent interaction. The division of B -values into ionic components is quite arbitrary and based on some assumptions, the validity of which may be questioned. The following methods have been used for the division of B -values in the ionic components:

- [1]. Cox and Wolfenden [241] carried out the division on the assumption that B_{ion} values of Li^+ and IO_3^- in LiIO_3 are proportional to the ionic volumes which are proportional to the third power of the ionic mobilities. The method of Gurney [242] and also of Kaminsky [192] is based on:

$$B_{K^+} = B_{Cl^-} \text{ (in water)} \quad (\text{II. 32})$$

The argument in favour of this assignment is based on the fact that the B -coefficients for KCl is very small and that the motilities' of K^+ and Cl^- are very similar over the temperature range 288.15–318.15K. The assignment is supported from other thermodynamic properties. Nightingale, [243] however preferred RbCl or CsCl to KCl from mobility considerations.

- [2]. The method suggested by Desnoyers and Perron [193] is based on the assumption that the Et_4N^+ ion in water is probably closest to be neither structure breaker nor a structure maker. Thus, they suggest that it is possible to apply with a high degree of accuracy of the Einstein's equation, [244]

$$B = 0.0025\overline{V}_o \quad (\text{II. 33})$$

Now, having an accurate value of the partial molar volume of the ion, \overline{V}_o , it is possible to calculate the value of 0.359 for $B_{\text{Et}_4\text{N}^+}$ in water at 298.15 K. Recently, Sacco *et al.* proposed the "reference electrolytic" method for the division of B -values.

Thus, for tetraphenylphosphonium tetraphenylborate in water, we have:

$$B_{BPh_4^-} = B_{PPh_4^+} = B_{BPh_4PPh_4} / 2 \quad (\text{II. 34})$$

$B_{BPh_4PPh_4}$ (Scarcely soluble in water) has been obtained by the following method:

$$B_{BPh_4PPh_4} = B_{NaBPh_4} + B_{PPh_4Br} - B_{NaBr} \quad (\text{II. 35})$$

The values obtained are in good agreement with those obtained by other methods. The criteria adopted for the separation of B -coefficients in non-aqueous solvents differ from those generally used in water. However, the methods are based on the equality of equivalent conductances of counter ions at infinite dilutions.

(a) Criss and Mastroianni assumed $B_{K^+} = B_{Cl^-}$ in ethanol based on equal mobilities of ions [245]. They also adopted $B_{Me_4N^+}^{25} = 0.25$ as the initial value for acetonitrile solutions.

(b) For acetonitrile solutions, Tuan and Fuoss [246] proposed the equality, as they thought that these ions have similar mobilities. However, according to Springer *et al.* [247] $\lambda_{25}^o(Bu_4N^+) = 61.4$ and $\lambda_{25}^o(Ph_4B^-) = 58.3$ in acetonitrile.

$$B_{Bu_4N^+} = B_{Ph_4B^-} \quad (\text{II. 36})$$

(c) Gopal and Rastogi [197] resolved the B -coefficient in N-methyl propionamide solutions assuming that $B_{Et_4N^+} = B_{I^-}$ at all temperatures.

(d) In dimethyl sulphoxide, the division of B -coefficients were carried out by Yao and Beunion [196] assuming:

$$B_{[(i-pe)_3Bu_4N^+]} = B_{Ph_4B^-} = \frac{1}{2} B_{[(i-pe)_3BuNPh_4B]} \quad (\text{II. 37})$$

at all temperatures.

Wide use of this method has been made by other authors for dimethyl sulphoxide, sulpholane, hexamethyl phosphotriamide and ethylene carbonate [248] solutions. The methods, however, have been strongly criticized by Krumgalz [249]. According to him, any method of resolution based on the equality of equivalent conductances for certain ions suffers from the drawback that it is impossible to select any two ions for which $\lambda_o^+ = \lambda_o^-$ in all solvents at all temperatures. Thus, though $\lambda_K^+ = \lambda_{Cl^-}$ at 298.15 K in methanol, but is not so in ethanol or in any other solvents. In addition, if

the mobilities of some ions are even equal at infinite dilution, but it is not necessarily true at moderate concentrations for which the B - coefficient values are calculated. Further, according to him, equality of dimensions of $(i-pe)_3BuN^+$ or $(i-Am)_3BuN^+$ and Ph_4B^- does not necessarily imply the equality of B -coefficients of these ions and they are likely to be solvent and ion-structure dependent. Krumgalz [249,250] has recently proposed a method for the resolution of B -coefficients. The method is based on the fact that the large tetraalkylammonium cations are not solvated [251,252] in organic solvents (in the normal sense involving significant electrostatic interaction). Thus, the ionic B -values for large tetraalkylammonium ions, R_4N^+ (where $R > Bu$) in organic solvents are proportional to their ionic dimensions. So, we have:

$$B_{R_4NX} = a + br^3 R_4N^+ \quad (\text{II. 38})$$

where $a = B_{X^-} B$ and b is a constant dependent on temperature and solvent nature.

The extrapolation of the plot of B_{R_4NX} ($R > Pr$ or Bu) against r^3 to R_4N to zero cation dimension gives directly B_{X^-} in the proper solvent and thus B -ion values can be calculated.

The B -ion values can also be calculated from the equations:

$$B_{R_4N^+} - B_{R'_4N^+} = B_{R_4NX} - B_{R'_4NX} \quad (\text{II. 39})$$

$$\frac{B_{R_4N^+}}{B_{R'_4N^+}} = \frac{r^3_{R_4N^+}}{r^3_{R'_4N^+}} \quad (\text{II. 40})$$

The radii of the tetraalkylammonium ions have been calculated from the conductometric data [253]. Gill and Sharma [231] used Bu_4NBPh_4 as a reference electrolyte. The method of resolution is based on the assumption, like Krumgalz, that Bu_4N^+ and Ph_4B^- ions with large R - groups are not solvated in non-aqueous solvents and their dimensions in such solvents are constant. The ionic radii of Bu_4N^+ (5.00 Å) and Ph_4B^- (5.35 Å) were, in fact, found to remain constant in different non-aqueous and mixed non-aqueous solvents by Gill and co-workers. They proposed the equations:

$$\frac{B_{Ph_4B^-}}{B_{Bu_4N^+}} = \frac{r^3_{Ph_4B^-}}{r^3_{Bu_4N^+}} = \left(\frac{5.35}{5.00} \right)^3 \quad (\text{II. 41})$$

$$B_{Bu_4NBPh_4} = B_{Bu_4N^+} B_{Ph_4B^-} \quad (\text{II. 42})$$

The method requires only the B -values of Bu_4NBPh_4 and is equally applicable to mixed non-aqueous solvents. The B -ion values obtained by this method agree well with those reported by Sacco *et al.* in different organic solvents using the assumption as given below:

$$B_{[(i-Am)_3Bu_4N^+]} = B_{Ph_4B^-} = \frac{1}{2} B_{[Bu_4NPh_4B]} \quad (\text{II. 43})$$

Recently, Lawrence and Sacco [234] used tetrabutylammonium tetrabutylborate (Bu_4NBBu_4) as reference electrolyte because the cation and anion in each case are symmetrical in shape and have almost equal Van der Waals volume. Thus, we have:

$$\frac{B_{Bu_4N^+}}{B_{Bu_4B^-}} = \frac{V_{W(Bu_4N^+)}}{V_{W(Bu_4B^-)}} \quad (\text{II. 44})$$

$$B_{Bu_4N^+} = \frac{B_{Bu_4NBPh_4}}{\left[1 + \frac{V_{W(Bu_4B^-)}}{V_{W(Bu_4N^+)}} \right]} \quad (\text{II. 45})$$

A similar division can be made for Ph_4PBPh_4 system.

Lawrence *et al.* also made the viscosity measurements of tetraalkyl (from propyl to heptyl) ammonium bromides in DMSO and HMPT.

The B -coefficients $B_{R_4NBr} = B_{Br^-} + a[f_x R_4N^+]$ were plotted as functions of the Vander Waal's volumes. The B_{Br^-} values thus obtained were compared with the accurately determined B_{Br^-} value using Bu_4NBBu_4 and Ph_4PBPh_4 as reference salts. They concluded that the 'reference salt' method is the best available method for division into ionic contributions.

Jenkins and Pritchett [254] suggested a least square analytical technique to examine additivity relationship for combined ion thermodynamics data, to effect apportioning into single-ion components for alkali metal halide salts by employing Fajan's competition principle [255] and 'volcano plots' of Morris [256]. The principle was extended to derive absolute single ion B coefficients for alkali metals and halides in

water. They also observed that $B_{Cs^+} = B_{I^-}$ suggested by Krungalz [251] to be more reliable than $B_{K^+} = B_{Cl^-}$ in aqueous solutions. However, we require more data to test the validity of this method.

It is apparent that almost all these methods are based on certain approximations and anomalous results may arise unless proper mathematical theory is developed to calculate B -values.

II. 5. 11. TEMPERATURE DEPENDENCE OF IONIC VISCOSITY B-VALUES

Regularity in the behaviour of B_{\pm} and dB_{\pm}/dT has been observed both in aqueous and non-aqueous solvents and useful generalizations have been made by Kaminsky. He observed that (i) within a group of the periodic table the B -ion values decrease as the crystal ionic radii increase, (ii) within a group of periodic system, the temperature coefficient of B_{Ion} values increase as the ionic radius. The results can be summarized as follows:

$$(i) \quad A \text{ and } dA/dT > 0 \quad (II. 46)$$

$$(ii) \quad B_{Ion} < 0 \text{ and } dB_{Ion}/dT > 0 \quad (II. 47)$$

characteristic of the structure breaking ions.

$$(iii) \quad B_{Ion} > 0 \text{ and } dB_{Ion}/dT < 0 \quad (II. 48)$$

characteristic of the structure making ions.

An ion when surrounded by a solvent sheath, the properties of the solvent in the solvational layer may be different from those present in the bulk structure. This is well reflected in the 'Co-sphere' model of Gurney, [257] A, B, C Zones of Frank and Wen [258] and hydrated radius of Nightingale [243].

Stokes and Mills gave an analysis of the viscosity data incorporating the basic ideas presented before. The viscosity of a dilute electrolyte solution has been equated to the viscosity of the solvent (η_0) plus the viscosity changes resulting from the competition between various effects occurring in the ionic neighborhood. Thus, the Jones-Dole equation:

$$\eta = \eta_0 + \eta^* + \eta^E + \eta^A + \eta^D = \eta_0 + \eta(A\sqrt{c} + Bc) \quad (II. 49)$$

where η^* , the positive increment in viscosity is caused by coulombic interaction. Thus,

$$\eta^E + \eta^A + \eta^D = \eta_o Bc) \quad (\text{II. 50})$$

B -coefficient can thus be interpreted in terms of the competitive viscosity effects.

Following Stokes, Mills and Krumgalz [249] we can write:

$$B_{Ion} = B_{Ion}^{Einst} + B_{Ion}^{Orient} + B_{Ion}^{Str} + B_{Ion}^{Reinf} \quad (\text{II. 51})$$

whereas according to Lawrence and Sacco:

$$B_{Ion} = B_W + B_{Solv} + B_{Shape} + B_{Ord} + B_{Discord} \quad (\text{II. 52})$$

B_{Ion}^{Einst} is the positive increment arising from the obstruction to the viscous flow of the solvent caused by the shape and size of the ions (the term corresponds to η^E or B_{Shape}).

B_{Ion}^{Orient} is the positive increment arising from the alignment or structure making action of the electric field of the ion on the dipoles of the solvent molecules (the term corresponds to η^A or B_{Ord}). B_{Ion}^{Str} is the negative increment related to the destruction of the solvent structure in the region of the ionic co-sphere arising from the opposing tendencies of the ion to orientate the molecules round itself centrosymmetrically and solvent to keep its own structure (this corresponds to η^D or $B_{Discord}$). B_{Ion}^{Reinf} is the positive increment conditioned by the effect of 'reinforcement of the water structure' by large tetraalkylammonium ions due to hydrophobic hydration. The phenomenon is inherent in the intrinsic water structure and absent in organic solvents. B_W and B_{Solv} account for viscosity increases and attributed to the Van der Waals volume and the volume of the solvation of ions. Thus, small and highly charged cations like Li^+ and Mg^{2+} form a firmly attached primary solvation sheath around these ions (B_{Ion}^{Orient} or η^E positive). At ordinary temperature, alignment of the solvent molecules around the inner layer also cause increase in B_{Ion}^{Orient} (η^A), B_{Ion}^{Orient} (η^D) is small for these ions. Thus, B_{Ion} will be large and positive as $B_{Ion}^{Einst} + B_{Ion}^{Orient} > B_{Ion}^{Str}$ However, B_{Ion}^{Einst} and B_{Ion}^{Orient} would be small for ions of greatest crystal radii (within a group) like Cs^+ or I^- due to small surface charge densities resulting in weak orienting and structure forming effect. B_{Ion}^{Str} would be

large due to structural disorder in the immediate neighbourhood of the ion due to competition between the ionic field and the bulk structure. Thus, $B_{lon}^{Einst} + B_{lon}^{Orient} < B_{lon}^{Str}$ and B_{lon} is negative. Ions of intermediate size (e.g., K^+ and Cl^-) have a close balance of viscous forces in their vicinity, i.e., $B_{lon}^{Einst} + B_{lon}^{Orient} = B_{lon}^{Str}$ so that B is close to zero.

Large molecular ions like tetraalkylammonium ions have large B_{lon}^{Einst} because of large size but B_{lon}^{Orient} and B_{lon}^{Str} would be small, i.e., $B_{lon}^{Einst} + B_{lon}^{Orient} \gg B_{lon}^{Str}$ would be positive and large. The value would be further reinforced in water arising from B_{lon}^{Reinf} due to hydrophobic hydrations.

The increase in temperature will have no effect on B_{lon}^{Einst} . But the orientation of solvent molecules in the secondary layer will be decreased due to increase in thermal motion leading to decrease in B_{lon}^{Str} . B_{lon}^{Orient} will decrease slowly with temperature as there will be less competition between the ionic field and reduced solvent structure. The positive or negative temperature co-efficient will thus depend on the change of the relative magnitudes of B_{lon}^{Orient} and B_{lon}^{Str} .

In case of structure-making ions, the ions are firmly surrounded by a primary solvation sheath and the secondary solvation zone will be considerably ordered leading to an increase in B_{lon} and concomitant decrease in entropy of solvation and the mobility of ions. Structure breaking ions, on the other hand, are not solvated to a great extent and the secondary solvation zone will be disordered leading to a decrease in B_{lon} values and increases in entropy of solvation and the mobility of ions. Moreover, the temperature induced change in viscosity of ions (or entropy of solvation or mobility of ions) would be more pronounced in case of smaller ions than in case of the larger ions. So, there is a correlation between the viscosity, entropy of solvation and temperature dependent mobility of ions. Thus, the ionic B -coefficient and the entropy of solvation of ions have rightly been used as probes of ion-solvent interactions and as a direct indication of structure making and structure breaking character of ions. The linear plot of ionic B -coefficients against the ratios of mobility viscosity products at two temperatures (a more sensitive variable than ionic mobility) by Gurney [257,258]

clearly demonstrates a close relation between ionic B -coefficients and ionic mobilities. Gurney also demonstrated a clear correlation between the molar entropy of solution values with B -coefficient of salts. The ionic B - values show a linear relationship with the partial molar ionic entropies or partial molar entropies of hydration (\bar{S}_h^o) as:

$$\bar{S}_h^o = \bar{S}_{aq}^o - \bar{S}_g^o \quad (\text{II.53})$$

Where, $\bar{S}_{aq}^o = \bar{S}_{ref}^o + \Delta S^o$, \bar{S}_g^o is the calculated sum of the translational and rotational entropies of the gaseous ions. Gurney obtained a single linear plot between ionic entropies and ionic B -coefficients for all mono atomic ions by equating the entropy of the hydrogen ion ($S_{H^+}^o$) to $-5.5 \text{ cal. mol}^{-1} \text{ deg}^{-1}$. Asmus [259] used the entropy of hydration to correlate ionic B values and Nightingale [243] showed that a single linear relationship could be obtained with it for both monoatomic and polyatomic ions. The correlation was utilized by Abraham *et al.*[260] to assign single ion B -coefficients so that a plot of ΔS_e^o [261,262] the electrostatic entropy of solvation or $\Delta S_{I,II}^o$ the entropic contributions of the first and second solvation layers of ions against B points (taken from the works of Nightingale) for both cations and anions lie on the same curve. There are excellent linear correlations between ΔS_e^o and ΔS_i^o and the single ion B - coefficients. Both entropy criteria (ΔS_e^o and $\Delta S_{I,II}^o$) and B - ion values indicate that in water the ions Li^+ , Na^+ , Ag^+ and F^- are not structure makers, and the ions Rb^+ , Cs^+ , Cl^- , Br^- , I^- and ClO_4^- are structure breakers and K^+ is a border line case.

II. 5. 12. THERMODYNAMICS OF VISCOUS FLOW

Assuming viscous flow as a rate process, the viscosity (η) can be represented from Eyring's [263] approaches as:

$$\eta = A e^{\frac{E_{vis}}{RT}} = \left(\frac{hN_A}{V} \right) e^{\frac{\Delta G^*}{RT}} = \left(\frac{hN_A}{V} \right) e^{\left(\frac{\Delta H^*}{RT} - \frac{\Delta S^*}{R} \right)} \quad (\text{II. 54})$$

where E_{vis} = the experimental entropy of activation determined from a plot of $\ln \eta$ against $1/T$. ΔG^* , ΔH^* and ΔS^* are the free energy, enthalpy and entropy of activation, respectively.

Nightingale and Benck [264] dealt in the problem in a different way and calculated the thermodynamics of viscous flow of salts in aqueous solution with the help of the Jones-Dole equation (neglecting the Ac term). Thus, we have:

$$R \left[\frac{d \ln \eta}{d\left(\frac{1}{T}\right)} \right] = r \left[\frac{d \ln \eta_o}{d\left(\frac{1}{T}\right)} \right] + \frac{R}{1+Bc} \frac{d(1+Bc)}{d\left(\frac{1}{T}\right)} \quad (\text{II. 55})$$

$$\Delta E_{\eta(\text{Soln})}^{\ddagger} = \Delta E_{\eta(\text{Soln})}^{\ddagger} + \Delta E_V^{\ddagger} \quad (\text{II. 56})$$

ΔE_V^{\ddagger} can be interpreted as the increase or decrease of the activation energies for viscous flow of the pure solvents due to the presence of ions, i.e., the effective influence of the ions upon the viscous flow of the solvent molecules. Feakins *et al.* [265] have suggested an alternative formulation based on the transition state treatment of the relative viscosity of electrolytic solution. They suggested the following expression:

$$B = \frac{(\phi_{v,2}^0 - \phi_{v,1}^0)}{1000} + \phi_{v,2}^0 \frac{(\Delta\mu_2^{0\ddagger} - \Delta\mu_1^{0\ddagger})}{1000RT} \quad (\text{II. 57})$$

where $\phi_{v,1}^0$ and $\phi_{v,2}^0$ are the partial molar volumes of the solvent and solute respectively and $\Delta\mu_2^{0\ddagger}$ is the contribution per mole of solute to the free energy of activation for viscous flow of solution. $\Delta\mu_1^{0\ddagger}$ is the free energy of activation for viscous flow per mole of the solvent which is given by:

$$\Delta\mu_1^{0\ddagger} = \Delta G_1^{0\ddagger} = RT \ln(\eta_0 \phi_{v,1}^0 / h N_A) \quad (\text{II. 58})$$

Further, if B is known at various temperatures, we can calculate the entropy and enthalpy of activation of viscous flow respectively from the following equations as given below:

$$\frac{d(\Delta\mu_2^{0\ddagger})}{dT} = -\Delta S_2^{0\ddagger} \quad (\text{II. 59})$$

$$\Delta H_2^{0\ddagger} = \Delta\mu_2^{0\ddagger} + T \Delta S_2^{0\ddagger} \quad (\text{II. 60})$$

II. 5. 13. EFFECTS OF SHAPE AND SIZE

Stokes and Mills have dealt in the aspect of shape and size extensively. The ions in solution can be regarded to be rigid spheres suspended in continuum. The hydrodynamic treatment presented by Einstein [244] leads to the equation:

$$\frac{\eta}{\eta_0} = 1 + 2.5\phi \quad (\text{II. 61})$$

where ϕ is the volume fraction occupied by the particles. Modifications of the equation have been proposed by (i) Sinha [266] on the basis of departures from spherical shape and (ii) Vand on the basis of dependence of the flow patterns around the neighboring particles at higher concentrations. However, considering the different aspects of the problem, spherical shapes have been assumed for electrolytes having hydrated ions of large effective size (particularly polyvalent monatomic cations). Thus, we have from equation (II. 61):

$$2.5\phi = A\sqrt{c} + Bc \quad (\text{II. 62})$$

Since $A\sqrt{c}$ term can be neglected in comparison with Bc and $\phi = c\phi_{v,1}^0$ where $\phi_{v,1}^0$ is the partial molar volume of the ion, we get:

$$2.5\phi_{v,1}^0 = B \quad (\text{II. 63})$$

In the ideal case, the B -coefficient is a linear function of partial molar volume of the solute, $\phi_{v,1}^0$ with slope to 2.5. Thus, B_{\pm} can be equated to:

$$B_{\pm} = 2.5\phi_{\pm}^0 = \frac{2.5 \times 4}{3} \frac{(\pi R_{\pm}^3 N)}{1000} \quad (\text{II. 64})$$

assuming that the ions behave like rigid spheres with a effective radii, R_{\pm} moving in a continuum. R_{\pm} , calculated using the equation (II. 64) should be close to crystallographic radii or corrected Stoke's radii if the ions are scarcely solvated and behave as spherical entities. But, in general, R_{\pm} values of the ions are higher than the crystallographic radii indicating appreciable solvation.

The number n_b of solvent molecules bound to the ion in the primary solvation shell can be easily calculated by comparing the Jones-Dole equation with the Einstein's equation:

$$B_{\pm} = \frac{2.5}{1000(\phi_i + n_b \phi_s)} \quad (\text{II. 65})$$

where ϕ_i is the molar volume of the base ion and ϕ_s , the molar volume of the solvent. The equation (II. 65) has been used by a number of workers to study the nature of solvation and solvation number.

II. 5. 14. VISCOSITY OF NON-ELECTROLYTIC SOLUTIONS

The equations of Vand, [267] Thomas, [268] and Moulik [269-271] proposed mainly to account for the viscosity of the concentrated solutions of bigger spherical particles have been also found to correlate the mixture viscosities of the usual nonelectrolytes. These equations are:

$$\text{Vand equation:} \quad \ln \eta_r = \frac{\alpha}{1-Q} = \frac{2.5V_h c}{1-QV_h c} \quad (\text{II. 66})$$

$$\text{Thomas equation:} \quad \eta_r = 1 + 2.5V_h c + 10.05cV_h^2 c \quad (\text{II. 67})$$

$$\text{Moulik equation:} \quad \eta^2 = I + Mc^2 \quad (\text{II. 68})$$

where η_r is the relative viscosity, a is constant depending on axial ratios of the particles, Q is the interaction constant, V_h is the molar volume of the solute including rigidly held solvent molecules due to hydration, c is the molar concentration of the solutes; I and M are constants. The viscosity equation proposed by Eyring and coworkers for pure liquids on the basis of pure significant liquid structures theory, can be extended to predict the viscosity of mixed liquids also. The final expression for the liquid mixtures takes the following form:

$$\eta_m = \frac{6N_A h}{\sqrt{2}r_m(V_m - V_{Sm})} \left[\sum_i^n \left\{ 1 - \exp\left(\frac{-\theta_i}{T}\right) \right\}^{-x_i} \right] \exp\left[\frac{a_m E_{Sm} V_{Sm}}{RT(V_m - V_{Sm})} \right] + \frac{V_m - V_{Sm}}{V_m} \left[\sum_i^n \frac{2}{3d_i^2} \left(\frac{m_i kT}{\pi^3} \right)^{\frac{1}{2}} x_i \right] \quad (\text{II. 69})$$

where n is 2 for binary and 3 for ternary liquid mixtures. The mixture parameters, r_m , E_{Sm} , V_m , V_{Sm} and a_m were calculated from the corresponding pure component parameters by using the following relations:

$$r_m = \sum_i^n x_i^2 r_i + \sum_{i \neq j} 2x_i x_j x_{ij} \quad (\text{II. 70})$$

$$E_{Sm} = \sum_i^n x_i^2 E_{Si} + \sum_{i \neq j} 2x_i x_j E_{Sij} \quad (\text{II. 71})$$

$$V_m = \sum_i^n x_i V_i \quad V_{Sm} = \sum_i^n x_i V_{Si} \quad a_m = \sum_i^n x_i a_i \quad (\text{II. 72})$$

$$r_{ij} = (r_i r_j)^{\frac{1}{2}} \quad \text{and} \quad E_{Sij} = (E_{Si} E_{Sj})^{\frac{1}{2}} \quad (\text{II. 73})$$

$$\theta = \frac{h}{\kappa 2\pi} \left(\frac{b}{m} \right)^{\frac{1}{2}} \quad (\text{II. 74})$$

$$b = 2Z\varepsilon \left[22.106 \left(\frac{N_A \sigma^2}{V_s} \right)^4 - 10.559 \left(\frac{N_A \sigma^3}{V_s} \right)^2 \right] \frac{1}{\sqrt{2}\sigma^2} \left(\frac{N_A \sigma^3}{V_s} \right)^{\frac{2}{3}} \quad (\text{II. 75})$$

where σ and ε are Lennard-Jones potential parameters and the other symbols have their usual significance.

For interpolation and limited extrapolation purposes, the viscosities of ternary mixture can be correlated to a high degree of accuracy in terms of binary contribution by the following equations [272-278].

$$\begin{aligned} \eta_m = & \sum_i^3 x_i \eta_i + x_1 x_2 [A_{12} + B_{12}(x_1 - x_2) + C_{12}(x_1 - x_2)^2] \\ & + x_2 x_3 [A_{23} + B_{23}(x_2 - x_3) + C_{23}(x_2 - x_3)^2] \\ & + x_3 x_1 [A_{31} + B_{31}(x_3 - x_1) + C_{31}(x_3 - x_1)^2] \end{aligned} \quad (\text{II. 76a})$$

The correlation of ternary is modified to the following form:

$$\begin{aligned} \eta_m = & \sum_i^3 x_i \eta_i + x_1 x_2 [A_{12} + B_{12}(x_1 - x_2) + C_{12}(x_1 - x_2)^2] \\ & + x_2 x_3 [A_{23} + B_{23}(x_2 - x_3) + C_{23}(x_2 - x_3)^2] \\ & + x_3 x_1 [A_{31} + B_{31}(x_3 - x_1) + C_{31}(x_3 - x_1)^2] \\ & + A_{123}(x_1 x_2 x_3) \end{aligned} \quad (\text{II. 76b})$$

However, a better result may be obtained using the following relation:

$$\begin{aligned} \eta_m = & \sum_i^3 x_i \eta_i + x_1 x_2 [A_{12} + B_{12}(x_1 - x_2) + C_{12}(x_1 - x_2)^2] \\ & + x_2 x_3 [A_{23} + B_{23}(x_2 - x_3) + C_{23}(x_2 - x_3)^2] \\ & + x_3 x_1 [A_{31} + B_{31}(x_3 - x_1) + C_{31}(x_3 - x_1)^2] \\ & + x_1 x_2 x_3 [A_{123} + B_{123} x_1^2 (x_2 - x_3)^2 + C_{123} x_1^3 (x_2 - x_3)^3] \end{aligned} \quad (\text{II. 76c})$$

where A_{12} , B_{12} , C_{12} , A_{23} , B_{23} , C_{23} , A_{31} , B_{31} and C_{31} , are constants for binary mixtures; A_{123} , B_{123} and C_{123} are constants for the ternaries; and the other symbols have their usual significance.

II. 5. 15. VISCOSITY DEVIATION

Viscosity of liquid mixtures can also provide information for the elucidation of the fundamental behaviour of liquid mixtures, aid in the correlation of mixture viscosities with those of pure components, and may provide a basis for the selection of physico-chemical methods of analysis. Quantitatively, as per the absolute reaction rates theory, [279] the deviations in viscosities ($\Delta\eta$) from the ideal mixture values can be calculated as:

$$\Delta\eta = \eta - \sum_{i=1}^j (x_i \eta_i) \quad (\text{II. 77})$$

where η is the dynamic viscosities of the mixture and $x_i \eta_i$ are the mole fraction and viscosity of i^{th} component in the mixture, respectively.

II. 5. 16. GIBBS EXCESS ENERGY OF ACTIVATION FOR VISCOUS FLOW

Quantitatively, the Gibbs excess energy of activation for viscous flow ΔG^* can be calculated as: [280]

$$\Delta G^E = RT \left[\ln \eta V - \sum_{i=1}^j (x_i \ln \eta_i V_i) \right] \quad (\text{II. 78})$$

where η and V are the viscosity and molar volume of the mixture; η_i and V_i are the viscosity and molar volume of i^{th} pure component, respectively.

II. 6. ULTRASONIC SPEED

Ultrasonic or ultrasound, derived from the Latine words “ultra,” meanibg beyond, and “sonic,” meanings sound, is a term used to describe sound waves that vibrate more rapidly than the human ear can detect. Ultrasonic waves thus have frequencies avove 20,000 Hz. During the 1880s, Curie brothers discovered the phenomenon of piezoelectricity. It may be defined as the ability of some materials like crystals (e.g. Quartz, Rochelle salt) and certain ceramics to generate an electric Field or electric potential in response to applied mechanical stress.

II. 6. 1. APPARENT MOLAL ISENTROPIC COMPRESSIBILITY

In recent years, there has been considerably progress in the determination of thermophysical, thermodynamic, acoustic and transport properties of working liquids from ultrasonic speeds, density and viscosity measurement. The study of ultrasonic speeds and isentropic compressibilities of liquids, solutions and liquid mixtures provide useful information about molecular interactions, association and dissociation. Various parameters like molar isentropic and isothermal compressibilities, apparent molal compressibility, isentropic compressibility, deviation in isentropic compressibility from ideality, etc. can very well be evaluated and studied from the measurement of ultrasonic speeds and densities in solutions. Isentropic compressibilities play a vital role in characterization of binary and ternary liquid mixtures particularly in cases where partial molar volume data alone fail to provide an unequivocal interpretation of the interactions.

Although for a long time attention has been paid to the apparent molal isentropic compressibility for electrolytes and other compounds in aqueous solutions [281-285] measurements in non-aqueous solvents are still scarce. It has been emphasized by many authors that the apparent molal isentropic compressibility data can be used as a useful parameter in elucidating the solute-solvent and solute-solute interactions. The most convenient way to measure the compressibility of a solvent/solution is from the speed of sound in it.

The isentropic compressibility (β_s) of a solvent/solution can be calculated from the Laplace's equation; [286]

$$\beta_s = \frac{1}{u^2 \rho} \quad (\text{II. 79})$$

where ρ is the solution density and u is the ultrasonic speed in the solvent/solution. The isentropic compressibility (β_s) determined by equation (II. 79) is adiabatic, not an isothermal one, because the local compressions occurring when the ultrasound passes through the solvent/solution are too rapid to allow an escape of the heat produced.

The apparent molal isentropic compressibility (ϕ_K) of the solutions was calculated using the relation:

$$\phi_K = \frac{M \beta_s}{\rho} + \frac{1000(\beta_s \rho_0 - \beta_0 \rho)}{m \rho \rho_0} \quad (\text{II. 80})$$

where β_0 is the isentropic compressibility of the solvent mixture, M is the molar mass of the solute and m is the molality of the solution.

The limiting apparent isentropic compressibility ϕ_K^0 may be obtained by extrapolating the plots of ϕ_K versus the square root of the molal concentration of the solutes by the computerized least- square method according to the equation.

$$\phi_K = \phi_K^0 + S_K^* \cdot \sqrt{m} \quad (\text{II. 81})$$

The limiting apparent molar isentropic compressibility (ϕ_K^0) and the experimental slope S_K^* can be interpreted in terms of solute-solvent and solute-solute interactions respectively. It is well established that the solutes causing electrostriction leads to the decrease in the compressibility of the solution [287,288]. This is reflected by the negative values of ϕ_K^0 of electrolytic solutions. Hydrophobic solutes often show negative compressibilities due to the ordering induced by them in the water structure. The compressibility of hydrogen-bonded structure, however, varies depending on the nature of the hydrogen bonding involved. However, the poor fit of the solute molecules [289,290] as well as the possibility of flexible hydrogen bond formation appear to be responsible for causing a more compressible environment and hence positive ϕ_K^0 values have been reported in aqueous non-electrolyte [291] and non-aqueous non-electrolyte [292] solutions.

II. 6. 2. DEVIATION IN ISENTROPIC COMPRESSIBILITY

The deviation in isentropic compressibility (ΔK_s) can be calculated using the following equation: [293-295]

$$\Delta\beta_s = \beta_s - \sum_{i=1}^j x_i \beta_{s,i} \quad (\text{II. 82})$$

where $x_i, \beta_{s,i}$ are the mole fraction and isentropic compressibility of i^{th} component in the mixture, respectively. The observed values of $\Delta\beta_s$ can be qualitatively explained by considering the factors, namely

- (i) the mutual disruption of associated species present in the pure liquids
- (ii) the formation of weak bonds by dipole-induced dipole interaction between unlike molecules
- (iii) Geometrical fitting of component molecules into each other structure.

The first factor contributes to positive $\Delta\beta_s$ values, whereas the remaining two factors lead to negative $\Delta\beta_s$ values [296]. The resultant values of $\Delta\beta_s$ for the mixtures are due to the net effect of the combination of (i) to (iii) [297].

Moreover, the excess or deviation properties ($V_m^E, \Delta\eta, \Delta G^E$ and $\Delta\beta_s$) have been fitted to Redlich-Kister [298] polynomial equation using the method of least squares involving the Marquardt algorithm [299] and the binary coefficients, α_i were determined as follows:

$$Y_{i,j}^E = x_1 x_2 \sum_{i=1}^j a_i (x_1 - x_2)^i \quad (\text{II. 83})$$

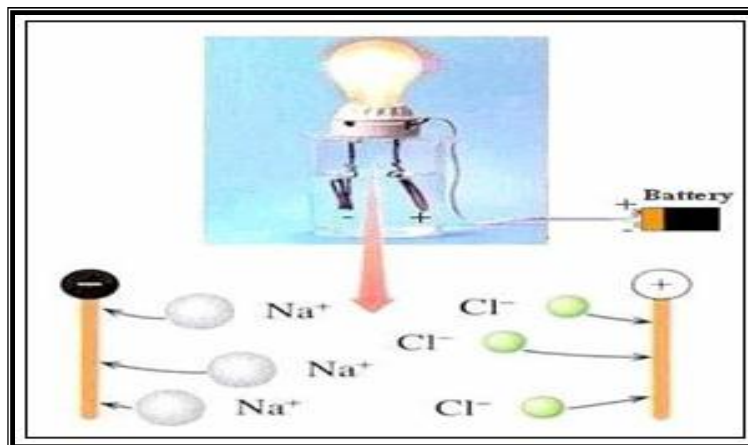
where $Y_{i,j}^E$ refers to an excess or deviation property and x_1 and x_2 are the mole fraction of the solvent 1 and solvent 2, respectively. In each case, the optimal number of coefficients was ascertained from an approximation of the variation in the standard deviation (σ). The standard deviation (σ) was calculated using,

$$\sigma = \sqrt{\frac{(Y_{\text{exp}}^E - Y_{\text{cal}}^E)^2}{n - m}} \quad (\text{II. 84})$$

where n is the number of data points and m is the number of coefficients.

II. 7. CONDUCTANCE

One of the most precise and direct technique available to determine the extent of the dissociation constants of electrolytes in aqueous, mixed and non-aqueous solvents is the “*conductimetric method.*” Conductance data in conjunction with viscosity measurements, gives much information regarding ion-ion and ion-solvent interaction.



Dissolved Ions Conduct Electricity

The studies of conductance measurements were pursued vigorously during the last five decades, both theoretically and experimentally and a number of important theoretical equations have been derived. We shall dwell briefly on some of these aspects in relation to the studies in aqueous, non-aqueous, pure and mixed solvents. The successful application of the Debye-Hückel theory of interionic attraction was made by Onsager, [300] to derive the Kohlrausch’s equation representing the molar conductance of an electrolyte. For solutions of a single symmetrical electrolyte the equation is given by:

$$\Lambda = \Lambda_0 - S\sqrt{c} \quad (\text{II. 85})$$

where,

$$S = \alpha\Lambda_0 + \beta \quad (\text{II. 86})$$

$$\alpha = \frac{(z^2)k}{3(2 + \sqrt{2})\epsilon_r kT \sqrt{c}} = \frac{82.406 \times 10^4 z^3}{(\epsilon_r T)^{\frac{3}{2}}} \quad (\text{II. 87a})$$

$$\beta = \frac{z^2 e F k}{3\pi\eta\sqrt{c}} = \frac{82.487 z^3}{\eta\sqrt{\epsilon_r T}} \quad (\text{II. 87b})$$

The equation took no account for the short-range interactions and also of shape or size of the ions in solution. The ions were regarded as rigid charged spheres in an electrostatic and hydrodynamic continuum, i.e., the solvent [301]. In the subsequent years, Pitts (1953) [302] and Fuoss and Onsager (1957) [303] independently worked out the solution of the problem of electrolytic conductance accounting for both long-range and short-range interactions. However, the Λ_o values obtained for the conductance at infinite dilution using Fuoss-Onsager theory differed considerably from that obtained using Pitt's theory and the derivation of the Fuoss-Onsager equation was questioned [304,305]. The original Fuoss-Onsager equation was further modified by Fuoss and Hsia [306,307] who recalculated the relaxation field, retaining the terms which had previously been neglected.

The results of conductance theories can be expressed in a general form:

$$\Lambda = \frac{\Lambda_o - \alpha\Lambda_o\sqrt{c}}{(1 + \kappa\alpha)} \left(\frac{1 + \kappa\alpha}{\sqrt{2}} \right) - \frac{\beta\sqrt{c}}{(1 + \kappa\alpha)} + G(\kappa\alpha) \quad (\text{II. 88})$$

where $G(\kappa\alpha)$ is a complicated function of the variable. The simplified form:

$$\Lambda = \Lambda_o - S\sqrt{c} + Ec \ln c + J_1c + J_2\sqrt[3]{c} \quad (\text{II. 89})$$

However, it has been found that these equations have certain limitations, in some cases it fails to fit experimental data. Some of these results have been discussed elaborately by Fernandez-Prini [308,309]. Further correction of the equation (II. 89) was made by Fuoss and Accascin. They took into consideration the change in the viscosity of the solutions and assumed the validity of Walden's rule. The new equation becomes:

$$\Lambda = \Lambda_o - S\sqrt{c} + Ec \ln c + J_1c + J_2\sqrt[3]{c} - F\Lambda c \quad (\text{II. 90})$$

where,

$$Fc = \frac{4\pi R^3 N_A}{3} \quad (\text{II. 91})$$

In most cases, however, J_2 is made zero but this leads to a systematic deviation of the experimental data from the theoretical equations. It has been observed that Pitt's equation gives better fit to the experimental data in aqueous solutions [310].

II. 7. 1. IONIC ASSOCIATION

The equation (II. 90) successfully represents the behaviour of completely dissociated electrolytes. The plot of Λ against \sqrt{c} (limiting Onsager equation) is used to assign the dissociation or association of electrolytes. Thus, if $\Lambda_{o\text{exp}}$ is greater than $\Lambda_{o\text{theo}}$, i.e., if positive deviation occurs (ascribed to short range hard core repulsive interaction between ions), the electrolyte may be regarded as completely dissociated but if negative deviation ($\Lambda_{o\text{exp}} < \Lambda_{o\text{theo}}$) or positive deviation from the Onsager limiting tangent ($\alpha\Lambda_o + \beta$) occurs, the electrolyte may be regarded to be associated. Here the electrostatic interactions are large so as to cause association between cations and anions. The difference in $\Lambda_{o\text{exp}}$ and $\Lambda_{o\text{theo}}$ would be considerable with increasing association [311].

Conductance measurements help us to determine the values of the ion-pair association constant, K_A for the process:



$$K_A = \frac{(1-\alpha)}{\alpha^2 c \gamma_{\pm}^2} \quad (\text{II. 93})$$

$$\alpha = 1 - \alpha^2 K_A c \gamma_{\pm}^2 \quad (\text{II. 94})$$

where γ_{\pm} is the mean activity coefficient of the free ions at concentration αc .

For strongly associated electrolytes, the constant K_A and Λ_o have been determined using Fuoss-Kraus equation [312] or Shedlovsky's equation [313].

$$\frac{T(z)}{\Lambda} = \frac{1}{\Lambda_o} + \frac{K_A}{\Lambda_o^2} \cdot \frac{c \gamma_{\pm}^2 \Lambda}{T(z)} \quad (\text{II. 95})$$

where $T(z) = F(z)$ (Fuoss-Kraus method) and $1/T(z) = S(z)$ (Shedlovsky's method).

$$F(z) = 1 - z(1 - z(1 - \dots)^{\frac{1}{2}})^{\frac{1}{2}} \quad (\text{II. 96a})$$

$$\text{and} \quad \frac{1}{T(z)} = S(z) = 1 + z + \frac{z^2}{2} + \frac{z^3}{8} + \dots \quad (\text{II. 96b})$$

A plot of $T(z)/\Lambda$ against $c\gamma_{\pm}^2\Lambda/T(z)$ should be a straight line having $1/\Lambda_0$ for its intercept and K_A/Λ_0^2 for its slope. Where K_A is large, there will be considerable uncertainty in the determined values of Λ_0 and K_A from equation (II. 95).

The Fuoss-Hsia conductance equation for associated electrolytes is given by:

$$\Lambda = \Lambda_0 - S\sqrt{\alpha c} + E(\alpha c)\ln(\alpha c) + J_1(\alpha c) - J_2(\alpha c)^{\frac{3}{2}} - K_A\Lambda\gamma_{\pm}^2(\alpha c) \quad (\text{II. 97})$$

The equation was modified by Justice [314,315]. The conductance of symmetrical electrolytes in dilute solutions can be represented by the equations:

$$\Lambda = \alpha(\Lambda_0 - S\sqrt{\alpha c} + E(\alpha c)\ln(\alpha c) + J_1R(\alpha c) - J_2R(\alpha c)^{\frac{3}{2}}) \quad (\text{II. 98})$$

$$\frac{(1-\alpha)}{\alpha^2 c \gamma_{\pm}^2} = K_A \quad (\text{II. 99})$$

$$\ln \gamma_{\pm} = \frac{-k\sqrt{q}}{(1+kR\sqrt{\alpha c})} \quad (\text{II. 100})$$

The conductance parameters are obtained from a least square treatment after setting, $R = q = \frac{e^2}{2\epsilon kT}$ (Bjerrum's critical distance).

According to Justice the method of fixing the J -coefficient by setting, $R = q$ clearly permits a better value of K_A to be obtained. Since the equation (II. 98) is a series expansion truncated at the $c^{3/2}$ term, it would be preferable that the resulting errors be absorbed as much as possible by J_2 rather than by K_A , whose theoretical interest is greater as it contains the information concerning short-range cation-anion interaction. From the experimental values of the association constant K_A , one can use two methods in order to determine the distance of closest approach, ' a ', of two free ions to form an ion-pair. The following equation has been proposed by Fuoss; [316]

$$K_A = \frac{4\pi N_A \alpha^3}{3000} \exp\left(\frac{e^2}{\alpha \epsilon kT}\right) \quad (\text{II. 101})$$

In some cases, the magnitude of K_A was too small to permit a calculation of a . The distance parameter was finally determined from the more general equation due to Bjerrum [317].

$$K_A = \frac{4\pi N_A \alpha}{1000} \int_{r=a}^{r=q} r^2 \exp\left(\frac{z^2 e^2}{r \epsilon k T}\right) dr \quad (\text{II. 102})$$

The equations neglect specific short-range interactions except for solvation in which the solvated ion can be approximated by a hard sphere model. The method has been successfully utilized by Douheret [318].

II. 7. 2. ION SIZE PARAMETER AND IONIC ASSOCIATION

For plotting, equation (II. 90) can be rearranged to the 'A' function as:

$$A_1 = A + S\sqrt{c} - Ec \ln c = A_o + J_1 c + J_2 \sqrt[3]{c} = A_o + J_1 c \quad (\text{II. 103})$$

with J_2 term omitted.

Thus, a plot of A_1 vs. c gives a straight line with A_o as intercept and J_1 as slope and 'a' values can be calculated from J_1 values. The 'a' values obtained by this method for DMSO were much smaller than would be expected from sums of crystallographic radii. One of the reasons attributed to it is that ion-solvent interactions are not included in the continuum theory on which the conductance equations are based. The inclusion of dielectric saturation results in an increase in 'a' values (much in conformity with the crystallographic radii) of alkali metal salts (having ions of high surface charge density) in sulpholane. The viscosity correction leads to a larger value of 'a' [319] but the agreement is still poor. However, little of real physical significance may be attached to the distance of closest approach derived from J_1 [320,321]. Fuoss [322] in 1975 proposed a new conductance equation. Latter he subsequently put forward another conductance equation in 1978 replacing the old one as suggested by Fuoss and co-workers.

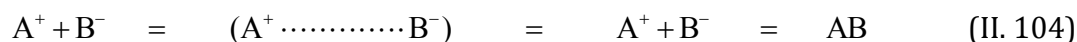
He classified the ions of electrolytic solutions in one of the three categories.

- (i) Ions finding an ion of opposite charge in the first shell of nearest neighbours (contact pairs) with $r_{ij} = a$. The nearest neighbours to a contact pair are the solvent molecules forming a cage around the pairs.
- (ii) Ions with overlapping Gurney's co-spheres (solvent separated pairs). For them $r_{ij} = a + ns$, where n is generally 1 but may be 2, 3 etc.; 's' is the diameter

of sphere corresponding to the average volume (actual plus free) per solvent molecule.

- (iii) Ions finding no other unpaired ion in a surrounding sphere of radius R , the diameter of the co-sphere (unpaired ions).

Thermal motions and interionic forces establish a steady state, represented by the following equilibria:



Solvent separated ion-pair Contact ion-pair Neutral molecule

Contact pairs of ionogens may rearrange to neutral molecules $A^+B^- = AB$, e.g., H_3O^+ and CH_3COO^- . Let γ be the fraction of solute present as unpaired ($r > R$) ions. If $c\gamma$ is the concentration of unpaired ion and α is the fraction of paired ions ($r \leq R$), then the concentration of unpaired ion and $c(1-\alpha)(1-\gamma)$ and that of contact pair is $\alpha c(1-\gamma)$.

The equilibrium constants for Eq. (II. 104) are:

$$K_R = \frac{(1-\alpha)(1-\gamma)}{c\gamma^2 f^2} \quad (\text{II. 105})$$

$$K_S = \frac{\alpha}{1-\alpha} = \exp\left(\frac{-E_S}{kT}\right) = e^{-\varepsilon} \quad (\text{II. 106})$$

where K_R describes the formation and separation of solvent separated pairs by diffusion in and out of spheres of diameter R around cations and can be calculated by continuum theory; K_S is the constant describing the specific short-range ion-solvent and ion-ion interactions by which contact pairs form and dissociate. E_S is the difference in energy between a pair in the states ($r = R$) and ($r = a$); ε is E_S measured in units of kT .

Now,

$$(1-\alpha) = \frac{1}{1+K_S} \quad (\text{II. 107})$$

and the conductometric pairing constant is given by:

$$K_A = \frac{(1-\alpha)}{c\gamma^2 f^2} = \frac{K_R}{1-\alpha} = K_R(1+K_S) \quad (\text{II. 108})$$

The equation determines the concentration, $c\gamma$ of active ions that produce long-range interionic effects. The contact pairs react as dipoles to an external field, X and contribute only to changing current. Both of the contact pairs and solvent separated pairs are gone as virtual dipoles by unpaired ions, their interaction with unpaired ions is, therefore, ignored in calculating long-range effects (activity coefficients, relaxation field ΔX and electrophoresis ($\Delta X \cdot \Delta A_e$)). The various patterns can be reproduced by theoretical fractions in the form:

$$A = p \left[A_o \left(\frac{1 + \Delta X}{X} \right) + \Delta A_e \right] = p \left[A_o (1 + R_x) + E_L \right] \quad (\text{II. 109})$$

which is a three parameter equation $A = A(c, A_o, R, E_s), \Delta X / X$ (the relaxation field) and ΔA_e (the electrophoretic counter current) are long range effects due to electrostatic interionic forces and p is the fraction of Gurney co-sphere.

The parameters K_R (or E_s) is a catch-all for all short range effects:

$$p = 1 - \alpha(1 - \gamma) \quad (\text{II. 110})$$

In case of ionogens or for ionophores in solvents of low dielectric constant, α is very near to unity ($-E_s/kT$) $\gg 1$ and the equation becomes:

$$A = \gamma \left[A_o \left(\frac{1 + \Delta X}{X} \right) \right] + \Delta A_e \quad (\text{II. 111})$$

The equilibrium constant for the effective reaction, $A^+ + B^- + AB$, is then

$$K_A = \frac{(1 - \gamma)}{c\gamma^2 f^2} \approx K_R K_S \quad (\text{II. 112})$$

as $K_S \gg 1$. The parameters and the variables are related by the set of equations:

$$\gamma = 1 - \frac{K_R c \gamma^2 f^2}{(1 - \alpha)} \quad (\text{II. 113})$$

$$K_R = \left(\frac{4\pi N_A R^3}{3000} \right) \exp\left(\frac{\beta}{R}\right) \quad (\text{II. 114})$$

$$-\ln f = \frac{\beta\kappa}{2(1 + \kappa R)}, \quad \beta = \frac{e^2}{\epsilon\kappa T} \quad (\text{II. 115})$$

$$\kappa^2 = 8\pi\beta\gamma\eta = \frac{\pi\beta N_A \gamma c}{125} \quad (\text{II. 116})$$

$$-\varepsilon = \ln \left[\frac{\alpha}{1-\alpha} \right] \quad (\text{II. 117})$$

The details of the calculations are presented in the 1978 paper [322]. The shortcomings of the previous equations have been rectified in the present equation that is also more general than the previous equations and can be used for higher concentrations (0.1 N in aqueous solutions).

II. 7. 3. LEE-WHEATON CONDUCTANCE EQUATION

As Fuoss 1978 conductance equation contained a boundary condition error, [323,324] Fuoss introduced a slight modification to his model [325,326]. According to him, the ion pairs (ion approaching with their Gurney co-sphere) are divided into two categories- contact pairs (with no contribution to conductance) and solvent separated ion pairs (which can only contribute to the net transfer of charge). To rectify the boundary errors contained in Fuoss 1978 conductance equation, Lee-Wheaton [327] in the same year described in the derivation of a new conductance equation, based on the Gurney co-sphere model and henceforth the new equation is referred to as the Lee-Wheaton equation [328]. The conductance data were analyzed by means of the Lee-Wheaton conductance equation [329] in the form:

$$A = \alpha_i \left[\frac{A_o \{1 + C_1 \beta \kappa + C_2 (\beta \kappa)^2 + C_3 (\beta \kappa)^3\}}{-\frac{\rho \kappa}{1 + \kappa R} \left\{ 1 + C_4 \beta \kappa + C_5 (\beta \kappa)^2 + \frac{\kappa R}{12} \right\}} \right] \quad (\text{II. 118})$$

The mass action law association [330] is

$$K_{A,c} = \frac{(1-\alpha_i)\gamma_A}{\alpha_i^2 c_i \gamma_{\pm}^2} \quad (\text{II. 119})$$

and the equation for the mean ionic activity coefficient:

$$\gamma_{\pm} = \exp \left[-\frac{q\kappa}{1 + \kappa R} \right] \quad (\text{II. 120})$$

where C_1 to C_5 are least square fitting coefficients as described by Pethybridge and Taba [331], A_o is the limiting molar conductivity, $K_{A,c}$, is the association constant, α_i is the dissociation degree, q is the Bjerrum parameter and γ the activity coefficient and $\beta = 2q$

. The distance parameter R is the least distance that two free ions can approach before they merge into ion pair. The Debye parameter κ , the Bjerrum parameter q and ρ are defined by the expressions:[332]

$$\kappa = 16000\pi N_A q c_i \alpha_i \quad (\text{II. 121})$$

$$q = \frac{e^2}{8\epsilon_o \epsilon_r \kappa T} \quad (\text{II. 122})$$

$$\rho = \frac{F e}{299.79 \times 3\pi\eta} \quad (\text{II. 123})$$

where the symbols have their usual significance [333].

The equation (II. 115) was resolved by an iterative procedure. For a definite R value the initial value of A_o and $K_{A,c}$, were obtained by the Kraus-Bray method.[333] The parameter A_o and $K_{A,c}$, were made to approach gradually their finest values by a sequence of alternating linearization and least squares optimizations by the Gauss - Siedel method [334] until satisfying the criterion for convergence. The best value of a parameter is the one when equation (II. 115) is best fitted to the experimental data corresponding to minimum standard deviation (σ_A) for a sequence of predetermined R value and standard deviation (σ_A) was calculated by the following equation:

$$\sigma_A^2 = \sum_{i=1}^n \frac{[A_{i(calc)} - A_{i(obs)}]^2}{n - m} \quad (\text{II. 124})$$

where n is the number of experimental points and m is the number of fitting parameters. The conductance data were investigated by fixing the distance of closest approach R with two parameter fit ($m=2$). For the electrolytes with no significant minima observed in the σ_A versus R curves, the R values were arbitrarily preset at the centre to centre distance of solvent-separated pair:

$$R = a + d \quad (\text{II. 125})$$

where $a = r_c^+ + r_c^-$, i.e., the sum of the crystallographic radii of the cation and anion and d is the average distance consequent to the side of a cell occupied by a solvent molecule. The definitions of d and related terms are described in the literature [335]. R was generally varied by a step 0.1 \AA and the iterative process was continued with equation (115).

II. 7. 4. LIMITING EQUIVALENT CONDUCTANCE

The limiting equivalent conductance of an electrolyte can be easily determined from the theoretical equations and experimental observations. At infinite dilutions, the motion of an ion is limited solely by the interactions with the surrounding solvent molecules as the ions are infinitely apart. Under these conditions, the validity of Kohlrausch's law of independent migration of ions is almost axiomatic. Thus:

$$\Lambda_0 = \lambda_o^+ + \lambda_o^- \quad (\text{II. 126a})$$

At present, limiting equivalent conductance is the only function which can be divided into ionic components using experimentally determined transport number of ions, i.e.,

$$\lambda_o^+ = t_+ \Lambda_0 \quad \text{and} \quad \lambda_o^- = t_- \Lambda_0 \quad (\text{II. 126b})$$

Thus, from accurate value of λ_o of ions it is possible to separate the contributions due to cations and anions in the solute-solvent interactions. However, accurate transference number determinations are limited to few solvents only.

In the absence of experimentally measured transference numbers it would be useful to develop indirect methods to obtain the ionic limiting equivalent conductances in solvents for which experimental transference numbers are not yet available. Various attempts were made to develop indirect methods to obtain the limiting ionic equivalent conductance, in ionic solvents for which experimental transference numbers are not yet available.

The method has been summarized by Krumgalz [336,337] and some important points are mentioned as follows:

(i) Walden equation[338]

$$(\lambda_o^\pm)_{\text{water}}^{25} \cdot \eta_{\text{o,water}} = (\lambda_o^\pm)_{\text{acetone}}^{25} \cdot \eta_{\text{o,acetone}} \quad (\text{II. 127})$$

(ii) $(\lambda_{\text{o,pic}} \cdot \eta_{\text{o}}) = 0.267$, $\lambda_{\text{o,Et}_4\text{N}^+} \cdot \eta_{\text{o}} = 0.269$ [338,339] (II. 128)

$$\text{based on } \Lambda_{\text{o,Et}_4\text{N}_{\text{pic}}} = 0.563$$

Walden considered the products to be independent of temperature and solvent. However, the $\Lambda_{\text{o,Et}_4\text{N}_{\text{pic}}}$ values used by Walden were found to differ considerably from

the data of subsequent more precise studies and the values of (ii) are considerably different for different solvents.

$$(iii) \quad \lambda_o^{25}(\text{Bu}_4\text{N}^+) = \lambda_o^{25}(\text{Ph}_4\text{B}^-) \quad (\text{II. 129})$$

The equality holds good in nitrobenzene and in mixture with CCl_4 but not realized in methanol, acetonitrile and nitromethane.

$$(iv) \quad \lambda_o^{25}(\text{Bu}_4\text{N}^+) = \lambda_o^{25}(\text{Bu}_4\text{B}^-) [340] \quad (\text{II. 130})$$

The method appears to be sound as the negative charge on boron in the Bu_4B^- ion is completely shielded by four inert butyl groups as in the Bu_4N^+ ion while this phenomenon was not observed in case of Ph_4B^- .

(v) The equation suggested by Gill[341,342] is:

$$\lambda_o^{25}(R_4N^+) = \frac{zF^2}{6\pi N_A \eta_o [r_i - (0.0103\varepsilon_o + r_y)]} \quad (\text{II. 131})$$

where Z and r_i are the charge and crystallographic radius of proper ion, respectively; η_o and ε_o are solvent viscosity and dielectric constant of the medium, respectively; r_y = adjustable parameter taken equal to 0.85 Å and 1.13 Å for dipolar non-associated solvents and for hydrogen bonded and other associated solvents respectively.

However, large discrepancies were observed between the experimental and calculated values [336]. In a paper, [337] Krumgalz examined the Gill's approach more critically using conductance data in many solvents and found the method reliable in three solvents e.g. butan-1-ol, acetonitrile and nitromethane.

$$(vi) \quad \lambda_o^{25}[(i-Am)_3 \text{BuN}^+] = \lambda_o^{25}(\text{Ph}_4\text{B}^-) [343] \quad (\text{II. 132})$$

It has been found from transference number measurements that the $\lambda_o^{25}[(i-Am)_3 \text{BuN}^+]$ and $\lambda_o^{25}(\text{Ph}_4\text{B}^-)$ values differ from one another by 1%.

$$(vii) \quad \lambda_o^{25}(\text{Ph}_4\text{B}^-) = 1.01\lambda_o^{25}[(i-Am)_4 \text{B}^-] [344] \quad (\text{II. 133})$$

The value is found to be true for various organic solvents.

Krumgalz suggested a method for determining the limiting ion conductance in organic solvents. The method is based on the fact that large tetraalkyl (aryl) onium ions are not solvated in organic solvents due to the extremely weak electrostatic interactions between solvent molecules and the large ions with low surface charge density and this phenomenon can be utilized as a suitable model for apportioning Λ_0 values into ionic components for non-aqueous electrolytic solutions.

Considering the motion of solvated ion in an electrostatic field as a whole, it is possible to calculate the radius of the moving particle by the Stokes equation:

$$r_s = \frac{|z|F^2}{A\pi\eta_0\lambda_o^\pm} \quad (\text{II. 134})$$

where A is a coefficient varying from 6 (in the case of perfect sticking) to 4 (in case of perfect slipping). Since the r_s values, the real dimension of the non-solvated tetraalkyl (aryl) onium ions must be constant, we have:

$$\lambda_o^\pm\eta_0 = \text{constant} \quad (\text{II. 135})$$

This relation has been verified using λ_o^\pm values determined with precise transference numbers. The product becomes constant and independent of the chemical nature of the organic solvents for the $i\text{-Am}_4\text{B}^-$, Ph_4As^+ , Ph_4B^- ions and for tetraalkylammonium cation starting with Et_4N^+ . The relationship can be well utilized to determine λ_o^\pm of ions in other organic solvents from the determined Λ_0 values

II. 7. 5. SOLVATION

Various types of interactions exist between the ions in solutions. These interactions result in the orientation of the solvent molecules towards the ion. The number of solvent molecules that are involved in the solvation of the ion is called *solvation number*. If the solvent is water, this is called *hydration number*. Solvation region can be classified as primary and secondary solvation regions. Here we are concerned with the primary solvation region. The primary solvation number is defined as the number of solvent molecules which surrender their own translational freedom and remain with

the ion, tightly bound, as it moves around, or the number of solvent molecules which are aligned in the force field of the ion.

If the limiting conductance of the ion i of charge Z_i is known, the effective radius of the solvated ion can be determined from Stokes' law. The volume of the solvation shell is given by the equation.

$$V_s = \left(\frac{4\pi}{3}\right)(r_s^3 - r_c^3) \quad (\text{II. 136})$$

where r_c is the crystallographic radius of the ion. The solvation number n_s would then be obtained from

$$n_s = \frac{V_s}{V_0} \quad (\text{II. 137})$$

Assuming Stokes' relation to hold well, the ionic solvated volume can be obtained, because of the packing effects, [345] from

$$V_s^o = 4.35r_s^3 \quad (\text{II. 138})$$

where V_s^o is expressed in $\text{mol}\cdot\text{lit}^{-1}$ and r_s in angstroms. However, this method is not applicable to ions of medium size though a number of empirical and theoretical corrections [346-349] have been suggested in order to apply it to most of the ions.

II. 7. 6. STOKES' LAW AND WALDEN'S RULE

The starting point for most evaluations of ionic conductances is Stokes' law that states that the limiting ionic Walden product (the product of the limiting ionic conductance and solvent viscosity) for any singly charged, spherical ion is as function only of the ionic radius and thus, under normal conditions, is constant. The limiting conductances λ_o^i of a spherical ion of radius R_i moving in a solvent of dielectric continuum can be written, according to Stokes' hydrodynamics, as

$$\lambda_o^i = \frac{|z_i e| e F}{6\pi\eta_o R_i} = \frac{0.819|z_i|}{\eta_o R_i} \quad (\text{II. 139})$$

where η_o = macroscopic viscosity by the solvent in poise, R_i is in angstroms. If the radius R_i is assumed to be the same in every organic solvent, as would be the case, in case of bulky organic ions, we get:

$$\lambda_o^i \eta_o = \frac{0.819 z_i}{R_i} = \text{constant} \quad (\text{II. 140})$$

This is known as the Walden rule [350,351]. The effective radii obtained using this equation can be used to estimate the solvation numbers. However, Stokes' radii failed to give the effective size of the solvated ions for small ions.

Robinson and Stokes, [352] Nightingale [349] and others [353-355] have suggested a method of correcting the radii. The tetraalkylammonium ions were assumed to be not solvated and by plotting the Stokes' radii against the crystal radii of those large ions, a calibration curve was obtained for each solvent. However, the experimental results indicate that the method is incorrect as the method is based on the wrong assumption of the invariance of Walden's product with temperature. The idea of microscopic viscosity [356] was invoked without much success [357,358] but it has been found that:

$$\lambda_o^i \eta_o = \text{constant} \quad (\text{II. 141})$$

where i is usually 0.7 for alkali metal or halide ions and $i = 1$ for the large ions [359,360]. Gill [361] has pointed out the inapplicability of the Zwanzig theory [362] of dielectric friction for some ions in non-aqueous and mixed solvents and has proposed an empirical modification of Stokes' Law accounting for the dielectric friction effect quantitatively and predicts actual solvated radii of ions in solution. This equation can be written as:

$$r_i = \frac{|z| F^2}{6\pi N_A \eta_o \lambda_o^i} + 0.0103D + r_y \quad (\text{II. 142})$$

where r_i is the actual solvated radius of the ion in solution and r_y is an empirical constant dependent on the nature of the solvent [361,362].

The dependence of Walden product on the dielectric constant led Fuoss to consider the effect of the electrostatic forces on the hydrodynamics of the system. Considering the excess frictional resistance caused by the dielectric relaxation in the solvent caused by ionic motion, Fuoss proposed the relation:

$$\lambda_o^i = \frac{F e |z_i|}{6\pi R_\infty} \left(\frac{1+A}{\epsilon R_\infty^2} \right) \quad (\text{II. 143})$$

$$\text{or,} \quad R_i = R_\infty + \frac{R}{\infty} \quad (\text{II. 144})$$

where R_∞ is the hydrodynamic radius of the ion in a hypothetical medium of dielectric constant where all electrostatic forces vanish and A is an empirical constant.

Boyd [347] gave the expression:

$$\lambda_o^i = \frac{Fe|z_i|}{6\pi\eta_o r_i \left[\left(1 + \frac{2}{27}\pi\eta_o\right) \cdot \left(\frac{z_i^2 e^2 \tau}{r_i^4 \epsilon_o}\right) \right]} \quad (\text{II. 145})$$

by considering the effect of dielectric relaxation in ionic motion; τ is the Debye relaxation time for the solvent dipoles. Zwanzig [348] treated the ion as a rigid sphere of radius r_i moving with a steady state viscosity, V_i through a viscous incompressible dielectric continuum. The conductance equation suggested by Zwanzig is:

$$\lambda_o^i = \frac{z_i^2 eF}{\left[A_V \pi \eta_o r_i + A_D \left\{ \frac{z_i^2 e^2 (\epsilon_r^o - \epsilon_r^\infty) \tau}{\epsilon_r^o (2\epsilon_r^o + 1) r_i^3} \right\} \right]} \quad (\text{II. 146})$$

where ϵ_r^o and ϵ_r^∞ are the static and limiting high frequency (optical) dielectric constants. $A_V = 6$ and $A_D = 3/8$ for perfect sticking and $A_V = 4$ and $A_D = 3/4$ for perfect slipping. It has been found that Born's and Zwanzig's equations are very similar and both may be written in the form:

$$\lambda_o^i = \frac{Ar_i^3}{r_i^4 + B} \quad (\text{II. 147})$$

The theory predicts [363] that λ_o^i passes through a maximum of $27^{\frac{1}{4}} A / 4B^{\frac{1}{4}}$ at $r_i = (3B)^{1/4}$. The phenomenon of maximum conductance is well known. The relationship holds good to a reasonable extent for cations in aprotic solvents but fails in case of anions. The conductance, however, falls off rather more rapidly than predicted with increasing radius. For comparison with results in different solvents, the equation (II. 146) can be rearranged as: [364]

$$\frac{z_i^2 eF}{\lambda_o^i \eta_o} = \frac{A_V \pi r_i + A_D z_i^2}{r_i^3} \cdot \frac{e^2 (\epsilon_r^o - \epsilon_r^\infty)}{\epsilon_r^o (2\epsilon_r^o + 1)} \left(\frac{\tau}{\eta_o} \right) \quad (\text{II. 148})$$

$$L^* = A_V \pi r_i + \frac{A_D z_i^2}{r_i^3 P^*} \quad (\text{II. 149})$$

In order to test Zwanzig's theory, the equation (II. 148) was applied for Me_4N^+ and Et_4N^+ in pure aprotic solvents like methanol, ethanol, acetonitrile, butanol and pentanol. [363-368] Plots of L^* against the solvent function P^* were found to be straight line. It is noted that relaxation effect is not the predominant factor affecting ionic mobility and these mobility differences could be explained quantitatively if the microscopic properties of the solvent, dipole moment and free electron pairs were considered the predominant factors in the deviation from the Stokes' law.

It is found that the Zwanzig's theory is successful for large organic cations in aprotic media where solvation is likely to be minimum and where viscous friction predominates over that caused by dielectric relaxation. The theory breaks down whenever the dielectric relaxation term becomes large, i.e., for solvents of high P^* and for ions of small r_i . Like any continuum theory Zwanzig has the inherent weakness of its inability to account for the structural features, [364] e.g.,

(i) It does not allow for any correlation in the orientation of the solvent molecules as the ion passes by and this may be the reason why the equation is not applicable to the hydrogen-bonded solvents [365].

(ii) The theory does not distinguish between positively and negatively charged ions and therefore, cannot explain why certain anions in dipolar aprotic media possess considerably higher molar concentrations than the fastest cations.

The Walden product in case of mixed solvents does not show any constancy but it shows a maximum in case of DMF + water and DMA + water [363-373] mixtures and other aqueous binary mixtures [373-378]. To derive expressions for the variation of the Walden product with the composition of mixed polar solvents, various attempts [379] have been made with different models for ion-solvent interactions but no satisfactory expression has been derived taking into account all types of ion-solvent interactions because

(i) it is difficult to include all types of interactions between ions as well as solvents in a single mathematical expression, and

(ii) it is not possible to account for some specific properties of different kinds of ions and solvent molecules.

Ions moving in a dielectric medium experience a frictional force due to dielectric loss arising from ion-solvent interactions with the hydrodynamic force. Though Zwanzig's expression accounts for a change in Walden product with solvent composition but does not account for the maxima. According to Hemmes [380] the major deviations in the Walden products are due to the variation in the electrochemical equilibrium between ions and solvent molecules of mixed polar solvent composition. In cases where more than one types of solvated complexes are formed, there should be a maximum and/or a minimum in the Walden product. This is supported from experimental observations. Hubbard and Onsager [380] have developed the kinetic theory of ion-solvent interaction within the framework of continuum mechanics where the concept of kinetic polarization deficiency has been introduced. However, quantitative expression is still awaited. Further, improvements [381-383] naturally must be in terms of (i) sophisticated treatment of dielectric saturation, (ii) specific structural effects involving ion-solvent interactions. From the discussion, it is apparent that the problem of molecular interactions is intriguing as well as interesting. It is desirable to explore this problem using different experimental techniques. We have, therefore, utilized four important methods, viz., volumetric, viscometric, interferometric and conductometric for the physico-chemical studies in different solvent media.

II. 7. 7. THERMODYNAMICS OF ION-PAIR FORMATION

The standard Gibbs energy changes (ΔG°) for the ion- association process can be calculated from the equation

$$\Delta G^\circ = -RT \ln K_A \quad (\text{II. 150})$$

The values of the standard enthalpy change, ΔH° and the standard entropy change, ΔS° , can be evaluated from the temperature dependence of values as follows;

$$\Delta H^\circ = -T^2 \left[\frac{d(\Delta G^\circ / T)}{dT} \right]_p \quad (\text{II. 151})$$

$$\Delta S^{\circ} = -T^2 \left[\frac{d(\Delta G^{\circ})}{dT} \right]_P \quad (\text{II. 152})$$

The values can be fitted with the help of a polynomial of the type:

$$\Delta G^{\circ} = c_0 + c_1(298.15 - T) + c_2(298.15 - T)^2 \quad (\text{II. 153})$$

And the coefficients of the fits can be compiled together with the $\sigma\sigma$ % values of the fits. The standard values at 298.15 K are then:

$$\Delta G_{298.15}^{\circ} = c_0 \quad (\text{II. 154})$$

$$\Delta S_{298.15}^{\circ} = c_1 \quad (\text{II. 155})$$

$$\Delta H_{298.15}^{\circ} = c_0 + 298.15c_1 \quad (\text{II. 156})$$

The major factors which oversee the standard entropy of ion-association of electrolytes are:

- (i) the size and shape of the ions,
- (ii) charge density on the ions,
- (iii) electrostriction of the solvent molecules around the ions,
- (iv) penetration of the solvent molecules inside the space of the ions, and the influence of these factors are discussed later.

The non-columbic part of the Gibbs energy ΔG° can also be calculated using the following equation:

$$\Delta G^{\circ} = N_A W_{\pm} \quad (\text{II. 157})$$

$$K_A = \left(\frac{4\pi N_A}{1000} \right) \int_a^R r^2 \exp\left(\frac{2q}{r} - \frac{W_{\pm}}{kT} \right) dr \quad (\text{II. 158})$$

where the symbols have their usual significance. The quantity $2q/r$ is Columbic part of the interionic mean force potential and W_{\pm} is its non-columbic part.

II. 7. 8 TRIPLE-ION FORMATIONS FROM ELECTRICAL CONDUCTANCE

While solutions of electrolytes in solvents of high and of intermediate dielectric constant have been studied extensively, similar solutions in solvents of very low dielectric constant have not been investigated systematically. We know only that such solutions generally are poor conductors and that the equivalent conductance falls rapidly with decreasing concentration. In addition to a number of isolated observations

on the conductance of solutions in benzene [384] and several series of measurements relating to the conductance of complex compounds in various solvents at relatively high concentrations, [385] the literature includes two important papers by Walden and his co-workers, [386] who investigated the conductance of a variety of *salts* in benzene, ether, carbon tetrachloride and similar solvents. In solvents of somewhat higher dielectric constant, the conductance passes through a minimum at moderate concentration and thereafter increases.

The influence of the dielectric constant on conductance is satisfactorily accounted for by the interionic attraction theory in solvents of high dielectric constant, it is not known to what extent interionic forces are primarily concerned in solvents of low dielectric constant. Due to the deviation of the conductometric curves from linearity in case of low dielectric constant solvents, the conductance data have been analyzed by the classical Fuoss-Kraus theory of triple-ion formation [387,388] in the form

$$\Lambda g(c)\sqrt{c} = \frac{\Lambda_0}{\sqrt{K_p}} + \frac{\Lambda_0^T K_T}{\sqrt{K_p}} \left(1 - \frac{\Lambda}{\Lambda_0}\right) c \quad (\text{II.159})$$

where $g(c)$ is a factor that lumps together all the intrinsic interaction terms and is defined by

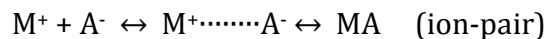
$$g(c) = \frac{\exp\{-2.303 \beta' (c\Lambda)^{0.5} / \Lambda_0^{0.5}\}}{\{1 - S(c\Lambda)^{0.5} / \Lambda_0^{1.5}\} (1 - \Lambda / \Lambda_0)^{0.5}} \quad (\text{II.160})$$

$$\beta' = 1.8247 \times 10^6 / (\epsilon_r T)^{1.5} \quad (\text{II.161})$$

$$S = \alpha \Lambda_0 + \beta = \frac{0.8204 \times 10^6}{(\epsilon_r T)^{1.5}} \Lambda_0 + \frac{82.501}{\eta(\epsilon_r T)^{0.5}} \quad (\text{II.162})$$

In all the above usable equations, the Λ_0 term signify the sum of the molar conductance of the simple ions at infinite dilution, the Λ_0^T is the sum of the conductance value of the two possible formation of triple-ions. Where the constants as K_P and K_T are implies that the ion-pair and triple-ion formation constants respectively and S is the limiting Onsager coefficient. If K_P is greater than K_T , indicates the electrolytes are exists as ion-pair with a major portion and as triple-ion with a minor portion. We know that the electrostatic ionic interactions are very large due to the higher force field effect, for very low relative permittivity solvents, i.e., $\epsilon_r < 10$. Therefore the formed ion-pairs were attracted by the free movable cations or anions present in the solution medium; as the

distance of the closest approach of the ions becomes minimum, these results in the formation of triple-ions, which acquires the charge of the respective ions, attracted from the solution bulk [388,389] i.e.;



where the symbols M^+ and A^- are implies for the cation and anions respectively. The effect of ternary association [390] thus clearly explained the non-linearity of the conductometric curve. According to the consequence of this ternary association, some formative non-conducting species MA, removed from solution and replaces by triple-ions which increase the conductance values evident by non-linearity observed in conductance curves.

Additionally, the ion-pair and triple-ion concentrations, C_P and C_T , respectively, at the minimum molar concentration of the salt solution have also been calculated using the K_P and K_T value by following set of equations [391]

$$\alpha = 1 / (K_P^{1/2} \cdot C^{1/2}) \quad (\text{II.163})$$

$$\alpha_T = (K_T / K_P^{1/2}) C^{1/2} \quad (\text{II.164})$$

$$C_P = C(1 - \alpha - 3\alpha_T) \quad (\text{II.165})$$

$$C_T = (K_T / K_P^{1/2}) C^{3/2} \quad (\text{II.166})$$

At this point, the fraction of ion-pairs (α) and triple-ions (α_T), present in the salt-solutions. From the appraisal of comparison of the C_P and C_T values, if C_P is higher with respect to C_T ; indicates the major portion of ions are present as ion-pair even at high concentration and a small fraction exist as triple-ion.

Using the K_P values, the interionic distance parameter a_{IP} has been calculated with the aid of the Bjerrum's theory of ionic association [390] in the form

$$K_P = \frac{4\pi N_A}{1000} \left[\frac{e^2}{\epsilon_r K T} \right]^3 Q(b) \quad (\text{II.167})$$

$$Q(b) = \int_2^b y^{-4} \exp(y) dy \quad (\text{II.168})$$

$$b = \frac{e^2}{a_{IP} \epsilon_r K T} \quad (\text{II.169})$$

The $Q(b)$ and b values have been calculated by the literature procedure [387].

The interionic distance a_{TI} for the triple ion can be calculated using the expressions [389]

$$K_T = \frac{2\pi N_A a_{IP}^3}{1000} I(b_3) \quad (\text{II.170})$$

$$b_3 = \frac{e^2}{a_{TI} \epsilon_r K T} \quad (\text{II.171})$$

$I(b_3)$ is a double integral tabulated in the literature [388] for a range of values of b_3 . Since $I(b_3)$ is a function of a_{TI} , the a_{TI} values have been calculated by an iterative computer program. These values also suggested the small fraction exist as triple-ion formation compared to the ion-pair.

II. 7. 9. SOLVATION MODELS (SOME RECENT TRENDS)

The interactions between particles in chemistry have been based upon empirical laws- principally on Coulomb's law. This is also the basis of the attractive part of the potential energy used in the SchÖdinger equation. Quantum mechanical approach for ion-water interactions was begun by Clementi in 1970. A quantum mechanical approach to salvation can provide information on the energy of the individual ion-water interactions provided it is relevant to solution chemistry, because it concerns potential energy rather than the entropic aspect of salvation. Another problem in quantum approach is the mobility of ions in solution affecting salvation number and coordination number. However, the Clementi calculations concerned stationary models and cannot have much to do with the dynamic salvation numbers. Covalent bond formation enters little into the aqueous calculations; however, with organic solvents the quantum mechanical approaches to bonding may be essential. The trend pointing to the future is thus the molecular dynamics technique. In molecular dynamic approach, a limited number of ions and molecules and Newtonian mechanics of movement of all particles in solution is concerned. The foundation of such an approach is the knowledge of the intermolecular energy of interactions between a pair of particles. Computer simulation approaches may be useful in this regard and the last decade (1990-2000) witnessed some interesting trends in the development of solvation models and computer software. Based on a collection of experimental free energy of solvation data, C.J.

Cramer, D.G. Truhlar and co-workers from the University of Minnesota, U.S.A. constructed a series of solvation models (SM1-SM5 series) to predict and calculate the free energy of solvation of a chemical compound [392-397]. These models are applicable to virtually any substance composed of H, C, N, O, F, P, S, Cl, Br and/or I. The only input data required are, molecular formula, geometry, refractive index, surface tension, Abraham's a (acidity parameter) and b (basicity parameter) values, and, in the latest models, the dielectric constants. The advantage of models like SM5 series is that they can be used to predict the free energy of self-solvation to better than 1 KJ/mole. These are especially useful when other methods are not available. One can also analyze factors like electrostatics, dispersion, hydrogen bonding, etc. using these tools. They are also relatively inexpensive and available in easy to use computer codes.

A. Galindo *et al.* [398,399] have developed Statistical Associating Fluid Theory for Variable Range (SAFT-VR) to model the thermodynamics and phase equilibrium of electrolytic aqueous solutions. The water molecules are modeled as hard spheres with four short-range attractive sites to account for the hydrogen-bond interactions. The electrolyte is modeled as two hard spheres of different diameter to describe the anion and cation. The Debye-Hückel and mean spherical approximations are used to describe the interactions. The relative permittivity becomes very close to unity, especially when the mean spherical approximation is used, indicating a good description of the solvent. E. Bosch *et al.*[400] of the University of Barcelona, Spain, have compared several "Preferential Solvation Models" specially for describing the polarity of dipolar hydrogen bond acceptor-cosolvent mixture.

II. 7. 10. CONDUCTANCE SOME RECENT TRENDS

Recently Blum, Turq and coworkers [401,402] have developed a mean spherical approximation (MSA) version of conductivity equations. Their theory starts from the same continuity and hydrodynamic equations used in the more classical treatment; however, an important difference exists in the use of MSA expressions for the equilibrium and structural properties of the electrolytic solutions. Although the differences in the derivation of the classical and MSA conductivity theories seem to be relatively small, it has been claimed that the performance of MSA equation is better

with a much wider concentration range than that covered by the classical equations. However, no through study of the performance of the new equation at the experimental uncertainty level of conductivity measurement is yet available in the literature, except the study by Bianchi *et al.* [403] They compared the results obtained using the old and new equations in order to evaluate their capacity to describe the conductivity of different electrolytic solutions. In 2000, Chandra and Bagchi [404] developed a new microscopic approach to ionic conductance and viscosity based on the mode coupling theory. Their study gives microscopic expressions of conductance and viscosity in terms of static and dynamic structural factors of charge and number density of the electrolytic solutions. They claim that their new equation is applicable at low as well as at high concentrations and it describes the cross over from low to high concentration smoothly. Debye-Huckel, Onsager and Falkenhagen expressions can be derived from this self-consistent theory at very low concentrations. For conductance, the agreement seems to be satisfactory up to 1 (M).

II. 8. REFRACTIVE INDEX

Optical data (refractive index, n_D) provide interesting information related to molecular interactions and structure of the solutions, as well as complementary data on practical procedures, such as concentration measurement or estimation of the extent of salvation of electrolytes/non-electrolytes in liquid systems [394,395].

The light bending property is a result of variation of the velocity with which light is transmitted. Refractive index (n_D) of liquid, changes not only with the wave length of light used but also with the temperature. Molar refractions are influenced by the arrangement of atoms in the molecule or by factors like unsaturation, ring closure etc. linear optical properties of liquids and liquid mixtures have been extensively studied to obtain information on their physical, chemical, and molecular properties. Fialkov *et al.* [405,406] stated that the refractive index is an additive property of pure components when composition is expressed in terms of volume fraction. Several researchers have estimated the refractivity of liquid systems using the well known mixing rules viz. Arago-Biot, Newton, Heller, Gladstone-Dale, Eyring-John, Eykman, Lorentz-Lorenz, Weiner and Oster relations [407-410]. These empirical approaches for calculating the

excess properties attempt to explain the non-ideality in terms of specific and non-specific intermolecular interactions. Refractive index or refractivity is a property of intrinsic interest in the fields of pharmaceutical research such as formulation of eye preparations, in optoelectronic and photonic applications.

The ratio of the speed of light in a vacuum to the speed of light in another substance is defined as the index of refraction (n_D) for the substance.

$$\text{Refractive Index } (n_D) = \frac{\text{Speed of light in vacuum}}{\text{Speed of light in solution systems}}$$

Whenever light changes speed as it crosses a boundary from one medium into another, its direction of travel also changes, i.e., it is refracted. The relationship between light's speed in the two mediums (V_A and V_B), the angles of incidence ($\sin \theta_A$) and refraction ($\sin \theta_B$) and the refractive indexes of the two mediums (n_A and n_B) is shown below:

$$\frac{V_A}{V_B} = \frac{\sin \theta_A}{\sin \theta_B} = \frac{n_B}{n_A} \quad (\text{II. 172})$$

Thus, it is not necessary to measure the speed of light in a sample in order to determine its index of refraction. Instead, by measuring the angle of refraction, and knowing the index of refraction of the layer that is in contact with the sample, it is possible to determine the refractive index of the sample quite accurately.

The refractive index of mixing can be correlated by the application of a composition-dependent polynomial equation. Molar refractivity, was obtained from the Lorentz-Lorenz relation [411,412] by using, n_D experimental data according to the following expression

$$R_M = \frac{(n_D^2 - 1)}{(n_D^2 + 2)} \left(\frac{M}{\rho} \right) \quad (\text{II. 173})$$

where M is the mean molecular weight of the mixture and ρ is the mixture density. n_D can be expressed as the following:

$$n_D = \sqrt{\frac{(2A+1)}{(1-A)}} \quad (\text{II. 174})$$

where A is given by:

$$A = \left[\left\{ \frac{(n_1^2 - 1)}{(n_1^2 + 2)} (1/\rho_1) \right\} - \left\{ \frac{(n_1^2 - 1)}{(n_1^2 + 2)} (w_2/\rho_1) \right\} + \left\{ \frac{(n_2^2 - 1)}{(n_2^2 + 2)} (w_2/\rho_2) \right\} \rho \right] \quad (\text{II. 175})$$

where n_1 and n_2 are the pure component refractive indices, w_j the weight fraction, ρ the mixture density, and ρ_1 and ρ_2 the pure component densities.

The molar refractivity deviation is calculated by the following expression:

$$\Delta R = R - \phi_1 R_1 - \phi_2 R_2 \quad (\text{II. 176})$$

where ϕ_1 and ϕ_2 are volume fractions and R , R_1 , and R_2 the molar refractivity of the mixture and of the pure components, respectively.

The deviations of refractive index were used for the correlation of the binary solvent mixtures:

$$\Delta n_D = n_D - x_1 n_{D1} - x_2 n_{D2} \quad (\text{II. 177})$$

where Δn_D is the deviation of the refractive index for this binary system and n_D , n_{D1} , and n_{D2} are the refractive index of the binary mixture, refractive index of component-1, and refractive index of component-2, respectively, 'x' is the mole fractions.

The computed deviations of refractive indices of the binary mixtures are fitted using the following Redlich-Kister expression [413].

$$\Delta n_{Dew} = w_e w_w \sum_{P=0}^S B_p (w_e w_w)^P \quad (\text{II. 178})$$

where B_p are the adjustable parameters obtained by a least squares fitting method, w is the mass fraction, and S is the number of terms in the polynomial.

In case of salt-solvent solution the binary systems were fitted to polynomials of the form:

$$n_{Ds,sol} = n_{Dsol} + \sum_{i=1}^N A_i m^i \quad (\text{II. 179})$$

where $n_{Ds,sol}$ is the refractive index of the salt + solvent system and n_{Dsol} is the refractive index of the solvent respectively, m is the molality of the salt in the solution, A_i are the fitting parameters, and N is the number of terms in the polynomial.

For the ternary systems of the salt + solvent-1 + solvent-2 solutions a polynomial expansion [414] has been employed, similar to that obtained for the salt + solvent solutions was used to represent ternary refractive indices:

$$n_D = n_{Dw} + \sum_{i=1}^P C_i m^i \quad (\text{II. 180})$$

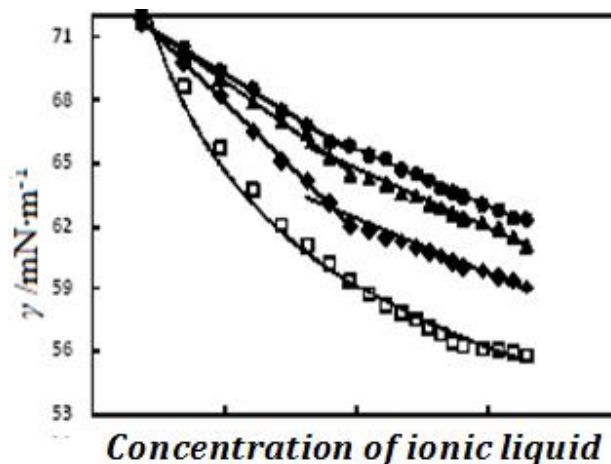
where n_D is the refractive index of the ternary solution, C_i are the parameters, and P is the number of terms in the polynomial.

There is no general rule that states how to calculate a refractivity deviation function. However, the molar refractivity is isomorphic to a volume for which the ideal activities may be expressed in terms of mole fraction: in this case smaller deviations occur but data are more scattered due to the higher sensitivity of the expression to rounding errors in the mole fraction. For the sake of completeness, both calculations of refractivity deviation function, molar refractivity deviation was fitted to a Redlich and Kister-type expression [413] and the adjustable parameters and the relevant standard deviation σ are calculated for the expression in terms of volume fractions and in terms of mole fractions, respectively.

II. 9. SURFACE TENSION

The surface tension experiments were done by platinum ring detachment method by means of a Tensiometer (K9, KRUSS; Germany) at the experimental temperature. The accuracy of the measurement was within $\pm 0.1 \text{ mN.m}^{-1}$. Temperature of the system has been maintained via circulating auto-thermostated water through a double-wall glass vessel containing the solution.

In case of inclusion complex formation study, the trends of the curves in surface tensions (γ) against concentration (molality) are similar to that of aq. Ionic liquid solution, but each curve clearly shows a break point in surface tension at a certain concentration, that is, the γ values increases with corresponding concentration, (Figure 8) reach a certain point (break point), and then become approximately steady, which obviously indicates the formation of inclusion complex.



The concentrations at which the inclusion occurred (or the break point of the surface tension) have been calculated by solving the equation of two straight lines. For instance, in case of the taken ionic liquid in $w_1=0.001$ mass fraction of α -cyclodextrin

$$\gamma = -307.8 c + 74.06$$

$$\gamma = -134.0 c + 67.72$$

$\gamma = 62.84$ and $c = 0.0364$.

II. 10. FTIR SPECTROSCOPY

The spectroscopic study has been established by the investigation of FTIR spectroscopy. The study has been taking into account to qualitative interpreting the molecular as well as ionic association of the electrolytes in the solutions. FTIR spectroscopy is one of the most appropriate optical properties which qualitatively interpreted the nature, mode, manner of the electrolytes and non-electrolytes in the solution system, eventually it also is able to give information about the configurational structure of the solute or solvents present in the solutions.

Infrared (IR) spectroscopy is one of the most widespread spectroscopic techniques used by organic and inorganic chemists. Simply, it is the absorption measurement of different IR frequencies by a sample positioned in the path of an IR beam. The main aspiration of IR spectroscopic analysis is to determine the chemical functional groups in the sample. Different functional groups absorb characteristic frequencies of IR radiation. Using assorted sampling accessories, IR spectrometers can accept a wide range of sample types such as gases, liquids, and solids. Thus, IR

spectroscopy is an imperative and popular tool for structural elucidation and compound identification.

Infrared radiation spans a section of the electromagnetic spectrum having wavenumbers from approximately 13,000 to 10 cm^{-1} , or wavelengths from 0.78 to 1000 μm . It is hurdle by the red end of the visible region at high frequencies and the microwave region at low frequencies.

IR absorption positions are commonly presented as either wavenumbers (ν) or wavelengths (λ). Wavenumber defines the number of waves per unit length. Thus, wavenumbers are directly proportional to frequency, by way of the energy of the IR absorption. The wavenumber unit (cm^{-1} , reciprocal centimeter) is more commonly used in modern IR instruments that are linear in the cm^{-1} scale. In contrast, wavelengths are inversely proportional to frequencies and their associated energy. Presently, the recommended unit of wavelength is μm (micrometers), but μ (micron) is used in a few older literatures. Wavenumbers and wavelengths can be interconverted using the following equation:

$$\nu (\text{cm}^{-1}) = \frac{1}{\lambda (\mu\text{m})} \times 10^4 \quad (\text{II.181})$$

IR absorption information is generally presented in the form of a spectrum with wavelength or wavenumber like the x-axis and absorption intensity or percent transmittance as the y-axis.

Transmittance, T , is the ratio of radiant power transmitted via the sample (I) to the radiant power incident on the sample (I_0). Absorbance (A) be the logarithm to the base 10 of the reciprocal of the transmittance (T).

$$A = \log_{10}(1/T) = -\log_{10}(T) = -\log_{10}\left(\frac{I}{I_0}\right) \quad (\text{II.182})$$

The transmittance spectra afford better contrast between intensities of strong and weak bands, since transmittance ranges from 0 to 100% T whereas absorbance ranges from infinity to zero. The analyst should be conscious that the same sample will give quite diverse profiles for the IR spectrum, which is linear in wavenumber, and the

IR plot, which is linear in wavelength. It will appear as if various IR bands have been contracted or expanded.

The IR region is normally divided into three smaller areas: near IR, mid IR, and far IR.

	Near IR	Mid IR	Far IR
Wavenumber	13,000–4,000 cm^{-1}	4,000–200 cm^{-1}	200–10 cm^{-1}
Wavelength	0.78–2.5 μm	2.5–50 μm	50–1,000 μm

This chapter focuses on the most frequently used mid IR region, between 4000 and 400 cm^{-1} (2.5 to 25 μm).

From the discussion, it is apparent that the problem of molecular interactions is intriguing as well as interesting. It is desirable to attack this problem using different experimental techniques. We have, therefore, utilized five important methods, viz., volumetric, viscometric, interferometric, conductometric and refractometric as the quantitative and FT-IR spectroscopy as the qualitative analysis for the studies of the thermophysical, physicochemical, thermodynamics, transport properties occurring in different studied liquid systems. Utilizing the theoretical and experimental results we have employed all the studies for application in different fields.

II. 11. NMR SPECTROSCOPY

Nuclear magnetic resonance spectroscopy determines the physical and chemical properties of atoms or the molecules in which they are contained. It relies on the phenomenon of nuclear magnetic resonance and can afford detailed information about the structure, dynamics, reaction state and chemical environment of molecules. The intermolecular magnetic field around an atom in a molecule changes the resonance frequency, thus giving access to particulars of the electronic structure of a molecule. NMR spectra are unique, well-resolved, analytically tractable and often and often highly predictable for small molecules. Thus, in organic chemistry practice, NMR analysis is used to confirm the identity of a substance. Different functional groups are obviously distinguishable, and identical functional groups with different neighbouring substituents still give distinguishable signals. NMR has largely replaced traditional wet chemistry tests for instance color reagents for identification. A disadvantage is that a

relatively large amount, 2-50 mg, of a purified substance is required, although it may be recovered. Preferably, the sample should be dissolved in a solvent, because NMR analysis of solids entails a dedicated MAS machine and may not give equally well-resolved spectra. The timescale of NMR is relatively long, and thus it is not suitable for observing fast phenomena, producing only an average spectrum. Although large amounts of impurities do show on an NMR spectrum, better methods exist for detecting impurities, as NMR is inherently not very sensitive.

The chemical shift provides information about the structure of the molecule. The conversion of the raw data to this information is labeled as *assigning* the spectrum. For example, for the ^1H NMR spectrum for ethanol ($\text{CH}_3\text{CH}_2\text{OH}$) (Figure 8), one would expect signals at each of three specific chemical shifts: one for the CH_3 group, one for CH_2 group and one for the OH group. A typical CH_3 group has a shift around 1 ppm, a CH_2 attached to an OH has a shift of around 4 ppm and an OH has a shift anywhere from 2-6 ppm depending on the solvent used and the quantity of hydrogen bonding. While the O atom does draw electron density away from the attached H through their mutual sigma bond, the electron lone pairs on the O bathe the H in their shielding effect.

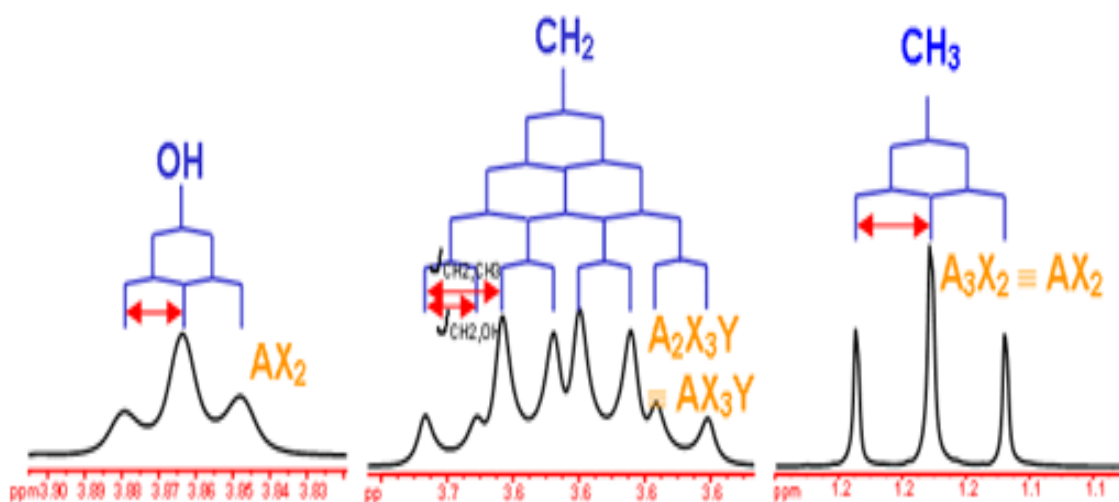


Figure 8: Expanded ^1H NMR spectrum of ethanol

CHAPTER-III

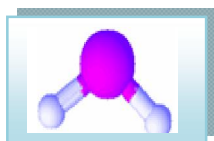
EXPERIMENTAL SECTION

III. 1 NAME, STRUCTURE, PHYSICAL PROPERTIES, PURIFICATION AND APPLICATIONS OF THE CHEMICALS USED IN THE RESEARCH WORK

III.1.1 SOLVENTS

The details of the aqueous and non-aqueous solvents used in the research work are given below:

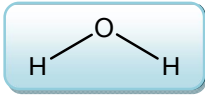
Water (H₂O):



Water is an all-pervading chemical essence is composed of hydrogen and oxygen and is indispensable for all known forms of life. In typical usage, water refers only to its liquid variety or state, but the substance also exists as solid state, ice, and a gaseous condition, water vapour or steam. Water is a good solvent and is often referred to as the universal solvent.

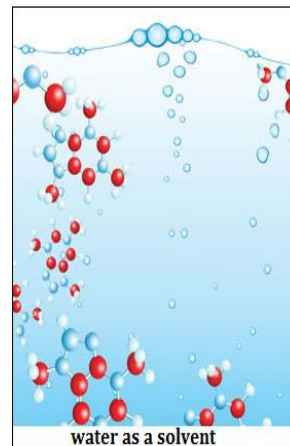
Source: Distilled water, distilled from fractional distillation method in Lab.

Purification: Water was first deionised and then distilled in an all glass distilling set along with alkaline KMnO₄ solution to eradicate any organic matter therein. The

WATER	
	
<i>Appearance</i>	:Liquid
<i>Molecular Formula</i>	:H ₂ O
<i>Molecular Weight</i>	:18.02 g·mol ⁻¹
<i>Boiling Point</i>	:373 K
<i>Melting Point</i>	:273 K
<i>Dielectric Constant</i>	:78.35 at 298.15K

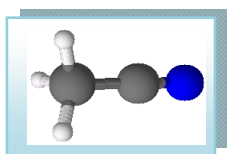
doubly distilled water was finally distilled using an all glass distilling set. Precautions were taken to prevent contamination from CO₂ and other impurities. The triply distilled water had specific conductance less than $1 \times 10^{-6} \text{ S}\cdot\text{cm}^{-1}$.

Application: Water is extensively used in chemical reactions as a solvent or reactant and fewer commonly as a solute or catalyst. In inorganic reactions, water is a common solvent, dissolving many ionic compounds. In recent times it has been a topic of research. Oxygen saturated supercritical water combusts organic pollutants proficiently. It is also used in various industries. It is a superb solvent, generally taken as the widespread solvent, due to the discernible polarity of the water molecule and its tendency to form hydrogen bonds



with other molecules. Life on earth totally depends on water. Not only a high percentage of living things, both plants and animals originate in water, all life on earth is thought to have arisen from water and the bodies of all living organisms are composed chiefly of water. About 70 to 90 percent of all organic substance is water. The chemical reactions in all plants and animals that support life take place in a water medium. Water not only provides the medium to compose these life sustaining reactions possible, but water itself is often an important reactant or product of these reactions. In short, the chemistry of life is water chemistry.

Acetonitrile (ACN):



Acetonitrile is the colourless liquid and one of the simplest organic nitriles. It is produced mainly as a byproduct of acrylonitrile manufacture.

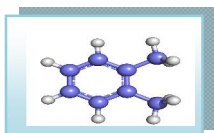
Source: Merck, India.

Acetonitrile	
	
<i>Appearance</i>	: Colourless Liquid
<i>Molecular Formula</i>	: CH ₃ CN
<i>Molecular Weight</i>	: 41.05 g·mol ⁻¹
<i>Boiling Point</i>	: 628.3 K
<i>Melting Point</i>	: 607.5 K
<i>Dielectric Constant</i>	: 35.95 at 298.15 K

Purification: Acetonitrile (ACN) obtained from Merck, India was used after further purification. It was distilled from P_2O_5 and then from CaH_2 in an all-glass distillation apparatus [1]. The middle fraction was collected. About 99% purified acetonitrile with specific conductivity $0.8 - 1.0 \times 10^{-8} \text{ S cm}^{-3}$ was obtained. The purity of the liquid was checked by measuring its density and viscosity which were in good agreement with the literature values [1,2] as shown in Table X.1.

Application: It is widely used in battery applications because of its relatively high dielectric constant and capability to dissolve electrolytes. For similar reasons it is a popular solvent in cyclic voltammetry. Its low viscosity and low chemical reactivity make it a popular choice for liquid chromatography. Acetonitrile plays a noteworthy role as the dominant solvent used in the manufacture of DNA oligonucleotides from monomers. Industrially, it is used as a solvent in the purification of butadiene and in the construct of pharmaceuticals and photographic film. Acetonitrile is a common two-carbon building block in organic synthesis as in the production of pesticides to perfumes.

o-Xylene:



o-Xylene (ortho-xylene) is an aromatic hydrocarbon, based on benzene with two methyl substituents bonded to adjacent carbon atoms in the aromatic ring (the ortho configuration).

Source: Sisco Research Laboratory Pvt. Ltd., Mumbai, India.

Purification: It was dried by passing through molecular sieves. [3]

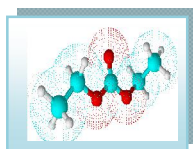
O-Xylene



<i>Appearance</i>	: Colourless Liquid
<i>Molecular Formula</i>	: C_8H_{10}
<i>Molecular Weight</i>	: $106.17 \text{ g} \cdot \text{mol}^{-1}$
<i>Boiling Point</i>	: 417.5 K
<i>Melting Point</i>	: 249 K
<i>Dielectric Constant</i>	: 2.60 at 298.15 K

Application: *o*-Xylene is largely used in the production of phthalic anhydride, and is generally extracted by distillation from an assorted xylene stream in a plant primarily designed for *p*-xylene production.

Diethyl carbonate (DEC):



Diethyl carbonate (DEC) is a carbonate ester of carbonic acid and ethanol having the formula $\text{OC}(\text{OCH}_2\text{CH}_3)_2$. At room temperature (25 °C) diethyl carbonate is a clear liquid with a low flash point.

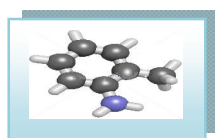
Source: Sisco Chem., India.

Purification: It was dried by passing through molecular sieves. [3]

Application: Diethyl carbonate is used as a solvent such as in erythromycin intramuscular injections. It can be used as a component of electrolytes in lithium batteries.

Diethyl carbonate	
<i>Appearance</i>	:Clear Liquid
<i>Molecular Formula</i>	: $\text{C}_5\text{H}_{10}\text{O}_3$
<i>Molecular Weight</i>	: $118.13 \text{ g}\cdot\text{mol}^{-1}$
<i>Boiling Point</i>	:401 K
<i>Melting Point</i>	:230 K
<i>Dielectric Constant</i>	:2.83 at 298.15 K

o-Toluidine:



o-Toluidine (ortho-toluidine) is an organic compound with the chemical formula $\text{C}_7\text{H}_9\text{N}$. This arylamine is a colorless to pale-yellow liquid with a poor solubility in water.

Source: Merck, Mumbai, India.

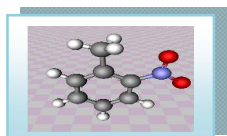
Purification: It was dried by passing

<i>o</i>-Toluidine	
<i>Appearance</i>	:Colourless or Pale Yellow Liquid
<i>Molecular Formula</i>	: $\text{C}_7\text{H}_9\text{N}$
<i>Molecular Weight</i>	: $107.16 \text{ g}\cdot\text{mol}^{-1}$
<i>Boiling Point</i>	:475K
<i>Melting Point</i>	:249.5 K
<i>Dielectric Constant</i>	:6.14 at 298.15 K

through molecular sieves. [3]

Application: *o*-Toluidine is used or applied in different circumstances. It is used mainly for dye, especially for coloring hair. The other usages of *o*-toluidine are specific determination of glucose in blood and the most recent one, the separation of toxic metal ions, which is still in the research phase.

2-Nitrotoluene:



2-Nitrotoluene or ortho-nitrotoluene is a pale yellow liquid. It can be made by nitrating toluene at above $-10\text{ }^{\circ}\text{C}$. 2-Nitrotoluene is a nitroaromatic compound. Multi-functional magnetic resins having elevated surface area and ion exchange efficiency were developed and were tested for desorption of 2-nitrotoluene. Its dioxygenation by nitrobenzene dioxygenase has been

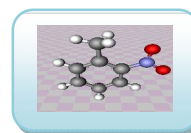
studied to assess the isotope fractionation. It has been reported as nitroaromatic explosive. Terbium-based magnetic metal-organic framework (MOF) nanospheres have been fabricated, which can detect the trace quantities of 2-nitrotoluene.

Source: Sisco Chem. Industries, Mumbai, India.

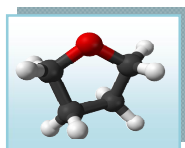
Purification: It was dried by passing through molecular sieves. [3]

Application: 2-Nitrotoluidine solvent is largely used in the production of phthalic anhydride, pigments and antioxidants. 2-Nitrotoluene may be employed as nitrogen supplement in the culture medium of *Pseudomonas* sp. strain CIS1. It may be utilized as carbon and energy supplement in the culture medium of *Pseudomonas* sp. strain JS42.

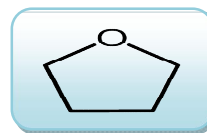
2-Nitrotoluene



<i>Appearance</i>	:Yellow Liquid
<i>Molecular Formula</i>	: $\text{C}_7\text{H}_7\text{NO}_2$
<i>Molecular Weight</i>	: $137.14\text{ g}\cdot\text{mol}^{-1}$
<i>Boiling Point</i>	:495K
<i>Melting Point</i>	:262.8 K
<i>Dielectric Constant</i>	:26.10 at 298.15 K

Tetrahydrofuran (THF):

Tetrahydrofuran (THF) is an organic compound having formula $(\text{CH}_2)_4\text{O}$. The compound is classified as heterocyclic compound, specifically a cyclic ether. It is a colorless, water-miscible organic liquid with low viscosity. THF has an odor akin to acetone. It is mainly used as a precursor to polymers. Being polar and having a wide liquid range, THF is a versatile solvent.

Tetrahydrofuran

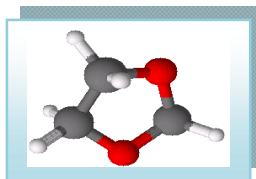
<i>Appearance</i>	:Colourless Liquid
<i>Molecular Formula</i>	: $\text{C}_4\text{H}_8\text{O}$
<i>Molecular Weight</i>	: $72.11 \text{ g}\cdot\text{mol}^{-1}$
<i>Boiling Point</i>	:339 K
<i>Melting Point</i>	:164.8 K
<i>Dielectric Constant</i>	:7.58 at 298.15 K

Source: Merck, Indian.

Purification: Tetrahydrofuran (THF), Merck, Indian was kept several days over potassium hydroxide (KOH), refluxed for 24 h and distilled over lithium aluminium hydride (LiAlH_4) described earlier [4]. The purified solvent had a boiling point of 339 K and a specific conductance of $0.81 \times 10^{-6} \text{ S cm}^{-3}$. The density and viscosity of the purified solvent were in good agreement with the literature data [5,6] as shown in Table X.1. The purity of the solvent was $\geq 98.9\%$.

Application: The main application of THF is as an industrial solvent for PVC and in varnishes. It is an aprotic solvent with a fairly polar solvent and can dissolve a wide range of non-polar and polar chemical compounds. THF is a popular solvent in the laboratory when a moderately higher-boiling ethereal solvent is required and its water miscibility is not an issue. Hence, like diethyl ether, THF can be used in hydroboration reactions to synthesize primary alcohols, and as a solvent for organometallic compounds such as organolithium and Grignard reagents. THF is often used in polymer science as dissolve polymers prior to determining their molecular mass using gel permeation chromatography, to PVC as well and thus it is the main ingredient in PVC adhesives. It can be used to liquefy old PVC cement, and is often used industrially to degrease metal parts. THF is also used as a component in mobile phases for reversed-phase liquid chromatography.

1,3-Dioxolane (1,3-DO):

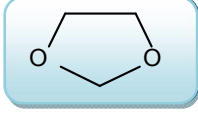


Dioxolane or 1,3-dioxolane is a heterocyclic acetal. No unusual toxic effects have been associated with the exploit of 1,3-dioxolane. The product is not explosive, not spontaneously flammable and has no disagreeable odour. Dioxolanes are a group of organic compounds sharing the dioxolane ring structure.

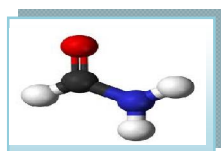
Source: Merck, India.

Purification: It is dried with KOH and then distilled from sodium [3].

Application: It is a very good solvent for pharmaceutical manufacturing, it is used as a substitute for many chlorinated solvents, in lithium battery electrolyte solvent component, as a copolymerization agent with trioxane and formaldehyde for manufacturing polyacetal resins, paint stripper, water solubilizing agent for pesticides, glue stabilizer, herbicides and wood preservatives.

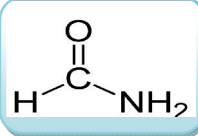
1,3-Dioxolane	
	
<i>Appearance</i>	: Colourless Liquid
<i>Molecular Formula</i>	: C ₃ H ₆ O
<i>Molecular Weight</i>	: 74.08 g·mol ⁻¹
<i>Boiling Point</i>	: 348 K
<i>Melting Point</i>	: 178 K
<i>Dielectric Constant</i>	: 7.34 at 298.15 K

Formamide (FA):



Formamide, also known as **methanamide**, is an amide derived from formic acid. It is a clear liquid which is miscible with water and has an odor akin to ammonia. It is chemical feedstock for the manufacture of sulfa drugs, other pharmaceuticals, herbicides, pesticides and the manufacture of hydrocyanic acid.

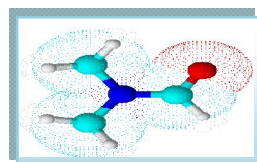
Source: Sigma Adrich, Germany

Formamide	
	
<i>Appearance</i>	: Colourless Liquid
<i>Molecular Formula</i>	: HCONH ₂
<i>Molecular Weight</i>	: 45.04 g·mol ⁻¹
<i>Boiling Point</i>	: 483 K
<i>Melting Point</i>	: 275-276 K
<i>Dielectric Constant</i>	: 109.5 at 298.15 K

Purification: The Spectrographic grade formamide used as procured, without further purification. The purity of the solvent is 99.5%.

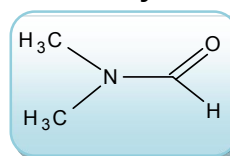
Application: It has been used as a softener for paper and fiber. It is a solvent for many ionic compounds. It has also been used as a solvent for resins and plasticizers. Formamide will commence to partially decompose into carbon monoxide and ammonia at 180°C. When heated strongly, formamide decomposes to hydrogen cyanide (HCN) and water vapor. It is also a ingredient of cryoprotectant vitrification mixtures used for cryopreservation of tissues and organs. Formamide is also used as an RNA stabiliser in gel electrophoresis by deionizing RNA. In capillary electrophoresis, it is employed for stabilizing (single) strands of denatured DNA. Another use is to add it in sol-gel solutions in order to avoid cracking during sintering. Formamide, in its pure state, has been utilized as an alternative solvent for the electrostatic self-assembly of polymer nano-films. It is used to prepare primary amines directly from ketones via their N-formyl derivatives, using the Leuckart reaction.

N,N-Dimethylformamide (DMF):



N, N, Dimethylformamide is an organic compound with the formula $(\text{CH}_3)_2\text{NC}(\text{O})\text{H}$. Commonly abbreviated as DMF (though this acronym is sometimes employed for dimethylfuran), this colourless liquid is miscible with water and the majority of organic liquids. DMF is a common solvent for chemical reaction. Pure dimethylformamide is odorless while technical grade or degraded dimethylformamide often has a fishy smell due to impurity of dimethylamine. Its name is derived from the fact that it is a derivative of formamide,

N,N-Dimethylformamide



<i>Appearance</i>	:Colourless Liquid
<i>Molecular Formula</i>	:(CH_3) ₂ NCHO
<i>Molecular Weight</i>	:73.09 $\text{g}\cdot\text{mol}^{-1}$
<i>Boiling Point</i>	:425-427 K
<i>Melting Point</i>	:212.7 K
<i>Dielectric Constant</i>	:36.71 at 298.15 K

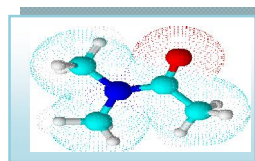
the amide of formic acid. DMF exists as polar (hydrophilic) aprotic solvent with a high boiling point. It facilitates reactions that follow polar mechanisms, such as S_N^2 reactions.

Source: Thomas Baker, India

Purification: In case of purification, it was dried by passing through Linde 4Å molecular sieves and then distilled [3].

Application: The primary use of dimethylformamide is as a solvent with small evaporation rate. DMF is used in the production of acrylic fibers and plastics. It is also used as a solvent in peptide coupling for pharmaceuticals, in the development and production of pesticides, adhesives, synthetic leathers, fibers, films, and surface coatings [7]. It is used as a reagent in the Bouveault aldehyde synthesis and in the Vilsmeier-Haack reaction, another valuable method of forming aldehydes. It is also a common catalyst used in the synthesis of acyl halides, in particular the synthesis of acyl chlorides from carboxylic acids using oxalyl or thionyl chloride [8]. DMF penetrates most plastics and makes them swell. This property makes it very suitable for solid phase peptide synthesis. It also frequently occurs as a constituent of paint strippers for this purpose. DMF is very effective at separating and suspending carbon nanotubes, and is recommended by the NIST for use in near infrared spectroscopy of such. DMF can be employed as a standard in proton NMR allowing for a quantitative determination of an unknown chemical. DMF is used as a solvent to recover olefins such as 1,3-butadiene via extractive distillation. It is also utilized in the manufacturing of solvent dyes as an important raw material. It is consumed during reaction. Pure acetylene gas cannot be compressed and stored devoid of the danger of explosion. Industrial acetylene gas is, therefore, dissolved in dimethylformamide and stored in metal cylinders or bottles. The casing is also filled with agamassan, which provides it safe to transport and use.

N,N-Dimethylacetamide (DMA):



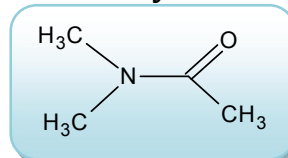
N,N-Dimethylacetamide is the organic compound with the formula $(\text{CH}_3)_2\text{NCOCH}_3$. This colorless, water-miscible, high boiling liquid is usually used as a polar solvent in organic synthesis. DMA, as it often abbreviated, is miscible with most other solvents, although it is feebly soluble in aliphatic hydrocarbons.

Source: Thomas Baker, India

Purification: It was dried by ephemeral through molecular sieves [3].

Application: DMA is useful solvent for reactions involving strong bases such as sodium hydroxide. Dimethylacetamide is normally used as a solvent for fibers (e.g., polyacrylonitrile, spandex) or in the adhesive industry [9]. It is also employed in the production of pharmaceuticals and plasticizers as a reaction medium.

N,N-Dimethylacetamide



<i>Appearance</i>	:Colourless Liquid
<i>Molecular Formula</i>	: $(\text{CH}_3)_2\text{NCOCH}_3$
<i>Molecular Weight</i>	: $87.12 \text{ g}\cdot\text{mol}^{-1}$
<i>Boiling Point</i>	: 438.2 K
<i>Melting Point</i>	: 253 K
<i>Dielectric Constant</i>	: $37.78 \text{ at } 298.15 \text{ K}$

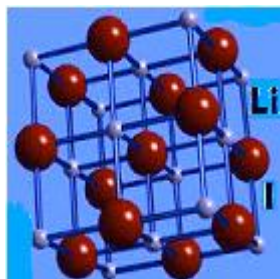
III.1.2 ELECTROLYTES AND NON-ELECTROLYTES

The electrolytes ionic liquids, and non-electrolytes and other chemicals than these two categories that are used in the research work have been describing follow:

III.1.2.1 Ionic Solids

Lithium Iodide

Lithium iodide, or LiI, is a compound of lithium and iodine. When exposed to air, it becomes yellow in color, Owing to the oxidation of iodide to iodine. It crystallizes as FCC lattice.



Appearance: White crystalline solid

M.F. LiI

M.W. 133.85 g/mol

M.P. 742 K

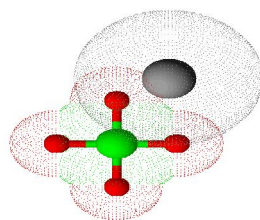
Source: Sigma Aldrich, Germany

Purification: Used as purchased. The purity of the ionic solid is >98.0%

Application: Lithium iodide is used as an electrolyte for high temperature batteries. It is also employed for long life batteries as required, for example, by artificial pacemakers. The solid is used as a phosphor for neutron detection. It is also used, in a complex with Iodine, in the electrolyte of dye-sensitized solar cells.

Lithium Perchlorate

Lithium perchlorate is the inorganic compound with the formula LiClO_4 . This white or colourless crystalline salt is noteworthy for its high solubility in a lot of solvents. It exists both in anhydrous form and as a trihydrate.



Appearance: White crystalline solid

M.F. LiClO_4

M.W. 106.39 g/mol

M.P. 509 K

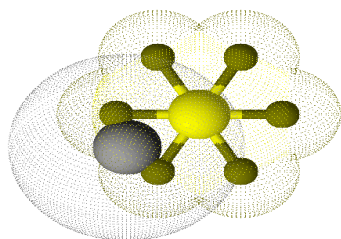
Source: Sigma Aldrich, Germany

Purification: Used as purchased. The purity of the ionic solid is >98.0%

Application: Lithium perchlorate is used as an electrolyte in lithium-ion batteries. Lithium perchlorate is also used as a source of oxygen in some chemical oxygen generators. In organic chemistry Lithium perchlorate is also used as a co-catalyst in the coupling of α,β -unsaturated carbonyls with aldehydes

Lithium Hexafluoroarsenate

Lithium hexafluoroarsenate is the inorganic compound with the formula LiAsF_6 .



Appearance: Powder

M.F. LiAsF_6

M.W. 195.85 g/mol

M.P. 622 K

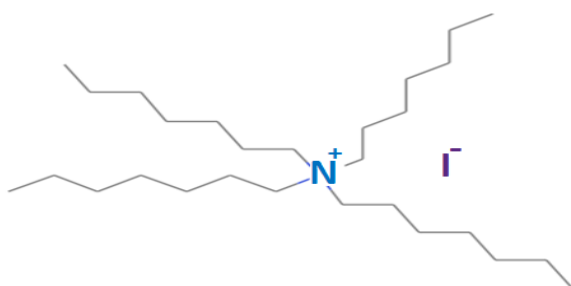
Source: Sigma Aldrich, Germany

Purification: Used as purchased. The purity of the ionic solid is >98.0%

Application: The surface chemistry of Li electrodes in ethereal LiAsF_6 was tested with new salts for potential battery systems. It is also used in the preparation of high energy batteries and lithium-ion batteries.

Tetraheptylammonium Iodide (Hept₄NI)

Tetraheptylammonium Iodide can be called as various other names such as, 1-Heptanammonium, N,N,N-triheptyl-, iodide; Ammonium, tetraheptyl-, iodide; Tetra-n-heptylammonium iodide etc. It contains a tertiary nitrogen atom which is linked with four heptyl (containing seven carbon atoms) groups.



Appearance: White crystalline solid

M.F. $\text{C}_{28}\text{H}_{60}\text{NI}$

M.W. 537.69 g/mol

M.P. 394 K-397 K

Source: Sigma Aldrich, Germany

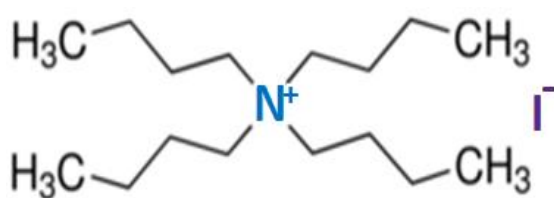
Purification: Used as purchased. purity of the ionic solid is >99.0%

Application: Hept₄NI used in this study has a number of applications such as it employed as phase transfer catalyst. Since this ionic solid has the tendency of locating at the interface of two phases (liquid-liquid or solid-liquid) for introducing

the continuity between two different phases, so it positively is said as phase transfer catalyst. It is also used as osmolytes.

Tetrabutylammonium Iodide (But₄NI)

Tetrabutylammonium Iodide is an ammonium based ionic solid having molecular formula (CH₃CH₂CH₂CH₂)₄N(I). It contains a tertiary nitrogen atom which is linked with four butyl (containing four carbon atoms) groups.



Appearance: White crystalline solid

M.F. C₁₆H₃₆NI

M.W. 369.67 g/mol

M.P. 414 K-416 K

Source: Sigma Aldrich, Germany

Purification: Used as purchased. The purity of the ionic solid is >99.0%

Application: The ionic solid has immense appliances in various fields such as in chemical reactions it acts as surface-active agents (due to the hydrophobic communications between the butyl groups and water molecules), solvents, Intermediates emulsifying means, pigment disperse and phase transfer catalyst [10,11]. Since but₄NI has the tendency of locating at the interface of two phases (liquid-liquid or solid-liquid) for introducing the continuity between two different phases, so it positively is said as phase transfer catalyst. Due to low cost and low toxicity of but₄NI in recent times it has appeared as a promising substitute as a catalyst for functionalization of C-H bonds [12,13]. In industrial usage but₄NI acts as active ingredient for conditioners, antistatic agent, detergent sanitizers, softener for textiles and paper products etc. In medicinal field it uses as antimicrobials, algacide, slimicidal agents, disinfection agents and sanitizers etc.

III.1.2.2 Ionic Liquids

1-Butyl-1-methylpyrrolidinium bromide

1-butyl-1-methylpyrrolidinium bromide is a pyrrolidinium based ionic liquid, having molecular formula $C_9H_{20}BrN$, which contains methyl and ethyl group with an active nitrogen atom in a five membered pyrrolidinium ring. This IL exists as a molten solid phase (white crystalline).



Appearance	: White Crystalline
Molecular Formula	: $C_9H_{20}BrN$
Molecular Weight	: $222.17 \text{ g}\cdot\text{mol}^{-1}$

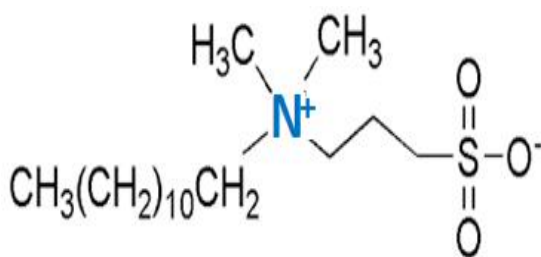
Source: Sigma Aldrich, Germany

Purification: Used as purchased. The purity of the ionic liquid is >99.0%

Application: This ionic liquid is an excellent example of neoteric solvents, novel types of solvents, or older resources that are finding new appliances as environmentally friendly (or eco-friendly) solvents, because of having their less vulnerability for human being as well as fewer toxicity for living organisms. This IL also used as recyclable solvents for organic reactions and separation processes, lubricating fluids, heat transfer fluids for processing biomass and electrically conductive liquids as electrochemical gadget (such as batteries and solar cells) in the field of electrochemistry.

N-Dodecyl N,N-dimethyl-3-ammonio-1-propanesulfonate

N-Dodecyl N,N-dimethyl-3-ammonio-1-propanesulfonate is a ammonio group based surface active ionic liquid (SAIL) which contains a very long dodecyl (having 12 carbon atoms) alkyl chain, two methyl groups, a tertiary nitrogen atom and a propanesulfonate group. This IL exists as a molten solid phase (white crystalline).



Appearance	: White Crystalline
Molecular Formula	: C₁₇H₃₇NO₃S
Molecular Weight	: 335.50 g·mol⁻¹

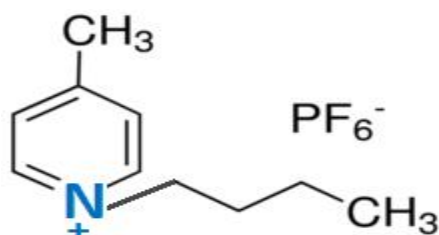
Source: Sigma Aldrich, Germany

Purification: Used as purchased. The purity of the ionic liquid is >99.0%

Application: Their relatively rapid emergence as alternative solvents has involved a rapidly growing number of examples of the application such as organic synthesis, chemical reactions, chemical separations, and material preparations [14,15]. ILs are composed of sterically mismatched ions that hinder crystal formation, thus molecular structure can be used to tune physicochemical properties. The design and synthesis of functional ILs that integrate structural or functional groups have been reported. ILs was designed as oriented solvents which could impact selectivity in reactions by ordering reactants [16]. Furthermore, functional ILs were also used as templates for the synthesis of mesoporous and zeolitic materials [17] and in the formation of ordered thin films [18,19]. Recently, ILs having a long alkyl chain group exhibited surface active properties in their aqueous solutions. Considering the special structures and properties of IL surfactant (zwitterionic detergent employed for protein solubilization), it is of interest to investigate their complexation behaviour using different techniques.

1-Butyl-4-methylpyridinium hexafluorophosphate

1-butyl-4-methylpyridinium hexafluorophosphate is basically a pyridinium based ionic liquid. It contains one butyl and one methyl attached with the nitrogen atom of group as cationic part, then again, hexafluorophosphate as an anionic part.



Appearance	: White Crystalline
Molecular Formula	: $C_{17}H_{37}NO_3S$
Molecular Weight	: $335.50 \text{ g}\cdot\text{mol}^{-1}$

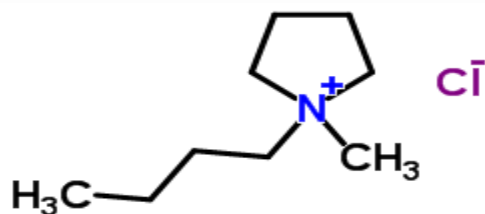
Source: Sigma Aldrich, Germany

Purification: Used as purchased. The purity of the ionic liquid is >99.0%

Application: This ionic liquid is an excellent example of neoteric solvents, novel types of solvents, or older resources that are finding new appliances as environmentally friendly (or eco-friendly) solvents, because of having their less vulnerability for human being as well as fewer toxicity for living organisms. The IL can selectively dissolve and remove gases and could be used for air purification on submarines and spaceships. It is also used in the present widely used in solvent extraction, liquid-liquid extraction process, electrochemical studies, dye-sensitized solar cells [20-23].

1-butyl-1-methylpyrrolidinium chloride

1-butyl-1-methylpyrrolidinium chloride is a pyrrolidinium based ionic liquid, having molecular formula $C_9H_{20}ClN$, which contains methyl and ethyl group with an active nitrogen atom in a five membered pyrrolidinium ring. This IL exists as a molten solid phase (white crystalline).



Appearance	: White Crystalline
Molecular Formula	: $C_9H_{20}ClN$
Molecular Weight	: $177.71 \text{ g}\cdot\text{mol}^{-1}$

Source: Sigma Aldrich, Germany.

Purification: Used as purchased. The purity of the ionic liquid is >99.0%

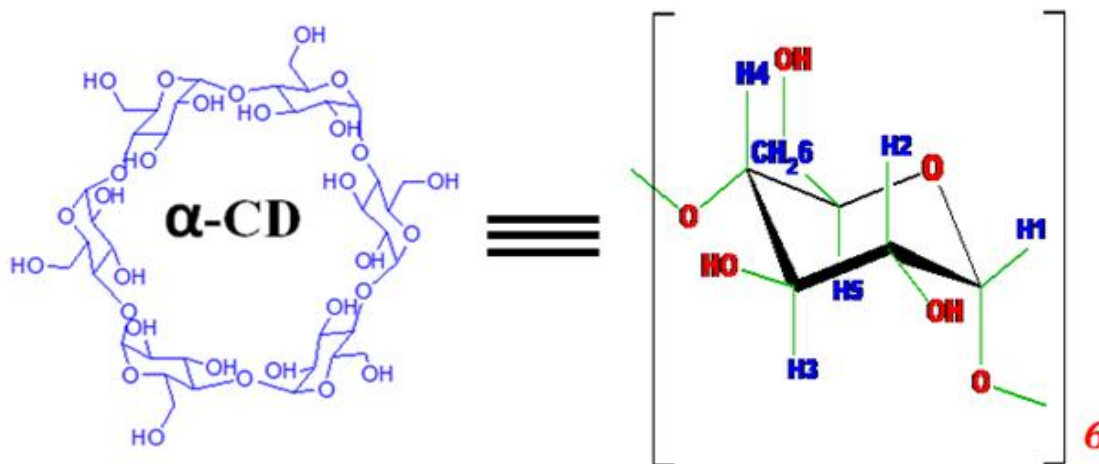
Application: This ionic liquid is an excellent example of neoteric solvents, novel types of solvents, or older resources that are finding new appliances as

environmentally friendly (or eco-friendly) solvents, because of having their less vulnerability for human being as well as fewer toxicity for living organisms. This IL also used as recyclable solvents for organic reactions and separation processes, lubricating fluids, heat transfer fluids for processing biomass and electrically conductive liquids as electrochemical gadget (such as batteries and solar cells) in the field of electrochemistry.

Non-Electrolytes

Alpha Cyclodextrin (α -CD)

α -CD is naturally occurring polysachharides of six glucose units and they are covalently attached via end to end α -1,4 linkage. It has hydrophobic inner cavity and hydrophilic outer surface. In aqueous medium hydrophobic inner core allow it to form host-guest inclusion colmplex with suitable hydrophobic molecules. Most of the cases it forms 1:1 inclusion complex due to its small cavity volume.



Appearance:	Crystalline Powder
Molecular Formula:	C ₃₆ H ₆₀ O ₃₀
Molecular Weight:	972.85 g/mol
Melting Point:	>551 K

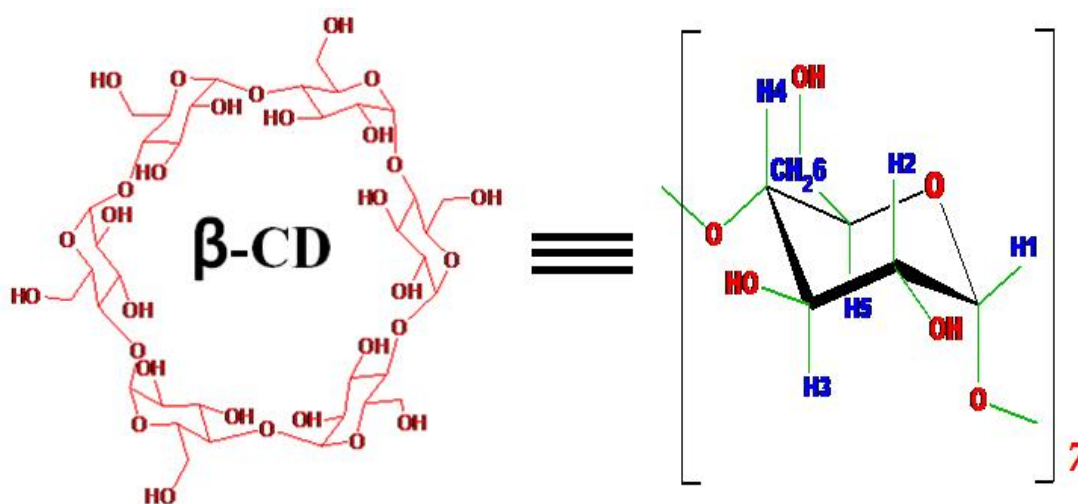
Source: Sigma Aldrich, Germany

Purification: Used as parched. The purity is 99.98%.

Application: α -Cyclodextrin is widely applied in production of medicine and food. It also used in cosmetics, paint, textile industries. In the production of medicine, it can strengthen the stability of medicine without being oxidized and resolving. On the other hand, it can improve the solubility. And the effect on living of medicine, lower the toxic and side-effect of medicine and cover the strange and bad smell. In the production of food, it can mainly cover strange and bad smell of food, improve the stability of perfume and condiment and keep food dry or wet at will. α -cyclodextrin is commonly used as a complexing agent in hormones, vitamins, and many bioactive compounds frequently used in tissue and cell culture applications.

Beta Cyclodextrin (β -CD)

β -Cyclodextrin is finely made from pure provision material-starch and translate enzyme, which is white powder and whose molecule structure is like a cylinder compounded from 7 glucose group with a key of 2-1.4. The function of β -Cyclodextrin depends on its cylinder molecule structure which can be easy to integrate other materials. That feature is applied widely in industry



Appearance:	Crystalline Powder
Molecular Formula:	C₄₂H₇₀O₃₅
Molecular Weight:	1134.98 g/mol
Melting Point:	563.15-573.15 K
Boiling Point	1814.33 K

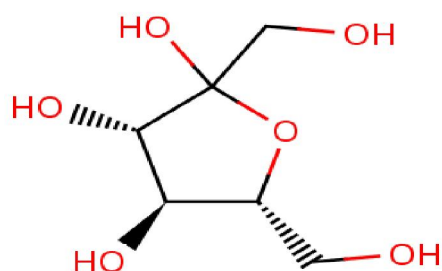
Source: Sigma Aldrich, Germany

Purification: Used as parched. The purity is 99.98%.

Application: β -Cyclodextrin is a new stuff which can be widely applied in production of medicine and food. It can be applied widely in production of medicine, food and cosmetics, whose function is improved stability, solubility and good smelled. In the production of medicine, it can strengthen the stability of medicine without being oxidized and resolving. On the other hand, it can improve the solubility. And the effect on living of medicine, lower the toxic and side-effect of medicine and cover the strange and bad smell. In the production of food, it can mainly cover strange and bad smell of food, improve the stability of perfume and condiment and keep food dry or wet at will. CD with a cavity diameter of 6.4-7.5 Å, is the most interest because its cavity size allows for the best special fit for many common guest moieties. For this reason, β -cyclodextrin is most commonly used as a complexing agent in hormones, vitamins, and many compounds frequently used in tissue and cell culture applications. This aptitude has also been of assistance for different applications in medicines, cosmetics, food technology, pharmaceutical, and chemical industries as well as in agriculture and environmental engineering as an encapsulating agent to protect sensitive molecules in antagonistic environment.

D(-)Fructose

Living system of every animal and man is composed of several molecules having specific functions are termed as biomolecules. Carbohydrates are one of the main classes of biomolecules. D(-)Fructose is one of the most important biomolecule. Fructose, or fruit sugar, is a simple ketonic monosaccharide found in lots of plants, where it is often bonded to glucose to form the disaccharide sucrose.



Appearance:	Crystalline Powder
Molecular Formula:	C₆H₁₂O₆
Molecular Weight:	180.16 g/mol
Melting Point:	376 K

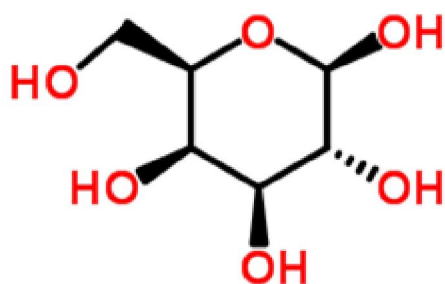
Source: Thomas Baker, Mumbai

Purification: Used as parched. The purity of the sample is 99.4%.

Application: D(-)Fructose usually act as a ubiquitous fuel for biological processes to supply necessary energy for the function of the living and their day's work. An unusual level of carbohydrate in human body fluid is a caution hint of a medical stipulation. Such as, an unbalanced concentration of carbohydrates in human blood or urine entails a biological dysfunction.

D(+)**Galactose**

Living system of every animal and man is composed of several molecules having specific functions are termed as biomolecules. Carbohydrates are one of the main classes of biomolecules. D(+)**Galactose** is one of the most important biomolecule. It is a monosaccharide sugar that is less sweet than glucose and fructose. It is a C-4 epimer of glucose. Galactan is a polymeric form of galactose found in hemicellulose.



Appearance:	Crystalline Powder
Molecular Formula:	C₆H₁₂O₆
Molecular Weight:	180.16 g/mol
Melting Point:	440 K

Source: Thomas Baker, Mumbai

Purification: Used as parched. The purity of the sample is 99.9%.

Application: D(+)**Galactose** usually act as a ubiquitous fuel for biological processes to supply necessary energy for the function of the living and their day's work. An unusual level of carbohydrate in human body fluid is a caution hint of a medical stipulation. Such as, an unbalanced concentration of carbohydrates in human blood or urine entails a biological dysfunction.

III. 2 EXPERIMENTAL METHODS

III.2.1 PREPARATION OF SOLUTIONS

A stock solution for each salt was prepared by mass (digital electronic analytical balance, Mettler Toledo, AG 285, Switzerland), and the working solutions were obtained by mass dilution of the stock solution. The uncertainty of concentration (molarity or molality) of different working solutions was evaluated to be ± 0.0002 .

III.2.2. PREPARATION OF MULTICOMPONENT LIQUID MIXTURES

The binary and multicomponent liquid mixtures can be prepared by any one of the methods discussed below:

(a) *Mole fraction*

(b) *Weight fraction*

(c) *Volume fraction*

(a) **Mole fraction:** The mole fraction (x_i) of the multicomponent liquid mixtures can be prepared using the following relation:

$$x_i = \frac{(w_i / M_i)}{\sum_{i=1}^n (w_i / M_i)}$$

where w_i , and M_i are weight and molecular weight of i^{th} component, respectively. The values of i depends on the number of components involved in the formation of a mixture.

(b) **Weight fraction:** The mole fraction (w_i) of the multicomponent liquid mixtures can be prepared using the following relation:

$$w_i = \frac{(x_i / M_i)}{\sum_{i=1}^n (x_i M_i)}$$

(c) **Volume fraction:** The volume fraction (ϕ_i) of the multicomponent liquid mixtures can be prepared by following employing three methods:

i. **Using volume:** The volume fraction (ϕ_i) of the multicomponent liquid mixtures can be prepared by following relation

$$\phi_i = \frac{V_i}{\sum_{i=1}^n V_i}$$

where V_i is the volume of pure liquid i .

ii. Using molar volume: The volume fraction (ϕ_i^l) of the multicomponent liquid mixtures can be prepared by following relation

$$\phi_i^l = \frac{x_i V_{mi}}{\sum_{i=1}^n (x_i V_{mi})}$$

where V_{mi} is the molar volume of pure liquid i .

iii. Using excess volume: The volume fraction (ϕ_i^{ex}) of the multicomponent liquid mixtures can be prepared by following relation

$$\phi_i^{ex} = \frac{x_i V_i}{\sum_{i=1}^n (x_i V_i) + V^E}$$

where V^E is the excess volume of the liquid mixture.

III.2.3. PREPARATION OF SOLVENT MIXTURES (MIXED SOLVENTS)

The research work has been carried out with binary or ternary solvent systems with acrylonitrile, tetrahydrofuran, methanol, ethylene glycol, 1,3-dioxolane etc. as primary solvents with some polar, weakly polar and non-polar solvents as well as with some electrolytes (ionic liquids & other electrolytes) and non-electrolytes (amino acids and other solutes).

For the preparation of solvent mixture, pure components were taken separately in glass stoppered bottles and thermostated at the desired temperature for sufficient time. When the thermal equilibrium was ensured, the required volumes of each component were transferred in a different bottle which was already cleaned and dried thoroughly. Conversion of required mass of the respective solvents to volume was accomplished by using experimental densities of the solvents at experimental temperature. It was then stoppered and the mixed contents were shaken well before use. While preparing different solvent mixtures care was taken to ensure that the same procedure was adopted throughout the entire work.

The physical properties of different pure and mixed solvents have been presented in the respective chapters.

Different types of binary and ternary solutions have been prepared and used for my research studies.

III.2.4 MEASUREMENTS OF EXPERIMENTAL PROPERTIES

III.2.4.1 MASS MEASUREMENT

Mass measurements were made on digital electronic analytical balance (Mettler Toledo, AG 285, Switzerland).

It can measure mass to a very high precision and accuracy. The weighing pan of a high precision (0.0001g) is inside a transparent enclosure with doors so that dust does not collect and so any air currents in the room do not affect the balance's operation.



Mettler Toledo, AG 285

Instrument Specification:

<i>Readability</i>	<i>: 0.1 mg/ 0.01mg</i>
<i>Maximum capacity</i>	<i>: 210 g/81g/41g</i>
<i>Taring range</i>	<i>: 0 ... 210 g</i>
<i>Repeatability</i>	<i>: 0.1 mg/ 0.05 mg</i>
<i>Linearity</i>	<i>: ±0.2 mg/±0.1 mg</i>
<i>Stabilization time</i>	<i>: 3 s/ 15 s</i>
<i>Adjustment with external weights</i>	<i>:200 g</i>
<i>Sensitivity</i>	<i>: ±0.003%</i>
<i>Display</i>	<i>: LCD</i>
<i>Interface</i>	<i>: LocalCAN universal interface</i>
<i>Weighing</i>	<i>: Φ 85 mm, stainless steel</i>
<i>Effective height above pan</i>	<i>: 240 mm</i>
<i>Dimensions(w/d/h)</i>	<i>: 205×330×310 mm</i>

*Net wt/with packaging**: 4.9 kg/7.25 kg*

III.2.4.2 CONDUCTIVITY MEASUREMENT

Conductivity measurement was done using Systronics Conductivity TDS meter-308. It can provide both automatic and manual temperature compensation.

Systronics Conductivity-TDS meter 308 is a microprocessor based instrument used for measuring specific conductivity of solutions. It can provide both automatic and manual temperature compensation. The instrument shows the conductivity of the solution under test at the existing temperature or with temperature compensation. Provision for storing the cell constant and the calibrating solution type, is provided with the help of battery back-up. This data can be further used for measuring the conductivity of an unknown solution, without recalibrating the instrument even after switching it off.



Systronic-308 Conductivity Bridge

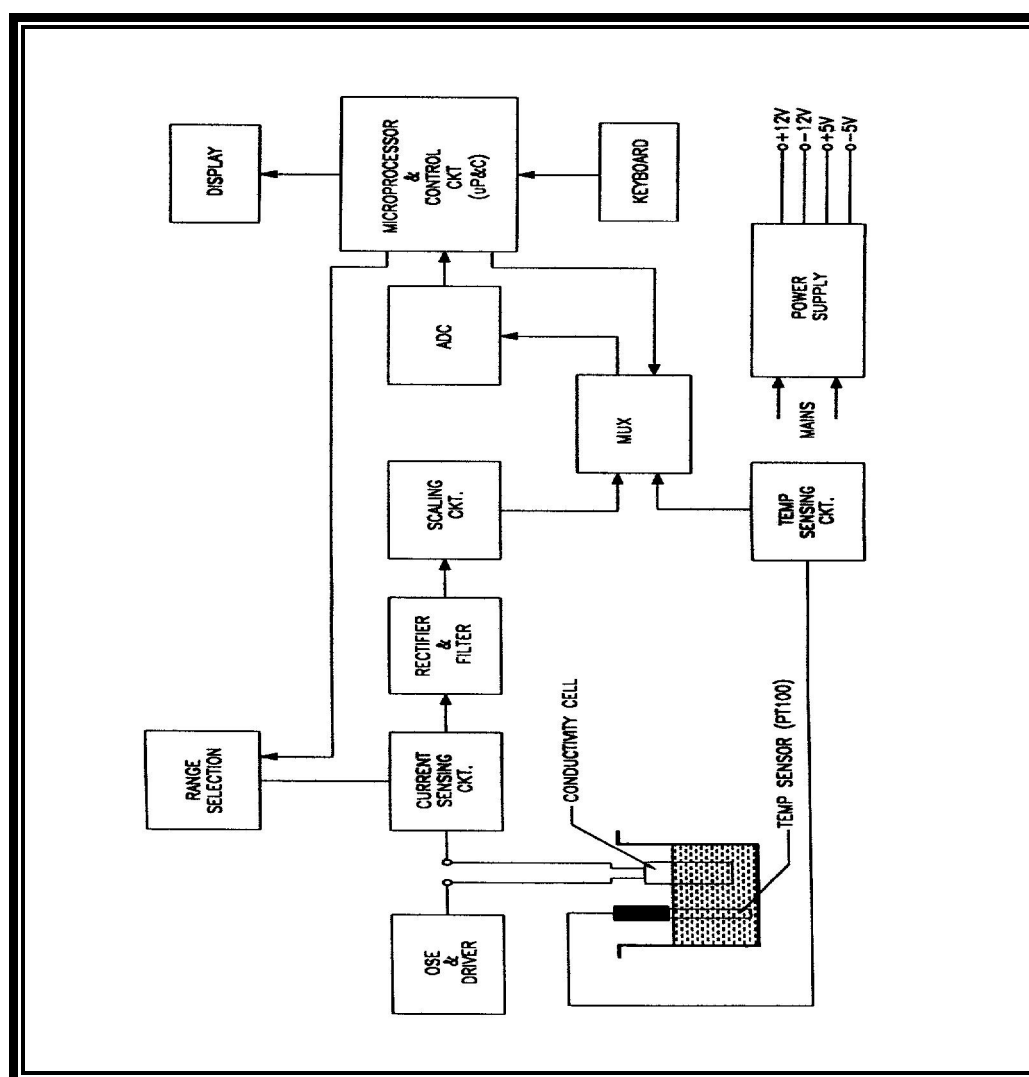
The conductance measurements were carried out on this conductivity bridge of accuracy $\pm 0.01\%$, using a dip-type immersion conductivity cell, CD-10 having a cell constant of approximately $(0.1 \pm 0.001) \text{ cm}^{-1}$. Measurements were made in a thermostate water bath maintained at $T = (298.15 \pm 0.01) \text{ K}$. The cell was calibrated by the method proposed by Lind et al [24], and cell constant was measured based on 0.01 M aqueous KCl solution [25]. During the conductance measurements, cell constant was maintained within the range $1.10\text{--}1.12 \text{ cm}^{-1}$. The conductance data were reported at a frequency of 1 kHz and the accuracy was $\pm 0.3\%$. The conductivity cell was sealed to the side of a 500 cm^3 conical flask closed by a ground glass fitted with a side arm through which dry and pure nitrogen gas was passed to prevent admission of air into the cell when solvent or solution was added. The

measurements were made in a thermostatic water bath maintained at the required temperature with an accuracy of ± 0.01 K by means of mercury in glass thermoregulator [26].

Instrument Specifications:

<i>Frequency</i>	<i>:100 Hz or 1 KHz Automatic</i>
<i>Conductivity</i>	
<i>Range</i>	<i>: 0.1 μS to 100 mS. (6 decadic range)</i>
<i>Accuracy</i>	<i>: $\pm 1\%$ of F.S. ± 1 digit</i>
<i>Resolution</i>	<i>: 0.001 μs</i>
<i>TDS</i>	
<i>Range</i>	<i>:0.1 ppm to 100 ppt. (6 decadic range)</i>
<i>Accuracy</i>	<i>: $\pm 1\%$ of F.S. ± 1 digit</i>
<i>Temperature</i>	
<i>Range</i>	<i>: 0°C to 100°C (Auto/Manual)</i>
<i>Accuracy</i>	<i>: ± 0.2 °C ± 1 digit</i>
<i>Resolution</i>	<i>: 0.1 °C</i>
<i>Cell Constant</i>	<i>: Acceptable from 0.1 to 5.0</i>
<i>Auto Temp. Compensation</i>	<i>: 0°C to 100°C with PT 100 sensor</i>
<i>Manual Temp. Compensation</i>	<i>: 0°C to 60°C user selectable</i>
<i>Conductivity temp. Co-efficient</i>	<i>: 0.0% to 9.9% user selectable</i>
<i>Display</i>	<i>: 7 digits, 7 segment LEDs (3 digits for TEMP/TEMPCO 4 digits for Conductivity/TDS) With automatic decimal point selection</i>
<i>TDS-factor</i>	<i>: 0.00 to 9.99 user selectable</i>
<i>Printer Port</i>	<i>: Epson compatible 80 Column Dot Matrix</i>
<i>Power</i>	<i>: 230V AC, $\pm 10\%$, 50 Hz</i>
<i>Dimensions</i>	<i>: 250(W)\times 205(D)\times 75(H)</i>
<i>Weight</i>	<i>: 1.25 Kg (Approx.)</i>
<i>Accessories</i>	<i>: i) Conductivity cell, cell constant 0.1 ii) Conductivity cell, cell constant 1.0 iii) Temp. Probe (PT-100 sensor) iv) Stand & Clamp</i>

Solutions were prepared by weight precise to $\pm 0.02\%$. The weights were taken on a Mettler electronic analytical balance (AG 285, Switzerland). The molarity being converted to molality as required. Several independent solutions were prepared and runs were performed to ensure the reproducibility of the results. Due correction was made for the specific conductance of the solvents at desired temperatures. The following figure shows the Block diagram of the Systronics Conductivity-TDS meter 308.



Block Diagram of the Instrument

III.2.4.3 DENSITY MEASUREMENT

The density measurement was performed with the help of Anton Paar DMA 4500M digital density-meter with a precision of $\pm 0.0005 \text{ g}\cdot\text{cm}^{-3}$.

In the digital density meter, the mechanic oscillation of the U-tube is e.g. electromagnetically transformed into an alternating voltage of the same frequency. The period τ can be measured with high resolution and stands in simple relation to the density ρ of the sample in the oscillator



Anton Paar DMA 4500M digital density-meter

In the digital density meter, mechanic oscillation of the U-tube is e.g. electromagnetically transformed into an alternating voltage of the same frequency. The period τ can be measured with high resolution and stands in simple relation to the density ρ of the sample in the oscillator:

$$\rho = A \cdot \tau^2 - B \quad (\text{III.1})$$

A and B are the respective instrument constants of each oscillator. Their values are resolute by calibrating with two substances of the precisely known densities ρ_1 and ρ_2 . Modern instruments calculate and store the constants A and B after the two calibration measurements, which are typically performed with air and water. They employ suitable measures to compensate various influences on the measuring result, e.g. the influence of the sample's viscosity and the non-linearity caused by the measuring instrument's finite mass. The instrument was calibrated by triply-distilled water and dry air.

III.2.4.3 VISCOSITY MEASUREMENT

Brookfield DV-III Ultra Programmable Rheometer: The viscosities (η) were measured using a Brookfield DV-III Ultra Programmable Rheometer with fitted spindle size-42. The viscosities were obtained using the following equation

$$\eta = (100 / RPM) \times TK \times \text{torque} \times SMC$$

where RPM , TK (0.09373) and SMC (0.327) are the speed, viscometer torque constant and spindle multiplier constant, respectively. The instrument was calibrated against the standard viscosity samples supplied through the instrument, water and aqueous CaCl_2 solutions [27]. The temperature was maintained to within $\pm 0.01^\circ\text{C}$ using Brookfield Digital TC-500 thermostat bath. The viscosities were measured with an accuracy of $\pm 1\%$. Each measurement reported herein is an average of triplicate reading with a precision of 0.3 %.



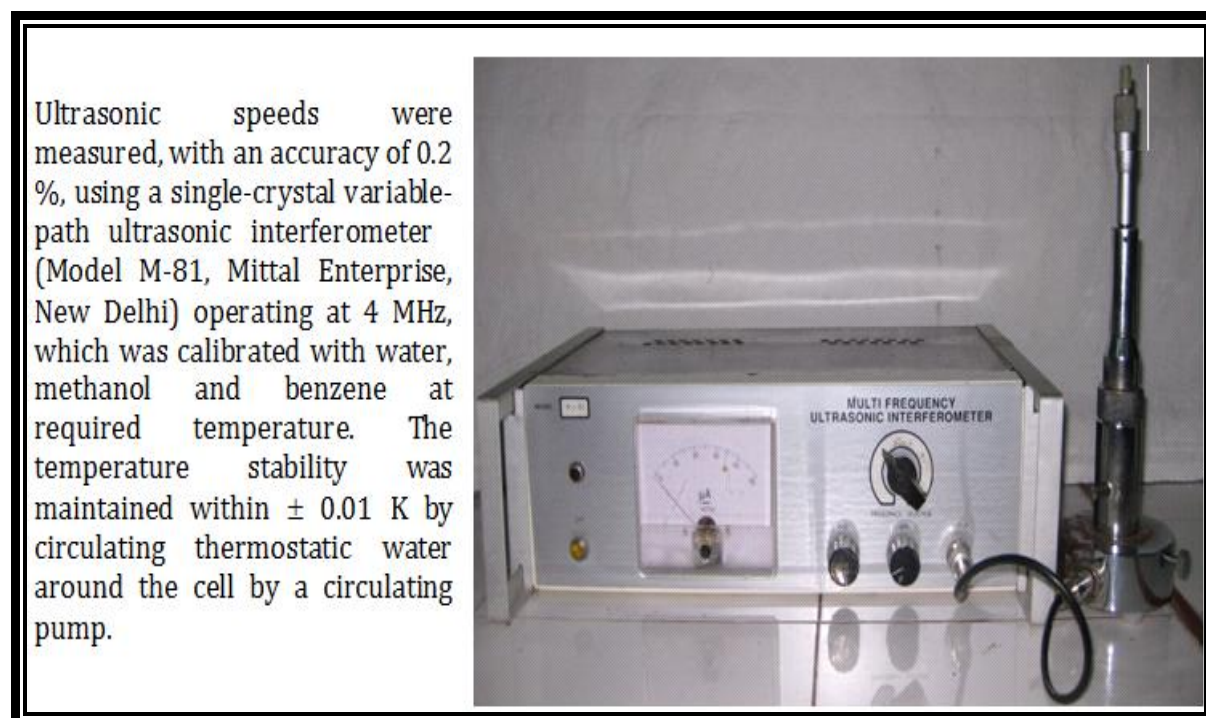
Instrument Specifications:

Range of Speed	: 0-250 RPM, 0.1 RPM increments
Viscosity Accuracy	: $\pm 1.0\%$ of full scale range for a specific spindle running at a specific speed.
Temperature sensing range	: -100°C to 300°C (-148°F to 572°F)
Accuracy of temperature	: $\pm 1.0^\circ\text{C}$ from -100°C to 150°C

	$\pm 2.0^{\circ}\text{C}$ from $+150^{\circ}\text{C}$ to 300°C
Analog Torque Output	: 0 - 1 Volt DC (0 - 100% torque)
Analog Temperature Output	: 0 - 4 Volts DC (10mv / $^{\circ}\text{C}$)

III.2.4.5 ULTRASONIC SPEED MEASUREMENT

The ultrasonic speed was measured with an accuracy of 0.2% using single-crystal variable-path ultrasonic interferometer (Model M-81 Mittal Enterprises, New Delhi) operating at 4MHz which was calibrated with water, methanol and benzene at required temperature.



Ultrasonic speeds were measured, with an accuracy of 0.2 %, using a single-crystal variable-path ultrasonic interferometer (Model M-81, Mittal Enterprise, New Delhi) operating at 4 MHz, which was calibrated with water, methanol and benzene at required temperature. The temperature stability was maintained within ± 0.01 K by circulating thermostatic water around the cell by a circulating pump.

Multifrequency Ultrasonic Interferometer

Instrument Specification:

<i>High Frequency Generator</i>	<i>: Single and Multi-frequency</i>
<i>Model No.</i>	<i>: M-81 Mittal Enterprises</i>
<i>Measuring Cell</i>	<i>: Four cell (1, 2,3, & 4 MHz)</i>
<i>Max. displacement of the reflector</i>	<i>: 20 mm</i>
<i>Required Quantity of liquid</i>	<i>: 10 c.c.</i>
<i>Least Count of micrometer</i>	<i>: 0.01mm/0.001 mm</i>

Accuracy	: 0.2%
Shielded Cable Impedance	: 50 Ω

Working Principle of Ultrasonic Interferometer

The principle used in the measurement of the ultrasonic speed (u) is based on the accurate determination of the wavelength (λ) in the medium. Ultrasonic waves of well-known frequency (f) are produced by a quartz crystal fixed at the base of the cell. These waves are reflected by a movable metallic plate kept parallel to the quartz crystal. If the separation between these two plates is accurately a whole multiple of the sound wavelength, standing waves are fashioned in the medium. This acoustic resonance provides rise to an electrical reaction on the generator pouring the quartz crystal and the anode current of the generator becomes a maximum.

If the distance is currently increased or decreased and the variation is exactly one half of wave length ($\lambda/2$) or integral multiples of it, anode current becomes maximum. From the knowledge of the wave length (λ), the speed (u) can be obtained by the relation.

$$\text{Ultrasonic speed } (u) = \text{Wave Length } (\lambda) \times \text{Frequency } (f) \quad (\text{III.5})$$

Experimental set-up - ultrasonic interferometer consists of the following parts,

- One high frequency generator.
- Measuring cell, 1, 2, 3 and 4 MHz.
- Shielded cable

The measuring cell is connected to the output terminal of the high frequency generator through a shielded cable. The cell is filled through the experimental liquid before switching on the generator. The ultrasonic waves shift normal from the quartz crystal till they are reflected back as of the movable plate and the standing waves are formed in the liquid in between the reflector plate and the quartz crystal. The micrometer is gradually moved till the anode current on the meter on the elevated frequency generator shows a maximum. A number of maxima readings of anode current are passed and their number (n) is counted. The total distance (d)

thus moved by the micrometer gives the value of the wavelength (λ) with the following relation.

$$d = n \times \lambda/2 \quad (\text{III.6})$$

Further, the velocity is determined from which the isentropic compressibility (β_s) is calculated by the following formula:

$$\beta_s = 1 / (u^2 \cdot \rho) \quad (\text{III.7})$$

where ρ is the density of the experimental liquid.

The following Figure shows the Multifrequency Ultrasonic Interferometer i.e.

- Cross-section of the measuring cell,
- Position of reflector vs. crystal current (Note: The extra peaks in between minima and maxima occurs due to a number of reasons, but these do not affect the value of $\lambda/2$) and)
- Electronic circuit diagram of the instrument

The Multifrequency Ultrasonic Interferometer

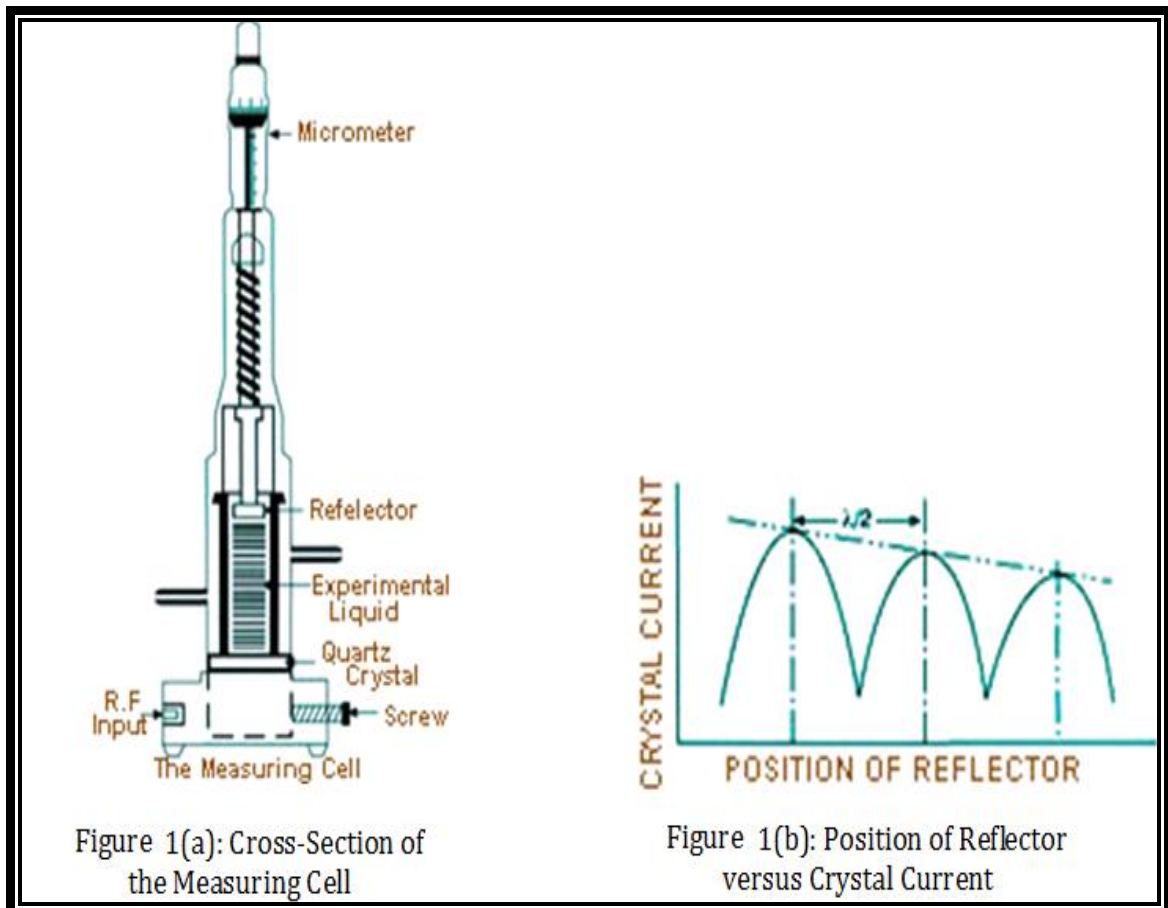


Figure 1(a): Cross-Section of the Measuring Cell

Figure 1(b): Position of Reflector versus Crystal Current

III.2.4.6 REFRACTIVE INDEX MEASUREMENT

Refractive index was be measure with the help of Digital Refractometer (Mettler Toledo 30GS).

Calibration was executed by measuring the refractive indices of double-distilled water, toluene, cyclohexane, and carbon tetrachloride at defined temperature. The accuracy of the instrument is ± 0.0005 . 2-3 drops of the sample was put onto the measurement cell and the reading was taken. The refractive index of a sample depends on temperature. During measurement, refractometer determines the temperature and then corrects the refractive index to a temperature as desired by the user.



Specifications-Refracto 30GS- extended RI measuring range

Model	: Refracto 30GS
Measurement range	: 1.32 -1.65; resolution: 0.0001
Accuracy	: +/- 0.0005
Measurement range BRIX	: 0 - 85 Brix%
Resolution	: 0.1 Brix%
Accuracy	: +/- 0.2 Brix%
Temperature range	: 10 - 40°
resolution	: 0.1°
display	: °C or °F
Trade Name	: 51324660

The ratio of the speed of light in a vacuum to the speed of light in another substance is defined as the index of refraction (also known as refractive index or n_D) for the substance.

$$\text{Refractive index of the substance } (n_D) = \frac{\text{Speed of light in vacuum}}{\text{Speed of light in substance}} \quad (\text{III.8})$$

Whenever light changes speed as it crosses a boundary from one medium into another its direction of travel also changes, i.e., it is refracted (Figure 1). (In the special case of the light traveling perpendicular to the boundary there is no change in direction upon entering the new medium.) The relationship between light's speed in the two mediums (v_A and v_B), the angles of incidence (θ_A) and refraction (θ_B) and the refractive indexes of the two mediums (n_A and n_B) is shown below:

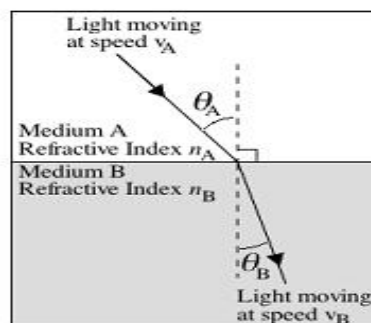


Figure 1. Light crossing from any transparent medium into another in which it has a different speed, is refracted, i.e., bent from its original path (except when the direction of travel is perpendicular to the boundary). In the case shown, the speed of light in medium A is greater than the speed of light in medium B

$$\frac{V_A}{V_B} = \frac{\sin \theta_A}{\sin \theta_B} = \frac{n_B}{n_A} \quad (\text{III.9})$$

Thus, it is not necessary to measure the speed of light in a sample in order to determine its index of refraction. Instead, by means of measuring the angle of refraction, and knowing the index of refraction of the layer to be precise in contact with the sample, it is probable to determine the refractive index of the sample quite accurately [28]. Nearly all refractometers utilize this principle, but may differ in their optical design.

A light source is projected through the illuminating prism, the bottom surface of which be ground (i.e., roughened like a ground-glass joint), so every point on this surface can be thought of as generating light rays traveling in all directions. Assessment of Figure 1 shows that light traveling from point A to point B will have the biggest angle of incidence (q_i) and therefore the largest possible angle of refraction (q_r) for that sample. All other rays of light inflowing the refracting prism will have smaller q_r and hence lie to the left of point C. As a consequence, a detector

located on the back side of the refracting prism would show a light region to the left and a dark region to the right.

III.2.4.7 SURFACE TENSION MEASUREMENT

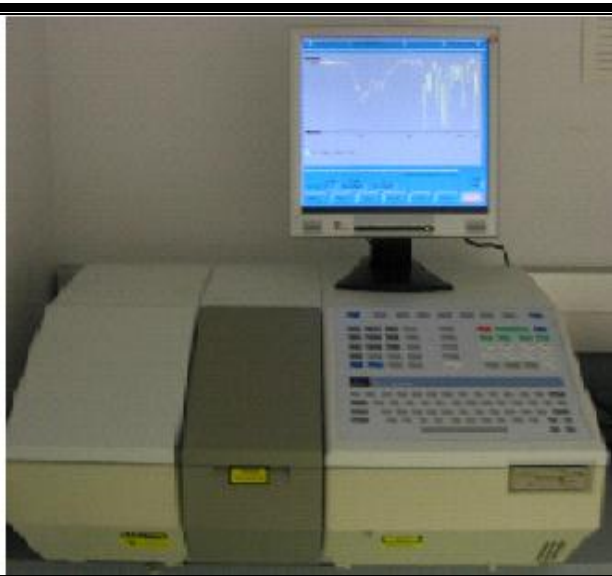
Surface tension was measured by using Digital Tensiometer KRÜSS K9 (Germany). The tensiometer is a precision instrument which will only perform reliably on a solid and vibration-free base. It places the same demands on its surroundings as a laboratory balance with a resolution of 0.1 mg. In addition surface tension measurements require a clean and dust-free atmosphere as atmospheric pollutants could directly falsify the results.



III.2.4.8 FTIR MEASUREMENT

Infrared spectra were recorded in 8300 FTIR spectrometer (Shimadzu, Japan).

It measures the intensity of light passing through the blank and measures the intensity of light passing through the sample. It is useful to calculate the transmittance and the absorbance



The intensity of light (I_0) passing through a blank is considered. The intensity is the number of photons per second. The blank is a solution that is identical to the sample solution except that the blank does not contain the solution that absorbs

light. The intensity of light (I) passing through the sample solution is calculated. (In practice, instrument measures the power somewhat than the intensity of the light. The power is the energy per second, which be the product of the intensity (photons per second) and the energy per photon. The experimental data is used to calculate two quantities: the transmittance (T) and the absorbance (A).

$$T = \frac{I}{I_0}; \quad A = -\log_{10} T \quad (\text{III.10})$$

The transmittance is simply the fraction of light in the original beam that passes through the sample and reaches the detector.

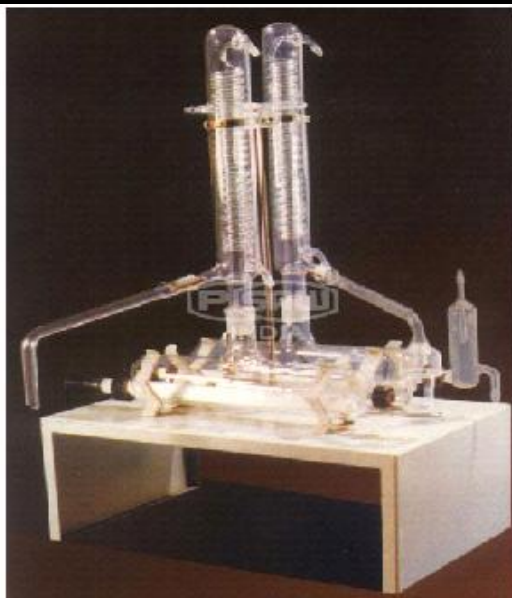
III.2.4.7 NMR MEASUREMENT

Nuclear Magnetic Spectra (NMR) spectroscopy is used to study the structure of molecules, the kinetics or dynamics of molecules and the composition of mixtures of biological or synthetic solutions or composites ^1H NMR spectra were recorded at 400MHz and 500 MHz using Bruker Avance instrument. Signals are quoted as δ values in ppm using residual protonated solvent signals as internal standard (D_2O : δ 4.79 ppm). Data are reported as chemical shift.

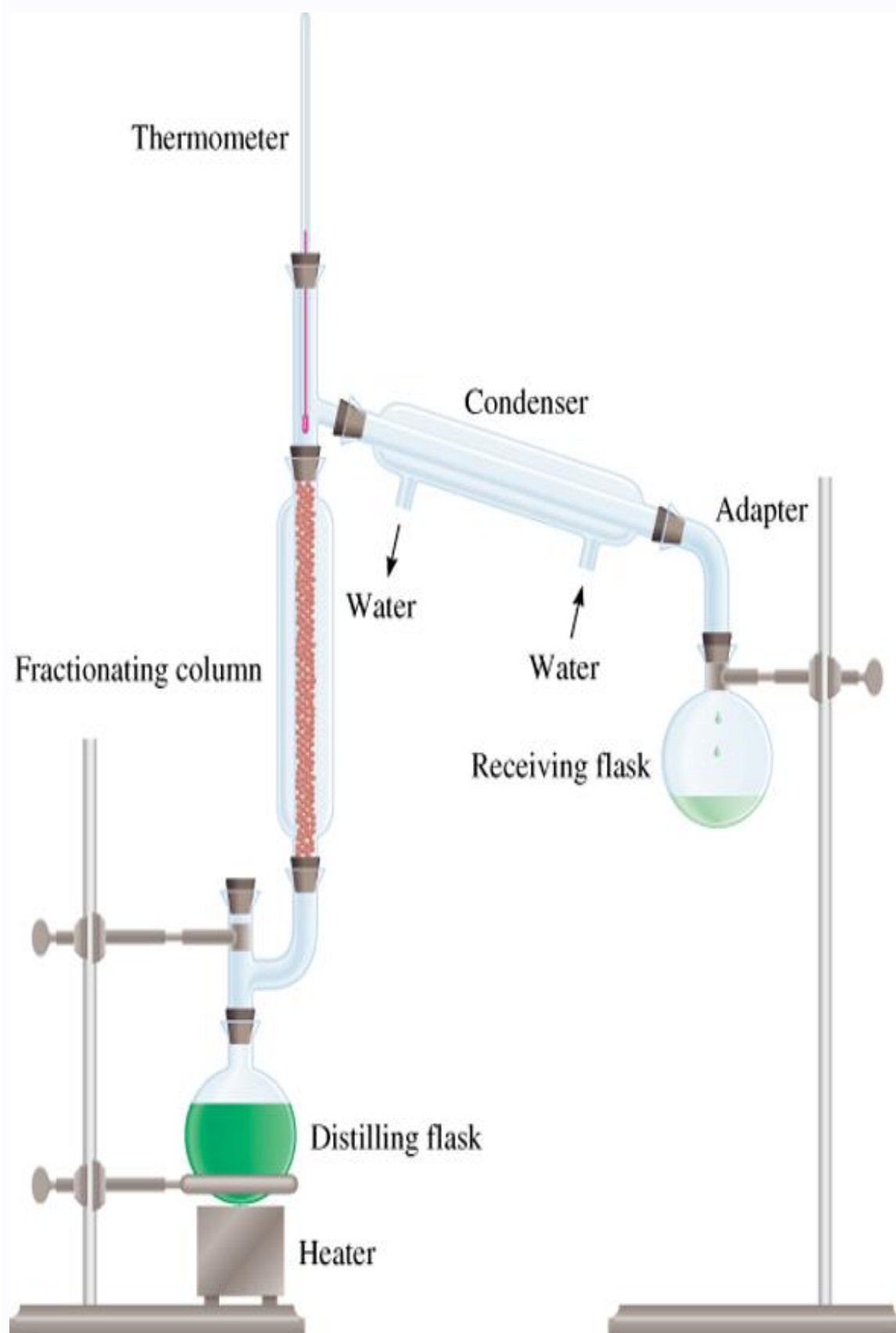


OTHER INSTRUMENTS USED:**III.2.4.8 WATER DISTILLER**

Water distillation units produce highly treated and disinfected water for laboratory usage. The distillation process removes minerals and microbiological contaminants and can reduce levels of chemical contaminants. A water distiller works by boiling water into water vapour, condensing it and then returning it to its liquid state. It is collected in a storage container.



Municipal or well water is physically or automatically fed into the distiller unit's boiling chamber. A heating element inside the boiling chamber heats the water awaiting it boils. The steam increases from the boiling chamber. Volatile contaminants (such as, gases) are discharged through a built-in vent. Minerals and salts are retained in the boiling chamber as hard deposits or scale. The steam penetrates a coiled tube (condenser), which is cooled by cold water. Water droplets form as condensation occurs. The distilled water is collected in a storage tank. If the unit is an automatic model, it is set to activate to fill the storage tank. The distillation apparatus consists of flask with heating elements embedded in glass and fused in spiral category coil internally of the base and tapered round glass, joints at the apex double walled condenser with B-40/B-50 ground glass joints, suitable to work on 220 volts, 50 cycles AC supply.

Fractional Distillation Apparatus

III.2.4.9 THERMOSTAT WATER BATH (Science India, Kolkata):

The measurements were carried out in thermostatic water bath maintained with an accuracy of ± 0.01 K of the desired temperature.



Laboratory water bath is a system in which a vessel containing the substance to be heated is placed into or over the one containing water and to rapidly heat it. These laboratory apparatus supplies are available in different volumes and construction with both digital and analogue controls and greater temperature uniformity, durability, heat retention and recovery. The chambers of water bath lab products are manufactured using rugged, leak proof and highly resistant stainless steel and other lab supplies.

CHAPTER-IV

Ionic Interplay of Lithium Salts in Binary Mixtures of Acetonitrile and Diethyl Carbonate Probed by Physicochemical Approach

IV.1. INTRODUCTION

Behavior of electrolytic solutions can be obtained by studying their thermodynamic and transport properties. The molecular interactions within the electrolytic solution can be studied in a better way by varying the properties of the solvents such as dielectric constant or viscosity which can be attained by using mixed solvent systems. A number of conductometric [1] and related studies of different electrolytes in non-aqueous solvents, especially mixed organic solvents, have made their optimal use in high-energy batteries [2] and for understanding organic reaction mechanisms [3]. The influence of the solvent mixtures on the ionic association of the electrolytes is due to the mode of solvation of the ions [4-8]. Solvent properties such as viscosity and the relative permittivity have been taken into consideration as these properties help in determining the extent of ion association and the solvent-solvent interactions. Thus, extensive studies on electrical conductances in various mixed organic solvents have been performed in recent years [9-13] to examine the nature and magnitude of ion-ion and ion-solvent interactions.

Volumetric and viscometric studies also render an insight into the molecular interactions prevailing in solution and helps in the better understanding of the behavior of electrolytic solutions. Studies on the apparent and limiting apparent molar volumes of the electrolyte and the dependence of viscosity on the concentration of salt have been employed as a function of studying ion-ion and ion-solvent interactions [14].

In this paper, conductometric, volumetric and viscometric studies have been carried out for lithium iodide (LiI), lithium perchlorate (LiClO_4) and lithium hexafluoroarsenate (LiAsF_6) in 0.25, 0.50, 0.75 mass fraction of acetonitrile (AN) in diethyl carbonate (DEC). The salts used in the study when mixed with organic solvents are very good electrolytes in lithium-ion batteries. Lithium-ion batteries are widely used in products such as portable consumer electronic devices. Hence, studying the behaviour of these lithium salts in different organic solvent systems will help in the production of more useful and cost effective batteries. The solvents i.e. acetonitrile and diethyl carbonate used in the study are also very useful in battery industries. By mixing these two solvents we obtained a wide variation in solvent properties.

IV.2. EXPERIMENTAL

IV.2.1 Source and purity of samples

Lithium iodide (LiI), lithium perchlorate (LiClO_4) and lithium hexafluoroarsenate (LiAsF_6) of puriss grade was procured from Aldrich, Germany. It was used as purchased as the purity assay of the salt was $\geq 98\%$. Acetonitrile (AN) procured from Thomas Baker, India and Diethyl carbonate (DEC) procured from Sisco Chem. Industries, India were purified using standard methods. [15]

IV.2.2 Apparatus and Procedure

A stock solution for the electrolyte was prepared by mass (Mettler Toledo AG285 with uncertainty 0.0003 g), and the working solutions were obtained by mass dilution at 298.15K. The uncertainty of molarity of different solutions was evaluated to $\pm 0.0001 \text{ mol dm}^{-3}$. The values of relative permittivity (ϵ) of the solvent mixtures was assumed to be an average of those of the pure liquids and calculated using the procedure as described by Rohdewald and Moldner [16].

The density (ρ) was measured by means of vibrating-tube Anton Paar density-meter (DMA 4500M) with a precision of $0.00005 \text{ g}\cdot\text{cm}^{-3}$. It was calibrated by double-distilled water and dry air.

The viscosity was also measured with the help Brookfield DV-III Ultra Programmable Rheometer with spindle size-42 fitted to a Brookfield Digital Bath TC-500.

The conductance measurements were carried out in a Systronic-308 conductivity meter (accuracy $\pm 0.01\%$) using a dip-type immersion conductivity cell, CD-10, having a cell constant of approximately $(0.1 \pm 0.001) \text{ cm}^{-1}$. Measurements were made in a water bath maintained within $T = (298.15 \pm 0.01) \text{ K}$ and the cell was calibrated by the method proposed by Lind et al. [17] The conductance data were reported at a frequency of 1 kHz and the accuracy was $\pm 0.3\%$.

IV.3. RESULTS AND DISCUSSION

The solvent properties are given in Table IV.1. The concentrations and molar conductances (Λ) of LiI, LiClO₄ and LiAsF₆ in different mass fraction of AN in DEC are given in Table IV.2. The molar conductance (Λ) has been obtained from the specific conductance (κ) value using the following equation.

$$\Lambda = (1000 \kappa) / c \quad (1)$$

Linear conductance curves (Λ versus \sqrt{c}) were obtained for the electrolytes in 0.50 and 0.75 mass fraction of AN in DEC and extrapolation of $\sqrt{c} = 0$ evaluated the starting limiting molar conductance for the electrolytes. But for the electrolytes in 0.25 mass fraction of AN in DEC, a deviation in the conductance curve was obtained and shows a decrease in conductance values upto a certain concentration and again an increase in the conductance value indicating triple-ion formation.

The conductance data for the electrolytes in 0.25 mass fraction of AN in DEC have been analysed using the classical Fuoss-Kraus equation [18] for triple-ion formation

$$\Lambda g(c) \sqrt{c} = \frac{\Lambda_0}{\sqrt{K_p}} + \frac{\Lambda_0^T K_T}{\sqrt{K_p}} \left(1 - \frac{\Lambda}{\Lambda_0} \right) c \quad (2)$$

$$g(c) = \frac{\exp\{ -2.303 \beta^l (c \Lambda)^{0.5} / \Lambda_0^{0.5} \}}{\{ 1 - S (c \Lambda)^{0.5} / \Lambda_0^{1.5} \} (1 - \Lambda / \Lambda_0)^{0.5}} \quad (3)$$

$$\beta^l = 1.8247 \times 10^6 / (\epsilon T)^{1.5} \quad (4)$$

$$S = \alpha \Lambda_0 + \beta = \frac{0.8204 \times 10^6}{(\epsilon T)^{1.5}} \Lambda_0 + \frac{82.501}{\eta(\epsilon T)^{0.5}} \quad (5)$$

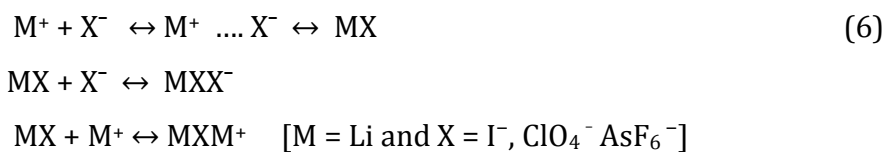
In the above equations, Λ_0 is the sum of the molar conductance of the simple ions at infinite dilution; Λ_0^T is the sum of the conductances of the two triple ions $\text{Li}(\text{X}_2)^-$ and $(\text{Li})_2^+\text{X}$ where $\text{X} = \text{I}^-, \text{ClO}_4^-, \text{AsF}_6^-$; $K_P \approx K_A$ and K_T are the ion pair and triple ion formation constants. To make equation (2) applicable, the symmetrical approximation of the two possible constants of triple ions equal to each other has been adopted [19] and Λ_0 values for the studied electrolytes have been calculated [20]. Λ_0^T is calculated by setting the triple ion conductance equal to $2/3\Lambda_0$ [21].

The ratio Λ_0^T/Λ_0 was thus set equal to 0.667 during linear regression analysis of equation (2).

Table IV.3 shows the calculated limiting molar conductances of simple ion (Λ_0), limiting molar conductances of triple ion Λ_0^T , slope and intercept of equation (2) for LiI, LiClO₄ and LiAsF₆ in 0.25 mass fraction of AN in DEC at 298.15 K.

Linear regression analysis of equation (2) for the electrolytes with an average regression constant, $R^2 = 0.9653$, gives intercepts and slopes. These permit the calculation of other derived parameters such as K_P and K_T listed in Table IV.4. It is observed from Figure IV.1 that Λ passes through a minimum as c increases. A perusal of Table IV.4 shows that the major portion of the electrolytes exists as ion-pairs and a minor portion as triple-ions. The value of $\log(K_T/K_P)$ is found to be highest in LiI as given in Table IV.4 so it has the highest tendency to form triple-ions.

At very low permittivity of the solvent, electrostatic ionic interactions are very large. So the ion-pairs attract the free +ve and -ve ions present in the solution medium as the distance of the closest approach of the ions become minimum. This results in the formation of triple-ions, which acquire the charge of the respective ions in the solution [22] i.e.



Furthermore, the ion-pair and triple-ion concentrations, c_P and c_T respectively of the electrolyte are also calculated at the minimum conductance concentration of LiI, LiClO₄ and LiAsF₆ in 0.25 mass fraction of AN in DEC using the following relations [23]:

$$\alpha = 1 / (K_P^{1/2} \cdot c^{1/2}) \quad (7)$$

$$\alpha_T = (K_T / K_P^{1/2}) c^{1/2} \quad (8)$$

$$c_P = c(1 - \alpha - 3\alpha_T) \quad (9)$$

$$c_T = (K_T / K_P^{1/2}) c^{3/2} \quad (10)$$

Here, α and α_T are the fraction of ion-pairs and triple-ions as given in Table IV.5 respectively.

Thus, c_P and c_T given in Table IV.5 indicates that the ions are mainly present as ion-pairs even at the minimum conductance concentration of each of the salts in the solvent and a small fraction existing as triple-ions. It is observed that at the minimum conductance concentration of the electrolytes in the solvent, LiAsF₆ has the minimum fraction of ion-pairs and triple-ions whereas LiI has the maximum fraction of ion-pairs and triple-ions present in 0.25 mass fraction of AN in DEC. Furthermore, c_P is maximum for LiAsF₆ and minimum for LiI and c_T is found to be highest for LiI and lowest for LiAsF₆.

The ion-pair formation in case of conductometric studies of LiI, LiClO₄ and LiAsF₆ in 0.50 and 0.75 mass fraction of AN in DEC was analysed using the Fuoss conductance equation [24]. With a given set of conductivity values ($c_j, \Lambda_j; j = 1 \dots n$), three adjustable parameters, i.e., Λ_0 , K_A and R have been derived from the Fuoss equation. Here, Λ_0 is the limiting molar conductance, K_A is the observed association constant and R is the association distance, i.e., the maximum centre to centre distance between the ions in the solvent separated ion-pairs. There is no precise method [25] for determining the R value but in order to treat the data in our system, R value is assumed to be, $R = a + d$, where a is the sum of the crystallographic radii of the ions and d is the average distance corresponding to the side of a cell occupied by a solvent molecule. The distance, d is given by:

$$d = 1.183 (M / \rho)^{1/3} \quad (11)$$

where M is the molar mass and ρ is the density of the solvent. For mixed solvents, M is replaced by the mole fraction average molar mass (M_{av}) which is given by,

$$M_{av} = M_1 M_2 / (W_1 M_2 + W_2 M_1) \quad (12)$$

where W_1 is the weight fraction of the first component of molar mass M_1 . Thus, the Fuoss conductance equation may be represented as follows:

$$\Lambda = P \Lambda_0 [(1 + R_x) + E_L] \quad (13)$$

$$P = 1 - \alpha(1 - \gamma) \quad (14)$$

$$\gamma = 1 - K_A c \gamma^2 f^2 \quad (15)$$

$$-\ln f = \beta \kappa / 2(1 + \kappa R) \quad (16)$$

$$\beta = e^2 / (\epsilon_r k_B T) \quad (17)$$

$$K_A = K_R / (1 - \alpha) = K_R / (1 + K_S) \quad (18)$$

where, Λ_0 is the limiting molar conductance, K_A is the observed association constant, R is the association distance, R_x is the relaxation field effect, E_L is the electrophoretic counter current, k is the radius of the ion atmosphere, ϵ is the relative permittivity of the solvent mixture, e is the electron charge, c is the molarity of the solution, k_B is the Boltzmann constant, K_S is the association constant of the contact-pairs, K_R is the association constant of the solvent-separated pairs, γ is the fraction of solute present as unpaired ion, α is the fraction of contact pairs, f is the activity coefficient, T is the absolute temperature and β is twice the Bjerrum distance.

The computations were performed using the program suggested by Fuoss. The initial Λ_0 values for the iteration procedure are obtained from Shedlovsky extrapolation of the data [26]. Input for the program is the no. of data, n , followed by ϵ , η (viscosity of the solvent mixture), initial Λ_0 value, T , ρ (density of the solvent mixture), mole fraction of the first component, molar masses, M_1 and M_2 along with c_j , Λ_j values where $j = 1, 2, \dots, n$ and an instruction to cover preselected range of R values.

In practice, calculations are performed by finding the values of Λ_0 and α which minimize the standard deviation, δ , whereby

$$\delta^2 = \sum [\Lambda_j(cal) - \Lambda_j(obs)]^2 / (n - m) \quad (19)$$

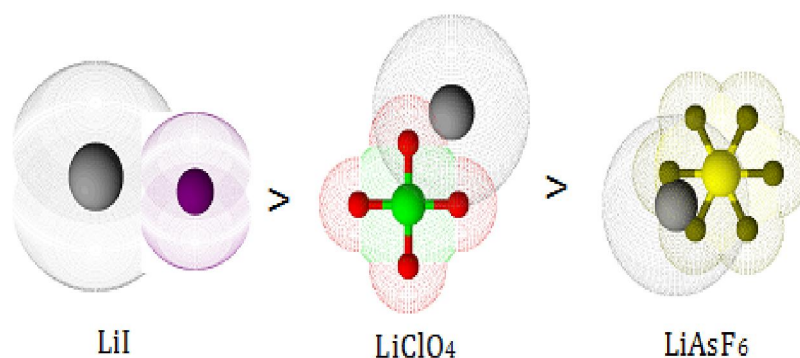
for a sequence of R values and then plotting δ against R , the best-fit R corresponds to the minimum of the δ - R versus R curve. So, an approximate sum is made over a fairly wide range of R values using 0.1 increment to locate the minimum but no significant minima is found in the δ - R curves, thus R values is assumed to be $R = a + d$, with terms having usual significance. Finally, the corresponding Λ_0 and K_A values are obtained which are reported in Table IV.6 along with R and δ for the all the solutions.

A perusal of Table IV.6 and Figure IV.2 shows that the limiting molar conductance (Λ_0) of LiAsF_6 is highest than the other two electrolytes and the conductance decrease with the increase in AN in the solvent mixture. It is evident from the association constant K_A values given in Table IV.6 that LiI is more solvated than the other two electrolytes and the solvation increase with the increase in the AN in the solvent mixture. This shows that with the increase in the viscosity of the solvent mixture the mobility of the ions decrease and hence the conductance also decreases.

The Gibb's energy change of solvation, ΔG° , is given by the following equation [27] and given in Table IV.7.

$$\Delta G^\circ = -RT \ln K_A \quad (20)$$

It is observed from the Table IV.7 that the values of the Gibb's free energy are all negative entire all over the solutions and is highly negative for LiI and the negativity increases with the increase in the mass fraction of AN in the solvent mixture. This result indicates the extent of solvation enhanced by the following order:



Ion-solvation can also be explained with the help of another characteristic property called the Walden Product. Λ_0 decreases for electrolytes with increasing

fraction of AN in DEC and the $\Lambda_0 \cdot \eta$ also decreases even though the viscosity of the solvent increases. This indicates the predominance of Λ_0 over η .

The measured values of densities and viscosities of LiI, LiClO₄ and LiAsF₆ in 0.25, 0.05 and 0.75 mass fraction of AN in DEC at 298.15K are listed in Table IV.8. The densities and viscosities of the electrolytes in different solvent mixtures increase linearly with the concentration at the experimental temperature. For the analysis of interaction of the electrolyte in binary solvent mixtures, limiting apparent molar volume are important. For this purpose, the apparent molar volumes ϕ_V given in Table IV.8 were determined from the solution densities using the following equation [28]

$$\phi_V = M / \rho_o - 1000(\rho - \rho_o) / c \rho_o \quad (21)$$

where M is the molar mass of the solute, c is the molarity of the solution, ρ and ρ_o are the densities of the solution and solvent mixtures, respectively. The limiting apparent molar volumes ϕ_V^0 were calculated using a least-squares treatment to the plots of ϕ_V versus $c^{1/2}$ using the following Masson equation [29]

$$\phi_V = \phi_V^0 + S_V^* \cdot \sqrt{c} \quad (22)$$

where ϕ_V^0 is the limiting apparent molar volume at infinite dilution and S_V^* is the experimental slope. The plots of ϕ_V against the square root of the molar concentration $c^{1/2}$ were found to be linear with negative slopes. The values of ϕ_V^0 and S_V^* are reported in Table 1V.8. The variation of ϕ_V^0 for all the electrolytes with the increase in the mass fraction of AN in the solvent mixture is shown in Figure IV.3.

ϕ_V^0 values for all the electrolytes are generally positive and increase with the amount of AN in the solvent mixture. This indicates the presence of strong ion-solvent interactions and these interactions increase with an increase in the amount of AN in the solvent mixtures under investigation, suggesting a larger electrostriction at higher amounts of AN in the mixture. It can also be seen from Table IV.8 that LiI has a stronger ion-solvent interaction than the rest of the electrolytes in all the solvent systems.

This result is in excellent agreement with the results drawn from the conductance data discussed earlier which shows that LiI has a higher association constant than the other electrolytes which results in greater solvation leading to lower conductance.

The S_V^* values which indicate ion-ion interactions show that the ion-ion interaction is higher for LiAsF₆ than the rest of the electrolytes and decreases with the increase in the mass fraction of AN in the solvent mixtures for all the electrolytes.

The values of viscosity of the solutions, η and $(\eta/\eta_0 - 1)/\sqrt{c}$ are listed in Table IV.9. These η/η_0 values have been utilized to calculate the viscosity A and B -coefficients analysed by the Jones-Dole equation [30]

$$(\eta/\eta_0 - 1)/\sqrt{c} = A + B\sqrt{c} \quad (23)$$

where η and η_0 are the viscosity of the solution and solvent mixtures respectively. The values of A and B are obtained from the straight line by plotting $(\eta/\eta_0 - 1)/\sqrt{c}$ against \sqrt{c} which are reported in Table IV.9. A perusal of Table IV.9 and Figure IV.4 shows that the values of the A -coefficient are very small for all the solutions under investigation at all composition ranges and indicate the presence of weak ion-ion interactions, and these interactions further decrease with an increasing amount of AN in the solvent mixture. It also indicates that the highest ion-ion interaction is seen in case of LiAsF₆. The viscosity B -coefficient [31] reflects the quantitative ion-solvent interactions in the solution. Table IV.9 shows that the viscosity- B coefficient value is the highest for LiI in all the solvent mixtures indicating more ion-solvent interaction in LiI than the other electrolytes. The table also shows that the viscosity- B coefficient values increase with the increase in the mass fraction of AN in the solvent mixtures indicating more ion-solvent interaction in solution containing higher mass fraction of AN in solvent mixtures. The viscosity A and B -coefficients are in excellent agreement with the results drawn from the conductance study and volumetric studies.

IV.4. CONCLUSION

A through conductometric, volumetric and viscometric studies indicates that LiAsF_6 is more conducting in all the solvent mixtures studied. In case of 0.25 mass fraction of AN in DEC, triple-ion formation was seen for the electrolytes. The result revealed that the major portion of the electrolytes exists as ion-pairs and a minor portion as triple-ions and it was observed that LiI has the highest tendency to form triple-ions among the three electrolytes. In case of 0.50 and 0.75 mass fraction of AN in DEC high solvation was seen in case of LiI in all the solvent mixtures studied. With the increase in the mass fraction of AN in the solvent mixture it was seen that the conductance of the electrolytes decreases which indicates that the lower mass fraction of AN in DEC gives better conductance of the electrolytes under study. The volumetric and viscometric studies were in excellent agreement with the conductance studies indicating more ion-solvent interaction in LiI solution which increase with the increase in the mass fraction of AN in DEC.

TABLES**Table IV.1:** Density (ρ), viscosity (η) and relative permittivity (ϵ) of the different mass fraction (w_1) of AN in DEC at 298.15K

w_1	$\rho \cdot 10^{-3}/\text{kg m}^{-3}$	$\eta/\text{mPa s}$	ϵ
0.25	0.82487	0.45	11.11
0.50	0.87325	0.57	19.39
0.75	0.92112	0.65	27.4

Table IV.2: The concentration (c) and molar conductance (Λ) of LiI, LiClO₄ and LiAsF₆ in different mass fraction of (w_1) of AN in DEC at 298.15 K.

$c \cdot 10^4/$ $\text{mol} \cdot \text{dm}^{-3}$	$\Lambda \cdot 10^4/$ $\text{S} \cdot \text{m}^2 \cdot \text{mol}^{-1}$	$c \cdot 10^4/$ $\text{mol} \cdot \text{dm}^{-3}$	$\Lambda \cdot 10^4/$ $\text{S} \cdot \text{m}^2 \cdot \text{mol}^{-1}$	$c \cdot 10^4/$ $\text{mol} \cdot \text{dm}^{-3}$	$\Lambda \cdot 10^4/$ $\text{S} \cdot \text{m}^2 \cdot \text{mol}^{-1}$
$w_1=0.25$					
LiI		LiClO ₄		LiAsF ₆	
1.1529	118.41	1.3381	128.12	1.3847	157.01
2.9879	85.93	3.5514	101.23	3.6272	134.23
4.3410	68.89	5.1940	87.28	5.2856	117.06
5.3780	54.75	6.4557	76.31	6.5578	106.41
6.1975	45.87	7.4542	67.59	7.5638	98.23
6.8614	40.12	8.2638	61.16	8.3792	90.02
7.4102	34.47	8.9333	56.32	9.0532	83.57
7.8713	29.91	9.7451	50.39	9.8704	77.79
8.4396	25.50	10.5758	45.21	10.7063	72.12
9.0319	20.00	10.9135	45.28	11.0460	68.74
9.4926	19.10	11.2115	44.51	11.3458	67.16
9.8613	21.00	11.5983	45.85	11.7349	65.53

10.2301	24.00	12.1522	48.42	12.2920	64.65
10.5772	26.10	12.5033	49.69	12.6451	65.51
10.7584	29.30	12.9168	54.11	13.0610	68.06
$w_1=0.50$					
	LiI		LiClO ₄		LiAsF ₆
1.4580	92.01	1.4923	96.51	1.4580	121.41
2.6730	87.34	2.7359	92.78	2.6730	116.50
3.7011	85.32	3.7882	89.55	3.7011	113.30
4.5823	83.21	5.4718	85.69	4.5823	110.59
5.3460	80.95	6.7593	83.52	5.3460	108.42
6.0143	79.19	7.7757	81.21	6.0143	106.11
7.1280	78.21	8.2077	80.00	6.6039	104.90
8.0190	76.49	8.9538	79.15	7.5969	104.05
8.7480	74.34	9.5756	76.91	8.0190	101.91
9.0650	74.51	10.1018	76.99	8.4009	101.89
9.3555	73.67	10.9436	75.98	9.6228	100.88
10.3101	72.79	12.0955	73.53	10.5077	98.43
10.6920	71.41	12.4116	73.27	11.4557	98.17
11.5830	70.57	13.0653	72.50	11.8175	97.40
12.8304	69.51	13.5072	71.79	12.5515	95.50
$w_1=0.75$					
	LiI		LiClO ₄		LiAsF ₆
2.2201	68.88	4.3681	75.73	4.1142	100.92
4.3681	64.78	6.8121	71.31	7.5426	94.41
8.9401	57.10	10.1761	67.57	10.4436	88.95
12.9302	52.08	14.0625	62.03	12.9302	86.21
16.8921	48.40	16.9725	59.63	15.0853	84.23
18.6347	46.90	20.1156	56.71	16.9709	81.31
21.4370	44.38	22.6300	54.92	18.6347	78.57

22.6279	43.08	24.6873	52.76	20.1137	78.51
25.2004	41.58	27.1560	51.35	21.4370	75.32
27.5625	39.58	28.4970	50.50	22.6279	74.26
28.1961	39.08	29.0957	49.81	23.7054	74.71
30.8025	36.58	29.6531	49.13	24.6850	73.69
33.6400	34.90	30.1733	49.16	26.3992	71.51
35.5216	32.88	30.6600	48.75	29.0930	69.82
38.1924	31.30	31.9482	47.62	31.9225	68.17

Table IV.3: The calculated limiting molar conductance of ion-pair (Λ_0), limiting molar conductances of triple ion Λ_0^T , experimental slope and intercept obtained from Fuoss-Kraus Equation for LiI, LiClO₄ and LiAsF₆ in 0.025 mass fraction of (w_1) of AN in DEC at 298.15 K.

Salts	$\Lambda \cdot 10^4$	$\Lambda_0^T \times 10^4$	Slope $\times 10^{10}$	Intercept
	/S·m ² ·mol ⁻¹	/S·m ² ·mol ⁻¹		$\times 10^{10}$
	$w_1=0.25$			
LiI	123.78	82.56	7.032	-48.20
LiClO ₄	133.58	89.10	1.318	-8.59
LiAsF ₆	169.87	113.30	1.218	-7.56

Table IV.4: Salt concentration at the minimum conductivity (C_{\min}) along with the ion-pair formation constant (K_P), triple ion formation constant (K_T) for LiI, LiClO₄ and LiAsF₆ in 0.025 mass fraction of (w_1) of AN in DEC at 298.15 K.

Salts	$c_{\min} \cdot 10^4 /$	$\log C_{\min}$	$K_P \cdot 10^{-22} /$	$K_T /$	K_T / K_P	$\log K_T / K_P$
	mol·dm ⁻³		(mol·dm ⁻³) ⁻¹	(mol·dm ⁻³) ⁻¹	$\cdot 10^{22}$	

$w_1=0.25$						
LiI	9.4926	-4.0226	0.0700	0.2187	3.1243	-21.505
LiClO ₄	11.2115	-2.9503	2.4200	0.2301	0.0951	-23.022
LiAsF ₆	12.2920	-2.9103	5.0536	0.2417	0.0479	-23.320

Table IV.5: Salt concentration at the minimum conductivity (c_{\min}), the ion pair fraction (α), triple ion fraction (α_T), ion pair concentration (c_P) and triple-ion concentration (c_T) for LiI, LiClO₄ and LiAsF₆ in 0.025 mass fraction of (w_1) of AN in DEC at 298.15 K.

Salts	$c_{\min} \cdot 10^4 /$ mol·dm ⁻³	$\alpha \cdot 10^{10}$	$\alpha_T \cdot 10^{14}$	$c_P \cdot 10^4 /$ mol·dm ⁻³	$c_T \cdot 10^{17} /$ mol ·dm ⁻³
$w_1=0.25$					
LiI	9.4926	12.267	25.468	9.4926	24.176
LiClO ₄	11.2115	1.9198	4.9527	11.211	5.5527
LiAsF ₆	12.2920	1.2692	3.7709	12.292	4.6351

Table IV.6: Limiting molar conductance (Λ_0), association constant (K_A), co-sphere diameter (R) and standard deviations of experimental Λ (δ) obtained from Fuoss conductance equation for LiI, LiClO₄ and LiAsF₆ in 0.025 mass fraction of (w_1) of AN in DEC at 298.15 K.

Salt	$\Lambda_0 \cdot 10^4 / \text{S} \cdot \text{m}^2 \cdot \text{mol}^{-1}$	$K_A / \text{dm}^3 \cdot \text{mol}^{-1}$	$R / \text{\AA}$	δ
$w_1=0.50$				
LiI	103.92	778.85	7.32	1.2757
LiClO ₄	107.83	670.96	7.15	0.7313
LiAsF ₆	131.21	486.18	8.25	0.5761
$w_1=0.75$				

LiI	87.03	1209.70	7.16	2.3758
LiClO ₄	97.17	790.45	7.14	1.0105
LiAsF ₆	121.09	536.01	8.09	0.9770

Table IV.7: Walden product ($\Lambda_0 \cdot \eta$) and Gibb's energy change (ΔG°) of LiI, LiClO₄ and LiAsF₆ in 0.025 mass fraction of (w_1) of AN in DEC at 298.15 K.

Salt	$\Lambda_0 \cdot \eta \cdot 10^4 /$ $S \cdot m^2 \cdot mol^{-1} mPa \cdot s$	$\Delta G^\circ /$ $kJ \cdot mol^{-1}$
$w_1 = 0.50$		
LiI	46.77	-16503.55
LiClO ₄	61.46	-16133.76
LiAsF ₆	85.28	-15335.43
$w_1 = 0.75$		
LiI	39.16	-17594.98
LiClO ₄	55.39	-16540.18
LiAsF ₆	78.71	-15577.28

Table IV.8: Concentration, c , density, ρ , apparent molar volume, ϕ_V , limiting apparent molar volume ϕ_V^0 and experimental slope for LiI, LiClO₄ and LiAsF₆ in 0.025 mass fraction of (w_1) of AN in DEC at 298.15 K.

Salts	$c /$ $mol \cdot dm^{-3}$	$\rho \cdot 10^{-3} /$ $kg \cdot m^{-3}$	$\phi_V \cdot 10^6 /$ $m^3 \cdot mol^{-1}$	$\phi_V^0 \cdot 10^6 /$ $m^3 \cdot mol^{-1}$	$S_V^* \cdot 10^6 /$ $m^3 \cdot mol^{-3/2} \cdot dm^{3/2}$
$w_1 = 0.25$					
LiI	0.005	0.82503	123.50	127.20	-52.79
	0.020	0.82557	119.71		
	0.035	0.82617	117.27		
	0.050	0.82680	115.45		

	0.065	0.82747	113.70		
	0.080	0.82817	112.31		
LiClO ₄	0.005	0.82498	102.13	105.4	-46.73
	0.020	0.82537	98.70		
	0.035	0.82580	96.70		
	0.050	0.82627	94.98		
	0.065	0.82678	93.40		
	0.080	0.82729	92.23		
LiAsF ₆	0.005	0.82558	65.72	67.54	-25.75
	0.020	0.82773	63.87		
	0.035	0.82992	62.66		
	0.050	0.83211	61.82		
	0.065	0.83433	60.96		
	0.080	0.83656	60.24		
$w_1=0.50$					
LiI	0.005	0.87334	132.50	138.07	-78.36
	0.020	0.87371	126.93		
	0.035	0.87416	123.56		
	0.050	0.87468	120.60		
	0.065	0.87526	117.94		
	0.080	0.87586	115.93		
LiClO ₄	0.005	0.87328	116.00	119.98	-56.84
	0.020	0.87342	111.92		
	0.035	0.87363	109.34		
	0.050	0.87389	107.20		
	0.065	0.87418	105.44		
	0.080	0.87450	104.00		
LiAsF ₆	0.005	0.88403	70.04	73.01	-42.58
	0.020	0.88424	66.92		

	0.035	0.88437	65.10		
	0.050	0.88448	63.46		
	0.065	0.88458	62.15		
	0.080	0.88466	61.00		
w ₁ =0.75					
LiI	0.005	0.92117	134.80	143.88	-136.18
	0.020	0.92151	124.00		
	0.035	0.92199	118.30		
	0.050	0.92260	113.10		
	0.065	0.92329	109.10		
	0.080	0.92402	105.90		
LiClO ₄	0.005	0.92114	111.60	121.00	-131.66
	0.020	0.92136	102.60		
	0.035	0.92175	96.00		
	0.050	0.92221	91.70		
	0.065	0.92275	88.00		
	0.080	0.92347	83.30		
LiAsF ₆	0.005	0.92172	81.50	88.92	-108.71
	0.020	0.92369	73.30		
	0.035	0.92577	68.50		
	0.050	0.92794	64.50		
	0.065	0.93019	61.10		
	0.080	0.93248	58.50		

Table IV.9: Concentration, c , viscosity, η , $\frac{(\eta_r - 1)}{\sqrt{c}}$, viscosity A and B coefficients

for LiI, LiClO₄ and LiAsF₆ in 0.025 mass fraction of (w_1) of AN in DEC at 298.15 K.

Salts	$c / \text{mol} \cdot \text{dm}^{-3}$	$\eta / \text{mPa} \cdot \text{s}$	$\frac{(\eta_r - 1)}{\sqrt{c}}$	B / $\text{dm}^3 \cdot \text{mol}^{-1}$	$A / \text{dm}^{3/2} \cdot \text{mol}^{-1/2}$
-------	---------------------------------------	------------------------------------	---------------------------------	--	---

$w_1=0.25$					
LiI	0.005	0.49	1.11	3.40	0.87
	0.020	0.54	1.34		
	0.035	0.58	1.51		
	0.050	0.61	1.63		
	0.065	0.65	1.73		
	0.080	0.68	1.83		
LiClO ₄	0.005	0.48	1.02	1.22	0.94
	0.020	0.52	1.12		
	0.035	0.55	1.17		
	0.050	0.57	1.21		
	0.065	0.59	1.26		
	0.080	0.61	1.28		
LiAsF ₆	0.005	0.50	1.62	1.12	1.54
	0.020	0.56	1.70		
	0.035	0.60	1.75		
	0.050	0.63	1.79		
	0.065	0.66	1.83		
	0.080	0.69	1.86		
$w_1=0.50$					
LiI	0.005	0.60	0.68	4.49	0.36
	0.020	0.65	0.99		
	0.035	0.70	1.20		
	0.050	0.74	1.36		
	0.065	0.79	1.49		
	0.080	0.83	1.64		
LiClO ₄	0.005	0.59	0.49	1.32	0.39
	0.020	0.62	0.58		
	0.035	0.64	0.65		

	0.050	0.66	0.69		
	0.065	0.68	0.73		
	0.080	0.69	0.77		
LiAsF ₆	0.005	0.62	1.13	1.28	1.03
	0.020	0.67	1.20		
	0.035	0.70	1.26		
	0.050	0.74	1.30		
	0.065	0.77	1.37		
	0.080	0.79	1.39		
w ₁ =0.75					
LiI	0.005	0.68	0.67	5.49	0.28
	0.020	0.75	1.05		
	0.035	0.81	1.32		
	0.050	0.87	1.51		
	0.065	0.93	1.69		
	0.080	0.99	1.83		
LiClO ₄	0.005	0.67	0.47	1.46	0.37
	0.020	0.70	0.57		
	0.035	0.73	0.65		
	0.050	0.75	0.70		
	0.065	0.77	0.74		
	0.080	0.79	0.77		
LiAsF ₆	0.005	0.70	1.12	1.32	1.01
	0.020	0.76	1.20		
	0.035	0.80	1.26		
	0.050	0.84	1.32		
	0.065	0.87	1.36		
	0.080	0.91	1.40		

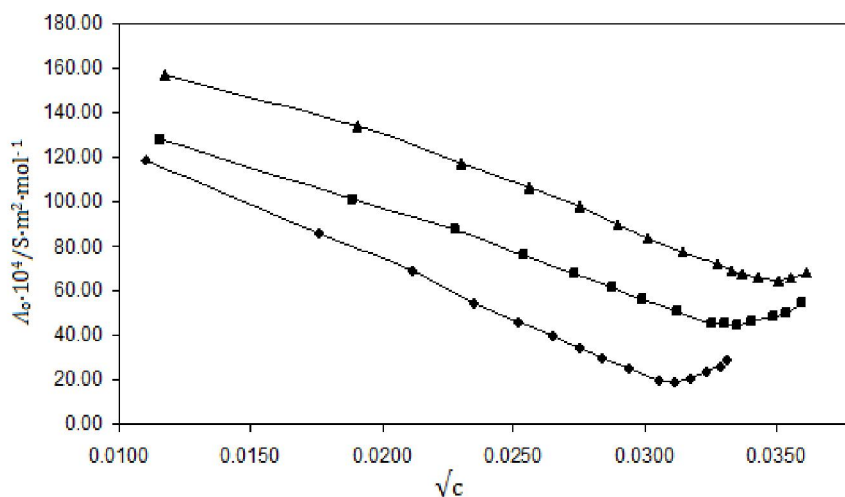
FIGURES

Figure IV.1: Plot of molar conductance (Λ) versus \sqrt{c} for LiI (—◆—), LiClO₄ (—■—) and LiAsF₆ (—▲—) in 0.025 mass fraction of AN in DEC at 298.15

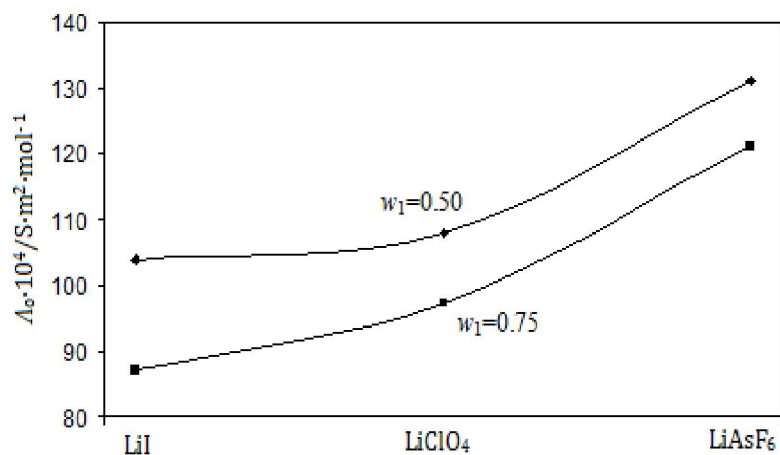


Figure IV.2: Plot of limiting molar conductance (Λ_0) for LiI, LiClO₄ and LiAsF₆ in 0.50 (—◆—) and 0.75 (—■—) mass fraction of AN in DEC at 298.15.

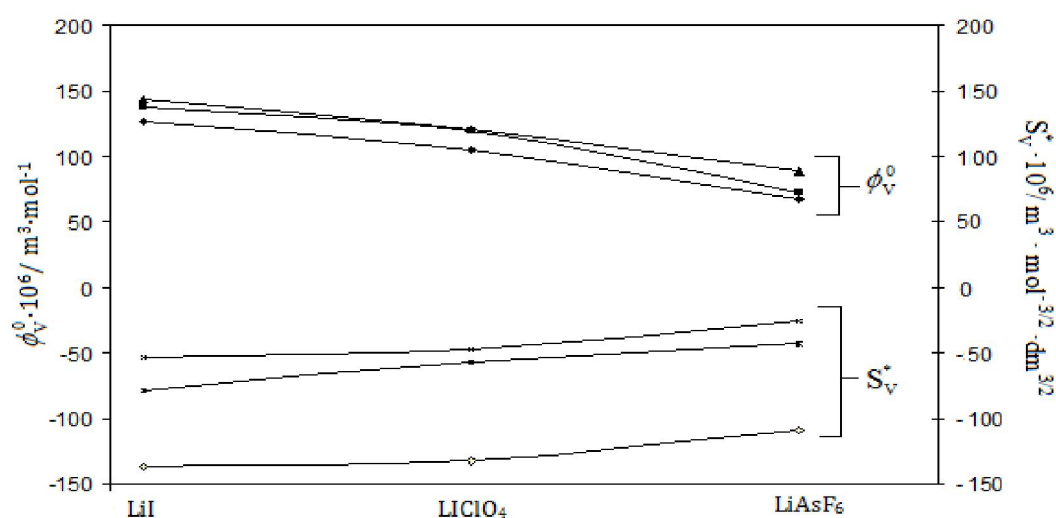


Figure IV.3: Limiting apparent molar volume (ϕ_V^0) for LiI, LiClO₄ and LiAsF₆ in 0.25(-♦-), 0.50(-■-) and 0.75 (-▲-) mass fraction of AN in DEC and experimental slope (S_V^*) for LiI, LiClO₄ and LiAsF₆ in 0.25 (-x-), 0.50(-*-) and 0.75 (-◇-) mass fraction of AN in DEC at 298.15 K

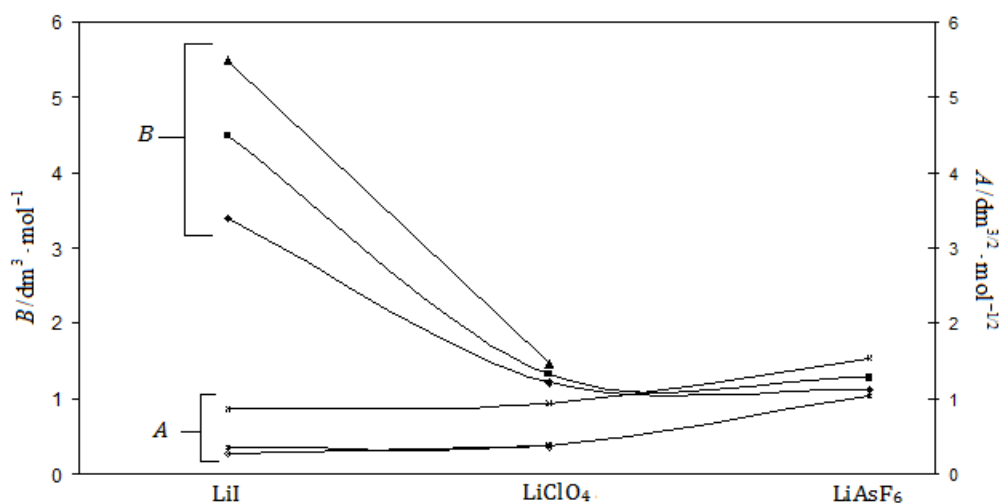
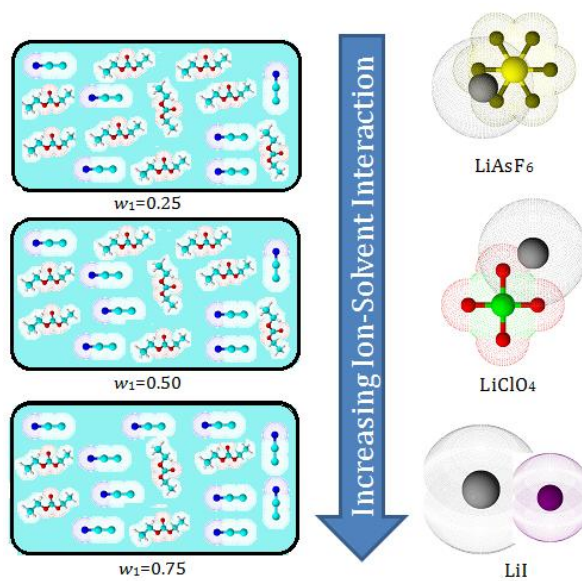


Figure IV.4: Viscosity B -coefficient for LiI, LiClO₄ and LiAsF₆ in 0.25(-♦-), 0.50(-■-) and 0.75 (-▲-) mass fraction of AN in DEC and viscosity A -coefficient for LiI, LiClO₄ and LiAsF₆ in 0.25 (-x-), 0.50(-*-) and 0.75 (-◇-) mass fraction of AN in DEC at 298.15 K.

SCHEMES**Scheme IV.1.** Trend in the ion solvent interaction

CHAPTER-V

Essential foundation of triple-Ion and ion-Pair formation of tetraheptylammonium iodide (Hept₄NI) salt in organic solvents investigated by physicochemical approach

V.1. INTRODUCTION

Behaviour of electrolytic solutions can be obtained by studying their thermodynamic and transport properties. The molecular interactions within the electrolytic solution can be studied in a better way by varying the properties of the solvents such as dielectric constant or viscosity. A number of conductometric [1] and related studies of different electrolytes in non-aqueous solvents, have been done in relation to the use of the electrolyte in high-energy batteries [2] and for understanding organic reaction mechanisms [3]. The formation of triple-ion in media having low permittivity ($\epsilon < 10$) [4] have been investigated from the conductivity studies of Hept₄NI [5,6]. The minima observed in conductometric curves (Λ versus \sqrt{c}) in this type of solvents were interpreted by the formation of M_2X^+ and MX_2^- triple-ion species [7].

Volumetric and viscometric studies also render an insight into the molecular interactions prevailing in solution and helps in the better understanding of the behavior of electrolytic solutions. Studies on the apparent and limiting apparent molar volumes of the electrolyte and the dependence of viscosity on the concentration of salt have been employed as a function of studying ion-ion and ion-solvent interactions [8].

In this paper, conductometric, volumetric and viscometric studies have been carried out for Hept₄NI in o-Toluidine, o-Xylene and 2-Nitrotoluidine. Hept₄NI used in this study has a number of applications such as it employed as phase transfer catalyst, it is also used as osmolytes. The solvent o-Toluidine used in the production of dyes. o-Xylene and 2-Nitrotoluidine solvents are largely used in the production of phthalic anhydride and pigments, antioxidants respectively.

V.2. EXPERIMENTAL

V.2.1 Materials

Hept₄NI of puriss grade was procured from Sigma Aldrich, Switzerland. It was used as purchased as the purity assay of the salt was $\geq 99\%$. o-Toluidine procured from Merck, India; o-Xylene procured from Sisco Research Laboratory Pvt. Ltd. Bombay, India and 2-Nitrotoluene procured from Sisco Chem. Industries, India. The solvents were purified using standard methods [9].

V.2.2 Apparatus and Procedure

A stock solution for the electrolyte was prepared by mass (Mettler Toledo AG285 with uncertainty 0.0003 g), and the working solutions were obtained by mass dilution at 298.15 K. The uncertainty of molarity of different solutions was evaluated to $\pm 0.0001 \text{ mol dm}^{-3}$.

The density (ρ) was measured by means of vibrating-tube Anton Paar density-meter (DMA 4500M) with a precision of $\pm 0.00005 \text{ g}\cdot\text{cm}^{-3}$. It was calibrated by double-distilled water and dry air [10]. The temperature was automatically kept constant within $\pm 0.01 \text{ K}$.

The viscosity was also measured with the help Brookfield DV-III Ultra Programmable Rheometer with spindle size-42 having an accuracy of $\pm 1.0\%$ range with displayed test data and fitted to a Brookfield Digital Bath TC-500.

The conductance measurements were carried out in a Systronic-308 conductivity meter (accuracy $\pm 0.01 \%$) using a dip-type immersion conductivity cell, CD-10, having a cell constant of approximately $(0.1 \pm 0.001) \text{ cm}^{-1}$. Measurements were made in a water bath maintained within $T = (298.15 \pm 0.01) \text{ K}$ and the cell was calibrated by the method proposed by Lind et al. [11] The conductance data were reported at a frequency of 1 kHz and the accuracy was $\pm 0.3\%$.

V.3. RESULTS AND DISCUSSION

The solvent properties are given in Table V.1. The concentrations and molar conductances (Λ) of o-Toluidine, o-Xylene, and 2-Nitrotoluidine are given in Table V.2. The molar conductance (Λ) has been obtained from the specific conductance (κ) value using the following equation.

$$\Lambda = (1000 \kappa) / c \quad (1)$$

Linear conductance curve (Λ versus \sqrt{c}) was obtained for the electrolyte in 2-Nitrotoluene, extrapolation of $\sqrt{c} = 0$ evaluated the starting limiting molar conductance for the electrolyte. But for the electrolyte in o-Xylene and o-Toluidine, a deviation in the conductance curve was obtained and shows a decrease in conductance values upto a certain concentration reaches a minimum and then increases indicating triple-ion formation.

The conductance data for the electrolyte in o-Xylene and o-Toluidine have been analysed using the classical Fuoss-Kraus equation [12] for triple-ion formation

$$\Lambda g(c) \sqrt{c} = \frac{\Lambda_0}{\sqrt{K_p}} + \frac{\Lambda_0^T K_T}{\sqrt{K_p}} \left(1 - \frac{\Lambda}{\Lambda_0} \right) c \quad (2)$$

$$g(c) = \frac{\exp\{ -2.303 \beta' (c \Lambda)^{0.5} / \Lambda_0^{0.5} \}}{\{ 1 - S (c \Lambda)^{0.5} / \Lambda_0^{1.5} \} (1 - \Lambda / \Lambda_0)^{0.5}} \quad (3)$$

$$\beta' = 1.8247 \times 10^6 / (\epsilon T)^{1.5} \quad (4)$$

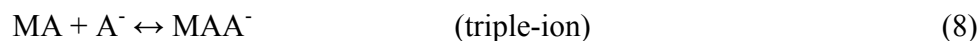
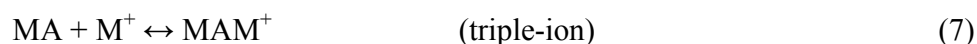
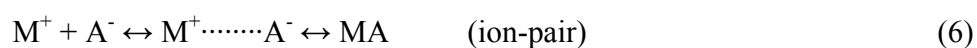
$$S = \alpha \Lambda_0 + \beta = \frac{0.8204 \times 10^6}{(\epsilon T)^{1.5}} \Lambda_0 + \frac{82.501}{\eta (\epsilon T)^{0.5}} \quad (5)$$

In the above equations, Λ_0 is the sum of the molar conductance of the simple ions at infinite dilution; Λ_0^T is the sum of the conductances of the two triple ions $[(\text{Hept})_4\text{N}]_2^+\text{I}$ and $(\text{Hept})_4\text{N}(\text{I})_2^-$. $K_p \approx K_A$ and K_T are the ion-pair and triple-ion formation constants. To make equation (2) applicable, the symmetrical approximation of the two possible constants of triple ions equal to each other has been adopted [13] and Λ_0 values for the studied electrolytes have been calculated [14]. Λ_0^T is calculated by setting the triple ion conductance equal to $2/3\Lambda_0$ [15].

The ratio Λ_0^T/Λ_0 was thus set equal to 0.667 during linear regression analysis of equation (2). A perusal of Table V.3, Figure V.1 and V.2 show that the limiting molar conductance (Λ_0) of Hept₄NI is higher in o-Toluidine than o-Xylene. Limiting molar conductance of triple-ions (Λ_0^T), slope and intercept of Eq. (2) for Hept₄NI in o-Toluidine and o-Xylene are given in Table V.3.

Linear regression analysis of equation (2) for the electrolytes with an average regression constant, $R^2 = 0.9653$, gives intercepts and slopes. These permit the calculation of other derived parameters such as K_P and K_T listed in Table V.4. It is observed from Figure V.1 and V.2 that Λ passes through a minimum as c increases. The K_P and K_T values predict that major portion of the electrolyte exists as ion-pairs with a minor portion as triple-ions (neglecting quadrupoles). The value of $\log(K_T/K_P)$ is found to be higher in o-Xylene than in o-Toluidine. This shows that o-Xylene has higher tendency to form triple-ion than o-Toluidine [16].

At very low permittivity of the solvent ($\epsilon < 10$) electrostatic ionic interactions are very large. So the ion-pairs attract the free +ve and -ve ions present in the solution medium as the distance of the closest approach of the ions becomes minimum. These results in the formation of triple-ions, which acquire the charge of the respective ions in the solution [17] i.e.



Where M^+ and A^- are Hept₄N⁺ and I⁻ respectively. The effect of ternary association [18] thus removes some non-conducting species, MA, from solution, and replaces them with triple-ions which increase the conductance manifested by non-linearity observed in conductance curves for the electrolyte in o-Toluidine and o-Xylene.

Furthermore, the ion-pair and triple-ion concentrations, c_P and c_T respectively of the electrolyte have also been calculated at the minimum conductance concentration of Hept₄NI in o-Toluidine and o-Xylene using the following relations [19].

$$\alpha = 1 / (K_P^{1/2} \cdot c^{1/2}) \quad (9)$$

$$\alpha_T = (K_T / K_P^{1/2}) c^{1/2} \quad (10)$$

$$c_P = c(1 - \alpha - 3\alpha_T) \quad (11)$$

$$c_T = (K_T / K_P^{1/2}) c^{3/2} \quad (12)$$

Here α and α_T are the fractions of ion-pairs and triple-ions present in the salt-solutions respectively and are given in Table V.5. Thus, the values of C_P and C_T also given in Table V.5 indicate that the ions are mainly present as ion-pairs even at high concentration and a small fraction existing as triple-ions. The ion-pair fraction (α), triple-ion fraction (α_T), ion-pair concentration (C_P) and triple-ion concentration (C_T) have also been calculated over the whole concentration range of [Hept₄NI] in o-Toluidine and o-Xylene and the data are provided in Table V.5.

The ion-pair formation in case of conductometric study of Hept₄NI in 2-Nitrotoluene was analysed using the Fuoss conductance equation [20]. With a given set of conductivity values ($c_j, \Lambda_j; j = 1 \dots n$), three adjustable parameters, i.e., Λ_0, K_A and R have been derived from the Fuoss equation. Here, Λ_0 is the limiting molar conductance, K_A is the observed association constant and R is the association distance, i.e., the maximum centre to centre distance between the ions in the solvent separated ion-pairs. There is no precise method [21] for determining the R value but in order to treat the data in our system, R value is assumed to be, $R = a + d$, where a is the sum of the crystallographic radii of the ions and d is the average distance corresponding to the side of a cell occupied by a solvent molecule. The distance, d is given by:

$$d = 1.183 (M / \rho)^{1/3} \quad (13)$$

where, M is the molar mass and ρ is the density of the solvent.

Thus, the Fuoss conductance equation may be represented as follows:

$$\Lambda = P\Lambda_0[(1+R_X) + E_L] \quad (14)$$

$$P = 1 - \alpha(1 - \gamma) \quad (15)$$

$$\gamma = 1 - K_A c \gamma^2 f^2 \quad (16)$$

$$-\ln f = \beta \kappa / 2(1 + \kappa R) \quad (17)$$

$$\beta = e^2 / (\epsilon_r k_B T) \quad (18)$$

$$K_A = K_R / (1 - \alpha) = K_R / (1 + K_S) \quad (19)$$

where, Λ_0 is the limiting molar conductance, K_A is the observed association constant, R is the association distance, R_X is the relaxation field effect, E_L is the electrophoretic counter current, k is the radius of the ion atmosphere, ϵ is the relative permittivity of the solvent mixture, e is the electron charge, c is the molarity of the solution, k_B is the Boltzmann constant, K_S is the association constant of the contact-pairs, K_R is the association constant of the solvent-separated pairs, γ is the fraction of solute present as unpaired ion, α is the fraction of contact pairs, f is the activity coefficient, T is the absolute temperature and β is twice the Bjerrum distance.

The computations were performed using the program suggested by Fuoss. The initial Λ_0 values for the iteration procedure are obtained from Shedlovsky extrapolation of the data [22]. Input for the program is the no. of data, n , followed by ϵ , η (viscosity of the solvent mixture), initial Λ_0 value, T , ρ (density of the solvent mixture), mole fraction of the first component, molar masses, M_1 and M_2 along with c_j , Λ_j values where $j = 1, 2, \dots, n$ and an instruction to cover preselected range of R values.

In practice, calculations are performed by finding the values of Λ_0 and α which minimize the standard deviation, δ , whereby

$$\delta^2 = \sum [A_j(cal) - A_j(obs)]^2 / (n - m) \quad (20)$$

for a sequence of R values and then plotting δ against R , the best-fit R corresponds to the minimum of the δ - R versus R curve. So, an approximate sum is made over a fairly wide range of R values using 0.1 increment to locate the minimum but no significant minima is found in the δ - R curves, thus R values is assumed to be $R = a + d$, with terms having usual

significance. Finally, the corresponding Λ_0 and K_A values are obtained which are reported in Table V.6 along with R and δ for the all the solutions.

Limiting molar conductance (Λ_0), association constant (K_A), co-sphere diameter (R) and standard deviations of experimental Λ (δ) obtained from Fuoss conductance equation for Hept₄NI in 2-Nitrotoluene at 298.15 K are given in Table V.6.

The Gibb's energy change of solvation, ΔG° , for Hept₄NI in 2-Nitrotoluene is given by the following equation [23]

$$\Delta G^\circ = -RT \ln K_A \quad (21)$$

It is observed from the Table V.7 that the value of the Gibb's free energy is entirely negative for 2-Nitrotoluene and it can be explained by considering the participation of specific covalent interaction in the ion-association process.

Table V.8 shows the value of ionic conductance (λ_0^\pm) and ionic Walden product ($\lambda_0^\pm \eta$) (product of ionic conductance and viscosity of the solvent) along with Stokes' radii (r_s) and Crystallographic Radii (r_c) of Hept₄NI in 2-Nitrotoluene. It is seen from this table that I⁻ has higher ionic conductance and Walden product than Hept₄N⁺ and in case of Stokes' radii and Crystallographic Radii reverse order of value is observed for I⁻ and Hept₄N⁺ of Hept₄NI.

The measured values of densities of Hept₄NI in o-Toluidine, o-Xylene and 2-Nitrotoluidine at 298.15 K are listed in Table V.9. The densities and viscosities of the electrolytes in different solvents increase linearly with the concentration at the experimental temperature. For this purpose, the apparent molar volumes ϕ_V given in Table V.9 were determined from the solution densities using the following equation [24]

$$\phi_V = M / \rho_0 - 1000(\rho - \rho_0) / c \rho_0 \quad (22)$$

where M is the molar mass of the solute, c is the molarity of the solution, ρ and ρ_0 are the densities of the solution and solvent, respectively. The limiting apparent molar volumes ϕ_V^0 were calculated using a least-squares treatment to the plots of ϕ_V versus $c^{1/2}$ using the following Masson equation [25]

$$\phi_V = \phi_V^0 + S_V^* \cdot \sqrt{c} \quad (23)$$

where ϕ_V^0 is the limiting apparent molar volume at infinite dilution and S_V^* is the experimental slope.

The plots of ϕ_V against the square root of the molar concentration $c^{1/2}$ were found to be linear with negative slopes. The values of ϕ_V^0 and S_V^* are reported in Table V.9. The variation of ϕ_V^0 for this electrolyte with the solvents is shown in Figure V.4. From Table V.9 it is seen that ϕ_V^0 values for this electrolyte are generally positive for all the solvents and is highest in case of Hept₄NI in 2-Nitrotoluene. This indicates the presence of strong ion-solvent interactions and the extent of interactions increases from o-Toluidine to 2-Nitrotoluene.

On the contrary, the S_V^* indicates the extent of ion-ion interaction. The values of S_V^* shows that the extent of ion-ion interaction is highest in case of o-Toluidine and is lowest in 2-Nitrotoluene. A quantitative comparison of the magnitude of ϕ_V^0 values is much greater in magnitude than S_V^* values, for the solutions. This suggests that ion-solvent interactions dominate over ion-ion interaction in all the solutions. The values of ϕ_V^0 also support the fact that higher ion-solvent interaction in 2-Nitrotoluene, leads to lower conductance of Hept₄NI in it than o-Toluidine and o-Xylene.

The viscosity data has been analysed by the Jones-Dole equation [26]

$$(\eta/\eta_0 - 1)/\sqrt{c} = A + B\sqrt{c} \quad (24)$$

where η and η_0 are the viscosities of the solution and solvent respectively. The values of A-coefficient and B-coefficient are obtained from the straight line by plotting $(\eta/\eta_0 - 1)/\sqrt{c}$ against \sqrt{c} which are reported in Table V.10.

An assessment of Table V.10 and Figure V.5 shows that the values of the A-coefficient are either very small positive or negative for the solutions under investigation

at all solvents indicating the presence of weak ion-ion interactions, and these interactions further decrease from o-Toluidine to 2-Nitrotoluene. The viscosity B -coefficient reflects the quantitative ion-solvent interactions in the solution and the values of viscosity B -coefficient for Hept₄NI in the solvent systems studied are positive [27,28], thereby suggesting the presence of strong ion-solvent interaction. The trends in B -coefficient values support the results discussed earlier on the basis of ϕ_V . This shows that with the increase in the viscosity B -coefficient of the solvent the mobility of the ions of the electrolyte solvated decrease [29] and hence the conductance also decreases. That is why, Hept₄NI salt is more solvated in 2-Nitrotoluene than the other two solvents.

The viscosity A -coefficient and B -coefficient values are in excellent agreement with the results drawn from the volumetric studies. The trend of ion-solvent interaction is o-Toluidine < o-Xylene < 2-Nitrotoluene.

V.4. CONCLUSION

The extensive study of Hept₄NI in o-Toluidine, o-Xylene and 2-Nitrotoluene leads to the conclusion that, the salt more associated in 2-Nitrotoluene than the other two studied solvents. It can also be seen that in the conductometric studies in o-Toluidine and o-Xylene the Hept₄NI remains as triple-ions and ion-pairs and the extent of triple-ion formation is higher in o-Xylene than o-Toluidine. But in 2-Nitrotoluene the Hept₄NI remains as only ion-pairs. The experimental values obtained from the volumetric and viscometric studies suggest that in solution there is more ion-solvent interaction than the ion-ion interaction and the extent of ion-solvent interaction of Hept₄NI is highest in 2-Nitrotoluene.

TABLES**Table V.1.** Density (ρ), viscosity (η) and relative permittivity (ϵ) of the different solvents o-Toluidine, o-Xylene and 2-Nitrotoluene.

Solvents	$\rho \cdot 10^{-3}/\text{kg m}^{-3}$	$\eta/\text{mPa s}$	ϵ
o-Toluidine	0.998	0.339	6.14
o-Xylene	0.87557	0.759	2.6
2-Nitrotoluene	1.163	2.218	26.1

Table V.2. Concentration (c) and molar conductance (Λ) of o-Toluidine, o-Xylene and 2-Nitrotoluene at 298.15 K.

$c \cdot 10^4/$ $\text{mol} \cdot \text{dm}^{-3}$	$\Lambda \cdot 10^4/$ $\text{S} \cdot \text{m}^2 \cdot \text{mol}^{-1}$	$c \cdot 10^4/$ $\text{mol} \cdot \text{dm}^{-3}$	$\Lambda \cdot 10^4/$ $\text{S} \cdot \text{m}^2 \cdot \text{mol}^{-1}$	$c \cdot 10^4/$ $\text{mol} \cdot \text{dm}^{-3}$	$\Lambda \cdot 10^4/$ $\text{S} \cdot \text{m}^2 \cdot \text{mol}^{-1}$
Hept ₄ NI					
o-Toluidine		o-Xylene		2-Nitrotoluene	
3.5044	14.82	3.3672	44.54	3.9720	56.31
4.4521	14.77	3.9641	44.50	4.7394	54.21
5.1938	14.72	4.7350	44.46	5.5180	52.31
5.8081	14.69	5.7600	44.41	6.2078	51.50
6.2001	14.68	6.6203	44.37	6.8164	50.20
6.9169	14.64	7.3984	44.33	7.2146	49.90
7.7841	14.60	8.2254	44.29	7.8414	48.50
8.7557	14.55	9.0721	44.27	8.2770	48.00
9.6534	14.51	10.1188	44.25	9.0000	46.40
10.6406	14.48	11.1422	44.25	9.7032	45.50
11.8542	14.44	11.9578	44.25	10.2400	44.70
13.3810	14.40	13.2642	44.27	11.0224	43.11

15.0777	14.38	14.2129	44.28	11.9025	42.90
16.4106	14.39	15.5000	44.31	12.9025	42.80
17.7241	14.42	16.4106	44.34	14.6459	42.00

Table V.3. Calculated limiting molar conductance of ion-pair (Λ_0), limiting molar conductances of triple ion Λ_0^T , experimental slope and intercept obtained from Fuoss-Kraus Equation for Hept₄NI in o-Toluidine and o-Xylene at 298.15 K.

Solvents	$\Lambda_0 \cdot 10^4$ /S·m ² ·mol ⁻¹	$\Lambda_0^T \times 10^4$ /S·m ² ·mol ⁻¹	Slope $\times 10^{-2}$	Intercept $\times 10^{-2}$
Hept ₄ NI				
o-Toluidine	69.12	46.10	0.20	0.15
o-Xylene	60.34	40.25	0.11	0.45

Table V.4. Salt concentration at the minimum conductivity (C_{\min}) along with the ion-pair formation constant (K_P), triple ion formation constant (K_T) for Hept₄NI in o-Toluidine and o-Xylene at 298.15 K.

Solvents	$c_{\min} \cdot 10^4$ / mol·dm ⁻³	$\log c_{\min}$	$K_P \cdot 10^{-5}$ / (mol·dm ⁻³) ⁻¹	K_T / (mol·dm ⁻³) ⁻¹	K_T / K_P ·10 ⁵	$\log K_T / K_P$
Hept ₄ NI						
o-Toluidine	9.92	-3.0034	0.36	48.96	136.4	-2.86
o-Xylene	9.24	-3.0343	0.32	75.33	235.4	-2.62

Table V.5. Salt concentration at the minimum conductivity (c_{\min}), the ion pair fraction (α), triple ion fraction (α_T), ion pair concentration (c_P) and triple-ion concentration (c_T) for Hept₄NI in o-Toluidine and o-Xylene at 298.15 K.

Solvents	$c_{\min} \cdot 10^4 /$ mol·dm ⁻³	$\alpha \cdot 10^5$	$\alpha_T \cdot 10^3$	$c_P \cdot 10^4 /$ mol·dm ⁻³	$c_T \cdot 10^6 /$ mol ·dm ⁻³
Hept ₄ NI					
O-Toluidine	9.92	16.6	8.13	9.68	8.1
O-Xylene	9.24	6.91	12.88	9.10	8.9

Table V.6. Limiting molar conductance (Λ_0), association constant (K_A), co-sphere diameter (R) and standard deviations of experimental Λ (δ) obtained from Fuoss conductance equation for Hept₄NI in 2-Nitrotoluene at 298.15 K.

Solvent	$\Lambda_0 \cdot 10^4 / \text{S} \cdot \text{m}^2 \cdot \text{mol}^{-1}$	$K_A / \text{dm}^3 \cdot \text{mol}^{-1}$	$R / \text{Å}$	δ
Hept ₄ NI				
2-Nitrotoluene	34.67	453.24	8.54	0.16

Table V.7. Walden product ($\Lambda_0 \cdot \eta$) and Gibb's energy change (ΔG°) of Hept₄NI in 2-Nitrotoluene at 298.15 K.

Solvent	$\Lambda_0 \cdot \eta \cdot 10^4 /$ S·m ² ·mol ⁻¹ mPa	$\Delta G^\circ /$ kJ·mol ⁻¹
Hept ₄ NI		
2-Nitrotoluene	76.90	-15.16

Table V.8. Limiting Ionic Conductance (λ_0^\pm), Ionic Walden Product ($\lambda_0^\pm \eta$), Stokes' Radii (r_s), and Crystallographic Radii (r_c) of Hept₄NI in 2-Nitrotoluene at 298.15 K.

Solvent	ion	λ_0^\pm (S·m ² ·mol ⁻¹)	$\lambda_0^\pm \eta$ (S·m ² ·mol ⁻¹ mPa)	r_s (Å)	r_c (Å)
2-Nitrotoluene	Hept ₄ N ⁺	10.15	22.51	3.64	5.88
	I ⁻	21.71	48.15	1.70	2.16

Table V.9. Concentration, c , density, ρ , apparent molar volume, ϕ_v , limiting apparent molar volume ϕ_v^0 and experimental slope for Hept₄NI in o-Xylene, o-Toluidine and 2-Nitrotoluene at 298.15 K.

Solvents	$c/$ mol·dm ⁻³	$\rho \cdot 10^{-3}/$ kg m ⁻³	$\phi_v \cdot 10^6/$ m ³ ·mol ⁻¹	$\phi_v^0 \cdot 10^6/$ m ³ ·mol ⁻¹	$S_v^* \cdot 10^6/$ m ³ · mol ^{-3/2} ·dm ^{3/2}
Hept ₄ NI					
o-Toluidine	0.005	0.99849	440.58	442.7	-29.47
	0.020	1.00000	438.58		
	0.035	1.00155	437.15		
	0.050	1.00312	436.17		
	0.065	1.00472	435.19		
	0.080	1.00634	434.32		
o-Xylene	0.005	0.87629	449.65	454.5	-69.97
	0.020	0.87854	444.51		
	0.035	0.88086	441.49		
	0.050	0.88324	438.91		
	0.065	0.88566	436.82		
	0.080	0.88814	434.66		

2-Nitrotoluene	0.005	1.16303	457.18	464.6	-103.60
	0.020	1.16328	450.30		
	0.035	1.16369	445.39		
	0.050	1.16421	441.53		
	0.065	1.16484	438.00		
	0.080	1.16550	435.47		

Table V.10. Concentration, c , viscosity, η , $\frac{(\eta_r - 1)}{\sqrt{c}}$, viscosity A and B coefficients for Hept₄NI in o-Xylene, o-Toluidine and 2-Nitrotoluene at 298.15 K.

Salts	c /mol·dm ⁻³	η /mPa·s	$\frac{(\eta_r - 1)}{\sqrt{c}}$	B /dm ³ ·mol ⁻¹	A /dm ^{3/2} ·mol ^{-1/2}
Hept ₄ NI					
o-Toluidine	0.005	0.34	0.13	1.9305	0.0032
	0.020	0.35	0.26		
	0.035	0.36	0.36		
	0.050	0.37	0.46		
	0.065	0.38	0.50		
	0.080	0.39	0.57		
o-Xylene	0.005	0.77	0.13	2.1570	-0.0006
	0.020	0.79	0.28		
	0.035	0.81	0.39		
	0.050	0.84	0.47		
	0.065	0.86	0.53		
	0.080	0.89	0.60		

2-Nitrotoluene	0.005	1.57	0.23	3.8380	-0.0537
	0.020	1.65	0.48		
	0.035	1.74	0.66		
	0.050	1.82	0.80		
	0.065	1.91	0.93		
	0.080	2.00	1.04		

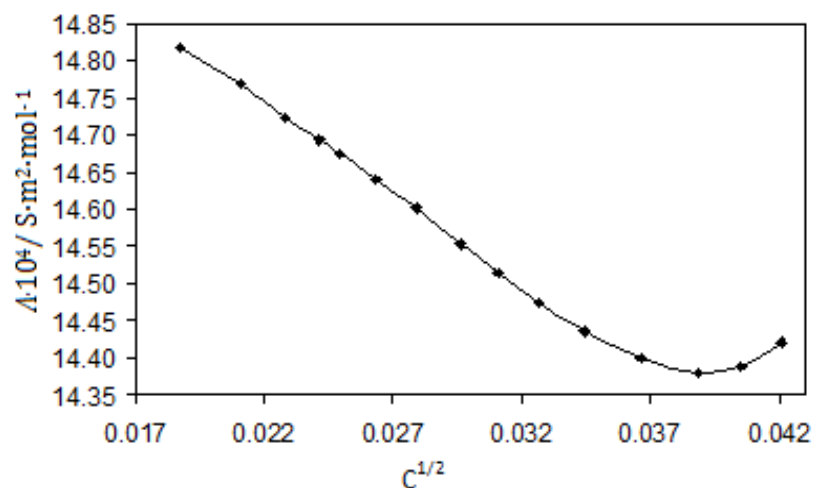
FIGURES

Figure V.1. Plot of molar conductance (Λ) versus $C^{1/2}$ for Hept₄NI in o-Toluidine at 298.15 K.

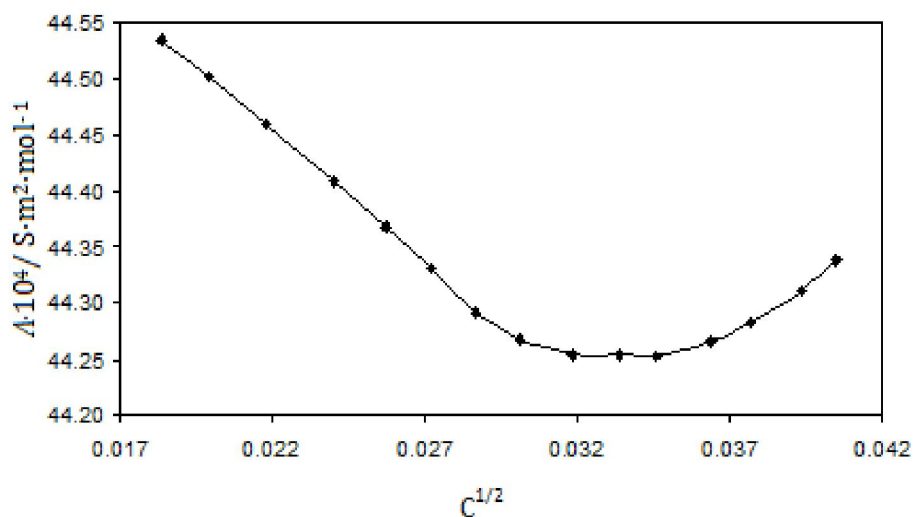


Figure V.2. Plot of molar conductance (Λ) versus $C^{1/2}$ for Hept₄NI in o-Xylene at 298.15 K.

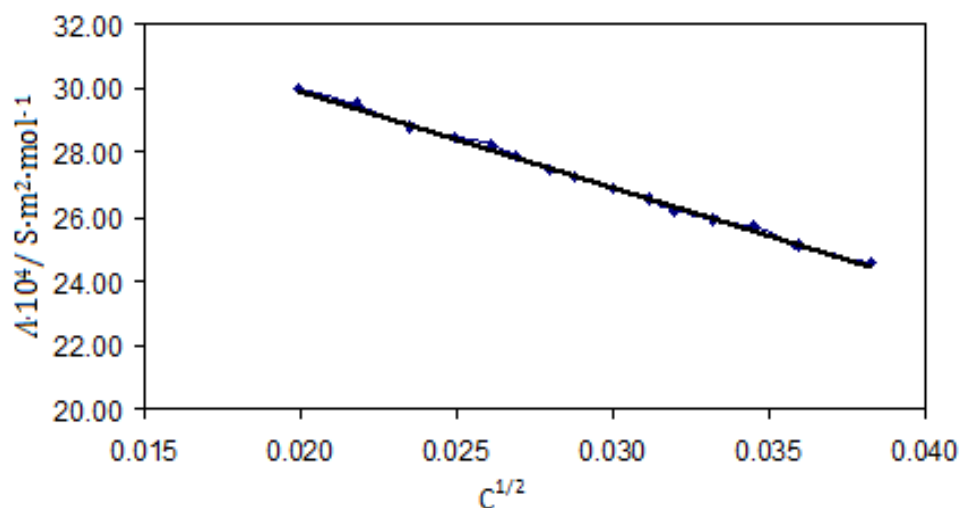


Figure V.3. Plot of molar conductance (Λ) versus $C^{1/2}$ for Hept₄NI in 2-Nitrotoluene at 298.15 K.

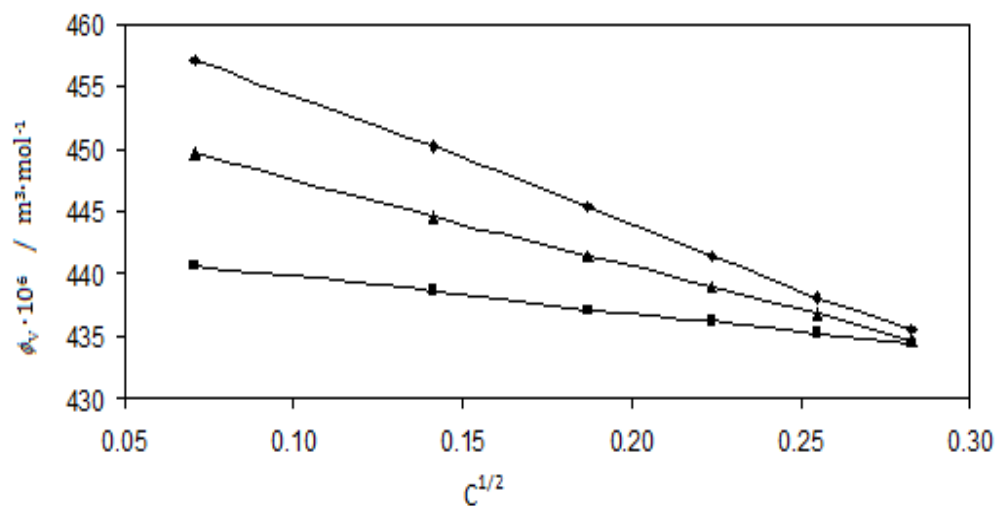


Figure V.4. Plot of $C^{1/2}$ versus Limiting apparent molar volume (ϕ_V^0) for Hept₄NI in o-Toluidine(—■—), o-Xylene(—▲—) and 2-Nitrotoluene(—◆—) at 298.15 K.

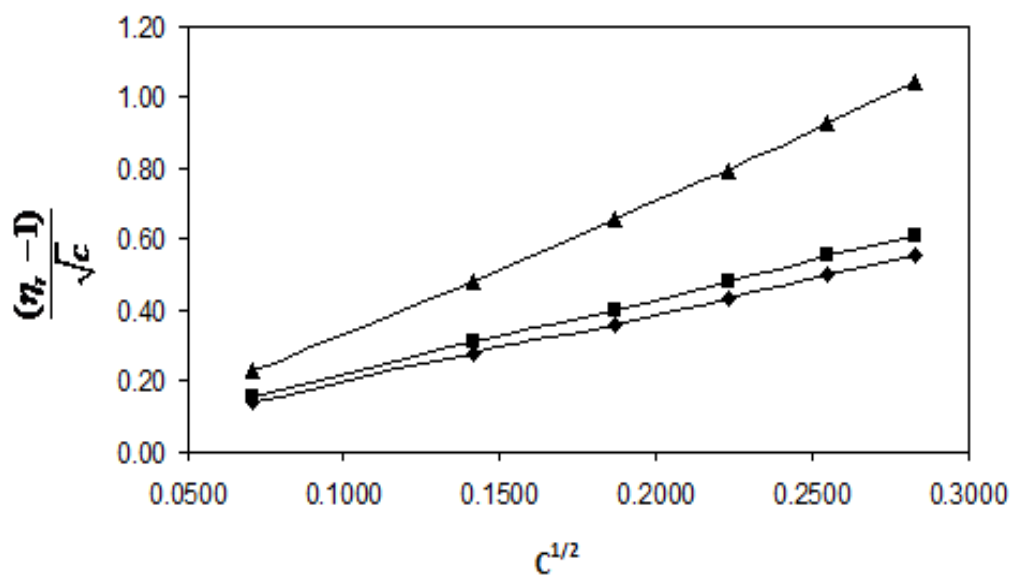


Figure V.5. Plot of $C^{1/2}$ versus $\frac{(\eta_r - 1)}{\sqrt{c}}$ for Hept₄NI in o-Toluidine(\blacklozenge), o-Xylene(\blacksquare) and 2-Nitrotoluene(\blacktriangle) at 298.15 K.

CHAPTER-VI

A study of NMR, density, viscosity and conductance vis-à-vis interactions of 1-butyl-1-methylpyrrolidinium chloride with oligosaccharides in aqueous environments

VI.1 INTRODUCTION

Ionic liquids (IL) have in recent times emerged as “green” and environment friendly solvents [1,2] for their use in the industrial manufacture of chemicals. Ionic liquids have been increasingly used for diverse applications such as organic synthesis, catalysis, electrochemical devices and solvent extraction of a variety of compounds. Ionic liquids are composed of cations and anions having low melting points (< 100 °C). The interest in ionic liquids was initiated because of their advantageous physicochemical properties such as negligible vapour pressure, high thermal and electrochemical stability, high solvating power etc [3-5]. Abundant current books, academic journal reviews and conference proceedings provide us an idea about the expansive band of research and latent manufacturing applications for ionic liquids. The important uses of [bmp]Cl are largely in catalysts, battery electrolytes, syntheses (excluding the catalysts group), and electrochemical relevances other than batteries.

Living system of every animal and man is composed of several molecules having specific functions are termed as biomolecules. Carbohydrates are one of the main classes of biomolecules. Carbohydrates (such as glucose, fructose, galactose etc.) are most important substances to all living organisms. They usually act as a ubiquitous fuel for biological processes to supply necessary energy for the function of the living and their day's work. Taken carbohydrates D(+)-galactose and D(-)-fructose are very significant variety of saccharide. An unusual level of carbohydrate in human body fluid

is a caution hint of a medical stipulation. Such as, an unbalanced concentration of carbohydrates in human blood or urine entails a biological dysfunction.

In spite of the “green” aspects of ILs, the potential toxicity of the ILs released into the environment could not be overlooked [6]. Since ILs are highly stable in water, they may be a health hazard by gathering in the ecological atmosphere and organisms. So, it is very important to determine the potential toxicity of ILs originate from the interface between ILs and biomolecules. Thus it is a progressive research topic to investigate the interactions between ILs and biomolecules such as carbohydrates.

In this present case, an attempt has been made to reveal the nature of various types of interactions prevailing an ionic liquid in aqueous carbohydrates [D(-)fructose and D(+)]galactose] solutions from conductometric, volumetric, viscometric and NMR measurements. Aim of the present work is to study the molecular interactions of IL in aqueous solutions of carbohydrates by physicochemical and thermodynamical studies, and the structural effect of carbohydrates as literature survey reveals that very ample work has been carried out in the present ternary systems especially given that theoretical foundations and significant information for studies on the potential toxicity of ILs. Such study helps in better understanding of the interactions occurring between carbohydrate molecules and entities present in mixed aqueous medium in the living cells through thermodynamics and transport properties. All of the derived parameters have been discussed in term of interactions between ionic liquid and carbohydrates.

VI.2 EXPERIMENTAL

VI.2.1 Source and purity of Materials

In this current research work, the chosen puriss graded IL was used as purchased (mass fraction purity of the IL $\geq 99\%$). The IL was acquired from Sigma-Aldrich, Germany.

D(-)fructose and D(+)]galactose were procured from Thomas Baker, Mumbai. The mass fraction purity of D(-)fructose and D(+)]galactose was $\geq 99.4\%$ and 99.9%

respectively. IL, D(-)fructose and D(+)galactose were dried in vacuum desiccator over P₂O₅ at room temperature for at least 72 h.

VI.2.2 Apparatus and Procedure

Using the mass property (weighed through Mettler Toledo AG-285 having uncertainty of 0.0003g), D(-)fructose, D(+)galactose and the electrolyte (IL) solutions were prepared. For conductance measurement the working solutions were obtained by mass dilution of the stock solutions [7-9].

The conductance measurements were carried out by means of the Systronics-308 conductivity bridge (accuracy $\pm 0.01\%$), using CD-10 conductivity cell having a dip-type immersion [cell constant $\approx (0.1 \pm 0.001) \text{ cm}^{-1}$]. Temperature of these entire measurements were maintained through a thermostat water bath held in reserve at $T = (298.15 \pm 0.01) \text{ K}$. The calibration of cell performed using the method proposed by Lind et al [10]. The conductance data were reported at a frequency of 1 kHz and the accuracy was $\pm 0.3\%$.

The vibrating u-tube Anton Paar digital density meter (DMA 4500M) (precision $\approx \pm 0.00005 \text{ g cm}^{-3}$) was used to determine the densities of the solvents and experimental solutions (ρ). The uncertainty of temperature was $\pm 0.01 \text{ K}$.

By means of a Brookfield DV-III Ultra Programmable Rheometer with fitted size-42 spindle fitted to a Brookfield digital bath TC-500 the viscosities of all the solutions were determined. The detailed descriptions of this apparatus are given in our earlier communication [11].

Using the Bruker ADVANCE 400 MHz instrument, NMR spectra were recorded in D₂O at 400 MHz at 298.15K. Signals are cited as δ values in ppm using residual protonated solvent signals as internal standard (D₂O : δ 4.79 ppm). Data are reported as chemical shift.

VI.3 RESULTS AND DISCUSSION

In the beginning it may be point out that there is no difference between D(+) and D(-) form of galactose and fructose in their physical properties in our experimental works.

Fructose, or fruit sugar, is a simple ketonic monosaccharide found in many plants and Galactose exists in both open-chain and cyclic form. The open-chain form has a carbonyl at the end of the chain. Four isomers are cyclic, two of them with a pyranose (six-membered) ring and another two isomers are with a furanose (five-membered) ring. Galactofuranose mostly occurs in bacteria, fungi and protozoa. In our experiment we have taken α -form of D(-)fructose and on the other hand D(+) Galactose taken in the experiment is in the form of 20% of α - and 80% of β -form. The solvent properties are given in Table VI.1.

Conductivity measurements have been carried out to obtain information on association behaviour and ion-solvent interactions [12,13] of the ionic liquid, [bmp]Cl, in (0.2, 0.4 and 0.6) mol kg⁻¹ aqueous D(-)fructose and D(+)galactose solutions at temperatures ranging from (298.15–308.15)K. The concentrations and molar conductances (Λ) of IL in aqueous solution of D(-)fructose and D(+)galactose at different temperatures are given in Table VI.2. The molar conductance (Λ) has been obtained from the specific conductance (κ) value using the following equation.

$$\Lambda = (1000 \kappa) / m \quad (1)$$

Linear conductance curves (Λ versus \sqrt{m}) were obtained for the electrolyte in aqueous solution of D(-)fructose. D(+) Galactose, extrapolation of $\sqrt{m} = 0$ evaluated the starting limiting molar conductance for the electrolyte. The values of K_A , Λ_0 and R obtained by this procedure are given in Table VI.3.

VI.3.1. Ion-pair Formation

The conductivity data of taken IL in aqueous solution of D(-)fructose and D(+)galactose at different temperatures were analyzed using the Fuoss conductance equation [14]. With a given set of conductivity values (m_j , Λ_j ; $j = 1, \dots, n$), three adjustable parameters, i.e., Λ_0 , K_A and R have been derived from the Fuoss equation. Here, Λ_0 is the limiting molar conductance, K_A is the observed association constant and R is the association distance, i.e., the maximum centre to centre distance between the ions in the solvent separated ion-pairs. There is no precise method [15] for determining the R value but in order to treat the data in our system, R value is

assumed to be, $R = a + d$, where a is the sum of the crystallographic radii of the ions and d is the average distance corresponding to the side of a cell occupied by a solvent molecule. The distance, d is given by [16]

$$d = 1.183 (M / \rho)^{1/3} \quad (2)$$

where, M is the molecular mass and ρ is the density of the solvent.

Thus, the Fuoss conductance equation may be represented as follows:

$$\Lambda = P\Lambda_0[(1 + R_x) + E_L] \quad (3)$$

$$P = 1 - \alpha(1 - \gamma) \quad (4)$$

$$\gamma = 1 - K_A m \gamma^2 f^2 \quad (5)$$

$$-\ln f = \beta \kappa / 2(1 + \kappa R) \quad (6)$$

$$\beta = e^2 / (\epsilon_r k_B T) \quad (7)$$

$$K_A = K_R / (1 - \alpha) = K_R / (1 + K_S) \quad (8)$$

where, Λ_0 is the limiting molar conductance, K_A is the observed association constant, R is the association distance, R_x is the relaxation field effect, E_L is the electrophoretic counter current, k is the radius of the ion atmosphere, ϵ is the relative permittivity of the solvent mixture, e is the electron charge, c is the molarity of the solution, k_B is the Boltzmann constant, K_S is the association constant of the contact-pairs, K_R is the association constant of the solvent-separated pairs, γ is the fraction of solute present as unpaired ion, α is the fraction of contact pairs, f is the activity coefficient, T is the absolute temperature and β is twice the Bjerrum distance.

The computations were performed using the program suggested by Fuoss. The initial Λ_0 values for the iteration procedure are obtained from Shedlovsky extrapolation of the data [17]. Input for the program is the no. of data, n , followed by ϵ , η (viscosity of the solvent mixture), initial Λ_0 value, T , ρ (density of the solvent mixture), mole fraction of the first component, molar masses, M_1 and M_2 along with m_j , Λ_j values where $j = 1, 2, \dots, n$ and an instruction to cover preselected range of R values.

In practice, calculations are performed by finding the values of Λ_0 and α which minimize the standard deviation, δ , whereby

$$\delta^2 = \sum [\Lambda_j(cal) - \Lambda_j(obs)]^2 / (n - m) \quad (9)$$

for a sequence of R values and then plotting δ against R , the best-fit R corresponds to the minimum of the δ - R versus R curve. So, an approximate sum is made over a fairly wide range of R values using 0.1 increment to locate the minimum but no significant minima is found in the δ - R curves, thus R values is assumed to be $R = a + d$, with terms having usual significance. Finally, the corresponding limiting molal conductance (Λ_0), association constant (K_A), co-sphere diameter (R) and standard deviations of experimental Λ (δ) obtained from Fuoss conductance equation for [bmp]Cl in aqueous solution of D(-)fructose and D(+)galactose at 298.15 K, 303.15 K and 308.15 K respectively are given in Table VI.4.

VI. 3.2. Limiting molal conductivities

Assessment of Table VI.2 and Table VI.3 allocate that the Λ_0 values of the ionic liquid decrease with increasing the concentration of D(-)fructose and D(+)galactose. This can be ascribed to the facts that with increase in D(-)fructose and D(+)galactose concentration (i) the microscopic viscosity of the mixtures increases thereby the mobility of ions decreases, and (ii) the solvated radii of ions become larger through an enhancement in the interactions between ionic liquid and D(-)fructose and D(+)galactose solution therefore, the mobility of ions decreases [18]. On the other hand, the Λ_0 values increase from D(-)fructose to D(+)galactose. Due to higher viscosity value of D(-)fructose than D(+)galactose Λ_0 values increase in D(+)galactose than in D(-)fructose. Λ_0 values increase in every solution with increase of temperature. With increasing temperature mobility of the concerned ions in solution increases, so Λ_0 values increase.

VI. 3.3. Thermodynamic of the ion-association process

Values of the association constant (K_A) for the ionic liquids in aqueous D(-)fructose and D(+)galactose solutions are shown in Table VI.4. It is obvious that at a fixed concentration of D(-)fructose and D(+)galactose, the K_A values decrease

from D(-)fructose to D(+)galactose and also decrease with increasing temperature in each solution. The association constant (K_A) for the ionic association reaction can serve to study the thermodynamic of this process. Consequently, the standard Gibbs energy (G_A^0) for the ion-association process were calculated according to the following equation [19]

$$\Delta G_A^0 = -RT \ln K_A \quad (10)$$

The obtained values of the standard Gibbs energy are collected in Table S6. Table S6 indicates that the ion-association process exhibits a negative value of (G_A^0) and becomes more negative in D(+)galactose than in D(-)fructose. This indicates that ion-association process is more feasible in D(+)galactose solution. Walden product value (Table VI.4) shows that ionic mobility is higher in case of D(+)galactose solution than in D(-)fructose solution and ionic mobility increases with increasing temperature.

Temperature-dependent of G_A^0 was expressed with the help of a polynomial [20]

$$\Delta G_A^0(T) = A_0 + A_1(298.15 - T) + A_2(298.15 - T)^2 \quad (11)$$

Entropy and enthalpy of ion association have been obtained as follows

$$\Delta S_A^0(T) = - \left(\frac{\partial \Delta G_A^0(T)}{\partial T} \right)_P = A_1 + 2A_2(298.15 - T) \quad (12)$$

$$\Delta H_A^0(T) = \Delta G_A^0(T) + T\Delta S_A^0(T) = A_0 + 298.15A_1 + (298.15^2 - T^2)A_2 \quad (13)$$

The values of the coefficients A_0 , A_1 and A_2 at different solvent compositions are given in Table VI.5. The calculated thermodynamic functions of IL in D(-)fructose and D(+)galactose solutions are listed in Table VI.6 and are represented graphically by Fig. 1, Fig. 2 and Fig. 3 respectively. Table VI.6 indicates that the ion-association process exhibits a negative value of ΔG_A^0 and becomes more negative with increasing temperature proposing the spontaneity and feasibility of the association process at high temperatures. In all cases, the ΔS_A^0 values are positive

over the whole temperature range. The positive ΔS_A^0 values may be attributed to the increasing number of degrees of freedom due to the release of solvent molecules from hydration shells as the association takes place. In other words, the solvation of the individual ions is weakened as soon as these ion-pairs are formed. The positive contribution of entropy resulting from the dehydration of ions during the association process dominates over the negative contribution from the formation of ion-pairs. It should be noted that the entropy term ($T\Delta S_A^0$) is sufficiently positive to exceed the positive contribution of the enthalpy (ΔH_A^0). Consequently, the ion-association process exhibits negative values of ΔG_A^0 and the process is driven by the change in entropy. Assessment of Table S6 also indicates that in case of [bmp]Cl in both aqueous solution of D(-)fructose than in D(+)galactose enthalpy decreases with increasing temperature and changes its sign from positive to negative at 308.15 K. This means that the association process is endothermic at lower temperature and exothermic at higher temperature. Furthermore, it means that ion-pair formation is entropy-driven at low temperatures, while it changes to enthalpy-driven process with increasing temperature. Enthalpy value of the IL is higher in case of D(-)fructose than in D(+)galactose. This means that the association process is more feasible in D(+)galactose than in D(-)fructose (Scheme VI.2). It was observed that the ion-association process exhibits a negative value of ΔG_A^0 and becomes more negative with increasing temperature proposing the spontaneity and feasibility of the association at high temperatures. It is also an attempt to explore the consequence of interaction of carbohydrates with ionic liquids, consequently, by means of the interaction between IL and biomolecules, the potential toxicity of ILs may originate.

VI. 3. 4. Apparent Molar Volume

From density measurement it is known that the densities of the IL in each aqueous D(-)fructose and D(+)galactose increase linearly with the concentration at the studied temperatures. The density values of IL are higher in aqueous D(-)fructose solution

than in aqueous D(+)galactose solution. For this purpose, the apparent molar volumes ϕ_V were determined from the solution densities using the following equation

$$\phi_V = M / \rho - (\rho - \rho_0) / m \rho_0 \rho \quad (14)$$

Where M is the molar mass of the solute, m is the molality of the solution, ρ and ρ_0 are the densities of the solution and solvent, respectively.

The limiting apparent molar volumes ϕ_V^0 were calculated using a least-squares treatment to the plots of ϕ_V versus \sqrt{m} using the following Masson equation [21].

$$\phi_V = \phi_V^0 + S_V^* \cdot \sqrt{m} \quad (15)$$

Where, ϕ_V^0 is the limiting apparent molar volume at infinite dilution and S_V^* is the experimental slope.

The limiting apparent molar volumes ϕ_V^0 are found to increase with increasing molality (m) of IL in each solvents and decrease with increasing temperature for the studied system. From Table VI.7 it is observed that ϕ_V^0 values are positive in both the solution systems and is higher in case of D(-)fructose compared to D(+)galactose. This indicates the presence of strong ion-solvent interactions and the extent of interactions increases in D(-)fructose than in D(+)galactose solution (Figure VI.4). On the contrary, the S_V^* indicates the extent of ion-ion interaction. The values of S_V^* shows that the extent of ion-ion interaction is higher in case of D(+)galactose than D(-)fructose. Owing to a quantitative comparison, the magnitude of ϕ_V^0 are much greater than S_V^* , in every solutions, suggests that ion-solvent interactions dominate over ion-ion interactions in all the solutions. The values of ϕ_V^0 also support the fact that higher ion-solvent interaction of IL leads to lower conductance in D(-)fructose than D(+)galactose, discussed earlier [22,23].

The transfer volumes, $\Delta_r \phi_V^0$ of D(-)fructose and D(+)galactose from water to aqueous [bmpy]Cl solutions have been calculated as follows [24]

$$\Delta_r \phi_V^0 = \phi_V^0(\text{in [bmp]Cl + aq. carbohydrate}) - \phi_V^0(\text{aq.}) \quad (16)$$

Where $\phi_V^0(\text{in}[\text{bmp}]\text{Cl} + \text{aq. carbohydrate})$ and $\phi_V^0(\text{aq.})$ are the standard partial molar volumes of [bmpy]Cl in aqueous carbohydrates [D(-)fructose and D(+)]galactose] and in water, respectively. The obtained values for the transfer volumes are given in Table S8. Here we have determined the standard partial molar volume of aqueous carbohydrates [25-27]. Perusal of Table VI.8 shows, the values of $\Delta_r\phi_V^0$ values are positive and increase with increase in the concentration of ionic liquid at each experimental temperatures. The following types of interactions are possible between solute [D(-)fructose and D(+)]galactose] and co-solute (ionic liquid) in ternary solutions being studied: (i) Hydrophilic-ionic interactions between the hydrophilic sites (-OH, -C=O, and -O-) of [D(-)fructose and D(+)]galactose] and the ions ([bmp]⁺/Cl⁻) of ionic liquid; (ii) Hydrophobic-ionic interactions between the hydrophobic parts of [D(-)fructose and D(+)]galactose] and the ions of ionic liquid. According to the co-sphere overlap model [28], type (i) interactions contribute positively, whereas the type (ii) interactions make negative contributions to $\Delta_r\phi_V^0$ values. The positive $\Delta_r\phi_V^0$ values obtained for D(-)fructose and D(+)]galactose] in the studied solutions suggest that the hydrophilic-ionic interactions predominate over the hydrophobic-ionic interactions.

Thus the interactions between IL and carbohydrate in water solutions can generally be summarized as, (a) the hydrogen bonding interaction between the H atoms of water with (i) -O atom of the -OH group attached to the carbohydrate and (ii) -N atom in the heterocyclic ring of IL; (b) the hydrogen bonding interaction between the O atom of water with the H atom associated with the -OH group attached to the carbohydrate. Therefore, more the number of interacting centres (-OH group) present in the carbohydrate, more is its interaction with the IL. A possible interaction between the plausible products (obtained with reaction between different carbohydrates and IL) with water is given in Scheme VI.1.

Interaction pattern between D(-)fructose, D(+)]galactose] and IL can be summarized such as [26]:

- a. The interactions between the -OH group of the saccharides and the ionic part of IL named as hydrophilic-ionic group interactions.
- b. The interactions occurring between the -OH group of the saccharides and N-atom of pyrrolidinium group present in IL termed as hydrophilic-hydrophilic interactions.
- c. The interactions present here in between the -OH group of the saccharides and the non-polar part of the IL can be said as hydrophilic-hydrophobic interactions.

The overall positive values of ϕ_V^0 (Table VI.7) for the systems reinforce the fact that the solute-solvent interactions are predominate. Therefore the mutual overlap of the hydration spheres of solute and co-solute molecules will lead to an increase in the magnitude of hydrogen bonding interactions between the plausible products (obtained with reaction between IL and different carbohydrates) with water. The observation shows that with increase in the number of the interacting centers (-OH groups) present in the studied carbohydrates, the solute-solvent interaction also increases [29-31]. The solute-solvent interaction in case of D(-)fructose is greater than D(+)galactose because of the presence of greater number of free -OH group in D(-)fructose. Also D(+)galactose is six-membered ring so there is some sort of structural restriction, whereas D(-)fructose is five-membered ring which containing more free -OH group favored H-bonding to a greater extent. Therefore, the solute-solvent interaction is superior in D(-)fructose compared to D(+)galactose solution.

VI. 3. 5. Temperature dependent limiting apparent molar volume

The temperature dependent general polynomial equation for ϕ_V^0 are as follows [32]

$$\phi_V^0 = a_0 + a_1T + a_2T^2 \quad (17)$$

Where, a_0 , a_1 , a_2 are the empirical and T is the Kelvin temperature. The values of these coefficients are presented in Table VI.9.

The limiting apparent molar expansibilities, ϕ_E^0 , can be obtained by the following equation,

$$\phi_E^0 = \left(\delta \phi_V^0 / \delta T \right)_P = a_1 + 2 a_2 T \quad (18)$$

Where, ϕ_E^0 is the change in magnitude with the change of temperature at constant pressure. The values of ϕ_E^0 for different solutions of the studied ILs at different Kelvin are reported in Table VI.10. The table reveals that ϕ_E^0 is positive for the IL in the studied solvent systems and studied temperatures. This fact can be ascribed to the absence of caging or packing effect for the IL in solutions.

Hepler [33] developed a technique of examining the sign of $\left(\delta \phi_E^0 / \delta T \right)_P$ for the solute in terms of long-range structure-making and breaking capacity of the solute in the mixed solvent systems using the general thermodynamic expression,

$$\left(\delta \phi_E^0 / \delta T \right)_P = \left(\delta^2 \phi_V^0 / \delta T^2 \right)_P = 2 a_2 \quad (19)$$

If the sign of $\left(\delta \phi_E^0 / \delta T \right)_P$ becomes positive or a small negative, the molecule is a structure maker; otherwise, it is a structure breaker [34]. From Table VI.10 the $\left(\delta \phi_E^0 / \delta T \right)_P$ values for the studied IL in both the solution of D(-)fructose and D(+)galactose are positive [in 0.2 (m) D-galactose solution small negative] imply predominantly that the IL is structure maker in all of the experimental solutions for D(-)fructose and D(+)galactose in aqueous ionic liquid solutions rather than water. This indicates that these saccharides behave as a structure breaker in aqueous system, on the other hand, the structure-breaking tendency decreases due to existence of ionic liquid. It can be mentioned here that in generally an enhancement in the solute-solvent interactions is conveyed by a decrease in the solute-cosolute interactions. Since with increasing temperatures, some slackly leaped carbohydrate molecules are released from the secondary solvation shells of the ions, so the solute-solvent interactions can become stronger with the increase of temperature [35].

VI. 3. 6. Viscosity calculation

The viscosity data have been analysed using Jones-Dole equation [36].

$$(\eta / \eta_0 - 1) / \sqrt{c} = A + B \sqrt{m} \quad (20)$$

Where, η and η_0 are the viscosities of the solution and solvent respectively. The viscosity co-efficient A - and B - represent ion-ion and ion-solvent interaction respectively. Perusal of Table VI.7 shows that the positive values of B -coefficients indicate greater ion-solvent interactions and small negative values of A - coefficients indicate smaller ion-ion interaction in solution. Thereby suggesting the ion-solvent interactions are dominant over the ion-ion interactions. The B -coefficient [37,38] value obtained from the viscosity measurements gives the important information regarding the extent of solvation of the solute molecules and the effects on the structure of the solvents in the local vicinity of the solute molecule in solution. The higher B -coefficient values are due to the solvated solutes molecule associated by the solvent molecules by solute-solvent interactions. These types of interactions are strengthened with rise in temperature and thus the values of B -coefficient increases with increase in temperature. As a consequence, the inclination of ion-solvent interaction is higher in case of D(-)fructose solution than in D(+)galactose solution (Figure VI.5). These results are in good agreement with those obtained from ϕ_V^0 and S_V^* values, discussed earlier.

Viscosity B -coefficients of transfer (ΔB) from water to different aqueous carbohydrate solutions have been determined using the relations [39,40]

$$\Delta B(IL) = B(IL + aq. carbohydrate) - B(aq.) \quad (21)$$

From Table VI.8 it is evident that ΔB values are positive and increases with a rise in temperature and with increasing concentration of carbohydrate, thereby suggesting the presence of strong solute-solvent interactions, and the interactions are strengthened with rise in temperature and increase of carbohydrate in aqueous mixture [41]. The observation supports the same results obtained from $\Delta_r \phi_V^0$ values discussed above.

The sign of dB/dT is another tool of structure-forming or -breaking ability of the solute [33]. It is found from Table VI.11 that the values of the B -coefficient increase with a rise in temperature (positive dB/dT values), suggesting the structure breaking tendency [28] of carbohydrates in the solution systems. Moreover, it is interesting to note that the B -coefficients of the studied carbohydrates show a linear relationship with the partial molar volumes ϕ_V^0 , i.e;

$$B = A_1 + A_2 \phi_V^0 \quad (22)$$

The coefficients A_1 and A_2 are included in Table VI.11. The positive slope (or A_2) shows the linear variation of B -coefficient with partial molar volumes ϕ_V^0 . This relationship is really expected, since both the viscosity B -coefficient and the partial molar volume reflect the privileged solute-solvent interactions in the solutions.

VI.4. ^1H NMR study

NMR study is one of the most imperative spectroscopic tools for deeply understanding the microscopic information about the ion-solvent interaction of the studied IL in carbohydrate solution systems. In our present work we have considered the interactions of an IL (*viz.*, [bmp]Cl) with D(-)fructose and D(+)galactose by ^1H NMR study taking 1:1 molar ratio of IL and CD in D_2O at 298.15K [Figure VI.6(a) and VI.6(b)]. ^1H NMR data of the IL, two carbohydrates and mixture of IL-Carbohydrates are listed in Table VI.12. Due to the analyzed interactions between the IL and the co-solvents, measurements of NMR are essential for the investigation of the solution state of ionic liquid in carbohydrates. In case of ^1H spectra of carbohydrates are often not first order, in which case line separations do not symbolize coupling constants. The protons of the IL show considerable chemical shift due to the interaction with the hydrophilic -OH groups present in the carbohydrate molecules. In the structure of D(-)Fructose the H1-H6 i.e. all the H-atoms situated in the moiety show the peak in NMR study. Similarly in case of D(+)Galactose the H1-H6 i.e. all the H-atoms situated in the carbohydrate moiety show the peak in NMR study. In case of IL the protons present in butyl as well as methyl group show NMR spectra. The chemical shifts for H-atoms of IL evidently show

highfield in presence carbohydrates [42]. It can be inferred that the interactions between the IL and carbohydrates would be mainly resolute by their dehydrations/hydrations in the processes. The change of chemical shift may be due to the disruption of the interionic hydrogen bonding network in ILs [43]. In case of mixture compositions, the variations of relative chemical shifts in thus commenced are interpreted in terms of specific and non-specific intermolecular interactions [44,45]. The results showed that the solvation process of carbohydrates is governed mainly by the interactions between the cationic part of the IL and carbohydrate molecules. The shifts of protons of IL are more in case D(-)fructose than that of D(+)galactose. This fact indicates that interaction between the IL and D(-)fructose is higher than that of IL and D(+)galactose. The NMR study provides a profound insight into other IL + biomolecule mixed systems, especially afforded theoretical foundations and imperative information for studies on the potential toxicity of ILs.

VI. CONCLUSION:

In our present research study, we have focused on the characteristic interfaces of some model biological systems [D(-)fructose and D(+)galactose], with an IL. The studied physicochemical properties provide us complete explanation for the interfaces of IL with carbohydrates. From the analysis of thermodynamic data, it is revealed that the association process for [bmp]Cl is higher in case of D(-)fructose than in D(+)galactose solution. This process is endothermic and entropy controlled at all the studied temperatures. Density and viscosity studies interpret limiting apparent molar volume, ϕ_V^0 and viscosity *B*-coefficient which describes that ion-solvent interaction is increased with increasing the conc. of D(-)fructose and D(+)galactose and decreased with increasing temperature. NMR study analysis reveals that no specific and stronger interactions occur between IL and carbohydrates. However the study confirms that interaction of IL with carbohydrates is higher in D(-)fructose than that of D(+)galactose. The study provides a profound insight into the potential toxicity of ILs in mixed systems of IL and biomolecules.

TABLES**Table VI.1.** Density (ρ), viscosity (η) and relative permittivity (ϵ) of the different concentration (m) of aqueous D(-)fructose and D(+)galactose at 298.15, 303.15 and 308.15 K^a respectively.

T (K)	$\rho \cdot 10^{-3}/\text{kg m}^{-3}$	$\eta/\text{mPa s}$	ϵ
<i>m</i> _{D(-)fructose} =0.2 mol kg ⁻¹			
298.15	1.0039	0.93	78.1
303.15	1.0025	0.91	76.3
308.15	1.0018	0.89	74.5
<i>m</i> _{D(-)fructose} =0.4 mol kg ⁻¹			
298.15	1.0051	0.93	77.4
303.15	1.0028	0.91	75.5
308.15	1.0021	0.90	73.8
<i>m</i> _{D(-)fructose} =0.6 mol kg ⁻¹			
298.15	1.0062	0.93	76.8
303.15	1.0049	0.92	74.9
308.15	1.0027	0.90	73.1
<i>m</i> _{D(+)galactose} =0.2 mol kg ⁻¹			
298.15	1.0037	0.93	78.1
303.15	1.0023	0.91	76.3
308.15	1.0015	0.90	74.5
<i>m</i> _{D(+)galactose} =0.4 mol kg ⁻¹			
298.15	1.0045	0.93	77.4
303.15	1.0025	0.92	75.5
308.15	1.0020	0.90	73.8
<i>m</i> _{D(+)galactose} =0.6 mol kg ⁻¹			
298.15	1.0059	0.93	76.8
303.15	1.0047	0.92	74.9

Communicated

308.15

1.0025

0.90

73.1

^aStandard uncertainties u are: $u(\rho) = \pm 5 \times 10^{-5} \text{ g}\cdot\text{cm}^{-3}$, $u(\eta) = \pm 1 \%$ and $u(T) = \pm 0.01\text{K}$

Table VI.2. Molar conductivities (Λ) of [bmp]Cl in aqueous D(-)fructose solutions as a function of ionic liquid molality (m) at different temperatures.

$c \cdot 10^4 /$ $\text{mol}\cdot\text{dm}^{-3}$	$\Lambda \cdot 10^4 /$ $\text{S}\cdot\text{m}^2\cdot\text{mol}^{-1}$	$c \cdot 10^4 /$ $\text{mol}\cdot\text{dm}^{-3}$	$\Lambda \cdot 10^4 /$ $\text{S}\cdot\text{m}^2\cdot\text{mol}^{-1}$	$c \cdot 10^4 /$ $\text{mol}\cdot\text{dm}^{-3}$	$\Lambda \cdot 10^4 /$ $\text{S}\cdot\text{m}^2\cdot\text{mol}^{-1}$
T=298.15K					
		T=303.15		T=308.15K	
$m_{\text{D(-)fructose}} = 0.2 \text{ mol kg}^{-1}$					
0.0114	101.10	0.0122	104.58	0.0132	107.60
0.0173	99.13	0.0223	101.91	0.0251	104.57
0.0239	96.45	0.0309	99.93	0.0320	103.13
0.0296	94.32	0.0383	98.20	0.0398	101.50
0.0345	92.40	0.0447	96.79	0.0469	99.90
0.0389	91.01	0.0503	95.34	0.0523	97.40
0.0427	89.91	0.0552	94.33	0.0579	96.80
0.0464	88.51	0.0596	93.18	0.0613	95.00
0.0512	87.91	0.0635	92.21	0.0647	94.26
0.0551	86.94	0.0670	91.44	0.0684	93.89
0.0593	85.50	0.0702	90.53	0.0715	92.03
0.0672	84.29	0.0731	89.91	0.0750	91.59
0.0715	83.11	0.0757	89.12	0.0765	90.53
0.0763	81.82	0.0782	88.09	0.0792	89.05
0.0841	80.20	0.0804	87.58	0.0815	89.78
$m_{\text{D(-)fructose}} = 0.4 \text{ mol kg}^{-1}$					
0.0121	99.43	0.0138	102.37	0.0142	105.85
0.0187	97.40	0.0235	100.75	0.0216	104.70
0.0241	95.04	0.0313	99.55	0.0285	103.58

Communicated

0.0310	93.62	0.0385	97.16	0.0346	102.62
0.0353	92.56	0.0465	95.91	0.0388	101.66
0.0395	90.90	0.0513	94.12	0.0438	100.70
0.0443	90.42	0.0544	93.40	0.0491	99.67
0.0475	88.35	0.0596	93.95	0.0551	97.57
0.0496	87.45	0.0635	92.88	0.0617	95.46
0.0542	85.76	0.0674	90.18	0.0675	93.24
0.0595	84.67	0.0715	89.52	0.0707	91.72
0.0657	83.63	0.0742	88.87	0.0731	89.29
0.0713	82.73	0.0774	88.09	0.0779	89.84
0.0765	81.62	0.0812	87.48	0.0821	88.79
0.0846	79.38	0.0851	86.83	0.0852	88.30

mD(-)fructose=0.6 mol kg⁻¹

0.0128	95.51	0.0143	98.99	0.0152	102.57
0.0185	94.48	0.0242	97.04	0.0271	100.17
0.0229	93.20	0.0316	95.70	0.0331	99.03
0.0282	91.54	0.0386	94.52	0.0423	97.20
0.0313	90.40	0.0451	93.13	0.0481	96.00
0.0351	89.27	0.0503	92.03	0.0542	94.75
0.0420	87.31	0.0557	91.06	0.0598	93.33
0.0456	86.00	0.0596	90.21	0.0631	92.92
0.0494	85.65	0.0635	89.45	0.0656	92.24
0.0499	84.91	0.0674	88.51	0.0699	90.17
0.0540	83.18	0.0730	87.35	0.0731	89.54
0.0591	82.23	0.0756	86.55	0.0763	88.91
0.0664	81.26	0.0785	86.05	0.0782	88.15
0.0719	80.09	0.0820	85.17	0.0819	87.99
0.0786	78.08	0.0841	84.73	0.0860	87.57

Table VI.3. Molar conductivities (Λ) of [bmp]Cl in aqueous D(+)-galactose solutions as a function of ionic liquid molality (m) at different temperatures.

$c \cdot 10^4 /$ mol·dm ⁻³	$\Lambda \cdot 10^4 /$ S·m ² ·mol ⁻¹	$c \cdot 10^4 /$ mol·dm ⁻³	$\Lambda \cdot 10^4 /$ S·m ² ·mol ⁻¹	$c \cdot 10^4 /$ mol·dm ⁻³	$\Lambda \cdot 10^4 /$ S·m ² ·mol ⁻¹
T=298.15K		T=303.15		T=308.15K	
m _{D(+)-galactose} =0.2 mol kg ⁻¹					
0.0118	102.50	0.0142	105.13	0.0129	108.95
0.0233	99.52	0.0254	102.86	0.0241	106.07
0.0311	97.58	0.0330	100.97	0.0303	105.43
0.0381	96.24	0.0396	99.54	0.0380	104.35
0.0445	94.71	0.0482	98.65	0.0449	102.63
0.0525	93.12	0.0521	97.54	0.0515	101.80
0.0558	92.12	0.0582	96.40	0.0560	100.96
0.0594	91.65	0.0616	95.20	0.0602	99.94
0.0638	90.48	0.0650	94.48	0.0629	99.06
0.0674	89.24	0.0687	93.74	0.0662	98.99
0.0715	88.10	0.0726	92.03	0.0707	98.76
0.0740	87.19	0.0752	91.84	0.0732	97.09
0.0774	85.91	0.0765	91.23	0.0749	96.82
0.0787	85.22	0.0792	91.95	0.0782	95.50
0.0815	84.76	0.0815	90.40	0.0821	94.60
m _{D(+)-galactose} =0.4 mol kg ⁻¹					
0.0124	100.33	0.0129	103.49	0.0142	107.87
0.0173	98.93	0.0196	102.40	0.0265	105.27
0.0249	97.37	0.0279	101.12	0.0325	104.03
0.0311	95.32	0.0352	99.76	0.0409	102.22
0.0355	94.46	0.0418	98.68	0.0464	101.11
0.0395	92.60	0.0472	97.80	0.0531	99.60
0.0443	91.50	0.0518	96.92	0.0567	98.89

0.0475	90.50	0.0562	95.40	0.0604	98.06
0.0496	90.06	0.0609	94.53	0.0654	96.85
0.0542	89.86	0.0670	93.51	0.0698	95.93
0.0599	88.77	0.0705	92.92	0.0727	95.20
0.0657	86.43	0.0736	91.25	0.0758	94.63
0.0721	85.63	0.0770	90.55	0.0784	94.24
0.0765	85.04	0.0807	89.01	0.0821	93.60
0.0844	83.30	0.0845	89.33	0.0880	92.13
<hr/>					
$m_{D(+)}_{\text{galactose}} = 0.6 \text{ mol kg}^{-1}$					
0.0153	97.11	0.0140	101.41	0.0150	105.25
0.0253	94.91	0.0215	99.83	0.0259	102.97
0.0331	92.80	0.0316	97.63	0.0329	101.53
0.0423	91.75	0.0371	96.60	0.0384	100.41
0.0481	90.28	0.0429	95.64	0.0430	99.19
0.0542	89.07	0.0494	94.32	0.0487	97.94
0.0598	88.11	0.0530	93.37	0.0527	97.11
0.0631	87.23	0.0583	92.44	0.0581	96.00
0.0656	86.21	0.0629	91.49	0.0624	95.17
0.0699	85.23	0.0652	91.03	0.0667	94.22
0.0731	84.16	0.0714	89.65	0.0715	92.95
0.0763	83.03	0.0744	88.93	0.0758	92.11
0.0782	81.93	0.0775	88.15	0.0785	91.67
0.0819	80.99	0.0812	87.71	0.0823	90.72
0.0862	80.33	0.0854	86.82	0.0859	90.08

Table VI.4. Ion association constants (K_A), limiting molar conductivities (Λ_0), distance parameters (R), Walden product ($\Lambda_0 \cdot \eta$) and standard deviations of experimental Λ (δ) obtained from Fuoss conductance equation of IL in aqueous D(-)fructose and D(+)galactose solutions as a function of ionic liquid molality (m) at different temperatures.

T (K)	$K_A(\text{dm}^3 \text{ mol}^{-1})$	$\Lambda_0(\text{S cm}^2 \text{ mol}^{-1})$	$10^{10}R(\text{m})$	$\Lambda_0 \cdot \eta(\text{S cm}^2 \text{ mPa s mol}^{-1})$	δ
$m_{\text{D}(-)\text{fructose}}=0.2 \text{ mol kg}^{-1}$					
298.15	52.18	107.16	9.53	99.66	1.165
303.15	51.78	110.11	9.59	100.20	0.729
308.15	50.21	114.22	9.65	101.66	0.572
$m_{\text{D}(-)\text{fructose}}=0.4 \text{ mol kg}^{-1}$					
298.15	54.21	100.79	9.52	93.73	1.478
303.15	52.91	105.10	9.55	95.64	1.261
308.15	51.12	108.26	9.58	97.43	1.173
$m_{\text{D}(-)\text{fructose}}=0.6 \text{ mol kg}^{-1}$					
298.15	56.23	99.41	9.45	92.45	1.659
303.15	55.29	103.39	9.49	95.12	1.392
308.15	52.98	107.93	9.54	97.43	1.281
$m_{\text{D}(+)\text{galactose}}=0.2 \text{ mol kg}^{-1}$					
298.15	50.24	108.35	9.61	100.77	1.086
303.15	48.36	111.27	9.63	101.26	0.695
308.15	46.91	115.92	9.66	104.33	0.425
$m_{\text{D}(+)\text{galactose}}=0.4 \text{ mol kg}^{-1}$					
298.15	51.22	105.54	9.56	98.15	1.321
303.15	50.53	107.03	9.60	98.47	1.053
308.15	49.62	113.25	9.62	101.93	0.915
$m_{\text{D}(+)\text{galactose}}=0.6 \text{ mol kg}^{-1}$					

298.15	50.45	104.18	9.50	96.89	1.114
303.15	49.28	106.34	9.57	97.83	0.992
308.15	48.38	111.05	9.69	99.95	0.711

Table VI.5. The values of coefficients in Eq. (11) A_0 , A_1 and A_2 at different solvent compositions.

Conc. (M)	$A_0 \cdot 10^{-6}$ (J mol ⁻¹)	A_1 (KJ mol ⁻¹ K ⁻¹)	A_2 (J mol ⁻¹ K ⁻²)
D(-)fructose			
0.2	-2.18	11.31	-18.82
0.4	-1.46	10.91	-18.15
0.6	-1.14	9.97	-16.60
D(-)galactose			
0.2	-2.02	10.28	-17.08
0.4	-1.35	8.49	-14.12
0.6	-1.05	8.09	-13.47

Table VI.6. Thermodynamic functions (ΔG_A^0 , ΔS_A^0 , ΔH_A^0) of IL in aqueous d(-)fructose and d(+)-galactose solutions as a function of ionic liquid molality (m) at different temperatures.

T (K)	ΔG_A^0 (kJ mol ⁻¹)	ΔS_A^0 (J mol ⁻¹ K ⁻¹)	ΔH_A^0 (kJ mol ⁻¹)
m _{D(-)fructose} =0.2 mol kg ⁻¹			
298.15	-9.59	263.30	68.91
303.15	-10.55	131.65	29.36
308.15	-10.58	11.31	-7.09
m _{D(-)fructose} =0.4 mol kg ⁻¹			

298.15	-9.76	253.90	65.76
303.15	-10.70	126.95	27.78
308.15	-10.75	10.91	-7.39
<hr/>			
<i>m_{D(-)}fructose=0.6 mol kg⁻¹</i>			
298.15	-9.92	232.33	59.35
303.15	-10.82	116.15	24.39
308.15	-10.90	9.97	-7.83
<hr/>			
<i>m_{D(+)}galactose =0.2 mol kg⁻¹</i>			
298.15	-9.92	238.80	61.28
303.15	-10.64	119.40	25.56
308.15	-10.68	10.28	-7.51
<hr/>			
<i>m_{D(+)}galactose =0.4 mol kg⁻¹</i>			
298.15	-10.01	197.50	48.87
303.15	-10.76	98.75	19.18
308.15	-10.81	8.49	-8.19
<hr/>			
<i>m_{D(+)}galactose =0.6 mol kg⁻¹</i>			
298.15	-10.14	188.50	46.06
303.15	-10.89	94.25	17.68
308.15	-10.92	8.09	-8.43

Table VI.7. Limiting apparent molar volume (ϕ_V^0), experimental slope (S_V^*), viscosity-B and A co-efficients of IL in aqueous d(-)fructose and d(+)galactose solutions at different temperatures.

T (K)	$\phi_V^0 \cdot 10^6 / \text{m}^3 \cdot \text{mol}^{-1}$	$S_V^* \cdot 10^6 / \text{m}^3 \cdot \text{mol}^{-1} \cdot \text{dm}^{3/2}$	$B / \text{dm}^3 \cdot \text{mol}^{-1}$	$A / \text{dm}^{3/2} \cdot \text{mol}^{-1/2}$
$m_{D(-)\text{fructose}} = 0.2 \text{ mol kg}^{-1}$				
298.15	120.56	-242.28	0.959	-0.0749
303.15	129.31	-259.39	1.108	-0.0780
308.15	140.91	-337.66	1.213	-0.0851
$m_{D(-)\text{fructose}} = 0.4 \text{ mol kg}^{-1}$				
298.15	124.73	-237.81	1.159	-0.0779
303.15	133.62	-249.15	1.301	-0.0868
308.15	149.67	-329.07	1.376	-0.0951
$m_{D(-)\text{fructose}} = 0.6 \text{ mol kg}^{-1}$				
298.15	129.03	-233.04	1.457	-0.0959
303.15	138.12	-246.93	1.529	-0.0967
308.15	155.35	-321.23	1.662	-0.0979
$m_{D(+)\text{galactose}} = 0.2 \text{ mol kg}^{-1}$				
298.15	114.05	-256.05	0.907	-0.0602
303.15	125.35	-269.07	1.088	-0.0685
308.15	134.08	-338.68	1.185	-0.0712
$m_{D(+)\text{galactose}} = 0.4 \text{ mol kg}^{-1}$				
298.15	121.38	-240.15	1.136	-0.0670
303.15	130.77	-257.67	1.273	-0.0794
308.15	144.43	-336.45	1.313	-0.0856
$m_{D(+)\text{galactose}} = 0.6 \text{ mol kg}^{-1}$				
298.15	126.29	-235.65	1.316	-0.0747

Communicated

303.15	135.72	-248.21	1.356	-0.0790
308.15	152.16	-324.43	1.462	-0.0841

Table VI.8. Values of $\phi_V^0(\text{aq})$, $\Delta\phi_{\text{tr}}^0$, $B(\text{aqueous})$, ΔB for IL in different solvent systems at different temperatures.

Temp /K	$\phi_V^0 \cdot 10^6(\text{aq})$ /m ³ ·mol ⁻¹	$\Delta\phi_{\text{tr}}^0 \cdot 10^6$ /m ³ ·mol ⁻¹	$B(\text{aq})$ /kg·mol ⁻¹	ΔB / kg·mol ⁻¹
$m_{\text{D}(-)\text{fructose}}=0.2 \text{ mol kg}^{-1}$				
298.15	112.01	8.55	0.890	0.069
303.15	112.23	17.08	1.033	0.075
308.15	112.71	28.20	1.129	0.084
$m_{\text{D}(-)\text{fructose}}=0.4 \text{ mol kg}^{-1}$				
298.15	112.95	11.78	1.085	0.074
303.15	113.03	20.59	1.22	0.081
308.15	113.11	36.56	1.283	0.093
$m_{\text{D}(-)\text{fructose}}=0.6 \text{ mol kg}^{-1}$				
298.15	113.21	15.82	1.377	0.080
303.15	113.27	24.85	1.44	0.089
308.15	113.35	42.00	1.563	0.099
$m_{\text{D}(+)\text{galactose}}=0.2 \text{ mol kg}^{-1}$				
298.15	112.01	2.04	0.842	0.065
303.15	112.23	13.12	1.016	0.072
308.15	112.71	21.37	1.102	0.083
$m_{\text{D}(+)\text{galactose}}=0.4 \text{ mol kg}^{-1}$				
298.15	112.95	8.43	1.065	0.071
303.15	113.03	17.74	1.197	0.076
308.15	113.11	31.32	1.234	0.079
$m_{\text{D}(+)\text{galactose}}=0.6 \text{ mol kg}^{-1}$				

298.15	113.21	13.08	1.242	0.074
303.15	113.27	22.45	1.275	0.081
308.15	113.35	38.81	1.369	0.093

Table VI.9. Values of empirical coefficients (a_0 , a_1 , and a_2) of eqn (17) for IL in different solvent systems.

Conc. (m)	$a_0 \cdot 10^{-6}$ (J mol ⁻¹)	a_1 (KJ mol ⁻¹ K ⁻¹)	a_2 (J mol ⁻¹ K ⁻²)
D(-)fructose			
0.2	0.0085	-0.0569	0.0097
0.4	0.0125	-0.0843	0.1432
0.6	0.0143	-0.0967	0.1628
D(+)galactose			
0.2	-0.0052	0.0332	-0.0510
0.4	0.0153	-0.1027	0.1734
0.6	0.0195	-0.1309	0.2202

Table VI.10. Limiting apparent molal expansibilities (ϕ_E^0) and $(\delta\phi_E^0/\delta T)_P$ for IL in different solvent systems at different temperatures.

T (K)	ϕ_E^0	$(\delta\phi_E^0/\delta T)_P$
m _{D(-)fructose} =0.2 mol kg ⁻¹		
298.15	57.78	0.194
303.15	58.75	0.194
308.15	59.72	0.194
m _{D(-)fructose} =0.4 mol kg ⁻¹		
298.15	85.30	0.286

Communicated

303.15	86.61	0.286
308.15	88.04	0.286
$m_{D(-)fructose} = 0.6 \text{ mol kg}^{-1}$		
298.15	100.20	0.336
303.15	101.76	0.336
308.15	103.44	0.336
$m_{D(+)}galactose = 0.2 \text{ mol kg}^{-1}$		
298.15	-29.84	-0.100
303.15	-30.04	-0.100
308.15	-30.84	-0.100
$m_{D(+)}galactose = 0.4 \text{ mol kg}^{-1}$		
298.15	103.29	0.347
303.15	105.02	0.347
308.15	106.76	0.347
$m_{D(+)}galactose = 0.6 \text{ mol kg}^{-1}$		
298.15	129.99	0.440
303.15	133.37	0.440
308.15	135.57	0.440

Table VI.11. Values of dB/dT , A_1 and A_2 coefficient of equation (22) for the IL in different solvent systems.

Conc. (m)	dB/dT	A_1	A_2
IL+aqueous D(-)fructose			
0.2	0.0071	-0.508	0.012
0.4	0.0076	0.161	0.008
0.6	0.0081	0.453	0.007
IL+aqueous D(+galactose			

0.2	0.0068	-0.480	0.014
0.4	0.0074	0.271	0.007
0.6	0.0077	0.586	0.005

Table VI.12. ^1H NMR data of [BMP]Cl, D(-)fructose, D(+)-galactose and IL-carbohydrates mixture

[BMP]Cl (300MHz, Solv: D ₂ O) δ /ppm	
0.91-0.96 (3H, t, $J = 7.29$ Hz), 1.34-1.41 (2H, m), 1.74-1.81(2H,m), 2.19 (4H, m), 3.02 (3H, s), 3.28-3.34 (2H, m), 3.48 (4H, m)	
D(-)fructose (300 MHz, Solv: D ₂ O)	D(+)-galactose (300 MHz, Solv: D ₂ O)
δ /ppm	δ /ppm
3.49-3.53 (2H, d), 3.64-3.68 (1H, m), 3.69-3.73 (1H, m), 3.77-3.84 (1H, m), 3.88-3.95 (1H, m), 3.94-4.06 (2H, d)	3.42-3.47 (2H, d), 3.58-3.61 (1H, m), 3.63-3.70 (1H, m), 3.72-3.79 (1H, m), 3.88-3.94 (1H, m), 4.53-4.55 (1H, d)
[BMP]Cl- D(-)fructose (1:1 molar ratio, 300 MHz, Solv: D ₂ O)	[BMP]Cl- D(+)-galactose (1:1 molar ratio, 300 MHz, Solv: D ₂ O)
δ /ppm	δ /ppm
0.87-0.92 (3H, t), 1.28-1.31 (2H, m), 1.72-1.80 (2H, m), 2.11-2.15 (4H, m), 2.98 (3H, s), 3.20-3.31 (2H, m), 3.40-3.46 (1H, m), 3.45-3.48 (2H, d), 3.59-3.65 (1H, m), 3.67-3.70 (1H, m), 3.71-3.79 (1H, m), 3.81-3.90 (1H, m), 3.91-4.01 (2H, d)	0.90-0.95 (3H, t), 1.29-1.39 (2H, m), 1.73- 1.81 (2H, m), 2.14-2.18 (4H, m), 3.00 (3H, s), 3.24-3.32 (2H, m), 3.46-3.48 (4H, m), 3.41-3.45 (2H, d), 3.56-3.60 (1H, m), 3.60-3.67 (1H, m), 3.69-3.76 (1H, m), 3.84-3.92 (1H, m), 4.51-4.53 (1H, d)

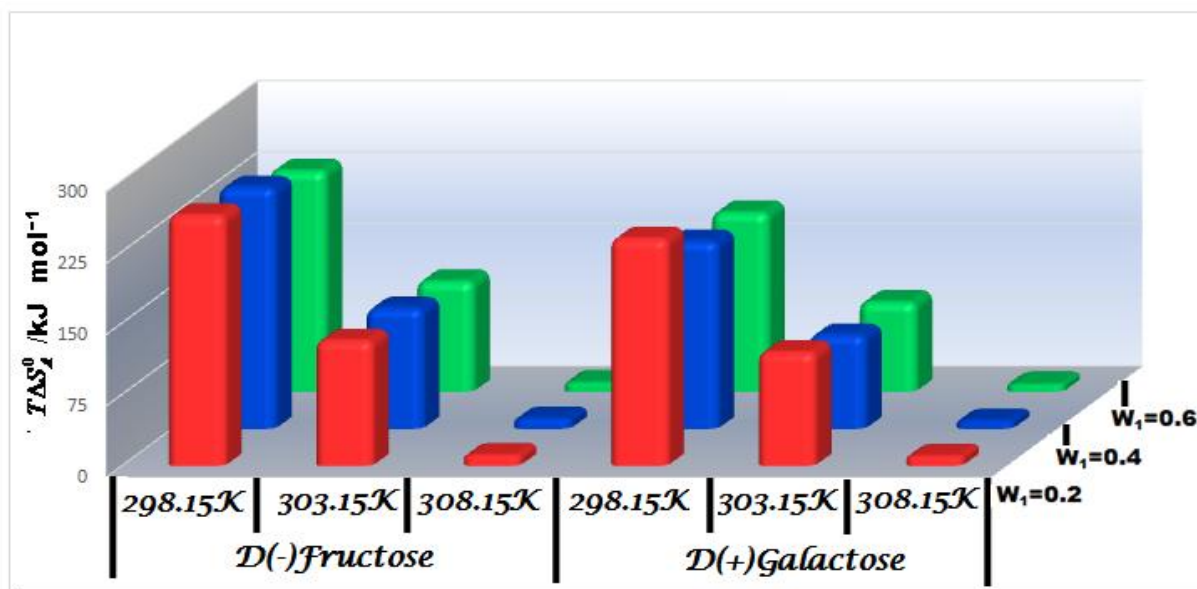
FIGURES

Figure VI.1. Plot of $T\Delta S_A^0$ of IL in different mass fractions of aqueous D(-)fructose and D(+)galactose solution respectively at different temperatures

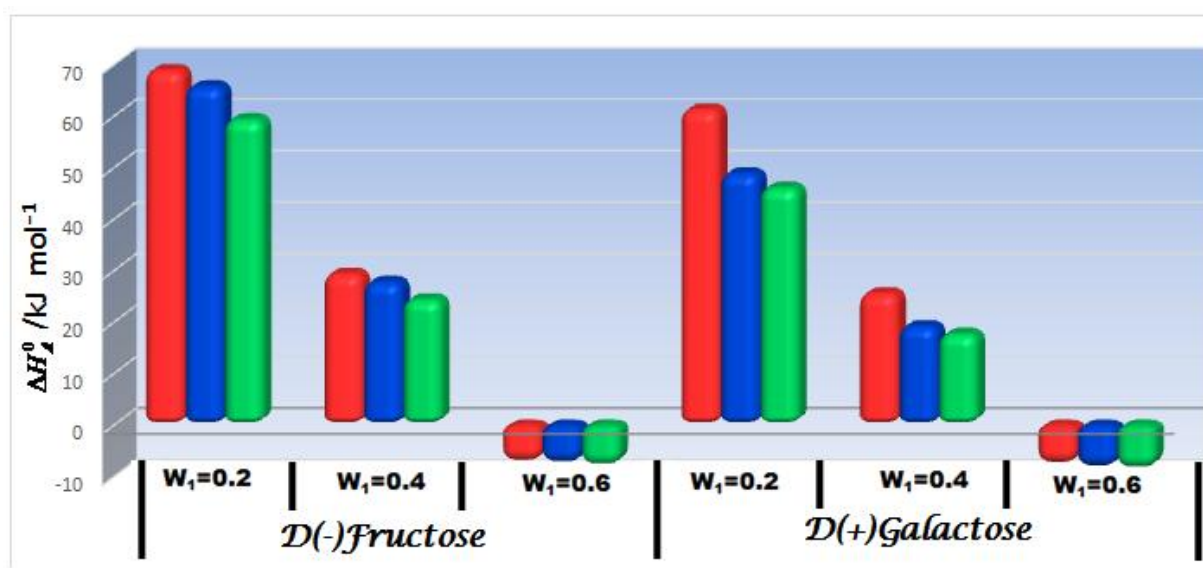


Figure VI.2. Plot of ΔH_A^0 of IL in different mass fractions of aqueous D(-)fructose and D(+)galactose solution respectively at 298.15 K (red), 303.15 K (blue) and 308.15 K (green) respectively

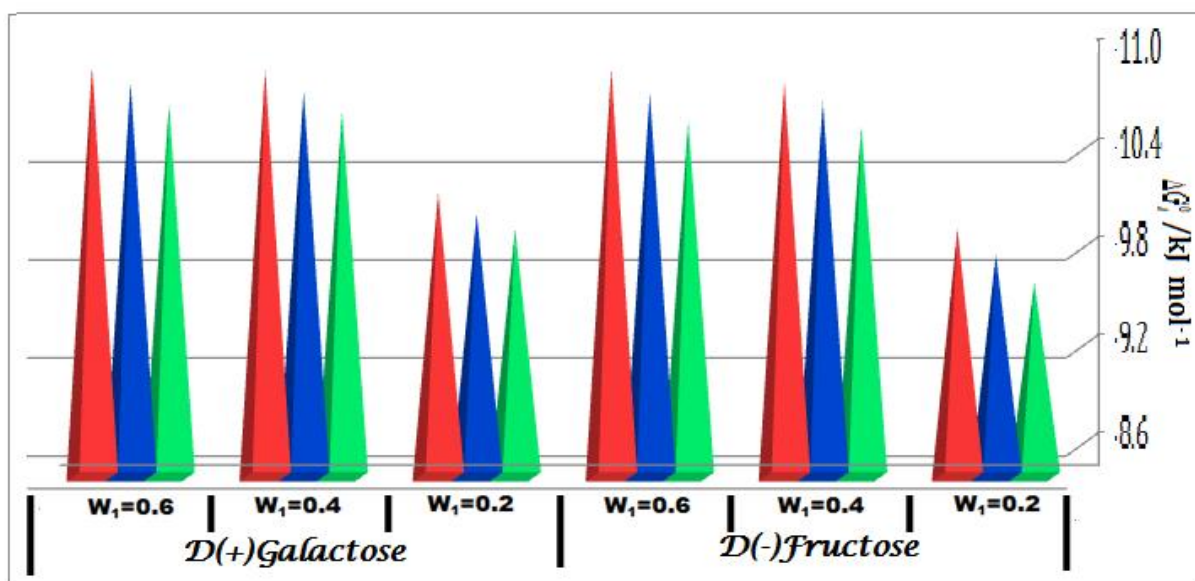


Figure VI.3. Plot of ΔG_A^0 of IL in different mass fraction of aqueous D(-)fructose and D(+)galactose solution respectively at 298.15 K (red), 303.15 K (blue) and 308.15 K (green) respectively

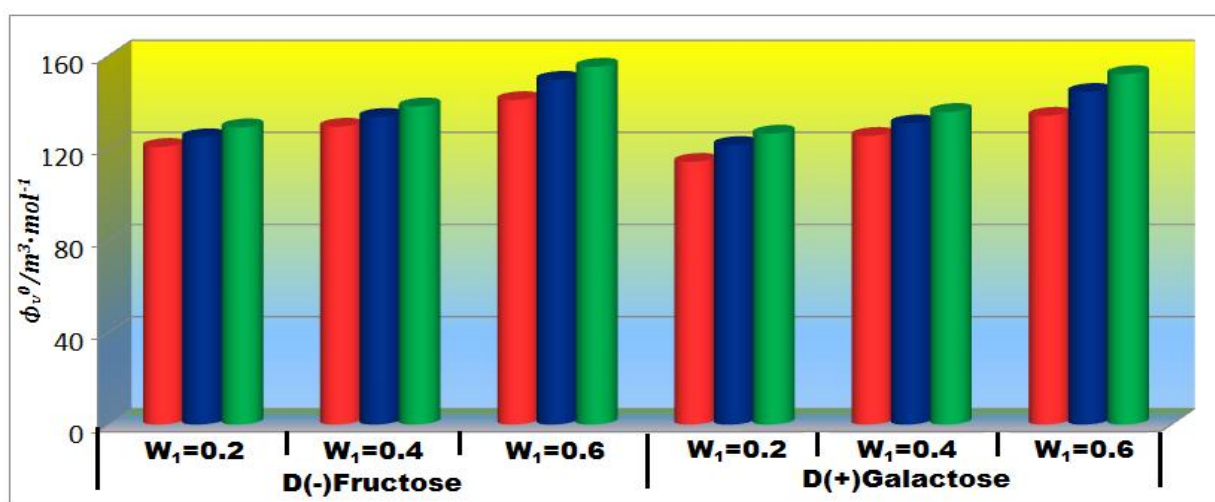


Figure VI.4. Plot of limiting molar volume (ϕ_V^0) of IL against mass fraction (w) of aqueous D(-)fructose and D(+)galactose at 298.15K (red), 303.15K (blue) and 308.15K (green) respectively

Communicated

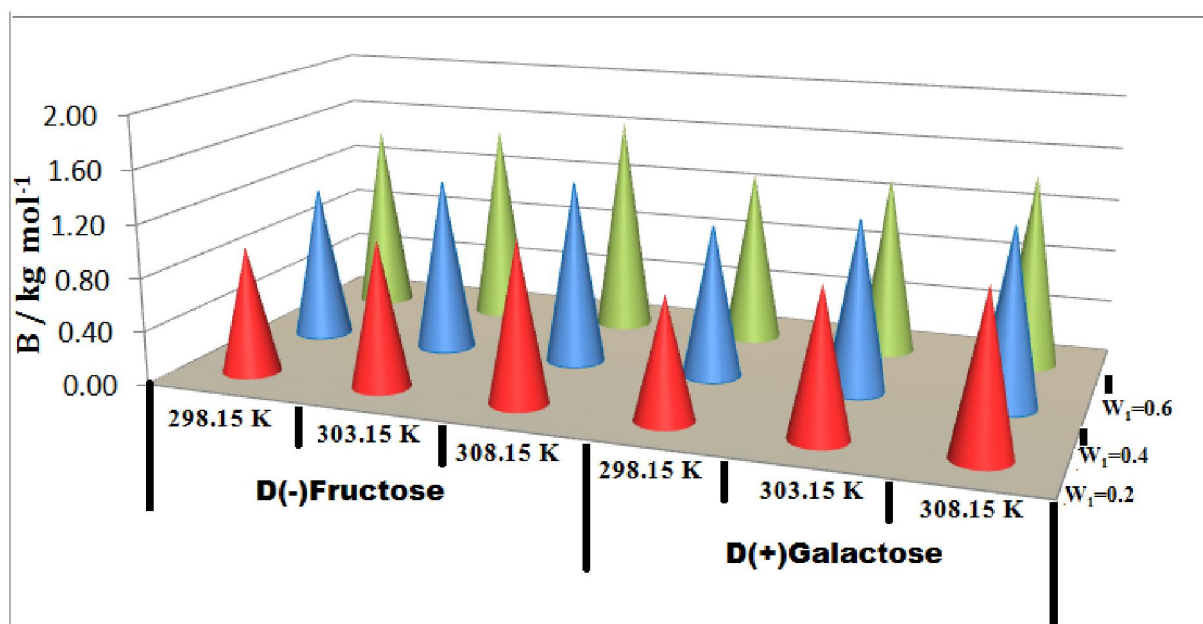


Figure VI.5. Plot of viscosity B -coefficient of IL against mass fraction (w) of aqueous D(-)fructose and D(+)-galactose at different temperatures

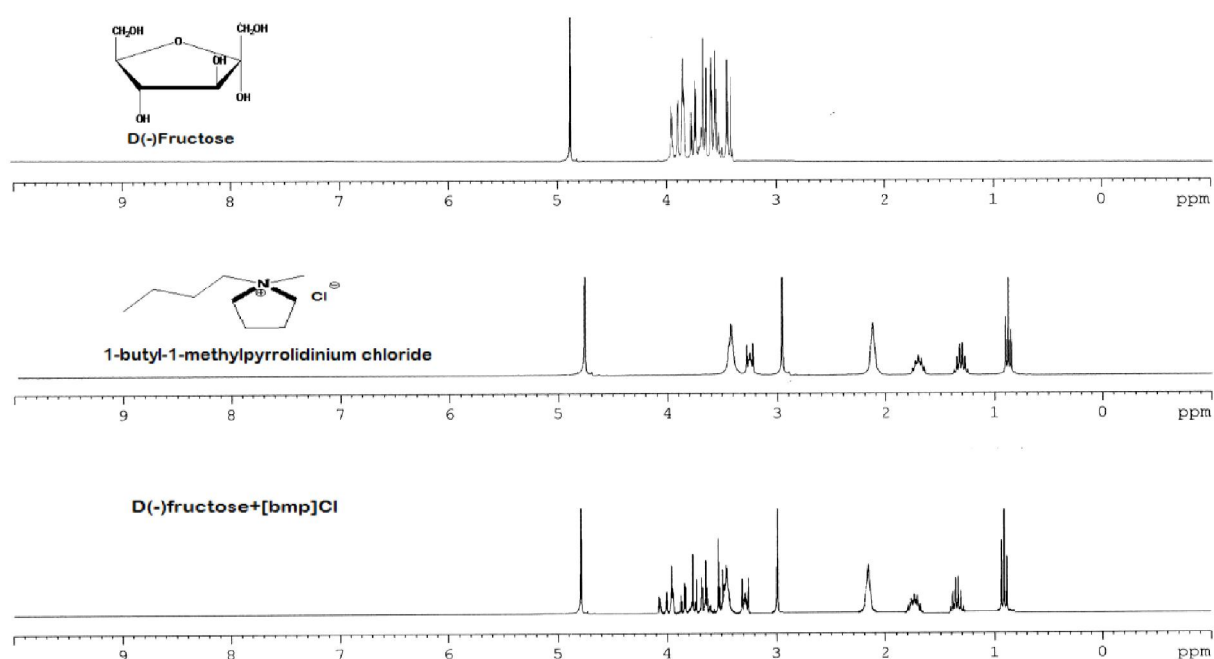


Figure VI.6(a). ^1H NMR Spectra of D(-)Fructose, [BMP]Cl and 1:1 molar ratio of D(-)Fructose + [BMP]Cl in D_2O in 298.15 K.

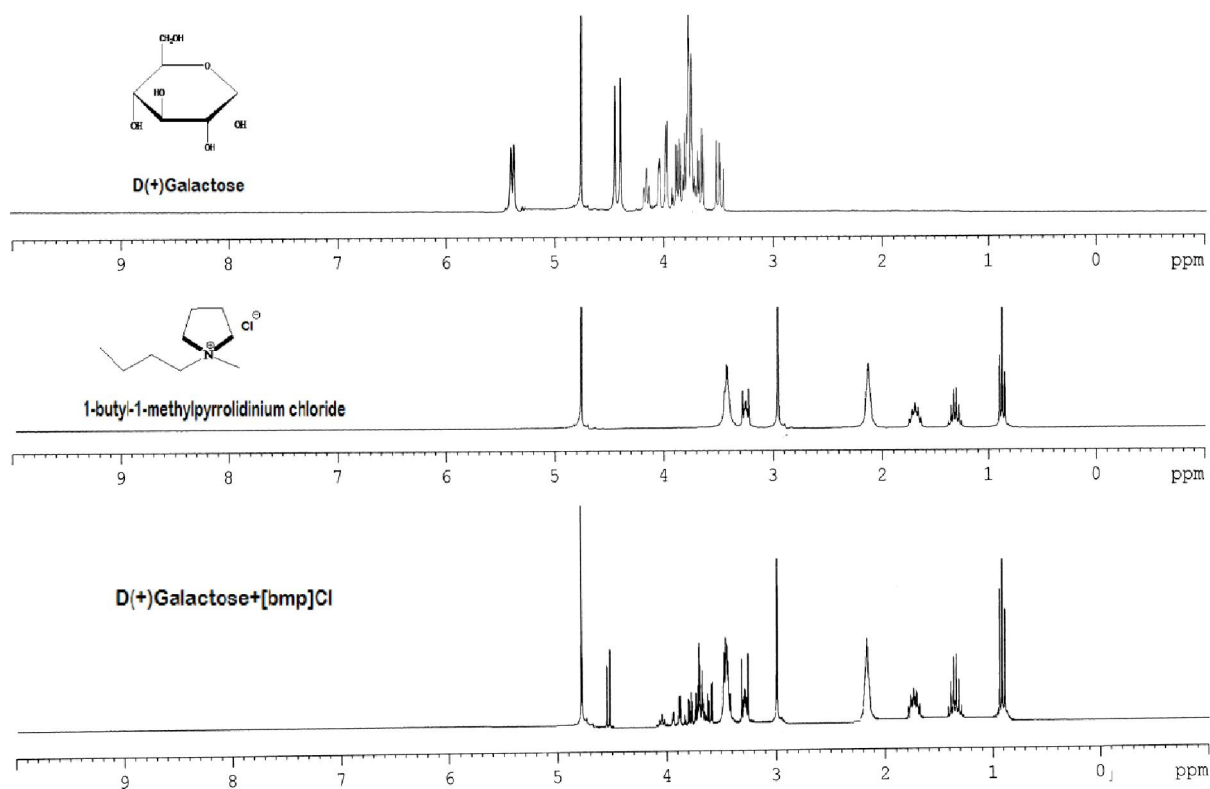
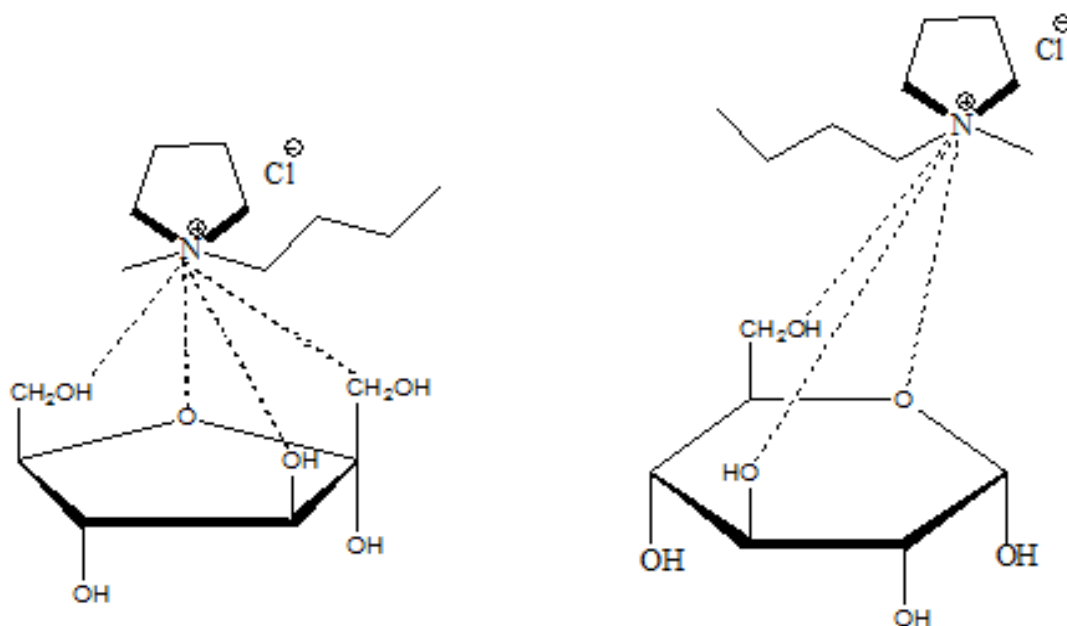


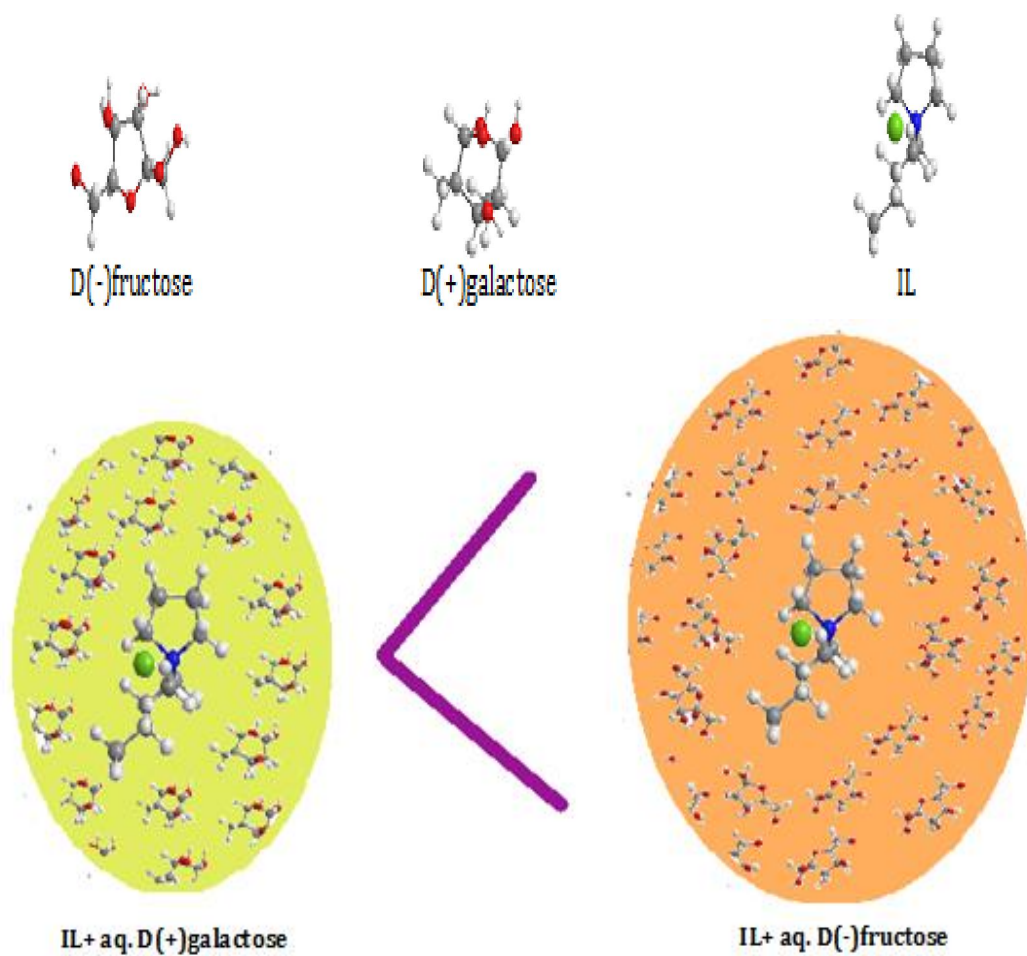
Figure. VI.6(b). ^1H NMR Spectra of D(+)-Galactose, [BMP]Cl and 1:1 molar ratio of D(+)-Galactose + [BMP]Cl in D_2O in 298.15 K.

SCHEMES:

Interaction between D(-)fructose and IL (I₁) Interaction between D(+)galactose and IL (I₂)

$I_1 > I_2$

Scheme VI.1: Plausible Interfaces between ionic liquid and diverse solvent systems



Scheme VI.2: Molecular structure of D(-)fructose, D(+)galactose, IL and Extent of ion-solvent interaction of ionic liquid in diverse solution systems.

CHAPTER-VII

Exploration of Miscellaneous Interfaces of a Green Liquid in Diverse Solvent Systems by the Process of Physicochemical Contrivances

VII.1. INTRODUCTION

Ionic liquids have unique intrinsic properties, such as negligible vapour pressure, large liquid range, ability of dissolving a variety of chemicals, high thermal stability, large electrochemical window and their potential as 'designer solvents' and 'green' replacements for volatile organic solvents[1-3] used in reactions involving inorganic and bio-catalysis etc. They are also utilized as heat transfer fluids for processing biomass and as electrically conductive liquids in electrochemistry (batteries and solar cells) [4-6]. In the modern technology, the application of the salt is well understood by studying the ionic solvation or ion association. Ionic association of electrolytes in solution depends on the mode of solvation of its ions [7-10] which in turn depends on the nature of the solvent/solvent mixtures. Such solvent properties as viscosity and the relative permittivity have been taken into consideration as these properties help in determining the extent of ion association and the solvent-solvent interactions. The non-aqueous system has been of immense importance [11,12] to the technologist and theoretician as many chemical processes occur in these systems. The volumetric, viscometric and interferometric behavior of solutes has been found to be very useful in elucidating the various interactions occurring in solutions. Studies on the effect of concentration (molarity), the apparent molar volumes of solutes have been extensively studied to obtain information on ion-ion, ion -solvent and solvent-solvent interactions [13-17].

In view of the above and in continuation of our studies, we have performed a systematic study on the conductance, density, viscosity, refractive index, ultrasonic

speed and FTIR study of 1-butyl-1-methylpyrrolidinium bromide [BMP][Br] in pure formamide (FA), N, N-dimethyl formamide (DMF) and N, N-dimethyl acetamide (DMA) at 298.15 K and we have attempted to report the limiting molar conductance (Λ_0), the association constant (K_A), the association diameter (R) and Walden product for ion-pair formation. Also the limiting apparent molar volume (ϕ_V^0), viscosity B -coefficients, molar refraction (R_M) and limiting apparent molar adiabatic compressibility (ϕ_K^0) for the [BMP][Br] in the same solvent systems.

VII.2. EXPERIMENTAL SECTION

VII.2.1. Materials

1-butyl-1-methylpyrrolidinium bromide [BMP][Br] of puriss grade was procured from Sigma-Aldrich, Germany and was used as purchased. The mass fraction purity of the IL has ≥ 0.99 . Formamide ($\geq 98.5\%$) and DMF ($\geq 99.5\%$) were obtained from Sd. Fine Chemicals, India. and DMA ($\geq 99.5\%$) has obtained from Thomas Beaker, India. The solvents were purified using standard methods. [18]

VII.2.2. Apparatus and Procedure

The conductance measurement was carried out in a Systronic-308 conductivity meter (accuracy $\pm 0.01\%$) using a dip-type immersion conductivity cell, CD-10, having a cell constant of approximately $0.1 \pm 0.001 \text{ cm}^{-1}$. Measurement was made in a water bath maintained within $T = 298.15 \pm 0.01 \text{ K}$ and the cell was calibrated by the method proposed by Lind et al. [19] The conductance data were reported at a frequency of 1 kHz and the accuracy was $\pm 0.3\%$.

Stock solutions for the IL in three different solvents were prepared by mass (Mettler Toledo AG285 with uncertainty 0.0003 g), and the working solutions were obtained by mass dilution at 298.15K. The uncertainty of molarity of different solutions was evaluated to $\pm 0.0001 \text{ mol dm}^{-3}$. The density (ρ) was measured by means of vibrating-tube Anton Paar density-meter (DMA 4500M) with a precision of 0.0005 $\text{g}\cdot\text{cm}^{-3}$. It was calibrated by double-distilled water and dry air.

The viscosity was measured with the help Brookfield DV-III Ultra Programmable Rheometer with spindle size-42 fitted to a Brookfield Digital Bath TC-500.

The refractive index was also measured with the help Refractive index was measured with the help of a Digital Refractometer Mettler Toledo. The light source was LED, $\lambda = 589.3$ nm. The refractometer was calibrated twice using distilled water, and calibration was checked after every few measurements. The uncertainty of refractive index measurement was ± 0.0002 units.

The ultrasonic velocities, u (ms^{-1}) were determined using an ultrasonic interferometer (Model M-83) from Mittal enterprises. The interferometer working at 2 MHz is based on the same principle as was used by Freyer et al. [20] and Kiyoharo et al. [21,22] The obtained velocities were corrected for diffraction errors as given by Subrahmayan et al. [23]. The maximum uncertainty in the velocity is ± 0.5 m s^{-1} . The temperature was controlled within ± 0.01 K using a Lauda thermostat for velocity measurements.

Infrared spectra were recorded in 8300 FT-IR spectrometer (Shimadzu, Japan). The details of the instrument have already been previously described [24].

VII.3. RESULTS AND DISCUSSION

VII.3.1. Conductance calculation

The solvent properties have been given in Table VII.1. The molar conductances (Λ) with corresponding concentrations of [BMP][Br] in FA, DMA and DMF have been given in Table VII.2. Linear conductimetric curves (Λ versus \sqrt{c}) have been obtained and extrapolation of $\sqrt{c} = 0$ evaluated the starting limiting molar conductance for the electrolyte. The conductance data for ion-pair formation have been analyzed using the Fuoss conductance equation [14]. For a given set of conductivity values ($c_j, \Lambda_j; j = 1, \dots, n$), three adjustable parameters, i.e., Λ_0, K_A and R have been derived from the Fuoss equation. Here, Λ_0 is the limiting molar conductance, K_A is the observed association constant and R is the association distance, i.e., the maximum centre to centre distance between the ions in the solvent separated ion-pairs. There is no precise

method [25] for determining the R value but in order to treat the data in our system, R value is assumed to be, $R = a + d$, where a is the sum of the crystallographic radii of the ions and d is the average distance corresponding to the side of a cell occupied by a solvent molecule. The distance, d , is given by:

$$d = 1.183 (M / \rho)^{1/3} \quad (1)$$

where M is the molar mass and ρ is the density of the solvent.

The Fuoss conductance equation may be represented as follows:

$$\Lambda = P\Lambda_0[(1 + R_x) + E_L] \quad (2)$$

$$P = 1 - \alpha(1 - \gamma) \quad (3)$$

$$\gamma = 1 - K_A c \gamma^2 f^2 \quad (4)$$

$$-\ln f = \beta \kappa / 2(1 + \kappa R) \quad (5)$$

$$\beta = e^2 / (\epsilon_r k_B T) \quad (6)$$

$$K_A = K_R / (1 - \alpha) = K_R / (1 + K_S) \quad (7)$$

here, Λ_0 is the limiting molar conductance, K_A is the observed association constant, R is the association distance, R_x is the relaxation field effect, E_L is the electrophoretic counter current, k is the radius of the ion atmosphere, ϵ_r is the relative permittivity of the solvent mixture, e is the electron charge, c is the molarity of the solution, k_B is the Boltzmann constant, K_S is the association constant of the contact-pairs, K_R is the association constant of the solvent-separated pairs, γ is the fraction of solute present as unpaired ion, α is the fraction of contact pairs, f is the activity coefficient, T is the absolute temperature and β is twice the Bjerrum distance.

The computations were performed using the program suggested by Fuoss [14]. The initial Λ_0 values for the iteration procedure are obtained from Shedlovsky extrapolation of the data [26]. Input for the program is the number of data, n , followed by ϵ_r , η (viscosity of the solvent mixture), initial Λ_0 value, T , ρ (density of the solvent mixture), mole fraction of the first component, molar masses, M_1 and M_2 along with c_j , Λ_j values where $j = 1, 2, \dots, n$ and an instruction to cover preselected range of R values. In practice, calculations are performed by finding the values of Λ_0 and α which minimize the standard deviation, δ , whereby

$$\delta^2 = \sum [A_j(cal) - A_j(obs)]^2 / (n - m) \quad (8)$$

for a sequence of R values and then plotting δ against R , the best-fit R corresponds to the minimum of the δ - R versus R curve. So, an approximate sum is made over a fairly wide range of R values using 0.1 increment to locate the minimum but no significant minima is found in the δ - R curves. Finally, the corresponding Λ_0 and K_A values have been obtained which are reported in Table VII.3 along with R and δ for the all the solutions.

A perusal of Table VII.3 and Figure VII.1 shows that the limiting molar conductance (Λ_0) of all the electrolytes studied is highest in case of DMF and lowest in case of FA among the studied solvents. The trend of Λ_0 for the electrolyte in three different solvents is as follows:



The more number of molecules interacting have been lead with the help greater ion-solvation. It has been seen that in case of FA, the K_A value are greater (Table VII.3), which obviously made the same inference that ion-solvent as well as ion-association is higher in FA. Similarly, the lower K_A value for DMF, suggesting the weakest ion-solvent interaction, is in lowest viscous solvent.

The Gibbs energy change of solvation, ΔG° , is determined by the following equation [27] and reported in Table VII.4.

$$\Delta G^\circ = -RT \ln K_A \quad (9)$$

The negative values of ΔG° can be explained by considering the participation of specific electrostatic interaction in the ion-association process [30]. The negative in ΔG° values have states that the ion-solvent interaction is more feasible in these solution systems. The decrease in the value of ΔG° , from DMF to FA, provides the spontaneity of the ion-solvent interactions, which have been trends from DMF to FA, as a results ion-association increases. This result indicates the extent of solvation enhanced by the following order:



The observed ion-solvent interactions can be explain as follow: In case of (IL+FA) binary solution, the positively charged N atom of [BMP]⁺ may interacts with more negative oxygen atom of FA. Again, negatively charged Br⁻ ion of IL interacts with positively charged N atom of resonance structure of formamide (Scheme VII.1). In DMA electrophilic character of N atom reduced due to presence of two -CH₃ groups, which exhibit +I affect. So, interaction between Br⁻ of IL and N atom of DMA decreases. On the other hand one -CH₃ is attached with C=O group present in DMA, which, increases the nucleophilic character of oxygen and the interaction between N atom of [BMP]⁺ and oxygen atom of DMA increases. But, in DMF electrophilic nature of N atom decreases due to +I effect of -CH₃ groups, therefore, interaction between Br⁻ and N atom of DMF decreases. Once again, there is no mesmerizing power in DMA, i.e., interaction mode of oxygen atom of DMF and N of [BMP]⁺ are lower (Scheme VII.1).

The ionic level of interaction has been interpreted from the results of ionic contribution of electrolyte. The starting point for most evaluations of ionic conductance is Stokes' law which states that the limiting Walden product ($\lambda_o^\pm \eta$), (the limiting ionic conductance-solvent viscosity product) for any singly charged, spherical ion is a function only of the ionic radius and thus, under normal conditions, is a constant. The ionic conductances λ_o^\pm for the cation [BMP]⁺ and the anion Br⁻ in all the solvents were calculated using tetrabutylammonium tetraphenylborate (Bu₄NBPh₄) as a 'reference electrolyte' following the scheme as suggested by B. Das et al. [28] The ionic limiting molar conductances λ_o^\pm for [BMP]⁺ and Br⁻ in all the solvents have been calculated by interpolation of conductance data from the literature [29] using cubic spline fitting. The λ_o^\pm values were in turn utilized for the calculation of Stokes' radii (r_s) according to the classical expression [30]

$$r_s = \frac{F^2}{6\pi N_A \lambda_o^\pm r_c} \quad (10)$$

where, r_c is the crystallographic radii, N_A is the Avogadro number, and F is the Faraday constant. The values of ionic limiting molar conductance λ_o^\pm , ionic Walden product $\lambda_o^\pm \eta$, Stokes' radii r_s , and crystallographic radii r_c are presented in Table VII.5. A perusal of table VII.5 shows the ionic conductance of cation [BMP]⁺ and anion Br⁻ is lower in case

of FA, compared to other two solvents, suggests that the ion-solvent interactions as well as ion-solvation of the individual ions are higher. Similar relation has been observed from Stokes' radii (r_s) for both cation and anion, are higher in FA than DMA, which is in turn higher than DMF; the results also indicate the higher solvation in FA than other two. The r_s value of cation [BMP]⁺ is higher for anion Br⁻, which results ion-solvation (ion-solvent interaction) is higher for [BMP]⁺ ion than Br⁻ in all investigated solvents.

VII.3.2. Density calculation

The measured values of densities of [BMP][Br] in FA, DMA and DMF at 298.15 K are listed in Table VII.6. The densities and viscosities of the electrolytes in different solvents increase linearly with the concentration at the studied temperature. For this purpose, the apparent molar volumes ϕ_V given in Table VII.9 were determined from the solution densities using the following equation [31]

$$\phi_V = M / \rho_o - 1000(\rho - \rho_o) / c \rho_o \quad (11)$$

where M is the molar mass of the solute, c is the molarity of the solution, ρ and ρ_o are the densities of the solution and solvent, respectively. The limiting apparent molar volumes ϕ_V^0 were calculated using a least-squares treatment to the plots of ϕ_V versus \sqrt{c} using the following Masson equation [32].

$$\phi_V = \phi_V^0 + S_V^* \cdot \sqrt{c}$$

(12)

where ϕ_V^0 is the limiting apparent molar volume at infinite dilution and S_V^* is the experimental slope.

The plots of ϕ_V against the square root of the molar concentration \sqrt{c} were found to be linear with negative slopes. The values of ϕ_V^0 and S_V^* are reported in Table VII.6. The variation of ϕ_V^0 for this electrolyte with the solvents is shown in Figure VII.2. From Table VII.6 it is observed that ϕ_V^0 values for this electrolyte are generally positive for all the solvents and is highest in case of [BMP][Br] in FA. This indicates the presence

of strong ion-solvent interactions and the extent of interactions increases from DMF to FA.

On the contrary, the S_V^* indicates the extent of ion-ion interaction. The values of S_V^* shows that the extent of ion-ion interaction is highest in case of DMF and is lowest in FA. Owing to a quantitative comparison, the magnitude of ϕ_V^0 are much greater than S_V^* , in every solutions. This suggests that ion-solvent interactions dominate over ion-ion interactions in all the solutions. The values of ϕ_V^0 also support the fact that higher ion-solvent interaction in FA, leads to lower conductance of [BMP][Br] in it than DMA and DMF, discussed earlier.

VII.3.3. Viscosity calculation

Another transport property of the solution is viscosity has been studied for comparison and conformation of the solvation of the electrolyte in the chosen solvents. The viscosity data has been analyzed using Jones-Dole equation [33].

$$(\eta/\eta_0 - 1)/\sqrt{c} = A + B\sqrt{c} \quad (13)$$

where η and η_0 are the viscosities of the solution and solvent respectively. The values of A -coefficient and B -coefficient are obtained from the straight line by plotting $(\eta/\eta_0 - 1)/\sqrt{c}$ against \sqrt{c} which are reported in Table VII.7.

The effects of ion-solvent interactions on the [BMP][Br] solution in FA, DMA and DMF viscosity can be inferred from the B -coefficient [34, 35]. The viscosity B -coefficient is a valuable tool to provide information concerning the solvation of the solutes and their effects on the structure of the solvent. From Table VII.7 and Figure VII.3 it is evident that the values of the B -coefficient are positive, thereby suggesting the presence of strong ion-solvent interactions, and strengthened with an increase the solvent viscosity value, are agreement with the results obtained from ϕ_V^0 values discussed earlier. An assessment of Table VII.7 and Figure VII.3 shows that the values of the A -coefficient are very small for the solutions under investigation at all solvents indicating

the presence of weak ion-ion interactions, and these interactions further decrease from FA to DMF. This shows that with the increase in the viscosity B -coefficient of the solvent the mobility of the ions of the solvated IL decrease and hence the conductance also decreases. That is why, [BMP][Br] is more solvated in DMF than the other two solvents. Thus, the trend of ion-solvent interaction is FA >DMA>DMF. The viscosity A - and B -coefficients are in excellent agreement with the results drawn from the volumetric studies.

VII.3.4. Refractive index calculation

The molar refraction, R_M can be evaluated from Lorentz-Lorenz relation [36]

$$R_M = \{(n_D^2 - 1) / (n_D^2 + 2)\} (M / \rho) \quad (14)$$

where R_M , n_D , M and ρ are the molar refraction, refractive index, molar mass and density of solution respectively. The refractive index of a compound describes its ability to refract light as it moves from one medium to another and thus, the higher the refractive index of a compound, the more the light is refracted. As stated by Deetlefs *et al.*[37] the refractive index of a substance is higher when its molecules are more tightly packed or in general when the compound is denser. Hence a perusal of Table VII.8 and Figure VII.4 shows that the refractive indices (n_D) and molar refractions (R_M) of all the electrolytes (0.05M) are highest in FA and lowest in case of DMF among the three solvents. The trend of n_D and R_M of the three ionic liquids in three different solvents is as follows:

$$FA > DMA > DMF$$

As R_M is directly proportional to molecular polarizability, it is evident from Table VII.8 and Figure VII.4 that the overall polarizability of all the electrolytes is highest in case of FA in comparison to the other solvents. It is also found that the refractive index (n_D) and molar refraction (R_M) of [BMP][Br] is highest in FA. So, according to the statement of Deetlefs *et al.* it is concluded that the molecules of [BMP][Br] are most tightly packed among in FA. The packing is least in the case of DMF.

VII.3.5. Ultrasonic speed calculation

The adiabatic compressibility (β) was evaluated from the following equation:

$$\beta = 1/u^2 \rho \quad (15)$$

[16].

$$\phi_K = M\beta / \rho + 1000(\beta \rho_o - \beta_o \rho) / c \rho \rho_o \quad (16)$$

where M is the molar mass and β_o, β are the adiabatic compressibility of the solvent and solution respectively and c is the molarity of the solution. Limiting partial molar adiabatic compressibilities (ϕ_K^0) and experimental slopes (S_K^*) were obtained by fitting ϕ_K against the square root of molarity of the electrolyte (\sqrt{c}) using the method of least squares.

$$\phi_K = \phi_K^0 + S_K^* \cdot \sqrt{c} \quad (17)$$

The values of ϕ_K^0 and S_K^* are presented in Table VII.9. Since the values of ϕ_K^0 and S_K^* are measures of solute-solvent and solute-solute interactions respectively, a perusal of Table VII.9 shows that the ϕ_K^0 values are in good agreement with those drawn from the values of ϕ_V^0 discussed earlier.

Acoustic relaxation time (τ) [38] is obtained using the relation:

$$\tau = \left(\frac{4\eta}{3\rho u^2} \right) \quad (18)$$

Relaxation time is the time taken for the excitation energy to appear as translational energy. The increase in acoustic relaxation time with concentration of solute suggests interactions among the components of solution. In the present case from Table VII.9 relaxation time increases with increase in concentration of IL. The increase of relaxation time indicates the presence of molecular interaction in the mixture and the order is FA > DMA > DMF.

The schematic representation of ion-solvation, for the particular ion in the studied solvents, in view of various derived parameters is depicted in Scheme VII.2.

VII.3.6. FT-IR calculation

With the help of FT-IR spectroscopy the molecular interactions existing between the solute and the solvents have been studied. At first the IR spectra of the pure solvents were studied. The stretching frequencies of the key groups are given in Table VII.10.

The FT-IR spectra of the ionic liquid in FA show that the peak for C=O at 1755cm^{-1} shifts to 1785.2 cm^{-1} for [BMP][Br] respectively due to the disruption of strong H-bonding [40] interaction in FA molecules leading to the formation of ion-dipole interaction between [BMP]⁺ and C=O dipole.

Similar types of interactions are observed in case of DMA where the sharp peak for C=O shifts from 1672 cm^{-1} to 1695.4 cm^{-1} . In this case the shifting is due to ion-dipole interaction between [BMP]⁺ and C=O dipole.

In case of DMF a sharp peak is obtained at 1654 cm^{-1} for C=O which shifts to 1675 cm^{-1} , on addition of the electrolyte [BMP][Br], due to the interaction of [BMP]⁺ with the C=O dipole showing ion-dipole interaction which is obviously responsible the disruption of H-bonding interaction in DMF molecules [41].

VII.4. CONCLUSION

The extensive conductometric study of [BMP][Br] in FA, DMA, and DMF leads the conclusion that the electrolyte more associated in FA than in the other two solvents. The reliable value of volumetric, viscometric and interferometric studies also intends to map the physicochemical behaviour in solution and suggests that in solution there is more ion-solvent interaction than ion-ion interaction. The molar refraction values also support the above fact that the highest ion-solvent interaction is seen in case of FA solvent. In all the solvents the electrolyte forms ion-dipole interactions as evident from the FT- IR studies.

TABLES**Table VII.1:** Density (ρ), viscosity (η), refractive index (n_D), ultrasonic speed (u) and relative permittivity (ϵ) of the different solvents FA, DMA and DMF.

Solvents	$\rho \cdot 10^{-3}/\text{kg m}^{-3}$	$\eta/\text{mPa s}$	n_D	u/ms^{-1}	E
FA	1.12110[39]	3.23[39]	1.4459[39]	1582.96[40]	110.21[42]
DMA	0.93660[41]	1.95[41]	1.4375[43]	1463.00[41]	38.60[42]
DMF	0.94430[41]	0.92[41]	1.4305[43]	1465.00[41]	36.71[42]

Table VII.2: Concentration (c) and molar conductance (Λ) of [BMP][Br] in Formamide, DMA and DMF at 298.15 K.

$c \cdot 10^4/\text{mol} \cdot \text{dm}^{-3}$	$\Lambda \cdot 10^4/\text{S} \cdot \text{m}^2 \cdot \text{mol}^{-1}$	$c \cdot 10^4/\text{mol} \cdot \text{dm}^{-3}$	$\Lambda \cdot 10^4/\text{S} \cdot \text{m}^2 \cdot \text{mol}^{-1}$	$c \cdot 10^4/\text{mol} \cdot \text{dm}^{-3}$	$\Lambda \cdot 10^4/\text{S} \cdot \text{m}^2 \cdot \text{mol}^{-1}$
[BMP][Br]					
Formamide		DMA		DMF	
0.6889	14.80	0.7056	40.70	0.7569	48.80
1.5625	14.40	1.8769	39.55	1.7956	47.70
2.6896	14.01	3.8809	38.50	3.0276	46.90
4.4521	13.67	6.1504	38.00	4.7524	45.80
5.8564	13.13	8.5849	37.00	7.1824	44.70
7.7284	12.92	12.0409	35.80	10.5625	43.60
9.4249	12.66	16.1604	34.80	14.2129	42.50
11.9025	12.33	19.0969	34.20	17.4724	41.50
14.8225	12.11	22.2784	33.10	20.4304	41.20
18.7489	11.95	25.2004	32.70	24.1081	40.40
21.6225	11.62	28.1961	32.04	28.6225	39.30
24.6016	11.31	30.8025	31.95	32.9476	38.70

29.0521	10.80	34.4569	31.05	37.0881	38.20
35.4025	10.40	40.0689	30.00	41.9904	37.60
42.7716	10.00	44.3556	29.30	45.6976	37.40

Table VII.3: Limiting molar conductance (Λ_0), association constant (K_A), co-sphere diameter (R) and standard deviations of experimental Λ (δ) obtained from Fuoss conductance equation for [BMP][Br] in Formamide, DMA and DMF at 298.15 K.

Solvent	$\Lambda_0 \cdot 10^4 / \text{S} \cdot \text{m}^2 \cdot \text{mol}^{-1}$	$K_A / \text{dm}^3 \cdot \text{mol}^{-1}$	$R / \text{\AA}$	δ
[BMP][Br]				
Formamide	14.66	169.83	22.57	0.18
DMA	40.94	138.64	43.51	0.20
DMF	48.56	109.08	37.27	0.45

Table VII.4: Walden product ($\Lambda_0 \cdot \eta$) and Gibb's energy change (ΔG°) of [BMP][Br] in Formamide, DMA and DMF at 298.15 K.

Solvents	$\Lambda_0 \cdot \eta \cdot 10^4 / \text{S} \cdot \text{m}^2 \cdot \text{mol}^{-1} \cdot \text{mPa}$	$10^3 \Delta G^\circ / \text{kJ} \cdot \text{mol}^{-1}$
[BMP][Br]		
Formamide	47.35	-12.73
DMA	80.08	-12.26
DMF	44.68	-11.63

Table VII.5: Limiting Ionic Conductance ($\lambda_{\sigma^{\pm}}$), Ionic Walden Product ($\lambda_{\sigma^{\pm}}\eta$), Stokes' Radii (r_s), and Crystallographic Radii (r_c) of [BMP][Br] in Formamide, DMA and DMF at 298.15 K.

Solvent	ion	$\lambda_{\sigma^{\pm}}$ (S·m ² ·mol ⁻¹)	$\lambda_{\sigma^{\pm}}\eta$ (S·m ² ·mol ⁻¹ mPa)	r_s (Å)	r_c (Å)
Formamide	[BMP] ⁺	3.06	9.87	8.30	5.05
	Br ⁻	11.60	37.48	2.19	1.33
DMA	[BMP] ⁺	8.53	16.73	4.90	5.05
	Br ⁻	32.41	63.51	1.29	1.33
DMF	[BMP] ⁺	10.12	9.31	8.80	5.05
	Br ⁻	38.44	35.36	2.32	1.33

Table VII.6: Concentration (c), density (ρ), apparent molar volume (ϕ_v), limiting apparent molar volume (ϕ_v^0) and experimental slope (S_v^*) for [BMP][Br] in Formamide, DMA and DMF at 298.15K and Experimental Pressure 0.1MPa.

Solvents	$c/$ mol·dm ⁻³	$\rho \cdot 10^{-3}/$ kg m ⁻³	$\phi_v \cdot 10^6/$ m ³ ·mol ⁻¹	$\phi_v^0 \cdot 10^6/$ m ³ ·mol ⁻¹	$S_v^* \cdot 10^6/$ m ³ · mol ^{-3/2} ·dm ^{3/2}
[BMP][Br]					
Formamide	0.005	1.13305	170.0	207.3	-541.0
	0.020	1.14312	130.0		
	0.035	1.15207	105.5		
	0.050	1.16055	86.4		
	0.065	1.16928	68.0		
	0.080	1.17679	56.0		
DMA	0.005	0.94410	114.0	139.2	-341.3
	0.020	0.95192	97.0		
	0.035	0.96035	81.4		

	0.050	0.96904	67.0		
	0.065	0.97950	52.0		
	0.080	0.98715	42		
DMF	0.005	0.95849	69.9	83.2	-193.4
	0.020	0.96695	60.0		
	0.035	0.97400	52.6		
	0.050	0.98228	45.2		
	0.065	0.99158	37.0		
	0.080	1.00223	28.8		

Table VII.7: Concentration (c) viscosity (η), $\frac{(\eta_r - 1)}{\sqrt{c}}$, viscosity A and B coefficients for [BMP][Br] in Formamide, DMA and DMF at 298.15K and Experimental Pressure 0.1MPa.

Solvents	c /mol·dm ⁻³	η /mPa·s	$\frac{(\eta_r - 1)}{\sqrt{c}}$	B /dm ³ ·mol ⁻¹	A /dm ^{3/2} ·mol ^{-1/2}
[BMP][Br]					
Formamide	0.005	3.24	0.026	0.304	0.0038
	0.020	3.25	0.047		
	0.035	3.26	0.061		
	0.050	3.28	0.072		
	0.065	3.29	0.080		
	0.080	3.31	0.088		
DMA	0.005	1.95	0.020	0.226	0.0042
	0.020	1.96	0.037		
	0.035	1.97	0.047		
	0.050	1.98	0.055		
	0.065	1.98	0.062		
	0.080	1.99	0.068		

DMF	0.005	0.94	0.016	0.161	0.0045
	0.020	0.94	0.027		
	0.035	0.95	0.034		
	0.050	0.95	0.041		
	0.065	0.96	0.046		
	0.080	0.96	0.050		

Table VII.8: Refractive indices (n_D) and molar refractions (R_M) of [BMP][Br] in Formamide, DMA and DMF at Temperature ($^n T$) 298.15K and Experimental Pressure 0.1MPa.

Solvents	n_D	$R_M/m^3 \cdot mol^{-1}$
	[BMP][Br]	
Formamide	1.5389	61.616
	1.5399	61.625
	1.5412	61.632
	1.5471	61.637
	1.5499	61.641
	1.5501	61.645
DMA	1.4376	61.269
	1.4377	61.289
	1.4379	61.295
	1.4381	61.314
	1.4383	61.327
	1.4383	61.333
DMF	1.4310	60.943
	1.4314	60.960
	1.4315	60.969
	1.4315	60.975
	1.4317	60.991
	1.4318	61.010

Table VII.9: Limiting partial adiabatic compressibility (ϕ_k^0) and experimental slope (S_k^*) of [BMP][Br] in Formamide, DMA and DMF at Temperature ($^n T$) 298.15K and Experimental Pressure 0.1MPa.

Solvents	$\phi_k^0 \times 10^{10}$	$S_k^* \times 10^4$	$\tau \times 10^{-6}$
	($\text{m}^3 \text{mol}^{-1} \text{Pa}^{-1}$)	($\text{m}^3 \text{mol}^{-3/2} \text{Pa}^{-1} \text{kg}^{1/2}$)	(Sec)
	[BMP][Br]		
Formamide	0.11	-0.98	12.17
DMA	0.01	-0.76	5.21
DMF	-0.08	-0.56	2.50

Table VII.10: Stretching frequencies of the functional groups present in the pure solvent and change of frequency after addition of 0.05(M) concentration of [BMP][Br] in Formamide, DMA and DMF.

Solvents	Stretching frequencies(cm^{-1})	
	Pure Solvent	Solvent + [BMP] Br
Formamide	C=O (1755)	C=O (1785.2)
DMA	C=O (1672)	C=O (1695.4)
DMF	C=O (1654)	C=O (1675.0)

FIGURES

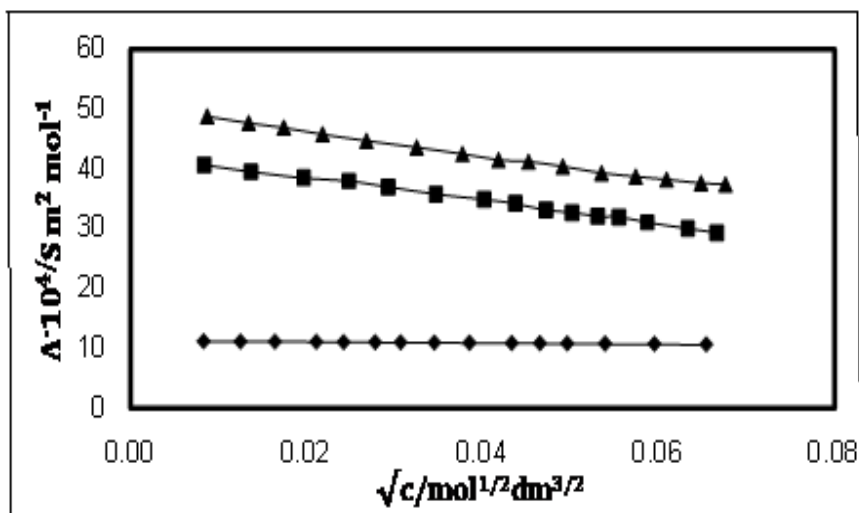


Figure VII.1: Plot of \sqrt{c} versus molar conductance (Λ) for [BMP][Br] in Formamide (—◆—), DMA (—■—) and DMF (—▲—) at 298.15 K.

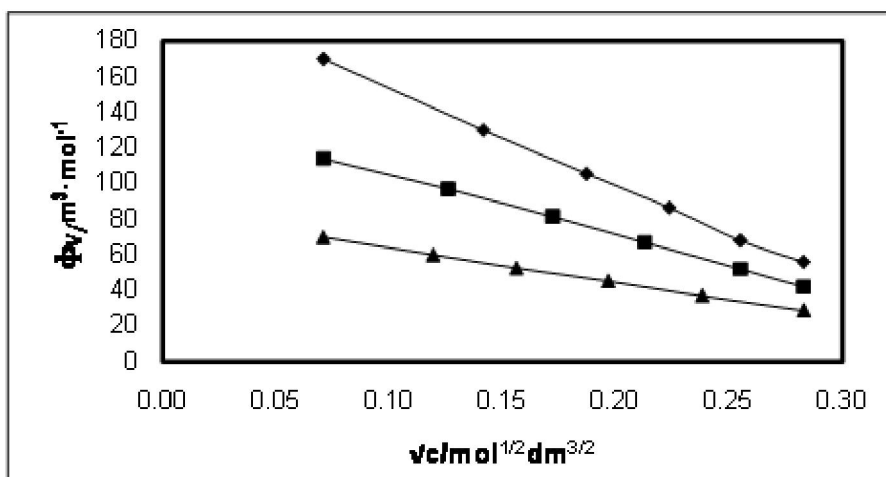


Figure VII.2: Plot of \sqrt{c} versus Limiting apparent molar volume (ϕ_v^0) for [BMP][Br] in Formamide (—◆—), DMA (—■—) and DMF (—▲—) at 298.15 K.

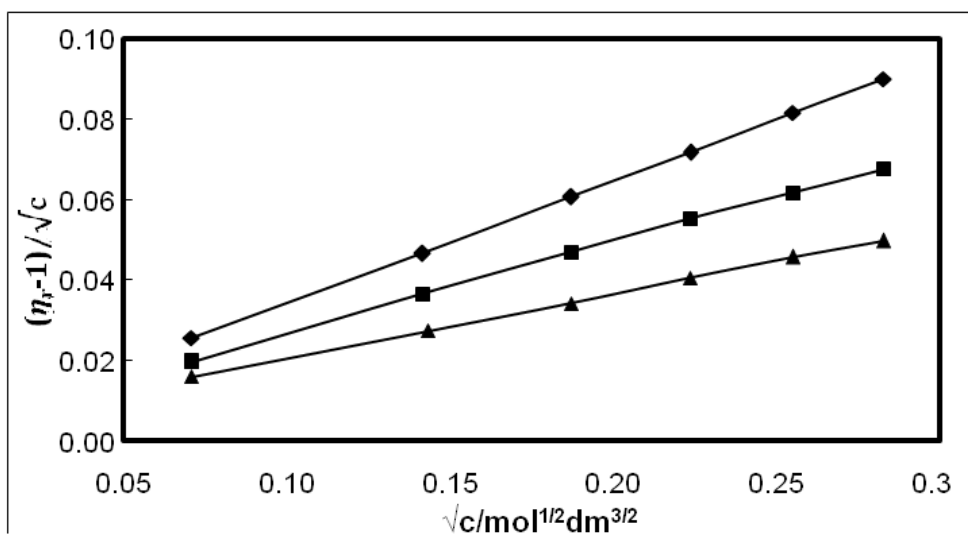


Figure VII.3: Plot of \sqrt{c} vs $\frac{(\eta_r - 1)}{\sqrt{c}}$ for [BMP][Br] in Formamide (\blacklozenge), DMA (\blacksquare) and DMF (\blacktriangle) at 298.15 K.

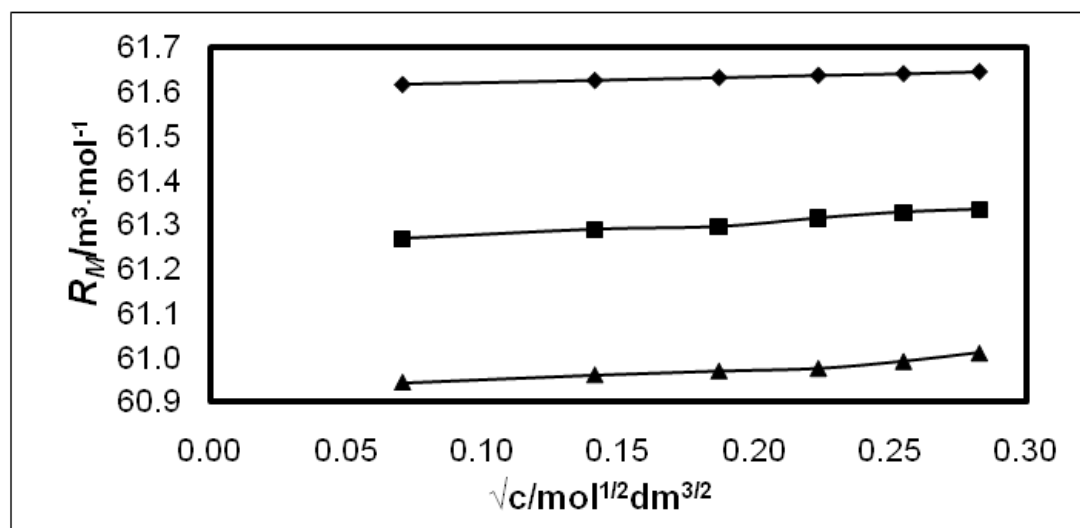
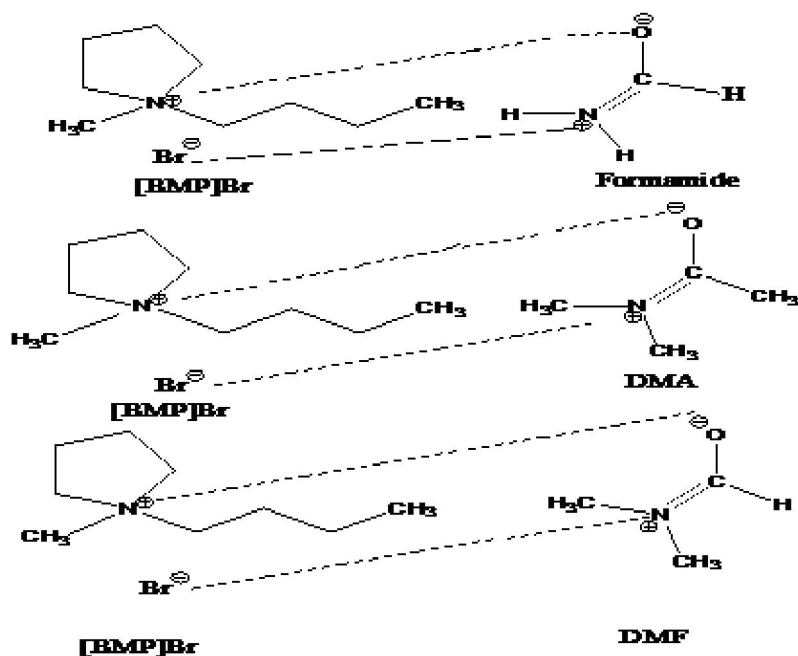
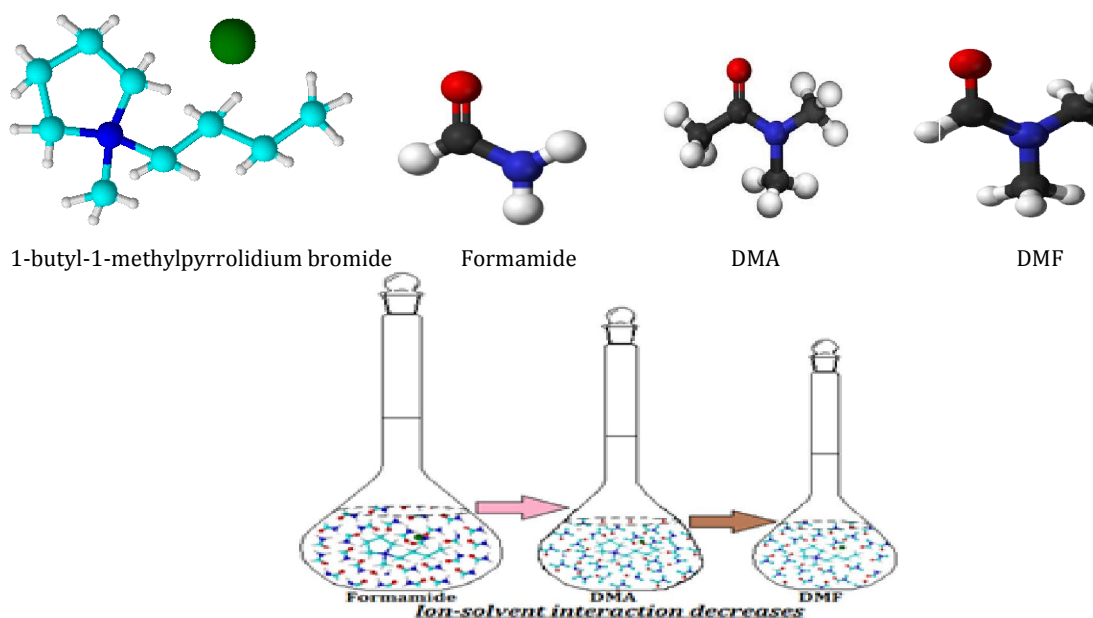


Figure VII.4: Plot of \sqrt{c} versus R_M for [BMP][Br] in Formamide (\blacklozenge), DMA (\blacksquare) and DMF (\blacktriangle) at 298.15 K.

SCHEMES



Scheme VII.1. Phase of interaction between [BMP]Br and Formamide, DMA and DMF respectively.



Scheme VII.2. Trend of Ion-solvent interaction between [BMP]Br and Formamide, DMA and DMF respectively.

CHAPTER-VIII

Inclusion complexation of tetrabutylammonium iodide by cyclodextrins

VIII.1. INTRODUCTION

In modern field of chemistry and biochemistry, cyclodextrins (CDs) are focused with immense interests due to the unique property of controlled release through the innovation of vast inclusion complex (IC) with guest molecules having hydrophobic cavity [1]. In diverse industries including pharmaceutical, food, textile, pesticides, cosmetics sectors Cyclodextrins have enormous applications [2]. CDs are cyclic oligomer of α -D-glucose having diverse numeral of glucopyranose units (6 in α -CD, 7 in β -CD and 8 in γ -CD) hop by α -(1-4) linkages [3]. CDs are truncated cone shaped with a quite rigid and distinct hydrophobic cavity of varying diameter and two separate rims, all secondary hydroxyl groups containing a wider rim and all the primary hydroxyl groups containing a narrow rim [3]. Hence CD is very proficient in forming stable supramolecular host-guest inclusion complex with variety of molecules for having a hollow-cylindrical shaped fragment [4]. Due to having the special structure and prospective application in the discovery of molecular switches, molecular machines and supramolecular polymers macrocyclic CD molecule always depict the concentration in this field of chemistry [5]. In some case due to micro-encapsulation of guest by CD various changes in physical and chemical properties occur such as very volatile substance fixation, masking the colour, smell and taste of substance etc. [6] In case of drug delivery devices and nano-sensors the molecular recognition of the host for functioning as nano-sensors is owing to conjugation of CD with a variety of nanoparticles [7].

Tetrabutylammonium Iodide (but_4NI) is mainly quaternary ammonium compounds of a group of ammonium salts in which all the four hydrogen atoms are substituted by four organic radicals (in this compound butyl group) which may be alkyl, aryl and aralkyl. but_4NI is a water soluble strong electrolyte which exhibits a assortment of physical, chemical and biological properties. The ionic solid has immense appliances in various fields such as in chemical reactions it acts as surface-active agents (due to the hydrophobic communications between the butyl groups and water molecules), solvents, Intermediates emulsifying means, pigment disperse and phase transfer catalyst [8,9]. Since but_4NI has the tendency of locating at the interface of two phases (liquid-liquid or solid-liquid) for introducing the continuity between two different phases, so it positively is said as phase transfer catalyst. Due to low cost and low toxicity of but_4NI in recent times it has appeared as a promising substitute as a catalyst for functionalization of C-H bonds [10,11]. In industrial usage but_4NI acts as active ingredient for conditioners, antistatic agent, detergent sanitizers, softener for textiles and paper products etc. In medicinal field it uses as antimicrobials, algacide, slimicidal agents, disinfection agents and sanitizers etc.

In this article the studied ionic solid, viz., tetrabutyl ammonium iodide (scheme VIII.1) is currently of interest in assorted industrial and medicinal aspects. Here we explored the creation of host-guest inclusion complexes (ICs) of the ionic solid with α and β -CD particularly towards their formation, stabilization, carrying and controlled release without chemical amendment by diverse reliable methods such as ^1H NMR, FT-IR, surface tension, conductivity, density, viscosity and refractive index measurements.

VIII.2. EXPERIMENTAL

VIII.2.1. Source and purity of samples

The preferred ionic solid and cyclodextrins of puriss grade were bought from Sigma-Aldrich, Germany and used as purchased. The mass fraction purity of but_4NI , α -cyclodextrin and β -cyclodextrin were ≥ 0.99 , 0.98 and 0.98 respectively.

VIII.2.2. Apparatus and Procedure

Each stock solutions of Ionic solid, α -CD and β -CD were prepared by mass (Mettler Toledo AG-285 with uncertainty 0.0001 g) and by mass dilution at 298.15 K the working solutions were obtained. To change molarity of the solutions to the molality of the solutions the density of the solutions was used [34].

Using Bruker ADVANCE 400 MHz instrument at 298.15K the NMR spectra were recorded in D2O at 400 MHz. Signals are cited as δ values in ppm using residual protonated solvent signals as internal standard (D2O : δ 4.79 ppm). As chemical shift all the Data are reported.

With the help of platinum ring detachment technique by a Tensiometer (K9, KRÜSS; Germany) surface tensions (Accuracy ± 0.1 mN·m⁻¹) of the solutions were measured at 298.15 K. Temperature of the system was maintained by circulating thermostated water through a double-wall glass vessel holding the solution.

Conductivities of the solutions were studied by Mettler Toledo Seven Multi conductivity meter having uncertainty 1.0 μ S·m⁻¹. The study was carried out in a thermostated water bath at 298.15K with uncertainty ± 0.01 K. HPLC grade water was used with specific conductance 6.0 μ S m⁻¹. The conductivity cell was calibrated using 0.01M aqueous KCl solution.

The densities (ρ) of the solutions were studied by vibrating U-tube Anton Paar digital density meter (DMA 4500M) having precision ± 0.00005 g cm⁻³ and uncertainty in temperature was ± 0.01 K. The density meter was calibrated by standard method [30].

Viscosities (η) were determined by Brookfield DV-III Ultra Programmable Rheometer with spindle size 42. The detail has already been represented in our ealier attempt [16].

Refractive indexes of the solutions were studied with a Digital Refractometer from Mettler Toledo having uncertainty ± 0.0002 units. The detail has already been described earlier [16].

To prepare both the solid inclusion complexes ([but₄NI] + α -CD and [but₄NI] + β -CD) 1:1 molar ratio of the ionic solid and cyclodextrin were taken. In both the cases 1.0 mmol cyclodextrin was dissolved in 20 mL water and 1.0 mmol ionic solid was

dissolved in 20 mL ethanol and stirred separately for 3 hrs. Then the ethanol solution of the ionic solid was added drop by drop to the aqueous CD solution. The mixture was then allowed to stir for 48 hrs at 50–55°C. It was filtered at this temperature, then cooled to 5°C and kept for 12 hrs. The resulting suspension was filtered and the white polycrystalline powder was found, which was washed with ethanol and dried in air.

Fourier transform infrared (FT-IR) spectra were recorded on a Perkin Elmer FT-IR spectrometer according to the KBr disk technique. Samples were prepared as KBr disks with 1 mg complex and 100 mg KBr. The FTIR spectroscopy measurements were performed in the scanning range of 4000–400 cm^{-1} at room temperature.

VIII.3. RESULTS AND DISCUSSION

VIII. 3.1. ^1H NMR study establishes inclusion

The inclusion phenomena of the guest ionic solid inside the host CD molecule are ascertained by the most imperative device NMR study. In this work we have studied the interactions of an ionic solid (but_4NI) with α and β -CD by ^1H NMR study taking 1:1 molar ratio of ionic solid and CD in D_2O at 298.15K (Figure VIII1). Table S1 shows the ^1H NMR data of the ionic solid, two CDs and two ICs. Due to the incorporation of guest ionic solid into the hydrophobic cavity of CD the protons of the CD molecule show considerable chemical shift [12]. In the structure of CD, the H1, H2 and H4 protons are found at the periphery of CD molecule while the H3 and H5 are located within the cavity, more specifically the location of H3 and H5 protons are near the wider rim and narrower rim respectively [13,14]. The H3 and H5 protons of CD show upfield chemical shift as a result of interaction with the guest during the insertion of guest ionic solid molecule inside the cavity of CD. It confirms the formation of host-guest inclusion complexes. The H3 protons located near the wider rim show higher shift than the H5 protons which are present near the narrower rim at the interior of CD due to insertion of guest ionic solid molecule inside the cavity of host CD through the wider rim (scheme S1). Due to the exterior protons upfield chemical shift is also observed but to trivial extent. The interacting protons of the studied ionic solid also show upfield chemical

shift. The shifts of four protons present in each butyl groups give four shifts which exemplifies the insertion mechanism. Moreover, the extent of shift of butyl protons are more in β -CD comparison to that in α -CD, signifying binding affinity of the former is higher compared to the latter.

VIII. 3.2. Surface tension study supports inclusion

Surface tension (γ) is an important consideration which furthermore recommends the inclusion complex formation of the considered ionic solid with both α and β -CD [15]. There shows no any considerable change to the surface tension of water when CD is added to pure water. This phenomenon indicates that both α and β -CD are almost surface inactive compounds [16]. In our present work the γ values of aqueous ionic solid have been determined with addition of α and β -CD at 298.15K (Table S4-S5). With increasing concentration of CDs the γ values substantially increase for this ionic solid but₄Ni. This is due to the removal of surface active ionic solid molecules from surface of the solution, i.e., α and β -CD form the host guest inclusion complexes after entering the hydrophobic tail of ionic solid into the hydrophobic cavity of α and β -CD [17,18] Figure VIII.2 and Table VIII.1 show the formation of 1:1 inclusion complex of ionic solid and CDs, since both the curves show a single break point and after that point the γ value becomes approximately steady. Inclusion complex formation with complex stoichiometry such as 1:2, 2:1, 2:2 etc occur if the surface tension curve shows more break points (scheme S2) [19,20]. Table VIII.1 shows the values of γ and corresponding concentration of CDs and ILs at each break. The breaks have been originated in certain concentration of ILs and CDs where their concentration ratio in the solution was almost 1:1. Hence this study proves the formation of 1:1 inclusion complex. In this case the γ value at the break point is higher for β -CD than that of α -CD which suggests that the former is superior to encapsulate the guests than the afterward.

VIII. 3.3. Conductivity study notifies inclusion

Conductivity (κ) study validates the construction of host-guest inclusion complex vp along with it also provides the stoichiometry of the assembly [21,22]. We have

measured the conductivity of the aqueous solution of the studied ionic solid having 10mmolL^{-1} concentration with successive addition of α and β -CD at 298.15K (table S4-S5). It has been found that the conductivity of the ionic solid decreases on a usual basis with escalating concentration of CDs (Figure VIII.3). Since the guest ionic solid molecules are inserted inside the cavity of the CD molecule, the number of free ions per unit volume reduces. Consequently the conductivity of the solution decreases. This surveillance is in concurrence with the development of inclusion complex. Perusal of Figure VIII.3 and Table VIII.2 show analogous result with surface tension study, each having a perceptible break, signifying the formation of Ionic salt-CD inclusion complex having stoichiometry 1:1. Table VIII.2 shows the values of κ and corresponding concentration of the ionic salt and CDs at each break point.

VIII. 3.4. Density study: interaction between host and guest

In our current study several expensive informations about the inclusion phenomenon between the ionic solid and CD molecules have been obtained applying density measurement. Apparent molar volume (ϕ_v) and limiting apparent molar volume (ϕ_v^0) are the two major parameters used for this intention. Apparent molar volume (ϕ_v) mainly describes the summation of the geometric volume of the central solute molecule and changes in the solvent volume as a result of interface with the solute around the co-sphere (here, solute = but_4NI and co-solvent = CD) [23]. For this system (ternary phase of Ionic solid + aqueous CD system) solute-solvent interaction is conveyed by limiting apparent molar volume. For this study ϕ_v have been calculated from the density of solution systems by means of equation (5) as revealed in SI at 298.15 K (Table S6). Least square method is employed to the plots of ϕ_v versus \sqrt{m} using the Masson equation (SI, equation 6, Table S7) for obtaining ϕ_v^0 value [24]. It is found that ϕ_v values repeatedly reduce and ϕ_v^0 values continually enhance for this studied ionic salt with increasing concentration of both the CDs. It is manifest from this fact that for but_4NI , in both the cases of α and β -CD the ion-hydrophilic group interactions are more efficient than ion-hydrophobic group interactions. The inspection of figure VIII.4 illustrates that the values of ϕ_v^0 increases with increasing mass fractions of both CDs and also found

grater for β -CD than α -CD, signifying the earlier interacts more with the ionic solid than the later. This may be explained as in case of but_4NI , two hydrophobic butyl group can be encapsulated into the cavity of CD and the single positively charged N atom show higher ion-hydrophilic interaction with the $-\text{OH}$ groups of CD. The larger diameter of β -CD helps in making more compact inclusion complex with the Ionic solid than α -CD with relatively smaller cavity size showing less hydrophobic interactions with this Ionic solid.

VIII. 3.5. Viscosity study: order of interactions

Viscosity study is also fruitful for the interpretation of interface between ILs and CDs [25]. In the present ternary system (but_4NI + aqueous CD), (table S3) the viscosity of the solutions show an escalating trend with increasing concentrations of the Ionic solid. The size and shape of the solute molecule recommend the solute-solvent interactions (here, solute = but_4NI and co-solvent = CD) which is designated as viscosity B -coefficients (table S7) [26]. All the viscosity B -coefficient values are found to be positive and depicted in figure VIII.5. Perhaps due to higher solvation and also greater Ionic solid-CD interaction the viscosity B values increase with increasing concentration of CDs [17]. Since the viscosity B values is again larger for β -CD than that of α -CD for the Ionic solid it suggest that inclusion is more constructive in case of former than the latter. The structural feature of the Ionic solid and CDs as explained earlier for which these trends of interactions have been acquired due to the relative consequence of viscosity B -coefficient of the Ionic solid and CDs has been found analogous as for the density study.

VIII. 3.6. Refractive index shows the compactness of the inclusion complexes

To establish the molecular interaction in the above mentioned ternary solution systems refractive index is one more important parameter to ascertain the molecular interaction [15]. Using the suitable equation (Table S3 and S6) refractive index (n_D) and molar refraction (R_M) values of the solutions have been estimated. The compactness

and density of the medium is determined by the greater values of R_M and the limiting molar refraction (R_M^0) (Table S7) [16,17]. In case of Ionic solid in both α and β -CD the R_M^0 values show an increasing trend with increasing concentrations of both CDs, which suggest that the IC of but₄NI with both the CDs are more closely packed perhaps due to greater hydrophobic as well as ion-hydrophilic interactions between the guest and host as described earlier. The R_M^0 values designate that β -CD is more competent than α -CD in case of formation of the ICs (Figure VIII.6). The earlier density and viscosity studies are in concurrence with the observations obtained from refractive index data.

VIII. 3.7. FT-IR Spectra of solid inclusion complexes

The inclusion phenomena in the solid inclusion complex are nicely proved by FT-IR spectrum [27-29]. Table S8 refers the characteristic IR frequencies of α -CD, β -CD, but₄NI and solid ICs. Characteristic broad peaks of -OH at about 3412.10 cm^{-1} and 3349.84 cm^{-1} are here in the spectrum for α and β -CD respectively. The characteristic FT-IR Spectra of but₄NI is showed due to the presence of peaks for -N-C-H-, -C-H (stretching), -C-H (bending for -CH₃ group), -C-H (bending for -CH₂ group) etc. bonds (Figure VIII.8 and Table S8). Yet, there are either absent or shifted several peaks of the Ionic solid due to the change in atmosphere of the guest after inclusion in the CD cavities. The -C-H bending bands for -CH₃ and -CH₂ of both the Ionic solid are shifted in the spectrum of the inclusion complex. The -O-H stretching of α -CD is shifted to lower frequency in the spectrum of the IC probably due to involvement of the -O-H groups of the host molecules in hydrogen bonding with the guest molecule. On the other hand the -O-H stretching of β -CD is shifted to higher frequency in the spectrum of the IC probably due to involvement of the -O-H groups of the host molecules in hydrogen bonding with the guest molecule. In the spectrum of the ICs the peak for the C-N group of the guest molecules are present. It is an indication of the fact that the hydrophobic side chains present on one side of the polar N atom of the guest molecules are encapsulated in the hydrophobic cavity of both the CDs.

VIII. 3.8. Binding constants: non-linear isotherms determined by conductivity method

1:1 host-guest inclusion complex formation of the ionic solid with α and β -CD can be articulated by this equilibrium



The corresponding equilibrium constant, K_f is given by

$$K_f = \frac{[IC]}{[IS][CD]} \times \frac{f(IC)}{f(IS)f(CD)} \quad (2)$$

where $[IC]$, $[IS]$, $[CD]$ and f represent the equilibrium molar concentrations of the inclusion complex, Ionic solid, CDs and the activity coefficients of the species respectively. Using the dilute solution system, the activity coefficient of uncharged macrocycle, $f(C)$, can be reasonably assumed as unity. The employ of Debye-Hückel limiting law, [30] conclude that $f(IS) \sim f(CD)$, so the activity coefficients in Equation (2) are cancelled. The complex formation constant in terms of the molar conductance, Λ , can be expressed as [31]

$$K_f = \frac{[IC]}{[IS][CD]} = \frac{(\Lambda_{IS} - \Lambda_{obs})}{(\Lambda_{obs} - \Lambda_{IC})[CD]} \quad (3)$$

Where

$$[CD] = CD_{ad} - \frac{IS_{ad}(\Lambda_{IS} - \Lambda_{obs})}{(\Lambda_{IS} - \Lambda_{IC})} \quad (4)$$

Here, Λ_{IS} represents molar conductance of the ionic solid before the addition of CD, Λ_{IC} the molar conductance of the inclusion complex, Λ_{obs} the molar conductance of the solution during titration, CD_{ad} the concentration of added cyclodextrin and $[IS]$ concentration of the ionic solid. The complex formation constant, K_f and the molar conductance of the complex, Λ_{IC} , were evaluated by using Equations (3) and (4). Therefore, through the application of a non-linear programme the K_f values (Table VIII.3) for the ICs were assessed from the binding isotherm.

K_f values indicate that the ionic solid has higher binding constant in β -CD than that of in α -CD. This fact may be occurring due to the larger cavity dimension of β -CD than that of in α -CD. So, inclusion complex formation is highly feasible in β -CD than in α -CD.

VIII. 3.9. Structural influence of cyclodextrin in inclusion complex formation

Size of the guest molecules and also on the cavity diameter of host, the formation of host-guest ICs between the Ionic solid and CDs is exclusively dependent. Between the two CDs β -CD has the higher cavity diameter (6.0-6.5Å) than that of α -CD (cavity diameter is 4.7-5.3Å). In view of the compatible size of the taken Ionic solid with β -CD, It is found that β -CD is more apt to form ICs than that of α -CD with the Ionic solid is possibly due to higher surface interaction, escalating the hydrophobic attractions, which is in concurrence with spectroscopic and physicochemical interpretations [1]. In case of ICs formation no covalent bonds are formed or broken; only the hydrophobic alkyl chains of the Ionic solid are encapsulated into the hydrophobic cavity of CD molecules. This is a very important factor in case of IC formation that the hydrophobic cavity of CD is engaged by polar water molecule, but it is unfavourable, so the water molecules are effortlessly replaced by more hydrophobic alkyl tails of Ionic solid. Furthermore due to release of the trapped water molecules in bulk of the solution entropy of the solution system is enhanced and the IC formation procedure becomes spontaneous. Due to the spontaneity of this procedure the system becomes very low energetic and stable. So, the ring strain of CD molecule becomes very low. Due to the difficulty of the trapping of another Ionic solid by CD molecule probably 1:1 host-guest inclusion complex formation occurs. The stability of the IC can be ascribed by structural feature such that the N atom present in the Ionic solid form H-bonds with the -OH groups present at the rim of CD.

IV.4. CONCLUSION

The above revealed various physicochemical studies help us to conclude that the ionic solid form host-guest ICs with both α and β -CD both in solution and solid state. With the help of ^1H NMR study it may be substantiated that inclusion occurs in the apolar cavity of both CD molecules, even as surface tension and conductivity data suggest 1:1 stoichiometry. Volumetric, viscometric and refractometric measurements are also in excellent concord with another study and furthermore suggested the

interactions between ionic solid and CD. The solid state of ICs have been characterised by FT-IR, confirming their creations also in solid state. In this study the inclusion phenomenon of ionic solid has been originated extra ensnared in case of β -CD than α -CD. The binding constants, evaluated using a non-linear programme by the conductivity method also supports the trend of IC formation. As a consequence, the exclusivity of our present research work is diverse appliances in the field of bio-chemistry such as drug delivery tools, recycling extraction agents and nano-sensors and so on.

TABLES:**Table VIII.1:** Values of surface tension (γ) at the break point with corresponding concentrations of cyclodextrins and but₄NI at 298.15 K^a.

Name of the Host	but ₄ NI		$\gamma^a / \text{mN}\cdot\text{m}^{-1}$
	Conc. of Host/mM	Conc of ionic Solid/mM	
α -CD	4.89	5.10	72.67
β -CD	4.77	5.23	73.52

Table VIII.2: Values of conductivity (κ) at the break point with corresponding concentrations of cyclodextrins and but₄NI at 298.15 K^a.

Name of the Host	but ₄ NI		$\kappa^a / \text{mS}\cdot\text{m}^{-1}$
	Conc. of Host/mM	Conc of ionic Solid/mM	
α -CD	5.91	4.09	0.40
β -CD	5.44	4.56	0.47

Table VIII.3: Formation constants of ionic solid-cyclodextrin inclusion complexes.

Cyclodextrin	$\log K_f^b (\text{M}^{-1})$		
	298.15 K ^a	303.15 K ^a	308.15 K ^a
α -CD	3.12	2.95	2.78
β -CD	3.38	3.15	2.99

^aStandard uncertainties in temperature are: $u(T) = \pm 0.01 \text{K}$. ^bMean errors in $K_b = \pm 0.01 \times 10^{-3} \text{M}^{-1}$

FIGURES

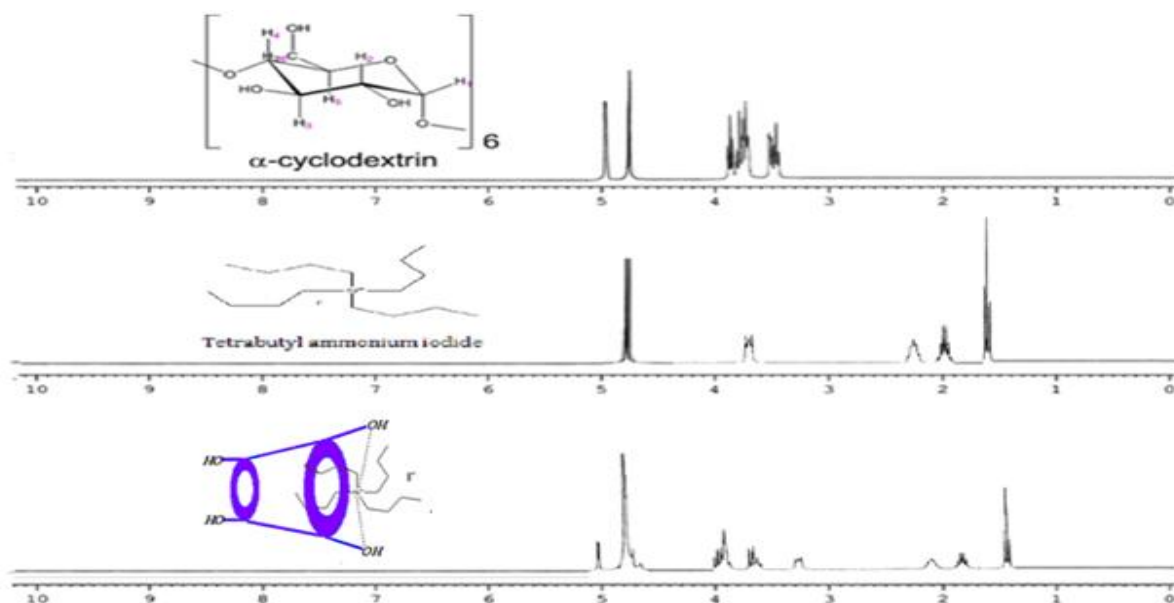


Figure VIII.1(a). ^1H NMR Spectra of α -CD, Tetrabutyl ammonium iodide and 1:1 molar ratio of α -CD + Ionic Solid in D_2O in 298.15 K.

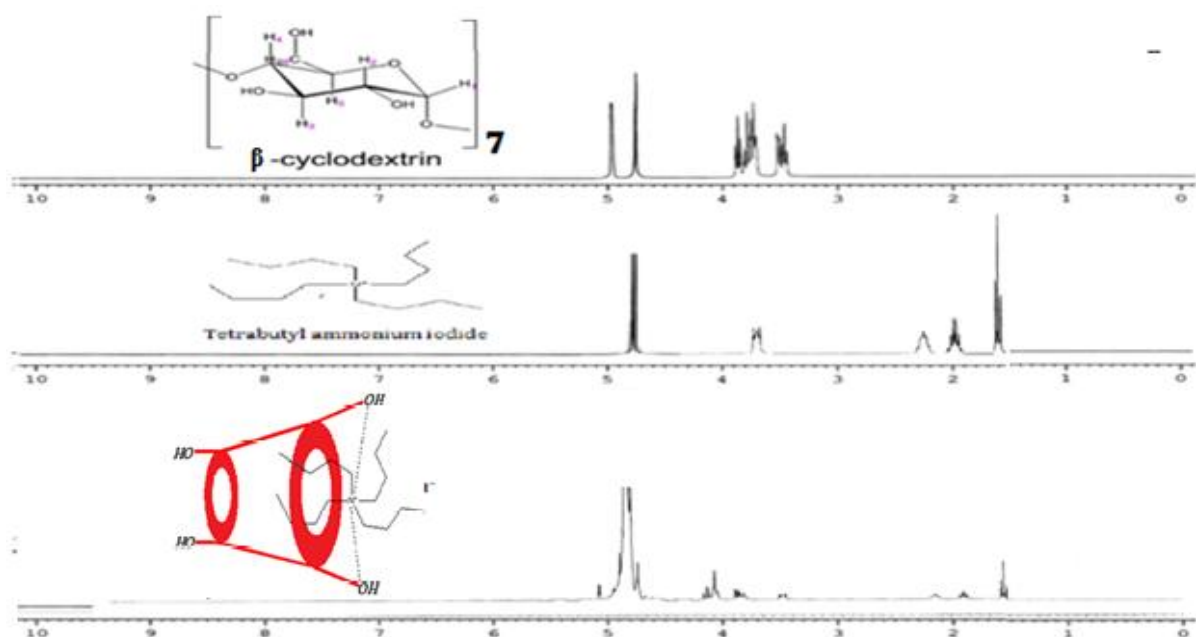


Figure VIII.1(b). ^1H NMR Spectra of β -CD, Tetrabutyl ammonium iodide and 1:1 molar ratio of β -CD + Ionic Solid in D_2O in 298.15 K.

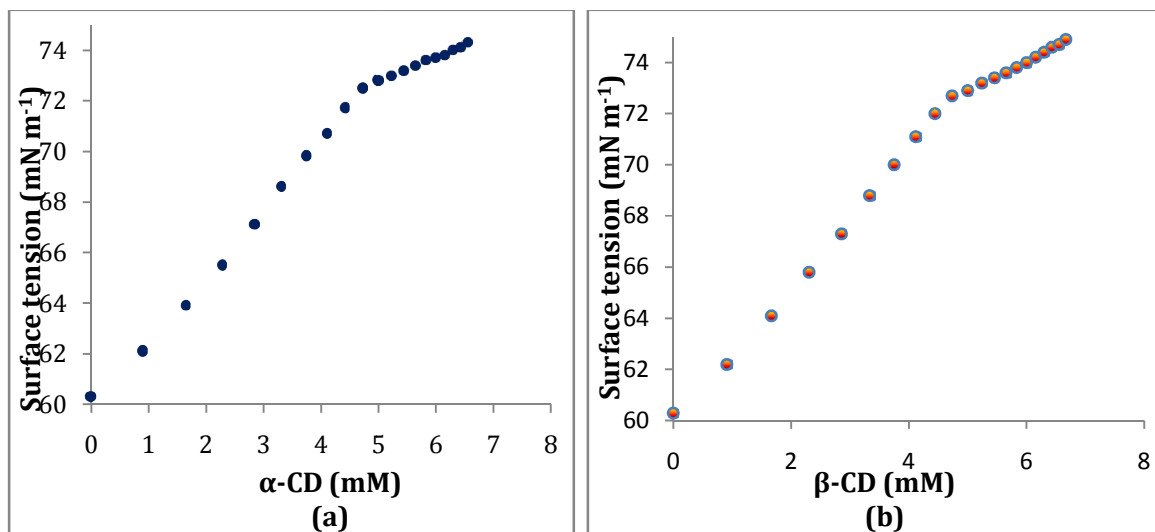


Figure VIII.2. Variation of surface tension of aqueous (a) but₄NI-α-CD and (b) but₄NI-β-CD systems respectively at 298.15 K.

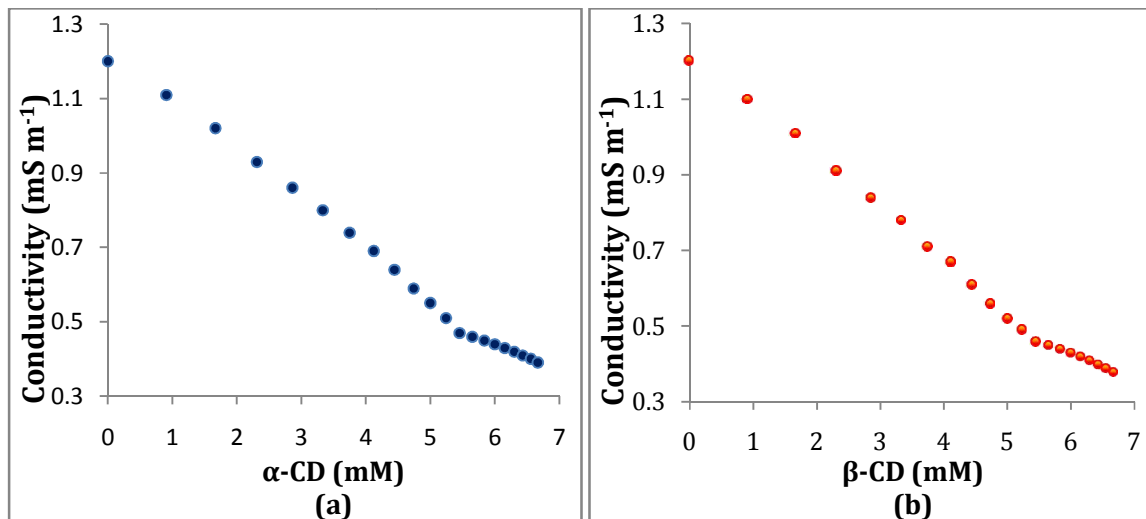


Figure VIII.3. Variation of conductivity of aqueous (a) but₄NI-α-CD and (b) but₄NI-β-CD systems respectively at 298.15 K.

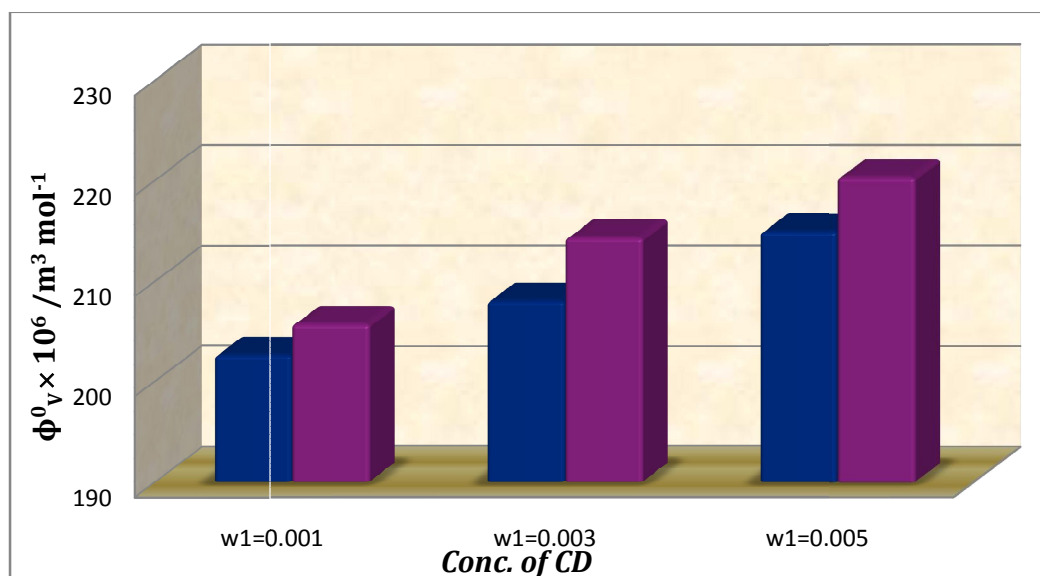


Figure VIII.4. Plot of limiting molar volume (ϕ^0_v) against mass fraction (w) of aqueous α -CD (blue) and aqueous β -CD (purple) for but₄NI at 298.15 K.

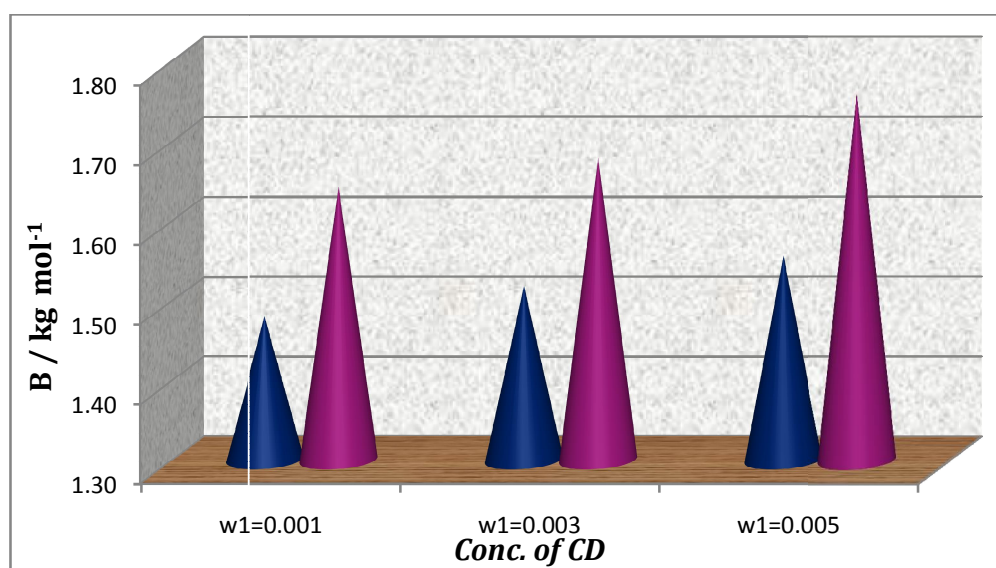


Figure VIII.5. Plot of viscosity B-coefficient against mass fraction (w) of aqueous α -CD (blue) and aqueous β -CD (purple) for but₄NI at 298.15 K.

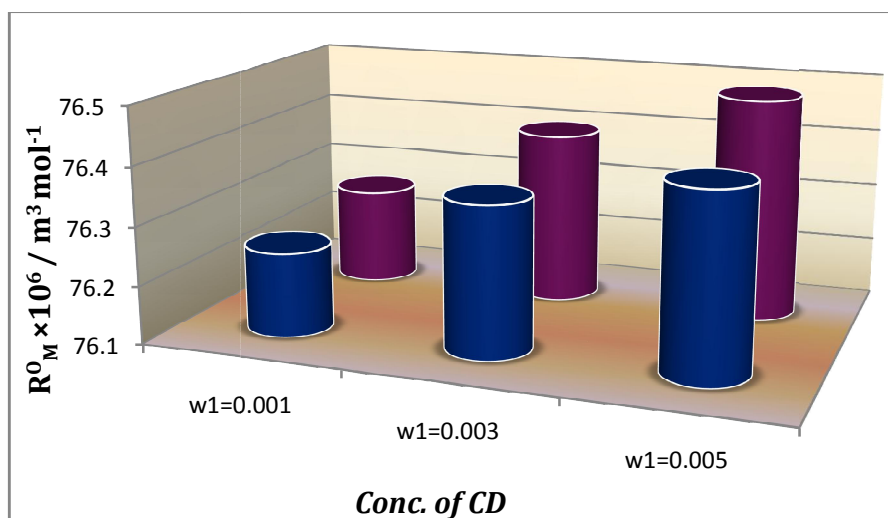


Figure VIII.6. Plot of limiting molar refraction (R_M^0) for but₄NI in different mass fractions (w) of aqueous α -CD (blue) and aqueous β -CD (purple) respectively at 298.15 K.

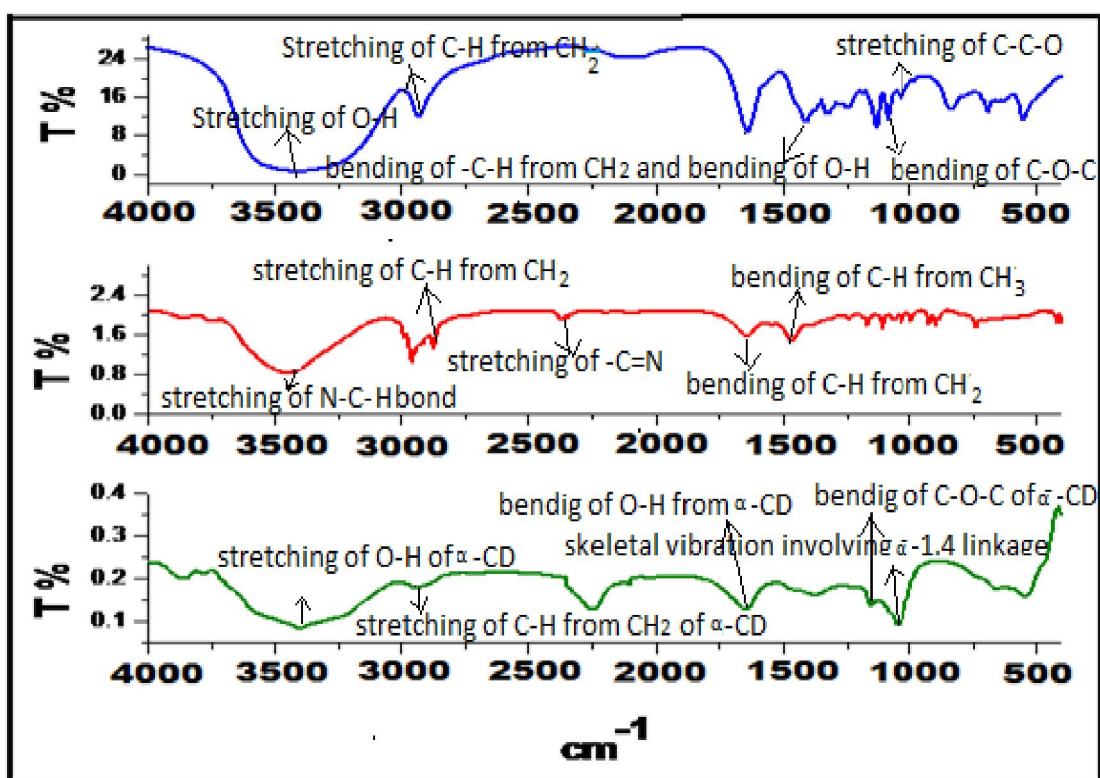


Figure VIII.7(a). FTIR spectra of α -CD (top), but₄NI (middle) and but₄NI- α -CD inclusion complex (bottom).

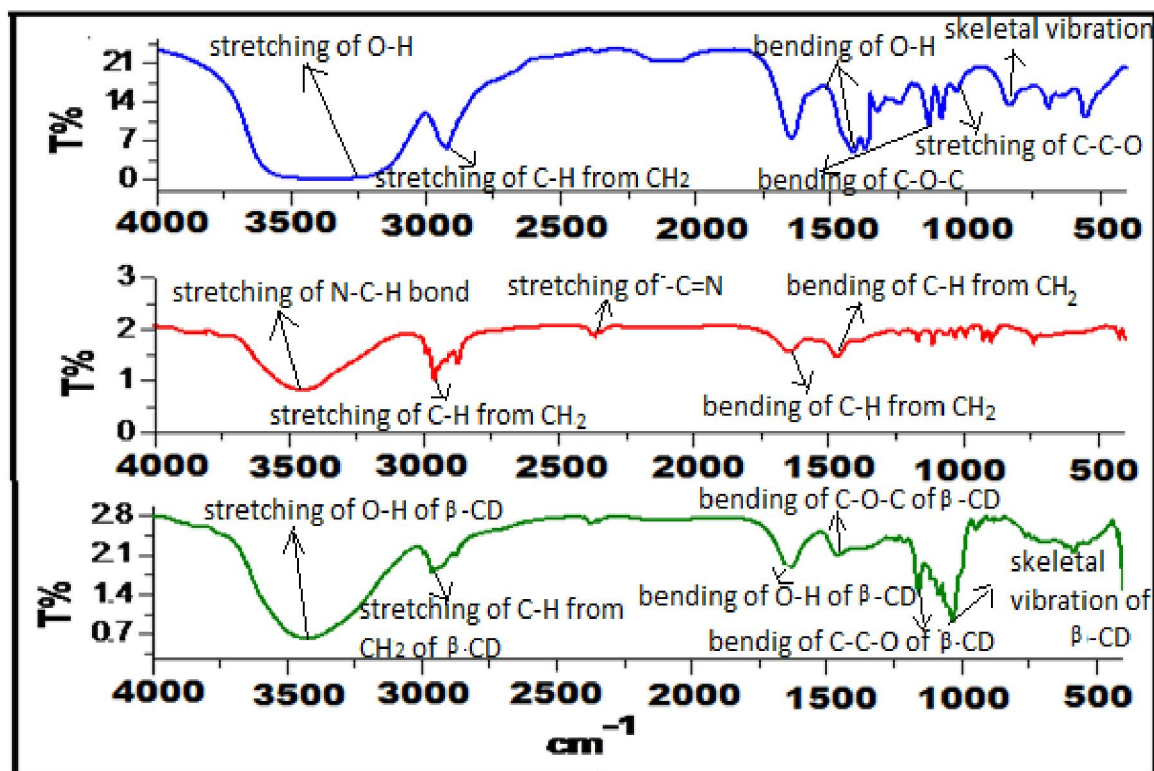
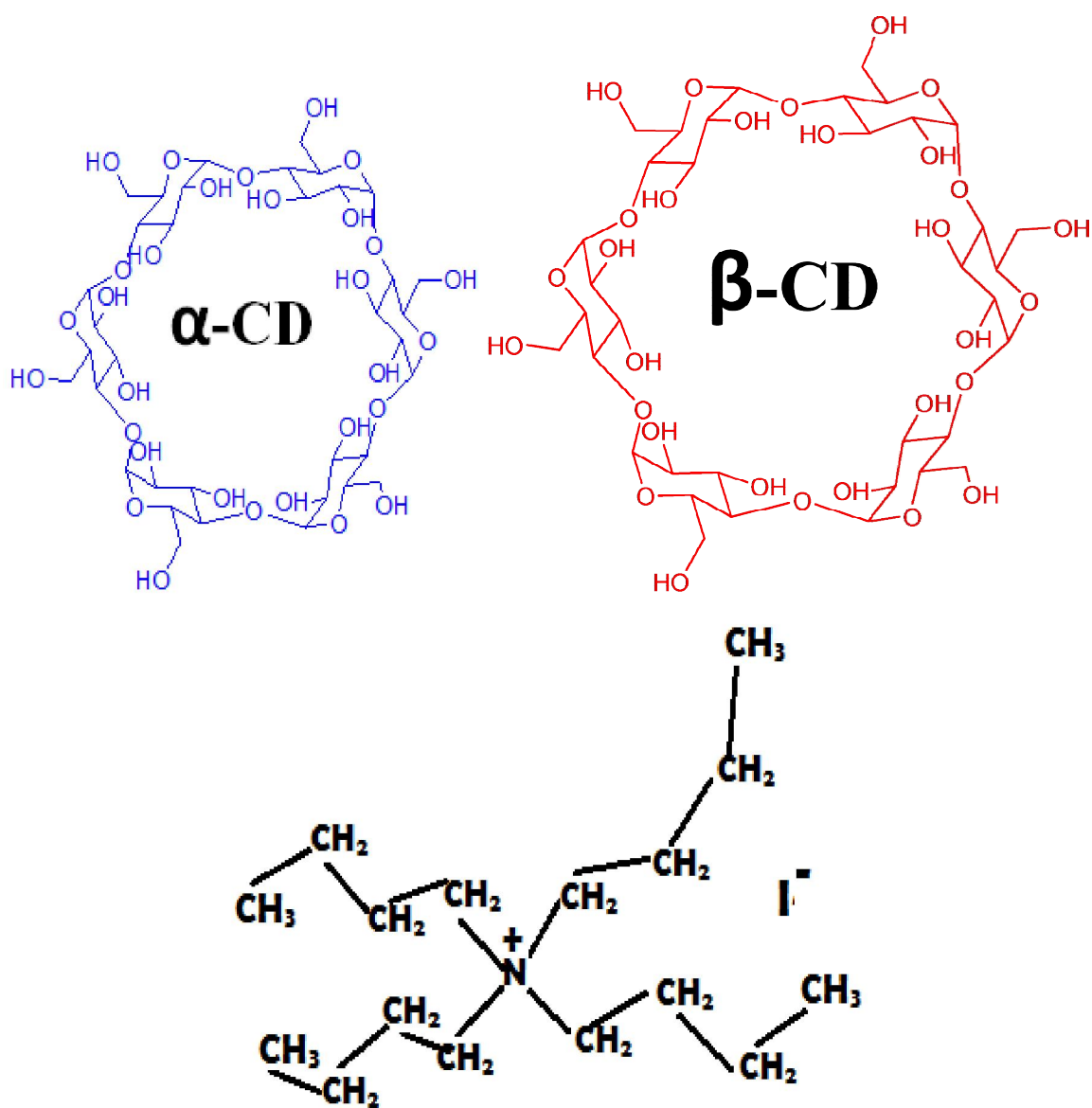


Figure VIII.7(b). FTIR spectra of β -CD (top), but_4NI (middle) and but_4NI - β -CD inclusion complex (bottom).

SCHEMES

Scheme VIII.1. Molecular structure of cyclodextrin molecules and tetrabutylammonium iodide.

CHAPTER- IX

Self assembly inclusion of ionic liquid into hollow cylinder oligosaccharides

IX. 1. INTRODUCTION

Cyclodextrins are hollow cylinder cyclic oligosaccharides containing six (α -CD), seven (β -CD) and eight (γ -CD) glucopyranose units, which are bound by α -(1-4) linkages forming a truncated conical structure, which have a hydrophobic interior and hydrophilic rims having primary and secondary $-OH$ groups [1]. Because of having unique structure, they can build up host-guest arrangement, *i.e.*, it can accommodate the hydrophobic moiety of a guest molecule into its hydrophobic cavity as well as the polar rims can stabilize the polar part of the guest, if any (e.g. ionic liquid) [2]. There has been an increasing attention in the use of cyclodextrins as a device for controlled liberation of active compounds due to their outstanding capability to form molecular inclusion complexes with hydrophobic guest molecules. It is well known that CDs are cyclic oligosaccharides of six to eight glucose units linked by α -1,4-linkages, which are known as α -, β - and γ -CD, respectively. Due to this special property, CDs have been used widely in pharmaceuticals, pesticides, foodstuffs, toilet articles, and textile processing [3,4]. In addition to these industrial applications, they are related to many interesting topics, such as molecular recognition, self assembly, selectivity, molecular encapsulation, chemical stabilization, and intermolecular interactions [4,5]. In an aqueous solution, the slightly apolar cavity of cyclodextrin is occupied by a small quantity of water molecules that are energetically unfavoured and therefore can be readily substituted by appropriate guest molecules that are less polar than water. The guest molecule prefers to penetrate the empty cavity, leading to the formation of an inclusion complex through host-guest interactions. In recent years, with increasing interest in macromolecular

recognition, ICs of polymers with CDs have been investigated extensively [6-14]. So-called molecular necklaces may be formed through penetrating CD molecules by a polymeric chain [15,16]. Moreover, lots of organometallic compounds also can form inclusion compounds with CDs [17,18]. Based on the well-known representative structure of α -, β - and γ -CDs, many different derivatives have been synthesized, which possess different inclusion capabilities [19,20].

Ionic liquids (ILs) are nonvolatile, nonflammable and thermally stable solvents, and also very promising replacements for the traditional volatile organic solvents. Their quite rapid emergence as alternative solvents has involved a rapidly growing number of examples of the application such as organic synthesis, chemical reactions, chemical separations, and material preparations [21,22]. ILs are composed of sterically mismatched ions that hinder crystal formation, thus molecular structure can be used to tune physicochemical properties. The design and synthesis of functional ILs that incorporate structural or functional groups have been reported. For example, ILs was designed as oriented solvents which could impact selectivity in reactions by ordering reactants [23]. Furthermore, functional ILs were also used as templates for the synthesis of mesoporous and zeolitic materials [24] and in the formation of ordered thin films [25,26]. Recently, ILs having a long alkyl chain group exhibited surface active properties in their aqueous solutions. These IL surfactants have been investigated by surface tension measurements [27-30]. There have been few reports on the combination of CDs and ILs. Qi et al. have used ILs as running electrolytes in capillary zone electrophoresis and CDs as a modifier for the separation of anthraquinones extract of Chinese herb [31]. Moreover, CDs or their derivatives dissolved in IL can be used to prepare stationary phases in gas chromatography [32]. Considering the special structures and properties of IL surfactant (Zwitterionic detergent used for protein solubilization), it is of interest to investigate their complexation behaviour using different techniques.

In this work, we investigated the hydrophobic and hydrophilic interfaces between oligosaccharides such as α - and β -CD and IL surfactant viz. n-dodecyl-n n-dimethyl-3-ammonio-1-propanesulfonate.

IX. 2. EXPERIMENTAL

IX.2.1 Materials

The considered compounds i.e. IL and oligosaccharides such as α - and β -cyclodextrins of puriss grade were procured from Sigma-Aldrich, Germany and used as purchased. The mass fraction purity of IL, α - and β -cyclodextrins was ≥ 0.99 , 0.98 and 0.98 respectively.

IX.2.1 Apparatus and procedure

Solubility of the chosen cyclodextrin in water (deionized, triply distilled, degassed water with a specific conductance of $1 \times 10^{-6} \text{ S}\cdot\text{cm}^{-1}$) and IL in aqueous α - and β -cyclodextrin, have been precisely checked to prior of the start of the experimental work, and seen that the selected IL soluble in all proportion of aq. α - and β -cyclodextrin. Aqueous binary solution of IL was prepared by mass (Mettler Toledo AG-285 with uncertainty $\pm 0.0003\text{g}$), and then the working solutions were obtained by mass dilution at 298.15 K. The conversion of molarity into molality was accomplished using experimental density values. All solutions were prepared afresh before use. The uncertainty in molality of the solutions is evaluated to $\pm 0.0001 \text{ mol kg}^{-3}$.

The surface tension experiments were done by platinum ring detachment method using a Tensiometer (K9, KRÜSS; Germany) at the experimental temperature. The accuracy of the measurement was within $\pm 0.1 \text{ mN}\cdot\text{m}^{-1}$. Temperature of the system has been maintained by circulating auto-thermostated water through a double-wall glass vessel containing the solution.

The conductance measurements were carried out in a Systronic-308 conductivity meter (accuracy $\pm 0.01 \%$) using a dip-type immersion conductivity cell, CD-10, having a cell constant of approximately $(0.1 \pm 0.001) \text{ cm}^{-1}$. Measurements were made in a

water bath maintained within $T = (298.15 \pm 0.01)$ K and the cell were calibrated by the method proposed by Lind et al [33]. The conductance data were reported at a frequency of 1 kHz and the accuracy was $\pm 0.3\%$.

IX.3. RESULTS AND DISCUSSION

IX.3.1. Surface tension:

It was reported that the IL with a long alkyl chain was surface active in aqueous solutions [34]. Then, if long alkyl chain IL can form inclusion complexes (ICs) with α - and β -CD, the surface tensions of their solutions would be distinctly affected by the addition of α - and β -CD. Therefore, surface tension measurements can be used to elucidate not only whether inclusion can happen or not but also the stoichiometry of inclusion complexes. The surface tension of aqueous solution of IL surfactant with various α - and β -CD concentrations were measured respectively, and the dependence of the surface tensions on α - and β -CD concentrations is shown in Figure IX.1 respectively. It is found that no remarkable change happens for the surface tensions of pure water when α - and β -CD is added (not shown here), indicating that α - and β -CD have no effect on the surface tensions of pure water. Thus, one may presume that the remarkable changes of surface tensions of aqueous solutions of IL surfactant are ascribed to the formation of the ICs. For aqueous solution of surface active ionic liquid (SAIL) the surface tensions increase remarkably with increasing concentration of α - and β -CD, indicating the formation of inclusion complexes between α - and β -CD and the IL surfactant.

The surface tensions (γ) with corresponding concentration of IL in different mass fraction [0.001, 0.003 and 0.005(M) respectively] of aq. α - and β -CD have been made at the temperature 298.15K. Each curve clearly shows a break point in surface tension at a certain concentration, that is, the γ values increase with corresponding concentration, reach a certain point (break point), and then become approximately steady, which obviously indicates the formation of inclusion complex. The formation of inclusion complexes is accountable for insertion of the hydrophobic (aliphatic) group of chosen

ionic liquid insight into the cavity of α - and β -CD. Single break, double break, and so on in the curve of surface tension indicate inclusion complex may have in different stoichiometries, like 1:1, 1:2, and so on (Scheme IX.2) ratios of CD and IL respectively. Since we noted in Figure XI.1, each curve shows a single break point, which further suggests that 1:1 inclusion complexes are formed.

For the aqueous solution of DDAPS, the surface tension values increase gradually with increasing the concentration of α - and β -CD (Figure IX.1), indicating the formation of inclusion complexes between α - and β -CD and DDAPS. For the SAIL the change in γ is suppressed with the increasing mass fraction of aq. α - and β -CD compared to aq. ionic liquid, i.e., the break point comes at the lower concentration of respective ionic liquid as well as the γ values come closer to that of aq. CDs, suggesting that inclusion becomes feasible with increasing amount of CD in solution. If we compare between aq. α -CD and β -CD, both the values of γ and concentration at the break point are lower in case of aq. β -CD than that of aq. α -CD (Table IX.1). This is evidently due to the fact that β -CD provides more viable attribute (either size or cavity diameter and volume) for formation of feasible inclusion complex than α -CD. The study ionic liquid, thus, form soluble 1:1 complexes with both the cyclodextrin in which we visualize the nonpolar tail group of the ionic liquid to be inserted via the wider rim, so as to make maximum contact with the cyclodextrin cavity (Scheme IX.3), while the charged polar head residue remains in the wider rim of cyclodextrin or in bulk solution. This is due to the fact that DDAPS has a long hydrophobic tail, thus a larger steric inhibition for penetrating into the cavity of α - and β -CD. Then after the addition of aqueous α - and β -CD, the number of α - and β -CD molecules increase with respect to the fixed number of ionic liquids, can pull or attract partially encapsulated hydrophobic tail of cationic part of IL; therefore, at the break point the hydrophobic tail group of DDAPS molecule is included into the apolar cavity of α - and β -CD molecule (Scheme IX.4) and finally form equimolar 1:1 inclusion. In consequence, it can be deduced that hydrophobicity plays an important role in the formation of inclusion complexes. Thus, the surface tension measurements indicate that the long chain tail of IL was included in the α - and β -CD

molecules. The studied IL, thus, form soluble 1:1 complexes with the cyclodextrin in which we visualize the nonpolar tail group of the IL to be inserted via the wider rim, make more contact with the cyclodextrin cavity, while the charged polar head residue remains in the wider rim of cyclodextrin or in bulk solution (Scheme IX.4). The hydrophilic part of the IL remains outside and can make H-bonds with the hydrophilic rim of cyclodextrin and also surrounded by water molecules.

If we compare between aq. α -CD and β -CD, both the values of γ and concentration at the break point are lower in case of aq. β -CD than that of aq. α -CD for SAIL (Scheme IX.5). This is obviously due to the fact that β -CD are provided more viable feature (either size or cavity diameter and volume) for formation of feasible inclusion complex than α -CD. Therefore, it can be deduced that hydrophobicity plays an important role in the formation of inclusion complexes. It has been reported that the choice of anion determines water miscibility and has the most dramatic effect on the properties of ILs [35]. ILs containing the sulphonate anion is very soluble in water, exhibiting a hydrophilic character and in the aqueous solution it pull the movable water molecules towards itself, as a result the cation of studied IL and α - and β -CD molecules are become free to interact each other in the solution which form the inclusion complex. It is suggested that the nature of the anion has significant influence on the inclusion complexes.

In general, therefore, there are four energetically favourable interactions that help shift the equilibrium towards the forward (Scheme IX.2) to form the inclusion complex:

- The displacement of exits polar water molecules from the apolar cavity of cyclodextrin.
- The formation of extended hydrogen bonds by the primary and secondary hydroxyl (-OH) groups and rest water molecules that open a face for enter the guest molecule.
- A reduction of the repulsive interactions between the hydrophobic guest and the aqueous environment.

- An increase in the hydrophobic interactions as the guest inserts itself into the apolar cyclodextrin cavity.

Association of the inclusion complex is not a rapid process because large number of water molecules in the surrounding environment is trapped by anionic part of the IL and it has the high charge surface density. The resulting concentration gradient shifts the equilibrium towards the right. (Scheme IX.2)

IX. 3.2. Conductance study:

Conductivity is a constructive method for studying the hydrophobic and hydrophilic interfaces and also inclusion phenomenon. So, it can be used to elucidate not only whether inclusion can occur but also the stoichiometry of the inclusion complexes (ICs) formed. If it forms an inclusion complex with α - and β -CD, the solution conductivity will be specifically affected by the accumulation of α - and β -CD. The conductivity of various α - and β -CD concentrations in aqueous IL are measured at 25°C, and the dependence of the conductivity on α - and β -CD concentration are shown in Figure IX.2. At a certain concentration in α - and β -CD, the linear decrease of molar conductance with ionic liquid concentration halted rather abruptly to show no or little further decrease with further addition of α - and β -CD, has been treated as the saturation point of the inclusion. From the perusal of Figure IX.2 it is seen that the conductivity of the ionic liquid decreased remarkably with increasing the concentration of α - and β -CD due to inclusion-complex formation between α - and β -CD and the hydrophobic part of IL. The decreasing tendency of the conductance-concentration curve clearly indicating that the α - and β -CD molecule attract or rapture the SAIL molecules one by one, as a results movement of the ionic liquid is restricted and which diminish the conductivity of overall solution system. If we compare between aq. α -CD and β -CD, both the values of conductance and concentration at the break point are lower in case of aq. β -CD than that of aq. α -CD for SAIL (Table IX.2). A discernible break in the conductivity curve occurred at a concentration of about 0.015 molL⁻¹ β -CD, suggesting that the stoichiometry of the β -CD-DDAPS ionic compound is equimolar. A

discernible break in the conductivity curve occurred at a concentration of about 0.016 molL^{-1} α -CD, suggesting that the stoichiometry of α -CD-DDAPS ionic compound is equimolar [36]. This indicates that the chief inclusion complex of β -CD and α -CD with IL in this range is 1:1 which indicates that the IL has been almost totally complex. This is also in correlation with the data from surface tension measurement discussing underway, undoubtedly establish that both the CDs have the favorable structure for the formation of inclusion complexes with the above selected IL and also β -CD is more efficient than α -CD in the formation of inclusion complexes with the above selected IL.

Structural influence of Cyclodextrins

Inclusion complex formation is a dimensional fit between host cavity of CD and SAIL molecule (Scheme IX.1). The most notable feature of cyclodextrin molecules (lipophilic cavity diameter of α - and β -CD is $4.7\text{-}5.3\text{\AA}$ and $6.0\text{-}6.5\text{\AA}$ respectively) provides a microenvironment into which appropriately sized non-polar moiety enters and form strong inclusion complexes [37] (Scheme IX.4). But, no covalent bonds are broken or formed during formation of the inclusion complex [38]. The main driving force is in aqueous solution the slightly apolar cyclodextrin cavity is occupied by water molecules which are energetically unfavoured (polar-apolar interaction), therefore can be readily substituted by more hydrophobic side chain group of IL molecules less polar than water, to attain an apolar-apolar association and decrease of cyclodextrin ring strain resulting in a more stable lower energy state [39]. One or two cyclodextrin molecules can entrap one or more IL molecules; therefore, the plausible host:guest ratio of the inclusion is 1:1, 1:2, 2:1, and 2:2, or even more complicated association complex, and higher order equilibria exist, approximately always simultaneous (Scheme IX.2). However, the simplest and most frequent case of host:guest ratio is 1:1 and 1:2 by the spirit of molecular encapsulation by α - and β -CD has been observed from surface tension and conductance study. Thus, after inclusion of an ionic liquid molecule, second molecule can trap by the cavity of the cyclodextrin. This is because, the cavity size (Scheme IX.1) and volume, allow two molecules accommodation through the wider or

secondary rim and both the narrow and wider rims are blocked (Scheme IX.3). The inclusion result state that the binding strength of IL- β -CD complex is well fits together on specific local interactions between surface atoms and form strong inclusion than IL- α -CD complex.

Based on these dimensions, the oligosaccharides such as α - and β -cyclodextrins and the selected SAIL can typically form complex with aliphatic side chain. Hence, the positive interfaces occurred to form the inclusion complex by

- The displacement of polar water molecules from the apolar cavity of cyclodextrin.
- Increased number of hydrogen bonds formed as the substituted water, returns to the larger pool.
- A reduction of the repulsive interactions between the hydrophobic group of surface active ionic liquid and the aqueous environment.
- An increase in the hydrophobic-hydrophobic interfaces as the inclusion of surface active ionic liquid itself into the apolar cavity of oligosaccharides.

IX.4. CONCLUSION

The extensive study of surface tension and conductance measurements concludes the hydrophobic interfaces of DDAPS in the apolar cavity of the oligosaccharides such as α and β -cyclodextrins favours the inclusion complex formation. The results point out that the oligosaccharides such as α and β -CD and the selected IL are finally form stable inclusion complexes (ICs) with a 1:1 stoichiometry. They both are promoting to each other due to the soluble nature by the formation of ICs, where α and β -CD molecules adopting a symmetrical conformation, and each glucose unit of α and β -CD being in a similar environment. The inclusion complex formation is more all-embracing in case of β -CD than in α -CD.

Hence, the generous culmination discussed and explained in this exertion exigent the exclusivity of the work and pertinent to the design for sundry applications.

TABLES:**Table IX.1.** Values of surface tension at the break point (γ) with corresponding concentration of IL (n-dodecyl-n n-dimethyl-3-ammonio-1-propanesulfonate) in different mass fraction of aqueous α and β -cyclodextrin respectively at 298.15K^a.

mass fraction (w)	conc (m)	γ /mNm ⁻¹
n-dodecyl-n, n-dimethyl-3-ammonio-1-propanesulfonate		
$w_1=0.001^b$	0.0441	77.81
$w_1=0.003^b$	0.0427	77.11
$w_1=0.005^b$	0.0421	76.26
$w_2=0.001^b$	0.0413	77.67
$w_2=0.003^b$	0.0405	77.06
$w_2=0.005^b$	0.0381	76.15

^a Standard uncertainty u is: $u(T) = 0.01\text{K}$ ^b w_1 and w_2 are mass fractions of α - and β -cyclodextrin in aqueous mixture respectively**Table IX.2.** Values of conductance at the break point (Λ) with corresponding concentration of IL (n-dodecyl-n n-dimethyl-3-ammonio-1-propanesulfonate) in different mass fraction of aqueous α and β -cyclodextrin respectively at 298.15K^a

mass fraction (w)	conc (m)	Λ (S m ² /mol)
n-dodecyl-n, n-dimethyl-3-ammonio-1-propanesulfonate		
$w_1=0.001^b$	0.01615	12.89
$w_1=0.003^b$	0.01546	14.89
$w_1=0.005^b$	0.01518	17.56
$w_2=0.001^b$	0.01892	13.16
$w_2=0.003^b$	0.01635	19.52
$w_2=0.005^b$	0.01486	19.83

^a Standard uncertainty u is: $u(T) = 0.01\text{K}$ ^b w_1 and w_2 are mass fractions of α - and β -cyclodextrin in aqueous mixture respectively

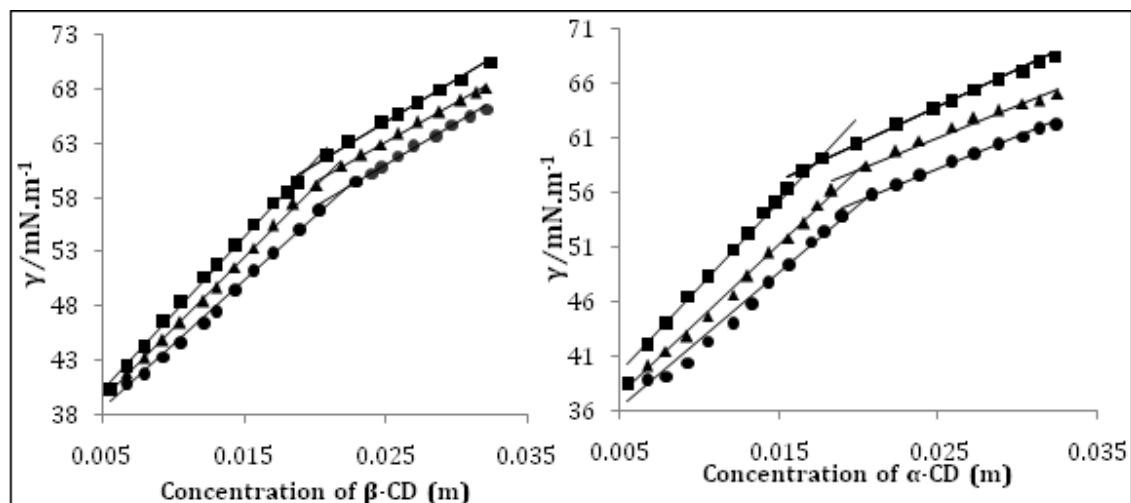
FIGURES

Figure IX.1. Plot of surface tension (γ) of ionic liquid corresponding to the added conc. of aq. β -CD (m) and aq. α -CD (m) in $w_1=0.001$ (\blacklozenge), $w_1=0.003$ (\blacktriangle), $w_1=0.005$ (\bullet) mass fraction of α -CD.

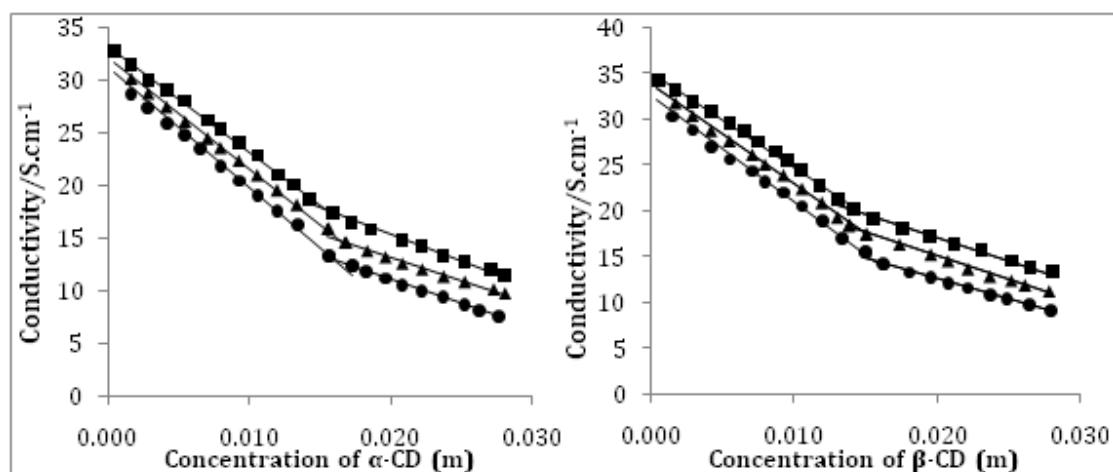
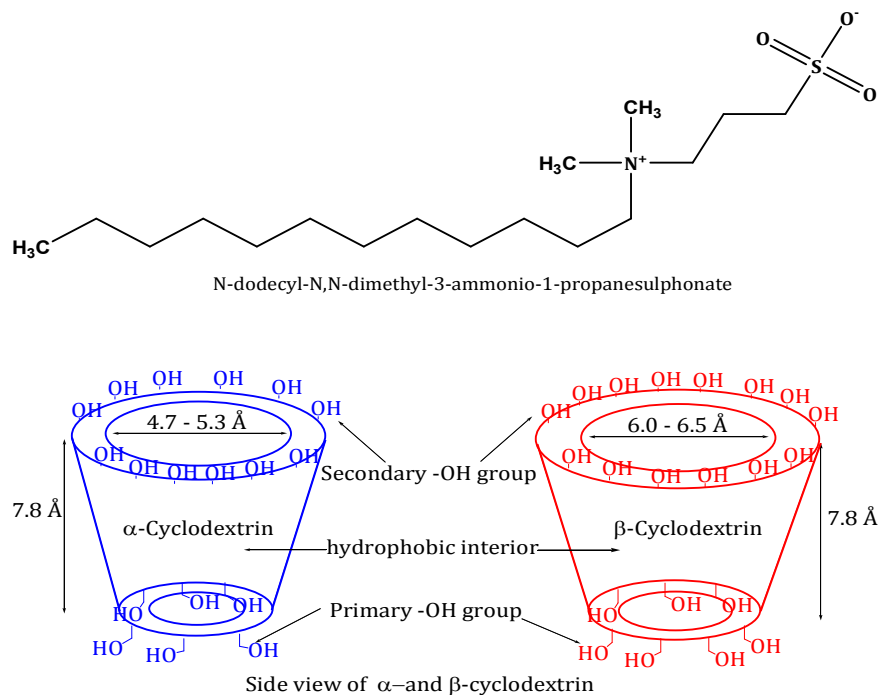
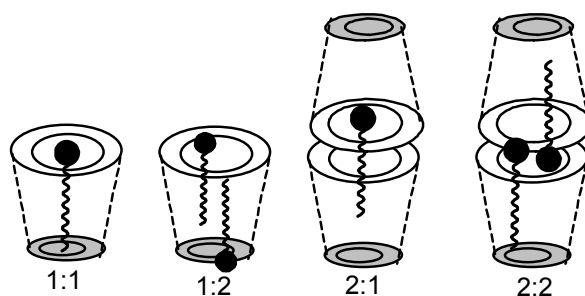


Figure IX.2. Plot of conductance of ionic liquid corresponding to the added conc of aq. α -CD (m) and aq. β -CD (m) in $w_1=0.001$ (\bullet), $w_1=0.003$ (\blacktriangle), $w_1=0.005$ (\blacksquare) mass fraction of β -CD respectively.

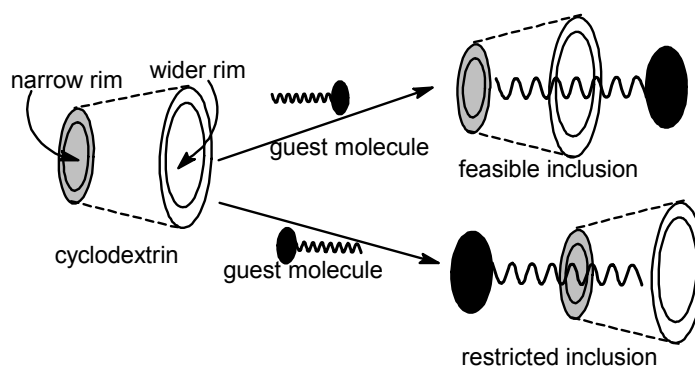
SCHEMES



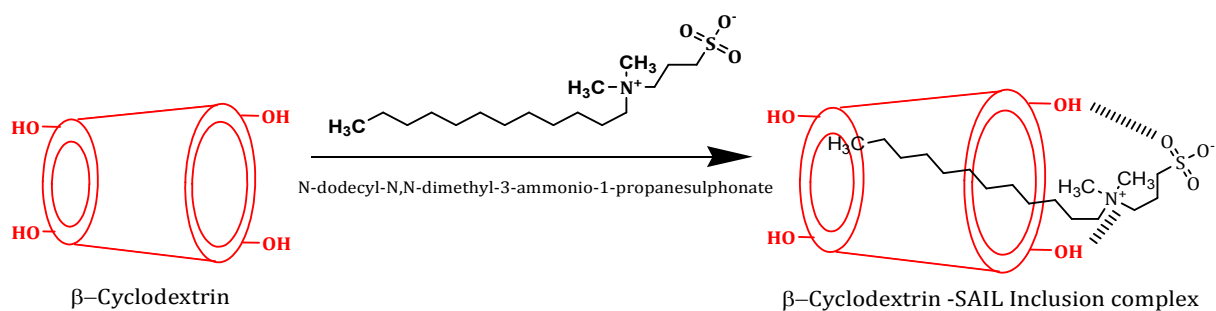
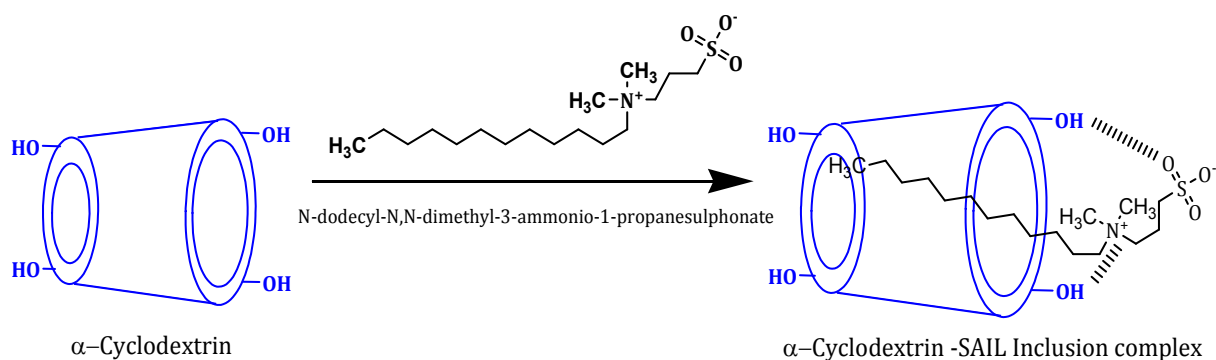
Scheme IX.1: The molecular structure of chosen ionic liquid and α - and β -cyclodextrin (α - CD 6 membered and β -CD 7 membered sugar ring molecules).



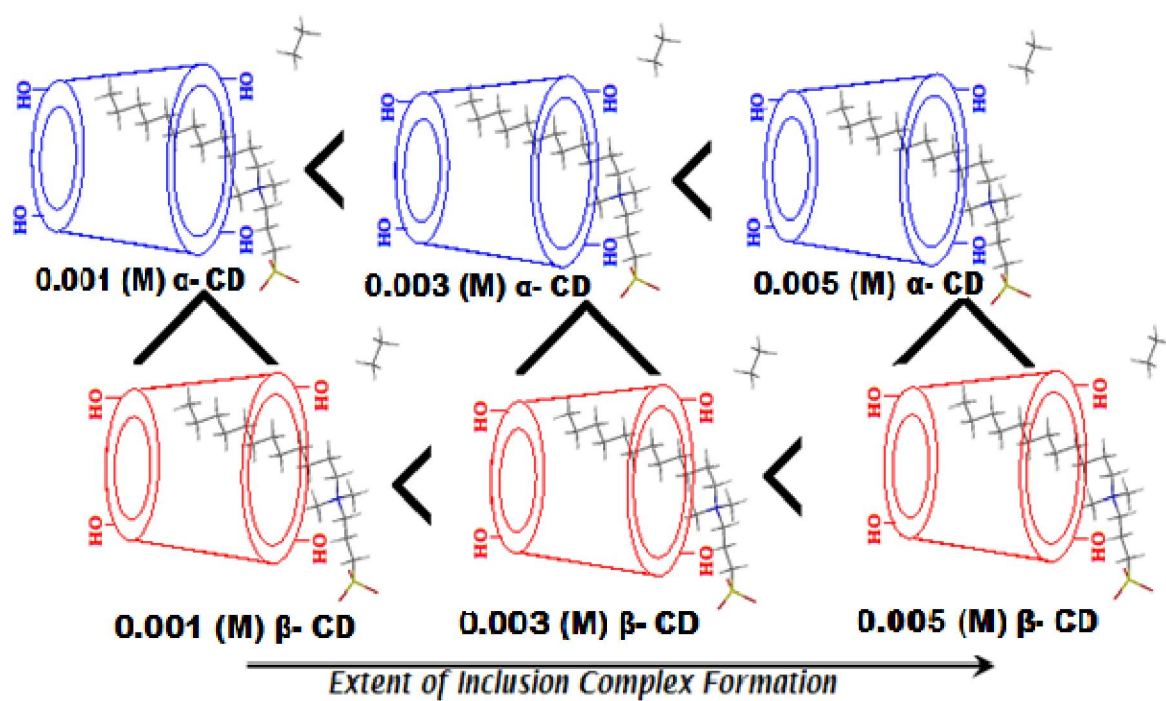
Scheme IX.2: The plausible stoichiometries inclusion ratio of host:guest molecule.



Scheme IX.3: The feasible and restricted inclusion of host:guest molecule.



Scheme IX.4: Schematic representation of convincing mechanism of 1:1 inclusion complexes insight into α - and β -cyclodextrin with the titled ionic liquid.



Scheme IX.5: Extent of inclusion complex formation insight into α - and β - CD with the titled ionic liquid.

CHAPTER-X

Physicochemical Study of Solution Behavior of Ionic Liquid Prevalent in Diverse Solvent Systems at Different Temperatures

X.1. INTRODUCTION

In existing times Ionic liquids (IL) have appeared as room temperature ionic liquids (RTILs) and atmosphere responsive solvents for the development of the manufacturing assemble of chemicals. Ionic liquids have been progressively more used for various commercial and potential applications such as organic synthesis, catalysis, electrochemical devices and solvent extraction of a variety of compounds. Most of the cases of ILs the cations may be organic or inorganic while the anions are inorganic [1]. Now a days the large attention in ionic liquids was commenced because of its usefulness as eco-friendly “green” solvents [2,3]. Ionic liquids offer the advantage of both homogeneous and heterogeneous catalysts. This is because preferred ionic liquids can be immiscible with the reactants and products but dissolve the catalysts. Enzymes are also stable in ionic liquids, opening the possibility for ionic liquids to be used in biological reactions, such as the synthesis of pharmaceuticals [4,5]. Ionizing radiation does not affect ionic liquids, so they could even be used to treat high-level nuclear waste. Ionic liquids can selectively dissolve and remove gases and could be used for air purification on submarines and spaceships. Ionic liquid used in the present widely used in solvent extraction, liquid-liquid extraction process, electrochemical studies, dye-sensitized solar cells [6-9]. Moreover, good thermal stability, variable viscosity, no effective vapor pressure, recyclability and conventional organic solvents have been replaced by ILs in organic synthesis is also great qualities of IL [10-12].

The utilized solvents in this study ascertain broad industrial usage. Acetonitrile (ACN) is largely used in battery industries and also used in pharmaceutical, perfume, rubber product, pesticide, acrylic nail remover preparation industries. For animal fatty acids and vegetable oils extraction ACN is chiefly used. Tetrahydrofuran (THF) is mainly used as a precursor to polymers. The other major applications of THF are an industrial solvent for PVC and in vernishes. 1,3-Dioxolane (DO) is a lower toxic versatile aprotic solvent. The oxygen atom present in DO acts as Lewis base, so it is able to solvate many inorganic compounds. DO is a very good industrial solvent which used prominently in the high energy battery industries and finds application in organic synthesis as manifested from the physicochemical studies in this medium [13]. Different standard compositions of the ionic liquid and the solvents taken can be used in the battery industry, dye industry and in many more industries. Thus, this work has a valuable contribution to these industries. These new solvent mixtures can make the products cheaper, easily available and more useful.

Currently physical chemists have long been of intense attention to the electrochemical study. The study of transport property is a helpful tool for understanding the performance of ions in solution. Furthermore, acquaintance of the thermodynamic properties is indispensable for the proper plan of industrial progressions. In both the theoretical and applied research areas have huge consequence of the perfect knowledge of thermodynamic properties of solution mixtures. In electrolyte solution systems the molecular interaction is afforded through the measurements of the bulk properties, such as density and viscosity of liquids. The above studies help us to understand the behaviour of IL in diverse solvent systems. Ion-ion and ion-solvent communications can be developed as a way to study on the apparent and partial molal volumes of the electrolyte and the dependence of viscosity on the concentration of electrolyte [14].

In continuation our earlier studies [15,16] an attempt has been made in this present study we have done the conductivity, density, viscosity and FTIR study of an IL, 1-butyl-4-methylpyridinium hexafluorophosphate ([bmpy]PF₆) in industrially imperative

solvents at three different temperatures to explore the solvation consequences of IL in diverse solvent systems.

X.2. EXPERIMENTAL

X.2.1 Source and purity of samples

In this current research work, the chosen IL puriss grade was purchased from Sigma-Aldrich, Germany and was used as purchased. The mass fraction purity of the ILs was ≥ 0.99 .

All the spectroscopic grade solvents having mass fraction of purity 0.995 were procured from Sigma-Aldrich, Germany and were used as procured. The IL was preserved in vacuum desiccator containing anhydrous P_2O_5 and any water content of the solvents was removed by using molecular sieves. The literature values as shown in Table X.1 were in excellent concurrence with assessment of measured density, viscosity and conductivity values of IL, which verified the purity [17] of the IL.

X.2.2 Apparatus and Procedure

All the stock solutions of the IL in considered solvents were prepared by mass (weighed by Mettler Toledo AG-285 with uncertainty 0.0003 g). In case of conductometric study the working solutions were achieved by mass dilution of the stock solutions.

Temperature of the solution was maintained to within ± 0.01 K using Brookfield Digital TC-500 temperature thermostat bath. The viscosities were measured with an accuracy of ± 1 %. Each measurement reported herein is an average of triplicate reading with a precision of 0.3 %.

The conductance measurements were carried out in a Systronics-308 conductivity bridge of accuracy $\pm 0.01\%$, using a dip-type immersion conductivity cell, CD-10 having a cell constant of approximately (0.1 ± 0.001) cm^{-1} . Measurements were made in a thermostat water bath maintained at $T = (298.15 \pm 0.01)$ K. The cell was calibrated by the method proposed by Lind et al.[18] and cell constant was calculated based on 0.01

(M) aqueous KCl solution. During the conductance measurements, cell constant was maintained within the range 1.10–1.12 cm⁻¹. The conductance data were reported at a frequency of 1 kHz and the accuracy was ±0.3%. During all the measurements, uncertainty of temperatures was ±0.01 K.

The density values of the solvents and experimental solutions (ρ) were measured using vibrating u-tube Anton Paar digital density meter (DMA 4500M) with a precision of ±0.00005 g cm⁻³ maintained at ±0.01 K of the desired temperature. It was calibrated by triply-distilled water and passing dry air.

The viscosity values were measured by means of a Brookfield DV-III Ultra Programmable Rheometer with fitted spindle size-42 fitted to a Brookfield digital bath TC-500. The viscosities were obtained using the following equation

$$\eta = (100 / RPM) \times TK \times \text{torque} \times SMC$$

where *RPM*, *TK* (0.09373) and *SMC* (0.327) are the speed, viscometer torque constant and spindle multiplier constant, respectively. The instrument was calibrated against the standard viscosity samples supplied with the instrument, water and aqueous CaCl₂ solutions [19]. The viscosities were measured with an accuracy of ± 1 %.

Fourier-transform infrared (FT-IR) was carried out on a Perkin Elmer FT-IR spectrometer (Spectra RXI) with sample prepared as 0.05 (M) solution of IL in the studied solvent systems. The spectra were acquired in the frequency range 4000–400 cm⁻¹ at a resolution of 4 cm⁻¹ with a total of 16 scans.

X.3. RESULTS AND DISCUSSION

Table X.1 demonstrates the solvent properties. The concentrations and molar conductances (Λ) of IL in ACN, THF and DO at 298.15, 303.15 and 308.15 K temperature are presented in Table S1. Due to diverse temperature based systems the molal conductance (Λ) has been acquired from the specific conductance (κ) value using the following equation.

$$\Lambda = (1000 \kappa) / m \quad (1)$$

Linear conductance curve (Λ vs \sqrt{m}) was achieved for the electrolyte in ACN extrapolation of $\sqrt{m} = 0$ evaluated the starting limiting molar conductance for the electrolyte. In conductometric study of IL in THF and DO triple-ion formation occurs. As there is the formation of the cluster in the concentrated solutions, we have discussed the conductometric study in the dilute solutions of the IL and the different solvents taken [20].

X.3.1. Ion-pair Formation

In conductometric study of ([bmpy]PF₆) in ACN the ion-pair formation is investigated using the Fuoss conductance equation [21]. Three adjustable parameters, i.e., Λ_0 , K_A and R have been derived from the Fuoss equation using a given set of conductivity values (c_j , Λ_j ; $j = 1 \dots n$). At this point, Λ_0 is the limiting molar conductance, K_A is the observed association constant and R is the association distance, i.e., the maximum centre to centre distance between the ions in the solvent separated ion-pairs. There is no particular method [22] to determine the R value but in order to treat the data in our system, R value is alleged to be, $R = d + a$, where d refers the average distance consequent to the side of a cell engaged by a solvent molecule and a refers the summation of the crystallographic radii of the ions. The distance, d refers above is specified as,

$$d = 1.183 (M / \rho)^{1/3} \quad (2)$$

where, M and ρ refer the molecular mass and the density of the solvent respectively.

Therefore, the Fuoss conductance equation may be embodied as follows:

$$\Lambda = P\Lambda_0[(1 + R_x) + E_L] \quad (3)$$

$$P = 1 - \alpha(1 - \gamma) \quad (4)$$

$$\gamma = 1 - K_A m \gamma^2 f^2 \quad (5)$$

$$-\ln f = \beta \kappa / 2(1 + \kappa R) \quad (6)$$

$$\beta = e^2 / (\epsilon_r k_B T) \quad (7)$$

$$K_A = K_R / (1 - \alpha) = K_R / (1 + K_S) \quad (8)$$

where, Λ_0 is the limiting molal conductance, K_A is the observed association constant, R is the association distance, R_X is the relaxation field effect, E_L is the electrophoretic counter current, k is the radius of the ion atmosphere, ϵ is the relative permittivity of the solvent mixture, e is the electron charge, m is the molality of the solution, k_B is the Boltzmann constant, K_S is the association constant of the contact-pairs, K_R is the association constant of the solvent-separated pairs, γ is the fraction of solute present as unpaired ion, α is the fraction of contact pairs, f is the activity coefficient, T is the absolute temperature and β is twice the Bjerrum distance.

The computations were executed using the program recommended by Fuoss. The initial Λ_0 values for the interaction process were obtained from Shedlovsky extrapolation of the data [23]. Attempt for the program is the no. of data, n , followed by ϵ , η (viscosity of the solvent), initial Λ_0 value, T , ρ (density of the solvent), mole fraction of the first component, molar masses, M_1 and M_2 along with m_j , Λ_j values where $j = 1, 2, \dots, n$ and an instruction to cover preselected range of R values.

Actually, estimates are executed through ruling the values of Λ_0 and α which minimize the standard deviation, δ , whereby

$$\delta^2 = \sum [\Lambda_j(cal) - \Lambda_j(obs)]^2 / (n - m) \quad (9)$$

for a sequence of R values and then plotting δ against R , the best-fit R corresponds to the minimum of the δ - R versus R curve. So, an approximate sum is made over a fairly wide range of R values using 0.1 increment to locate the minimum but no significant minima is found in the δ - R curves, thus R values is assumed to be $R = d + a$, with terms having usual significance. Finally, the corresponding limiting molar conductance (Λ_0), association constant (K_A), co-sphere diameter (R) and standard deviations of experimental Λ (δ) achieved from Fuoss conductance equation for ([bmpy]PF₆) in ACN at 298.15, 303.15 and 308.15K are given in Table X.2. The variation of equivalent conductance with square root of concentrations for ACN has been shown in Figure X.1 (Scheme X.2).

The standard Gibbs free energy change of solvation, ΔG° , for ([bmpy]PF₆) in ACN can be determined with help of the following equation [24],

$$\Delta G^\circ = -RT \ln K_A \quad (10)$$

The perusal of Table X.3 shows that the value of Gibbs free energy is entirely negative in ACN at all the three studied temperatures. It can also be enlightened by considering the participation of specific non-covalent interaction such as electrostatic forces of attraction, van der Waals forces etc. in the ion-association process (Scheme X.3).

The increase in the values of ΔG° of IL in ACN with increasing temperatures show that degree of association is lower with the increase of temperatures. Commencing the scrutiny of Table X.2 it may be concluded that Λ_0 increases with increase in temperature while K_A value decreases with increase in temperature for IL in ACN. It be originate that ΔG° decreases the negativity with increasing the temperature which indicates the spontaneity of the ion-association process.

By use of tetrabutylammonium tetraphenylborate (Bu_4NBPh_4) as a "reference electrolyte" [25] the ionic conductances λ_0^\pm (for $[\text{bmpy}]^+$ cation and $[\text{PF}_6]^-$ anion) were derived in solvent ACN. The values of ionic conductance λ_0^\pm and the product of ionic conductance and viscosity of the solvent named ionic Walden product ($\lambda_0^\pm \eta$) along with Stokes' radii (r_s) and Crystallographic Radii (r_c) of $[\text{bmpy}]\text{PF}_6$ in ACN at different temperatures are given in Table X.4.

Ion-solvation can also be explained with the help of another characteristic property called the Walden product [26] ($\Lambda_0 \eta$) (Table X.3). Λ_0 increases for the electrolyte in ACN with increasing temperature and the $\Lambda_0 \eta$ also increases even though the viscosity of the solvent decreases. This fact indicates the prevalence of Λ_0 over η .

X.3.2. Thermodynamic parameters

The variation of conductance of an ion with temperature can be treated as similar to the variation of the rate constant with temperature which is given by the Arrhenius equation [27],

$$\Lambda_o = A.e^{-E_a/RT} \quad (11)$$

$$\log \Lambda_o = \log A - \frac{E_a}{2.303RT} \quad (12)$$

Where A is an Arrhenius constant, E_a is the activation energy of the rate process which determines the rate of movement of ions in solution. The slope of the linear plot of $\log \Lambda_o$ Vs $1/T$ (Fig not shown) gives the value of E_a (Table X.5). From the Arrhenius equation it has been found that activation energy is positive. This indicates the higher mobilities of ions in solution increases. So Λ_o (limiting conductance) value increases with increase in temperature. Conductance of an ion is dependent on the rate of movement of ion. Here the changes of number of ions are not accounted quantitatively but, due to the formation of ion-pair available number of free ion will decrease and consequently molar conductivity of the solution decreases.

Thermodynamic parameters of association such as ΔH_a , ΔG_a and ΔS_a were also calculated on the basis of the following equations

$$\Delta H_a = \frac{RT^2 \ln K_a}{dT} \quad (13)$$

$$\Delta G_a = -RT \ln K_a \quad (14)$$

$$\Delta S_a = \frac{\Delta H_a - \Delta G_a}{T} \quad (15)$$

The change in enthalpy of the process of association (ΔH_a) is calculated from the slope of the plot of $\log K_a$ Vs $1/T$ (Fig not shown). ΔG_a was calculated at various temperatures and the average value was considered. ΔS_a was obtained from equation (15) at different temperatures and the average value was noted down. From the perusal of Table X.5 it can be assumed that the negative value of ΔG_a indicates the spontaneity of the ion-association process. The positive value of ΔH_a indicates that the ion-association processes are endothermic. The positive value of ΔS_a indicates the randomness increases from lower temperature to higher temperature.

X.3.3. Triple-ion Formation

There are several numbers of models which show the minimum value of equivalent conductivity of an electrolyte solution as the function of concentration by concerted fundamental studies including the pioneering work of Kohlrausch, Walden, Debye-Huckel and Fuoss-Kraus [28]. Since dielectric constant is dependent on several factors [29], there is clarity in ion-transport property governed by salt concentration.

According to Kohlrausch an empirical description was developed focusing on the concentration dependence of the molar conductivity. By the theoretical basis of this theory further developed by Debye-Hückel-Onsager considered that an ionic cloud is present about the central ion. Afterward including the effects of electrophoresis, the relaxation field and finite ion sizes Fuoss have been changed this model.

There may present a range of cation-anion interactions that result in what is somewhat slackly named as "ionic association". These interactions effect in extensive survival and discrete ionic species whose existence can be spectroscopically identified. The power of these interactions leads to electronic redistribution within bonds that result in the shifts of normal mode frequency.

Fuoss and Kraus at first described the typical behavior of ionic conductance of ionic species in solvents having low dielectric constant. In case of low dielectric constant ($\epsilon < 10$) solutions at very dilute region with increasing salt concentration decrease of Λ attributed as ion-pair formation or solvent separated ion-pairs. The decrease of Λ at high salt conc. is usually attributed to the increase of bulk viscosity in the liquids [30]. This increase has been attributed to the formation of charged triple-ion aggregates (Figure X.2) [31].

Now the conductivity values of ACN, THF and dioxane are tried to fit in Fouss ion-pair formation equation but, only the ACN conductivity values are fitted properly. Hence, the conductivity values of THF and dioxane are tried to fit in Fouss triple-ion formation equation and gives the concerned proper values obtained from Fouss triple-ion formation equation. So, we can say that in our studied systems (THF and dioxane) among many models triple-ion formation occurs. So, it can be explicitly state that here

we employed the triple ion model with no reasons other than that the fitting worked well.

For this IL in THF and DO solvent system the conductance data have been analysed using the classical Fuoss-Kraus equation [31] for triple-ion formation,

$$\Lambda g(c) \sqrt{c} = \frac{\Lambda_0}{\sqrt{K_p}} + \frac{\Lambda_0^T K_T}{\sqrt{K_p}} \left(1 - \frac{\Lambda}{\Lambda_0} \right) c \quad (16)$$

$$g(c) = \frac{\exp\{ -2.303 \beta' (c \Lambda)^{0.5} / \Lambda_0^{0.5} \}}{\{ 1 - S (c \Lambda)^{0.5} / \Lambda_0^{1.5} \} (1 - \Lambda / \Lambda_0)^{0.5}} \quad (17)$$

$$\beta' = 1.8247 \times 10^6 / (\epsilon T)^{1.5} \quad (18)$$

$$S = \alpha \Lambda_0 + \beta = \frac{0.8204 \times 10^6}{(\epsilon T)^{1.5}} \Lambda_0 + \frac{82.501}{\eta (\epsilon T)^{0.5}} \quad (19)$$

In the above equations, Λ_0 is the sum of the molar conductance of the simple ions at infinite dilution; Λ_0^T is the sum of the conductances of the two triple ions $\text{bmpy}^+\text{PF}_6^-$ and $\text{bmpy}^+(\text{PF}_6)_2^-$. $K_P \approx K_A$ and K_T are the ion-pair and triple-ion formation constants. To make equation (16) applicable, the symmetrical approximation of the two possible constants of triple ions equal to each other has been adopted [32] and Λ_0 values for the studied electrolytes have been calculated. Λ_0^T is calculated by setting the triple ion conductance equal to $2/3\Lambda_0$ [33].

During linear regression analysis of equation (16) the ratio Λ_0^T/Λ_0 was set equal to 0.667. Table 6 demonstrates the limiting molar conductance of triple-ions (Λ_0^T), slope and intercept of Eq. (16) for $[\text{bmpy}]\text{PF}_6$ in THF and DO at different temperatures. By the inspection of Table X.6 and Figure X.2 it may be stated that the limiting molar conductance (Λ^0) of $[\text{bmpy}]\text{PF}_6$ is higher in THF than in DO.

Linear regression analysis of equation (16) for the electrolyte in THF and DO with an average regression constant, $R^2 = 0.9653$, gives intercepts and slopes. These permit the calculation of other derived parameters such as K_P and K_T listed in Table X.7. It is observed that Λ passes through a minimum as c increases. The K_P and K_T values predict that major portion of the electrolyte exists as ion-pairs with a minor portion as triple-

ions (neglecting quadrupoles). Since the value of $\log (K_T/K_P)$ is found to be higher in DO than in THF, DO has privileged affinity of triple ion formation than THF.

Electrostatic ionic interactions become very large when permittivity of the solvent is very low (less than 10). In this situation ion-pairs present in solution attract the free +ve and -ve ions of the same medium. Due to the minimum distance of closest approach of the ions in lower permittivity media there is a possibility of greater aggregation by H-bonding [34,35]. The extent of triple-ion formation increases with decreasing the permittivity of the solvent. The above described phenomena exhibit triple-ion formation, which achieve the charge of the relevant ions in the concerned solution system [36] i.e.,



Due to the formation of ternary association in THF and DO triple-ion removes some non-conducting species from solution system. So, after the achievement of minimum conductance values up to a certain concentrations then increase which is manifested by the non-linear conductance curves for the electrolyte in THF and DO.

Moreover, the ion-pair and triple-ion concentrations, c_P and c_T respectively of the electrolyte have also been calculated at the minimum conductance concentration of [bmpy][PF₆] in THF and DO using the following relations: [37]

$$\alpha = 1 / (K_P^{1/2} \cdot c^{1/2}) \quad (23)$$

$$\alpha_T = (K_T / K_P^{1/2}) c^{1/2} \quad (24)$$

$$c_P = c(1 - \alpha - 3\alpha_T) \quad (25)$$

$$c_T = (K_T / K_P^{1/2}) c^{3/2} \quad (26)$$

Here α and α_T are the fractions of ion-pairs and triple-ions present in the salt-solutions respectively and are given in Table X.8. From Table X.8, it is observed that with increasing temperature the number of free ions per unit volume decreases resulting in an increase of K_P and K_T values. Thus, the values of C_P and C_T given in Table

X.8 indicate that the ions are mainly present as ion-pairs even at high concentration and a small fraction existing as triple-ions. With increasing the temperature C_P and C_T values increase and both C_P and C_T values are higher in THF than in DO.

The ion-solvent interaction of IL in DO is higher than in THF and ACN due to the interaction between The N atom of IL with two, one O atom of DO and one N atom of THF (Scheme X.1). From conductivity values it came to know that ion-solvent interaction occurs between the IL and the corresponding solvents. Ion-pair is formed in between IL and ACN and in THF and DO triple-ion is formed (Scheme X.2). Through the conductivity measurements we found the trend of association of IL with diverse solvent systems



X.3.4. Apparent molar volume

The density and viscosity values of [bmpy]PF₆ in ACN, THF and DO at 298.15, 303.15 and 308.15K respectively are stated in Table S2. At a particular temperature the density values of electrolyte in various solvent systems increase linearly with increasing the concentration of electrolyte. However the density values of IL in a particular solvent systems decreases with increase of temperature. By means of the following equations the apparent molar volumes ϕ_V were determined from the density values of solutions (Table S2).

$$\phi_V = M / \rho - (\rho - \rho_0) / m \rho_0 \rho \quad (22)$$

where M is the molar mass of the solute, m is the molality of the solution, ρ and ρ_0 are the densities of the solution and solvent, respectively. The apparent molar volumes ϕ_V were found to decrease with increasing molality (m) of IL in different solvents and increase with increasing temperature for the system under study. The limiting apparent molar volumes ϕ_V^0 were calculated using a least-squares treatment to the plots of ϕ_V versus \sqrt{m} using the following Masson equation [38]

$$\phi_V = \phi_V^0 + S_V^* \cdot \sqrt{m} \quad (23)$$

where ϕ_V^0 is the limiting apparent molar volume at infinite dilution and S_V^* is the experimental slope.

The plots of ϕ_V Vs square root of the molar concentration (\sqrt{c}) were found to be linear with negative slopes. The values of ϕ_V^0 and S_V^* are shown in Table X.9, reveals that ϕ_V^0 values for this electrolyte are generally positive [39] in all the solvent systems and is highest in DO. The variation of ϕ_V^0 values for this studied IL in different solvent systems at different temperatures has shown in Figure X.3. This indicates the presence of strong ion-solvent interactions of IL in DO. The extent ion-solvent interaction is highest in DO and in ACN ion-solvent interaction is lowest (scheme X.4).

In contrast, the S_V^* values designate the extent of ion-ion interaction. All the S_V^* values are negative, which indicates the presence of less ion-ion interaction in the medium. Such S_V^* values also show that extent of ion-ion interactions are highest in case of ACN and are lowest in DO. The above facts reveal that ion-solvent interactions govern over ion-ion interactions in all the studied solvent systems. According to Gurney co-sphere overlap model here overlap of the co-spheres of two ions form positive volume change. This result supports that higher values of ϕ_V^0 in DO sustain the higher ion-solvent interaction [40]. This fact lead to lower conductance of [bmpy]PF₆ in DO than in THF and ACN as conferred in above section. With increasing the temperature ϕ_V^0 values increase and S_V^* values decrease in every solution which indicates higher ion-solvent interaction than ion-ion interaction.

X.3.5. Temperature dependent limiting apparent molar volume:

The variation of ϕ_V^0 with the temperature of the IL in different solvents can be expressed by the general polynomial equation as follows,

$$\phi_V^0 = a_0 + a_1T + a_2T^2 \quad (24)$$

where a_0 , a_1 , a_2 are the empirical coefficients depending on the solute, mass fraction (w_1) of IL, and T is the temperature range under study in Kelvin. The values of these coefficients of the above equation for the IL in ACN, THF and DO are reported in Table X.10.

The limiting apparent molar expansibilities, ϕ_E^0 , can be obtained by the following equation,

$$\phi_E^0 = \left(\delta \phi_V^0 / \delta T \right)_P = a_1 + 2a_2T \quad (25)$$

The limiting apparent molar expansibilities, ϕ_E^0 , change in magnitude with the change of temperature. The values of ϕ_E^0 of the studied IL at (298.15, 303.15, and 308.15) K are accounted in Table X.10. The table reveals that ϕ_E^0 is positive for IL in all the studied solvents and studied temperatures. This fact can ascribed to the absence of caging or packing effect for the IL in solutions.

Hepler [41] built-up a method to examine the sign of $\left(\delta \phi_E^0 / \delta T \right)_P$ for the solute in terms of the structure-making and -breaking capability of the solute in diverse solvent systems using the under mentioned general thermodynamic expression,

$$\left(\delta \phi_E^0 / \delta T \right)_P = \left(\delta^2 \phi_V^0 / \delta T^2 \right)_P = 2a_2 \quad (26)$$

The molecule is a structure maker when the sign of $\left(\delta \phi_E^0 / \delta T \right)_P$ is positive or a small negative; if not, then it is a structure breaker [42]. From Table X.11, it is manifested that $\left(\delta \phi_E^0 / \delta T \right)_P$ values for the considered IL in all the solvents are small negative. This fact predominately shows the structure making tendency of IL in concerned solution systems. Further here effects of electrostriction are accounted due to variation of temperature. With increasing temperature the electrostriction effect of ions increases and electrostricted solvent molecules would be released which consign the structure breaking capacity.

X.3.6. Viscosity calculation

The comparison and conformation of solvation of the electrolyte in the solvent systems can be explored very simply by viscosity measurement. Here we use the following Jones-Dole equation [43] to evaluate the viscosity data

$$(\eta/\eta_0 - 1)/\sqrt{c} = A + B\sqrt{m} \quad (27)$$

where η and η_0 are the viscosities of the solution and solvent respectively. Table X.9 shows the values of viscosity B - and A - coefficients, obtained from the straight line by plotting $(\eta/\eta_0 - 1)/\sqrt{m}$ vs \sqrt{m} . Viscosity B -coefficient is an important device to offer information concerning the solvation of the solutes and their effects on the structure of the solvent. The viscosity B -coefficient reflects the quantitative ion-solvent interactions in the solution. A perusal of Table X.9 and Figure X.4 shows that the values of the B -coefficient are positive [44]. It suggests the presence of strong ion-solvent interactions which reinforce the increase of solvent viscosity value. The decrease of A -coefficient with increase of temperature shows very weak solute-solute interactions. The viscosity A and B -coefficients are in excellent agreement with the results drawn from the conductance and volumetric studies.

The values of the B - and A -coefficient obtained from viscometric measurement support the ϕ_V^0 and S_V^* values respectively obtained from the volumetric study. The viscosity B -coefficient is an expensive tool to provide information concerning the solvation of solutes and their effects on the structure of the solvent in the local vicinity of the solute molecules. Positive values of the B -coefficient (Table X.9) of IL in the studied solvent systems evident the presence of strong ion-solvent interactions and these types of interactions are strengthened from ACN to DO in the solvent mixtures. These conclusions are in excellent agreement with those drawn from ϕ_V^0 values discussed earlier. Due to the association of solvated solute molecules by the solvent molecules through solute-solvent interaction a resistance occur. So, viscosity B -coefficient values become higher in viscous solution system. With the elevation of temperature this type of interactions are strengthened [40]. From the accord of the

above discussions, it may be stated that, the solute-solvent interaction occurs by several types of interaction procedure such as hydrogen-bonding, dipole-dipole and solvophobic interactions [45]. At higher viscosity the triple-ion formation becomes more significant. In this situation, due to the formation of triple-ion equivalent conductivity starts increasing after passing through a minimum value.

The viscosity *B*- and *A*- coefficients are in superb concurrence with the results drawn from the volumetric studies. The ion-solvent interaction is highest in case of DO and lowest in ACN.

X.3.7. FTIR Spectroscopic Study

Molecular interface between IL and miscellaneous solvent systems can be qualitatively interpreted with the aid of FTIR spectroscopy. In case of ion-solvent and solvent-solvent interactions it is used as a supportive confirmation for the bond infringement and bond development (electrostatic bond) study. Table X.12 shows measured IR stretching frequencies of the functional groups of the pure solvents as well as the solutions of mixture ([bmpy]PF₆+Solvents).

For ACN the C≡N stretching vibration shows a sharp peak at $\nu_o = 2251.9 \text{ cm}^{-1}$. Mixture of ACN and IL (i.e. [bmpy]PF₆+CH₃CN) shows a peak at $\nu_s = 2275.1 \text{ cm}^{-1}$. Due to the distraction of dipole-dipole interface present in acetonitrile [46] and construction of ion-dipole interface between [bmpy]⁺ and PF₆⁻ ions with C≡N bond the shift of C≡N stretching frequency is occurred. The change in stretching frequency of C-H bond [47] is 3.4 cm^{-1} of CH₃CN is negligible which shows that C-H bond does not contribute in interaction.

A sharp peak for C-O is obtained at 1042.8 cm^{-1} in case of THF. After addition of IL this peak shifts to 1061.6 cm^{-1} , due to the interaction of [bupy]⁺ with the C-O dipole [47]. The ion-dipole interaction is formed due to the distraction of the H-bonding interface in the THF molecules. The change in stretching frequency of C-H bond 2.6 cm^{-1} of THF shows negligible contribution of C-H group.

After the addition of IL in DO the peak for C-O at 1158.2 cm^{-1} shift to 1175.5 cm^{-1} . Due to an ion-dipole interaction between $[\text{bmpy}]^+$ and the C-O dipole the shift of C-O peak is arised. The change in stretching frequency of C-H bond 2.3 cm^{-1} of DO again shows negligible contribution of C-H group.

In view of the observed derived parameter the ion-solvation happening in studied solution systems $\{[\text{bmpy}][\text{PF}_6]+\text{Solvent}\}$ have been represented in Scheme X.4.

IV.4. CONCLUSION

Commencing the prevalent study of the IL, $[\text{bmpy}]\text{PF}_6$ in different solvent systems it leads to conclude that the IL is more associated in DO than in THF and ACN. The results originated from the conductometric study evidently demonstrate that the IL in DO and THF mostly remains as triple-ions rather than ion-pairs, but in ACN the IL remains as ion-pairs. The investigational assessments achieved form the volumetric and viscometric studies at different temperatures also afford the similar concurrence as derived from the study of transport property. Further, due to the diverse permittivity of the inspected solvents the extent of ion-solvent interaction of $[\text{bmpy}]\text{PF}_6$ is amplified in the following order:



TABLES**Table X.1:** Density (ρ), viscosity (η), relative permittivity (ϵ) and Conductance (Λ) of the different solvents Acetonitrile, Tetrahydrofuran and 1,3 Dioxolane at different temperatures^a.

Temp.	$\rho^a \cdot 10^{-3}/\text{kg m}^{-3}$	$\eta^a/\text{mPa s}$	ϵ	$\Lambda^a \cdot 10^4/\text{S m}^2 \text{mol}^{-1}$
Acetonitrile				
298.15	0.78601	0.35	35.94	0.0695
303.15	0.78283	0.34	35.01	0.0702
308.15	0.78005	0.33	34.30	0.0705
Tetrahydrofuran				
298.15	0.88611	0.48	7.58	0.0677
303.15	0.88596	0.44	7.24	0.0683
308.15	0.88583	0.40	7.09	0.0687
1,3 Dioxolane				
298.15	1.05877	0.59	7.34	0.0659
303.15	1.05870	0.57	7.18	0.0664
308.15	1.05862	0.53	7.02	0.0669

^a Standard uncertainties u are: $u(\rho)=\pm 5 \times 10^{-5} \text{ g}\cdot\text{cm}^{-3}$, $u(\eta)=\pm 1 \%$, $u(\Lambda)=\pm 0.01\%$ and $u(T)=\pm 0.01\text{K}$

Table X.2: Limiting molar conductance (Λ_0), association constant (K_A), co-sphere diameter (R) and standard deviations of experimental Λ (δ) obtained from Fuoss conductance equation of [bmpy]PF₆ in Acetonitrile at 298.15 K, 303.15 K and 308.15 K respectively.

T/K	$\Lambda_0 \cdot 10^4/\text{S}\cdot\text{m}^2\cdot\text{mol}^{-1}$	$K_A/\text{dm}^3\cdot\text{mol}^{-1}$	$R/\text{\AA}$	δ
298.15	188.77	713.48	9.54 \pm 0.10	3.58
303.15	196.61	633.28	9.42 \pm 0.10	3.48
308.15	203.36	565.45	9.33 \pm 0.10	4.02

Table X.3: Walden product ($\lambda_0 \cdot \eta$) and Gibb's energy change (ΔG°) of [bmpy]PF₆ in Acetonitrile at 298.15 K, 303.15 K and 308.15 K respectively.

T/K	$\lambda_0 \cdot \eta \cdot 10^4 /$ $S \cdot m^2 \cdot mol^{-1} mPa$	$\Delta G^\circ \cdot 10^{-3} /$ $kJ \cdot mol^{-1}$
298.15	66.07	-16.29
303.15	66.85	-16.26
308.15	67.11	-16.24

Table X.4: Limiting Ionic Conductance (λ_0^\pm), Ionic Walden Product ($\lambda_0^\pm \eta$), Stokes' Radii (r_s), and Crystallographic Radii (r_c) of [bmpy]PF₆ in ACN at 298.15 K, 303.15 K and 308.15 K respectively.

T/K	ion	λ_0^\pm ($S \cdot m^2 \cdot mol^{-1}$)	$\lambda_0^\pm \eta$ ($S \cdot m^2 \cdot mol^{-1} mPa$)	r_s (Å)	r_c (Å)
298.15	Bmpy ⁺	88.58	31.00	3.21	2.27
	PF ₆ ⁻	101.99	35.70	2.23	1.99
303.15	Bmpy ⁺	92.12	31.32	3.19	2.28
	PF ₆ ⁻	105.52	35.87	2.22	2.01
308.15	Bmpy ⁺	95.43	31.49	3.18	2.29
	PF ₆ ⁻	108.95	35.95	2.20	2.02

Table X.5: Average computed thermodynamic parameters for [bmpy]PF₆ in Acetonitrile.

$\Delta G_a^0 / kJ \cdot mol^{-1}$	$\Delta H_a^0 / kJ \cdot mol^{-1}$	$\Delta S_a^0 / J K^{-1} mol^{-1}$	$E_a / kJ \cdot mol^{-1}$
-16.29	9.28	85.76	5.69

Table X.6: The calculated limiting molal conductance of ion-pair (Λ_0), limiting molar conductances of triple ion Λ_0^T , experimental slope and intercept obtained from Fuoss-Kraus Equation for [bmpy]PF₆ in THF and DO at 298.15 K, 303.15 K and 308.15 K respectively.

Solvents	$\Lambda_0 \cdot 10^4$ /S·m ² ·mol ⁻¹	$\Lambda_0^T \cdot 10^4$ /S·m ² ·mol ⁻¹	Slope $\times 10^{-2}$	Intercept $\times 10^{-2}$
298.15 K				
THF	44.86	29.92	0.18	-5.25
1,3 DO	36.31	24.22	0.11	-6.95
303.15 K				
THF	48.64	32.44	0.37	-5.48
1,3 DO	38.49	25.67	0.28	-7.02
308.15 K				
THF	54.51	36.36	0.57	-5.70
1,3 DO	43.53	29.03	0.44	-7.91

Table X.7: Salt concentration at the minimum conductivity (C_{\min}) along with the ion-pair formation constant (K_P), triple ion formation constant (K_T) for [bmpy]PF₆ in THF and 1,3 DO at 298.15 K, 303.15 K and 308.15 K respectively.

Solvents	$c_{\min} \cdot 10^4$ / mol·dm ⁻³	$\log c_{\min}$	$K_P \cdot 10^2$ / (mol·dm ⁻³) ⁻¹	$K_T \cdot 10^3$ / (mol·dm ⁻³) ⁻¹	$K_T/K_P \cdot 10^5$	$\log K_T/K_P$
298.15 K						
THF	5.45	0.7364	5.59	58.54	10.47	1.019
1,3 DO	5.26	0.7209	5.28	63.25	11.98	1.078
303.15 K						
THF	7.49	0.8745	5.29	65.19	12.32	1.090
1,3 DO	5.46	0.7372	5.18	68.85	13.29	1.123

308.15 K						
THF	7.54	0.8774	5.08	67.05	13.19	1.120
1,3 DO	5.49	0.7396	5.05	71.86	14.23	1.153

Table X.8: Salt concentration at the minimum conductivity (c_{\min}), the ion pair fraction (α), triple ion fraction (α_T), ion pair concentration (c_P) and triple-ion concentration (c_T) for [bmpy]PF₆ in THF and DO at 298.15 K, 303.15 K and 308.15 K respectively.

Solvents	$c_{\min} \cdot 10^4 /$ mol·dm ⁻³	$\alpha \cdot 10^{-2}$	$\alpha_T \cdot 10^2$	$c_P \cdot 10^{-3} /$ mol·dm ⁻³	$c_T \cdot 10^{-2} /$ mol·dm ⁻³
298.15 K					
THF	6.93	15.14	59.42	0.98	3.24
DO	5.26	17.50	61.41	0.97	3.23
303.15 K					
THF	6.91	15.32	74.79	1.69	5.60
DO	5.38	18.45	65.78	1.08	3.59
308.15 K					
THF	6.89	18.62	76.58	1.73	5.77
DO	5.09	17.21	67.89	1.12	3.73

Table X.9: Limiting apparent molal volume (ϕ_V^0), experimental slope (S_V^*), viscosity -B and -A coefficient for [bmpy]PF₆ in ACN, THF and DO at 298.15 K, 303.15 K and 308.15 K respectively.

Solvents	$\phi_V^0 \cdot 10^6 /$ m ³ ·mol ⁻¹	$S_V^* \cdot 10^6 /$ m ³ · mol ^{-3/2} · dm ^{3/2}	$B /$ dm ³ · mol ⁻¹	$A /$ dm ^{3/2} · mol ^{-1/2}
298.15 K				
ACN	250.69	-123.17	1.6567	0.1069
THF	262.63	-130.94	1.6699	-0.0117

DO	271.10	-162.01	1.8868	-0.1540
303.15 K				
ACN	258.73	-128.02	1.7741	0.1048
THF	275.96	-172.73	1.7790	-0.0188
DO	282.02	-163.90	2.0042	-0.1659
308.15 K				
ACN	265.71	-129.58	1.9134	0.1036
THF	281.33	-177.27	1.9375	-0.0338
DO	288.72	-168.75	2.1761	-0.1757

Table X.10: Values of empirical coefficients (a_0 , a_1 , and a_2) of Equation 4 for IL in ACN, THF and DO.

solvents	$a_0 \cdot 10^6$	$a_1 \cdot 10^6$	$a_2 \cdot 10^6$
	/m ³ ·mol ⁻¹	/m ³ ·mol ⁻¹ ·K ⁻¹	/m ³ ·mol ⁻¹ ·K ⁻²
ACN	-2144.9	14.356	-0.0212
THF	-14921.0	98.393	-0.1592
DO	-8008.5	52.934	-0.0844

Table X.11: Limiting apparent molal expansibilities (ϕ_E^0) for IL in different solvents (ACN, THF and DO) at 298.15K to 308.15K respectively.

solvent mixture	$\phi_E^0 \cdot 10^6$ /m ³ ·mol ⁻¹ ·K ⁻¹			$(\partial\phi_E^0/\partial T)_P \cdot 10^6$
				/m ³ ·mol ⁻¹ ·K ⁻²
ACN+IL				
T/K	298.15	303.15	308.15	
	1.714	1.502	1.290	-0.042

THF+IL				
T/K	298.15	303.15	308.15	
	3.462	1.870	0.278	-0.318
DO+IL				
T/K	298.15	303.15	308.15	
	2.606	1.762	0.918	-0.168

Table X.12: Stretching frequencies of the functional groups present in the pure solvent and change of frequency after addition of IL in the solvents.

Stretching frequencies			
Solvents	Functional Group	Pure Solvent (ν_0 cm ⁻¹)	{(bmpy)PF ₆ +Solvents} (ν_{IL} cm ⁻¹)
CH ₃ CN	C≡N	2253.2	2275.1
	C-H	2918.9	2922.3
THF	C-O	1043.1	1062.4
	C-H	2914.3	2917.2
DO	C-O	1158.2	1175.5
	C-H	2915.7	2918.2

FIGURES

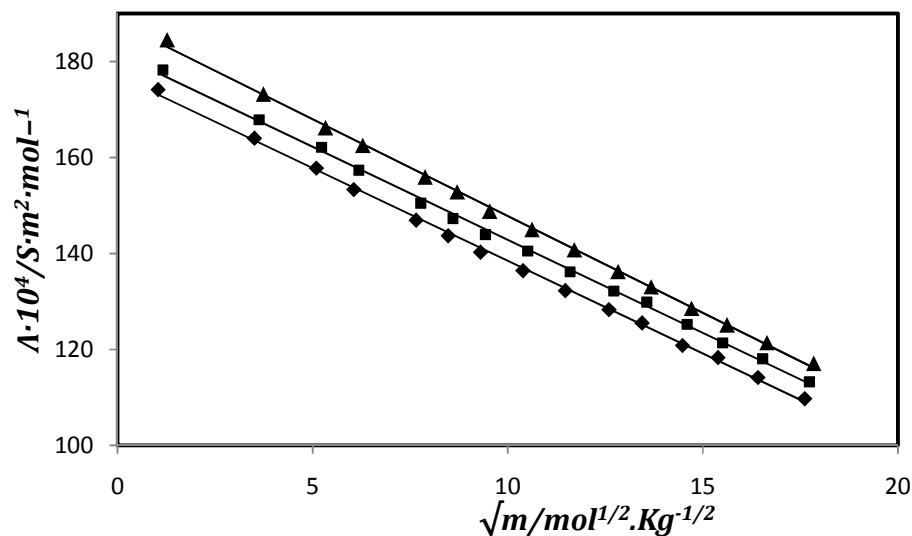


Figure X.1: Plot of molal conductance (Λ) versus \sqrt{m} for [bmpy]PF₆ in ACN at 298.15 K (◆), 303.15 K (■) and 308.15 K (▲).

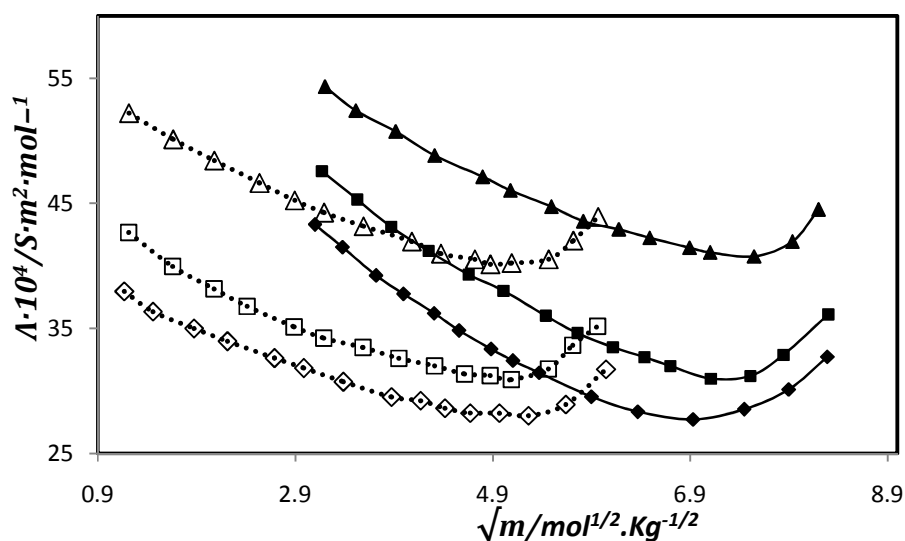


Figure X.2: Plot of molal conductance (Λ) versus \sqrt{m} for [bmpy]PF₆ in THF at 298.15 K (◆), 303.15 K (■), 308.15 K (▲) and in DO at 298.15 K (◇), 303.15 K (□), 308.15 K (Δ).

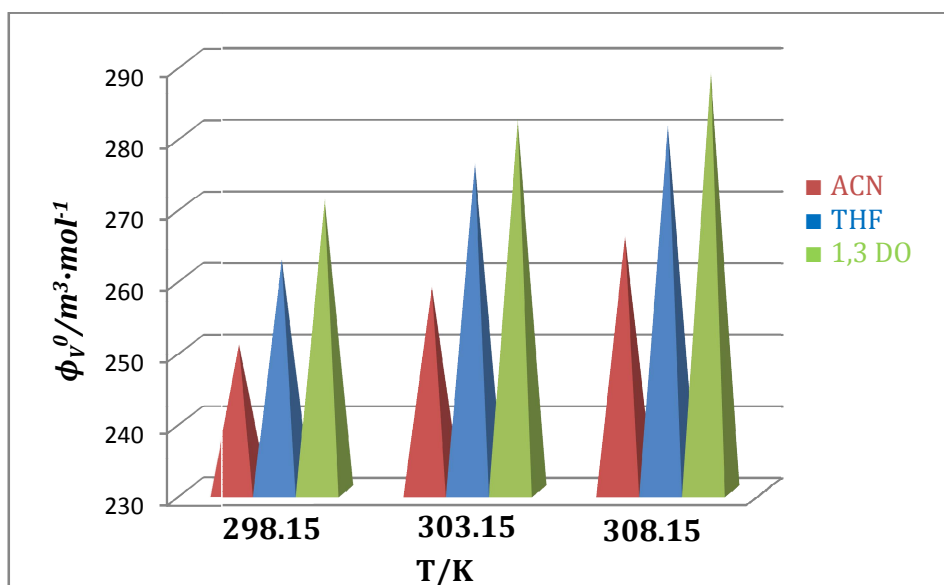


Figure X.3: Plot of temperature versus limiting apparent molal volume (ϕ_v^0) for [bmpy]PF₆ in ACN (red) , THF (blue) and 1,3 dioxolane (green).

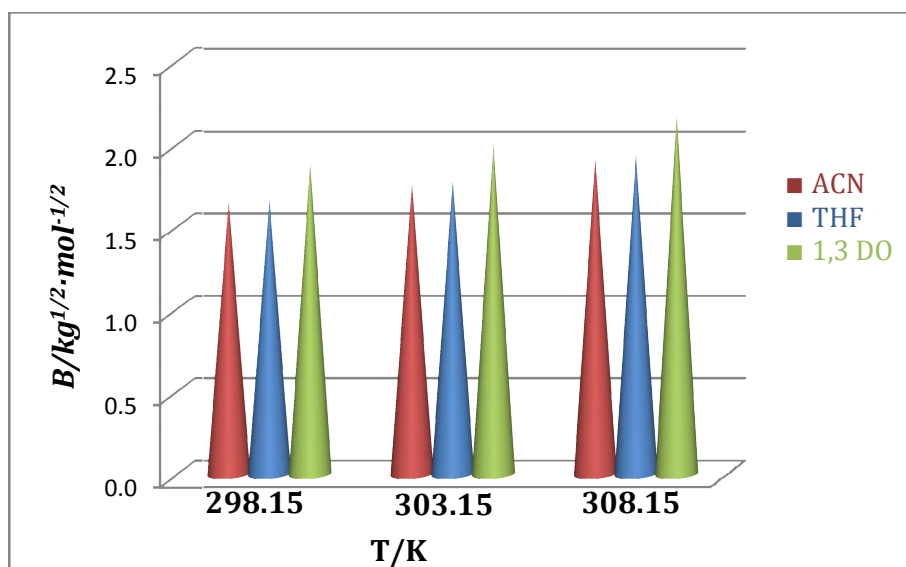
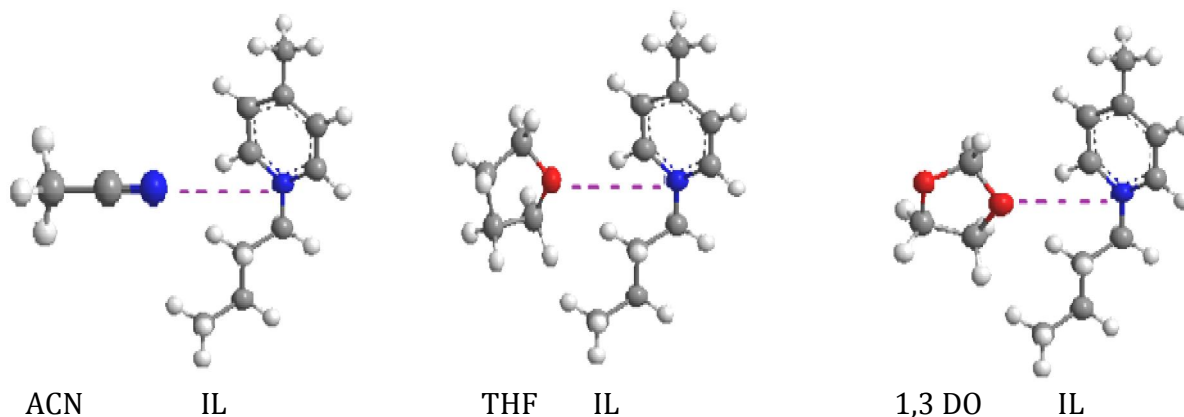
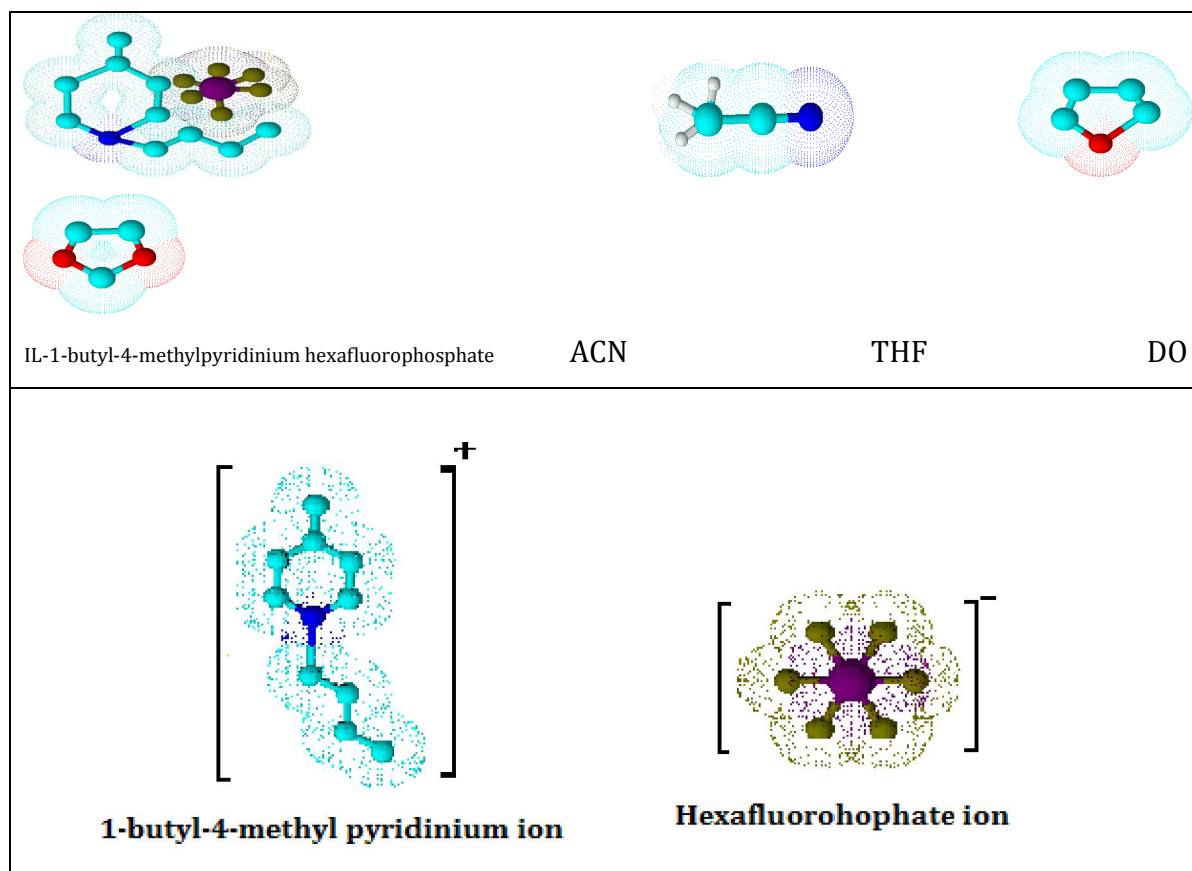
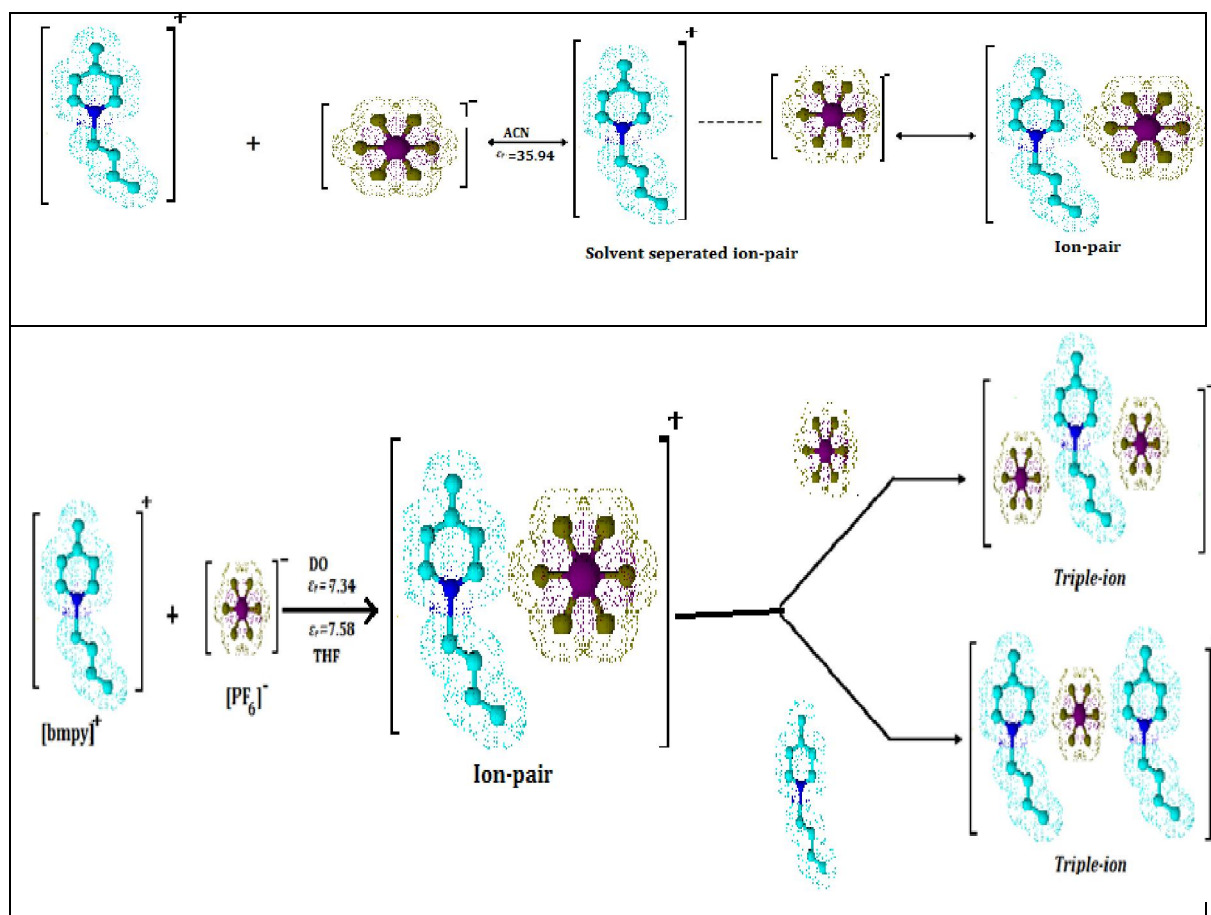


Figure X.4: Plot of temperature versus Viscosity B -Coefficient for [bmpy] PF₆ in ACN (red), THF (blue) and 1,3 dioxolane (green).

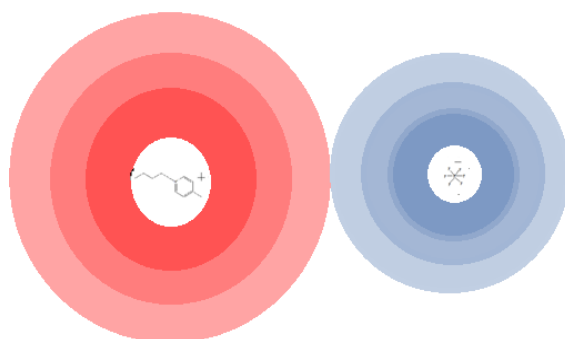
SCHEMES

Scheme X.1. Plausible interfaces between the ionic liquid and diverse solvent systems.

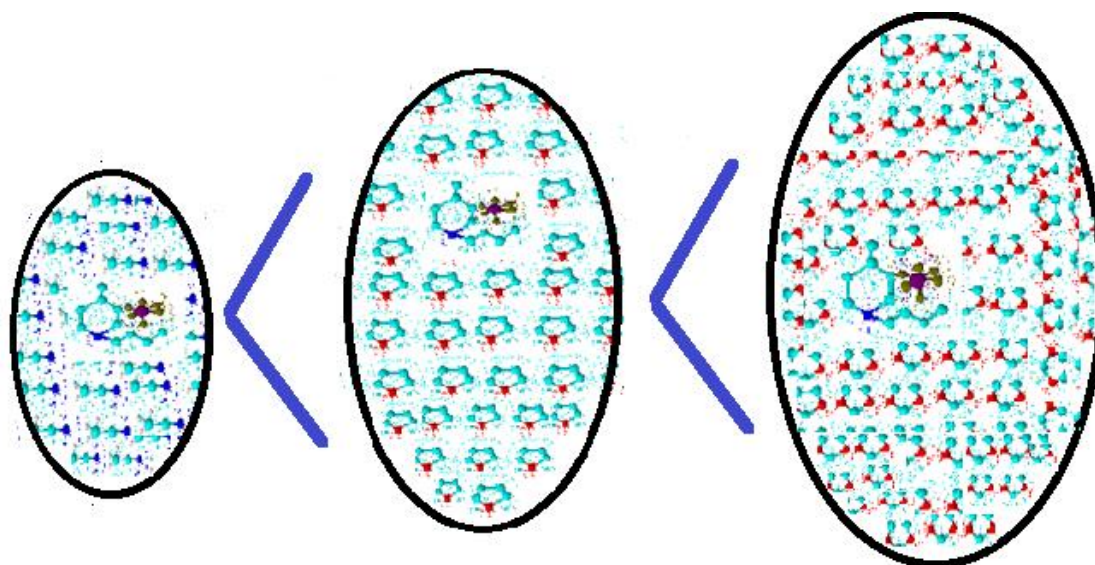




Scheme X.2. Molecular structures of the IL and the solvents and pictorial representation of ion-pair and triple-ion formation for the electrolyte in diverse solvent systems.



Scheme X.3. Electrostatic Forces of Attraction.



Scheme X.4. Extent of ion-solvent interaction of IL in miscellaneuous solvent systems

CHAPTER- XI

CONCLUDING REMARKS

In this thesis, I have studied the molecular interactions of ionic solids and ionic liquids in miscellaneous solvent systems and also host-guest inclusion complexation of ionic solid and ionic liquid with diverse host molecules. Molecular interfaces have been studied with the help of thermophysical, thermodynamic, transport, surface tension, optical properties of solutions along with FTIR and NMR studies.

The research reported in this dissertation explains the procedures and results as well as the studies of the molecular interactions that have been carried out on ionic liquids and amino acids. The overall goal of initiating an understanding of the structure property relationship of ionic liquids has been reached. This was done through work on several ionic liquids differing mainly in their cationic and anionic parts. By looking at thermophysical, thermodynamic and transport properties of these materials, a more complete knowledge of phosphonium, ammonium, imidazolium, pyridinium and pyrrolidinium -based ionic liquids and ionic solids was achieved.

The volumetric, viscometric, interferometric, conductometric refractive index studies helped us to evaluate the extent of molecular interaction in a particular solution quantitatively whereas the FTIR measurements gave an insight into the type of molecular interaction occurring in any solution systems. Various types of interactions exist between the ions in solutions, and of these, ion-ion and ion-solvent interactions are of current interest in all branches of chemistry. These interactions help in better understanding the nature of solute and solvent, that is, whether the solute modifies or distorts the structure of the solvent.

Mixed solvents enabled the variation of properties such as dielectric constant or viscosity, and therefore the ion-ion and ion-solvent interactions occurring in the

solutions systems could be better understood. Moreover, different quantities strongly influenced by solvent properties could be derived from concentration dependence of the electrolyte conductivity. Consequently, a number of conductometric and related studies of different electrolytes in nonaqueous solvents, especially mixed organic solvents, have been made for their optimal use in high-energy batteries and for understanding organic reaction mechanisms. Ionic association of electrolytes in solution depends upon the mode of solvation of its ions, which in turn depends on the nature of the solvent or solvent mixtures. Such solvent properties as viscosity and the relative permittivity have been taken into consideration as these properties help in determining the extent of ion association and the solvent-solvent interactions. Thus, extensive studies on electrical conductance in mixed organic solvents have been performed to examine the nature and magnitude of ion-ion and ion-solvent interactions.

Thus, the discussion of the molecular interactions throughout the thesis has been concluded **chapter** wise as follows:

The present **Chapter IV** reveals a through conductometric, volumetric and viscometric studies indicate that LiAsF_6 is more conducting in all the solvent mixtures studied. In case of 0.25 mass fraction of AN in DEC, triple-ion formation was seen for the electrolytes. The result revealed that the major portion of the electrolytes exists as ion-pairs and a minor portion as triple-ions and it was observed that LiI has the highest tendency to form triple-ions among the three electrolytes. In case of 0.50 and 0.75 mass fraction of AN in DEC high solvation was seen in case of LiI in all the solvent mixtures studied. With the increase in the mass fraction of AN in the solvent mixture it was seen that the conductance of the electrolytes decreases which indicates that the lower mass fraction of AN in DEC gives better conductance of the electrolytes under study. The volumetric and viscometric studies were in excellent agreement with the conductance studies indicating more ion-solvent interaction in LiI solution which increase with the increase in the mass fraction of AN in DEC.

The **Chapter V** deals an extensive study of Hept₄NI in o-Toluidine, o-Xylene and 2-Nitrotoluene leads to the conclusion that, the salt more associated in 2-Nitrotoluene than the other two studied solvents. It can also be seen that in the conductometric studies in o-Toluidine and o-Xylene the Hept₄NI remains as triple-ions and ion-pairs and the extent of triple-ion formation is higher in o-Xylene than o-Toluidine. But in 2-Nitrotoluene the Hept₄NI remains as only ion-pairs. The experimental values obtained from the volumetric and viscometric studies suggest that in solution there is more ion-solvent interaction than the ion-ion interaction and the extent of ion-solvent interaction of Hept₄NI is highest in 2-Nitrotoluene.

In **Chapter VI**, we have focused on the characteristic interfaces of some model biological systems [D(-)fructose and D(+)-galactose], with an IL. The studied physicochemical properties provide us complete explanation for the interfaces of IL with carbohydrates. From the analysis of thermodynamic data, it is revealed that the association process for [bmp]Cl is higher in case of D(-)fructose than in D(+)-galactose solution. This process is endothermic and entropy controlled at all the studied temperatures. Density and viscosity studies interpret limiting apparent molar volume, ϕ_V^0 and viscosity *B*-coefficient which describes that ion-solvent interaction is increased with increasing the conc. of D(-)fructose and D(+)-galactose and decreased with increasing temperature. NMR study analysis reveals that no specific and stronger interactions occur between IL and carbohydrates. However the study confirms that interaction of IL with carbohydrates is higher in D(-)fructose than that of D(+)-galactose. The study provides a profound insight into the potential toxicity of ILs in mixed systems of IL and biomolecules.

The **Chapter VII** shows The extensive conductometric study of [BMP][Br] in FA, DMA, and DMF leads the conclusion that the electrolyte more associated in FA than in the other two solvents. The reliable value of volumetric, viscometric and interferometric studies also intends to map the physicochemical behaviour in solution and suggests that in solution there is more ion-solvent interaction than ion-ion

interaction. The molar refraction values also support the above fact that the highest ion-solvent interaction is seen in case of FA solvent. In all the solvents the electrolyte forms ion-dipole interactions as evident from the FT- IR studies.

The **Chapter VIII** helps us to conclude that the ionic solid form host-guest ICs with both α and β -CD both in solution and solid state. With the help of ^1H NMR study it may be substantiated that inclusion occurs in the apolar cavity of both CD molecules, even as surface tension and conductivity data suggest 1:1 stoichiometry. Volumetric, viscometric and refractometric measurements are also in excellent concord with another study and furthermore suggested the interactions between ionic solid and CD. The solid state of ICs have been characterised by FT-IR, confirming their creations also in solid state. In this study the inclusion phenomenon of ionic solid has been originated extra ensnared in case of β -CD than α -CD. The binding constants, evaluated using a non-linear programme by the conductivity method also supports the trend of IC formation. As a consequence, the exclusivity of our present research work is diverse appliances in the field of bio-chemistry such as drug delivery tools, recycling extraction agents and nano-sensors and so on.

In **Chapter IX** the extensive study of surface tension and conductance measurements concludes the hydrophobic interfaces of DDAPS in the apolar cavity of the oligosaccharides such as α and β -cyclodextrins favours the inclusion complex formation. The results point out that the oligosaccharides such as α and β -CD and the selected IL are finally form stable inclusion complexes (ICs) with a 1:1 stoichiometry. They both are promoting to each other due to the soluble nature by the formation of ICs, where α and β -CD molecules adopting a symmetrical conformation, and each glucose unit of α and β -CD being in a similar environment. The inclusion complex formation is more all-embracing in case of β -CD than in α -CD. Hence, the generous culmination discussed and explained in this exertion exigent the exclusivity of the work and pertinent to the design for sundry applications.

In **Chapter X** commencing the prevalent study of the IL, [bmpy]PF₆ in different solvent systems it leads to conclude that the IL is more associated in DO than in THF and ACN. The results originated from the conductometric study evidently demonstrate that the IL in DO and THF mostly remains as triple-ions rather than ion-pairs, but in ACN the IL remains as ion-pairs. The investigational assessments achieved from the volumetric and viscometric studies at different temperatures also afford the similar concurrence as derived from the study of transport property. Further, due to the diverse permittivity of the inspected solvents the extent of ion-solvent interaction of [bmpy]PF₆ is amplified in this order: DO>THF>ACN

More extensive studies of the different thermophysical, thermodynamic and transport properties of the electrolytes will be of sufficient help in understanding the nature of the ion-solvent interactions and the role of solvents in different chemical processes. The study of the viscous behavior of pharmaceuticals, foodstuffs, cosmetics and industrial products etc. is essential for confirming that their viscosity is appropriate for the contemplated use of the products.

The proper understanding of the ion-ion and ion-solvent interactions may form the basis of explaining quantitatively the influence of the solvents and ions in solution and thus pave the way for real understanding of different phenomena associated with solution chemistry. However, it is necessary to remember that molecular interactions are very complex in nature. There are strong forces existing in the molecule and it is not really possible to separate them all. Nevertheless, if careful judgement is used, valid conclusions can be drawn in many cases relating to degree of structure and order of the system.

The broad studies of the different physicochemical, thermodynamic, transport and spectral properties of the ionic solids and ionic liquids in different solvents will be of sufficient in understanding the nature of the ion-solvent interactions and the role of solvents in different chemical processes. Here in this research work I have also tried to explore the formation of host-guest inclusion complexes of ionic solids and ionic liquids with several host molecules such as α and β cyclodextrins. This host-guest complexation has been confirmed by conductance, surface tension, FTIR and NMR

spectroscopy. These studies are very much important in pharmaceutical industries, food industries, paint industries, cosmetic and hygiene industries and in also enhance the speed of diagnostic test reaction.

So, it may be concluded that our research work has adequate significance in the different branches of sciences and demands a far reaching effect for the augmentation of the advance research.

In the near future we endeavor to widen our research work with ionic solids and ionic liquids which I hope will certainly compliment our present findings. In recent years, with the advent of new synthetic technologies such as catalytic symmetric/asymmetric synthesis, phase transfer catalysis, and catalysis, the diversity of molecular interactions that can be studied, has increased to the highest degree.

I hope this thesis provides substantial launching point for the readers to begin their own investigation into the chemical nature of remarkable ionic solids and ionic liquids. With gradual discovery of newer ionic liquids and solids, the possibility for development of synthetic methods and research in academic, industry and biological field grows up as well. I anticipate this thesis contributes plenty of knowledge in different sectors.

BIBLIOGRAPHY

REFERENCES OF CHAPTER-I

- [1] X. Li, X. Xu and C. Zhou, Chem. Commun. 48 (2012) 12240.
- [2] Z. J. Liu, J. Zhang, S. L. Chen, E. Shi, Y. Xu and X. B. Wan, Angew. Chem. Int. Ed. 51 (2012) 3231.
- [3] A. Triolo, O. Russina, H. J. Bleif and E. Di Cola, J. Phys. Chem. B 111 (2007) 4641.
- [4] P. Vanysek, CRC Handbook of Chemistry and Physics, 82nd Edition, CRC Press, Boca Raton (2001-2002).
- [5] G. Charlot and B. Tremillon, Chemical Reactions in Solvents and Melts, Pergamon, Oxford (1969).
- [6] H. A. Laitinen, Chemical Analysis, McGraw Hill, New York (1960).
- [7] T. O'Donnell, Superacids and Acidic Melts, VCH, Weinheim (1993).
- [8] The Structure and Properties of Ionic Melts, Discuss. Faraday Soc., 32, University Press, Aberdeen (1962).
- [9] J. O'M Bockris and A. K. N. Reddy, Modern Electrochemistry, Plenum, New York (1970).
- [10] Xing Ma and Yanli Zhao, Chem. Rev. 115 (2015) 7794.
- [11] D. K. Meck, The Chemistry of Non- Aqueous solvents, Academic Press, New York (1996).
- [12] O. Popovych and R. O. Bates, Crit. Rev. Anal. Chem. 1 (1970) 73-117.
- [13] F. Franks, Physico-Chemical Processes in Mixed Aqueous Solvents, Heinemann Educational Books Ltd., London (1967).
- [14] R. G. Bates, Determination of pH Theory and Practice, John Wiley and sons: New York (1973).
- [15] (a) R. G. Bates, Solute –solvent Interactions, Marcel Dekker, New York (1969).
(b) R. G. Bates and A. J. Parker, Chemical Physics of Ionic solutions, John Wiley and Sons. Inc, New York (1966).

- [16] A. J. Parker and J. H. Sharp, Proceeding of the Royal Australian Chemical Institute (1972).
- [17] A. J. Parker, *Electrochim. Acta.* 21 (1976) 671.
- [18] C. M. Criss and M. Salomon, *J. Chem. Educ.* 53 (1976) 763.
- [19] Y. Mercus, *Ion-solvation*, Wiley, Chinchester (1986).
- [20] E. J. King, *Acid-Base Equilibria*, Pergamon Press, London (1965).
- [21] O. Ppovych and R. T. P. Tomkins, *Non-Aqueous solution Chemsitry*, John Wiley and Sons, New York (1981).
- [22] R. R. Dogonadze, E. Kalman, A. A. Kornyshev and J. Ulstrup, *The Chemical Physics of Solvation*, Elsevier, Amsterdam (1988).
- [23] Faraday, Discussion of the Chemical Society, No. 67 (1977).
- [24] E. L. Herric and J. G. Brewer, *J. Chem. Eng. Data.* 14 (1969) 55.
- [25] B. V. Clineschmidt, D. J. Pettibone, V. J. Lotti, H. B. Hucker, B. M. Sweeney, D. R. Reiss, E. V. Lis, J. R. Huff and J. Vacca, *J Pharmacol Exp Ther.* 245 (1988) 32.
- [26] M. N. Roy and A. Sinha, *Fluid Phase Equilib.* 243 (2006) 133.
- [27] J. H. Dymond, *Chem. Soc. Rev.* 14 (1985) 417.
- [28] B. Giner, S. Martin, H. Artigas, M. C. Lopez and C. J. Lafuente, *J. Phys. Chem. B* 110 (2006) 17683.
- [29] B. Garcia, R. Alcalde, S. Aparicio, J. M. Leal, *Phys. Chem. Chem. Phys.* 4 (2002) 5833.
- [30] M. I. Aralaguppi, T. M. Aminabhavi, S. B. Harogoppad and R. H. Balundgi, *J. Chem Eng. Data* 37 (1992) 298.
- [31] A. F. Fucaloro, *J. Chem. Educ.* 79 (2002) 865.
- [32] B. Giner, C. Lafuente, A. Villares, M. Haro and M. C. Lopez, *J. Chem. Thermodyn.* 39 (2007) 148.
- [33] A. Pineiro, P. Brocos, A. Amigo, M. Pintos and Bravo R, *Phys. Chem. Liq.* 38 (2000) 251.
- [34] G. S. Kell, C. M. Daries and J. Jarynski *Water and Aqueous Solution, Structure, Thermodynamics and Transport Process*, Ed. Horne RA, Wiley (1972).

REFERENCES OF CHAPTER-II

- [1] M. Freemantle, An introduction to ionic Liquids, Cambridge, United Kingdom: The Royal Society of Chemistry (2010).
- [2] M. Armand et al., Nat. Mater 8 (2009) 621.
- [3] R. K. T. Katakabe and M. Watanabe, Electrochemical and Solid-State Letters 10 (2007) F23.
- [4] S. Seki et. al., J. Electrochem. Soc. 154 (2007) A173.
- [5] R. F. de Souza et. al., Electrochem. Comm. 5 (2003) 728.
- [6] C. Y. H. Yang, Q. Song, Y. Xia, F. Li, Z. Chen, X. Li, T. Yi and C. Huang, Chem. Mater 18 (2006) 5173.
- [7] M. Gorlov and L. Kloo, Dalton Trans. 20 (2008) 2655.
- [8] J. L. Anderson, J. Ding, T. Welton, D. W. Armstrong, J. Am. Chem. Soc. 124 (2002), 14247.
- [9] S. Pandey, Anal. Chim. Acta 556 (2006) 38.
- [10] P. Lozano, T. De Diego, D. Carrie, M. Vaultier and J. L. Iborra, J. Mol. Catal. B 21 (2003) 9.
- [11] J. A. Laszlo and D. L. Compton, Biotechnol. Bioeng. 75 (2001) 181.
- [12] B. M. Quinn, Z. Ding, R. Moulton and A. J. Bard, Langmuir 18 (2002) 1734.
- [13] C. Lagrost, D. Carrie, M. Vaultier and P. Hapiot, J. Phys. Chem. A 107 (2003) 745.
- [14] S. Carda-Broch, A. Berthod and D. W. Armstrong, Anal. Bioanal. Chem. 375 (2003) 191.
- [15] P. Wang, S. M. Zakeeruddin, P. Comte, I. Exnar and M. Gra'tzel, J. Am. Chem. Soc. 125 (2003) 1166.
- [16] T. Welton, Chem. Rev. 99 (1999) 2071.
- [17] P. Bonhote, A. P. Dias, N. Papageorgiou, K. Kalyanasundaram and M. Gra'tzel, Inorg. Chem. 35 (1996) 1168.
- [18] C. D. Tran and S. H. P. Lacerda, Anal. Chem. 74 (2002) 5337.

- [19] P. Wasserscheid and T. Welton, *Ionic Liquids in Synthesis*, 2nd Ed., Wiley VCH: (2008).
- [20] F. Endres, A. Abbott and D. MacFarlane, *Electrodeposition from Ionic Liquids*, 1st Ed., Wiley VCH: (2008).
- [21] J. D. Holbrey, *Chimica Oggi*. 22 (2004) 35.
- [22] K. N. Marsh, J. A. Boxall and R. Lichtenthaler, *Fluid Phase Equilib.* 219 (2004) 93.
- [23] A. Heintz, *J. Chem. Thermodyn.* 37 (2005) 525.
- [24] M. J. Earle, K. R. Seddon, *Pure and Applied Chemistry* 72 (2000) 1391.
- [25] D. Chaturvedi, *Current Organic Chemistry* 15 (2011) 1239.
- [26] N. V. Plechkova and K. R. Seddon, *Chem. Soc. Rev.* 37 (2008) 123.
- [27] F. Endres and S. El Abedin Zein, *Phys. Chem. Chem. Phys.* 8 (2006) 2101.
- [28] P. Wang, S. M. Zakeeruddin, J. E. Moser and M. Graätzel, *J. Phys. Chem. B* 107 (2003) 13280.
- [29] D. Das, B. Das and D. K. Hazra, *J. Sol. Chem.* 31 (2002) 425.
- [30] C. Guha, J. M. Chakraborty, S. Karanjai and B. Das, *J. Phys. Chem. B* 107 (2003) 12814.
- [31] D. Das, B. Das and D. K. Hazra, *J. Sol. Chem.* 32 (2003) 77.
- [32] M. N. Roy, D. Nandi and D. K. Hazra, *J. Ind. Chem. Soc.* 70 (1993) 123.
- [33] O. Popvych, R. P. T. Tomkins *Nonaqueous Solution Chemistry*, Chapter 4; Wiley-Interscience: New York (1981).
- [34] A. J. Matheson, *Molecular Acoustics*; Wiley-Interscience: London (1971).
- [35] K. Mikami, *Green reactions media in organic synthesis*, Oxford, UK: Blackwell (2005).
- [36] N. V. Plechkova and K. R. Seddon, *Chem. Soc. Rev.* 37 (2008) 123.
- [37] A. Stark, K. R. Seddon and Kirk-Othmer *Encyclopedia of Chemical Technology*. Vol., *Ionic Liquids*, John Wiley & Sons, Inc. 26 (2008) 836.
- [38] V. E. Dickinson, M. E. Williams, S. M. Hendrickson, H. Masui R. W. Murray, *J. Am. Chem. Soc.* 121 (1999) 613.
- [39] B. Datta, S. Barman and M. N. Roy, *J. Mol. Liq.* 214 (2016) 264.
- [40] S. V. Dzyuba and R. A. Bartsch, *Chem. Phys. Chem.* 3 (2002) 161.

- [41] M. Freemantle, Chem. Eng. News, 76 (1998) 32.
- [42] J. F. Brennecke and E. J. Maginn, AIChE J. 47 (2001) 2384.
- [43] J. D. Holbrey and K. R. Seddon, Clean Products and Processes 1 (1999) 223.
- [44] K. R. Seddon, A. Stark and M. J. Torres, Pure Appl. Chem. 72 (2000) 2275.
- [45] E. D. Bates, R. D. Mayton, I. Ntai and J. H. Davis, J. Am. Chem. Soc. 124 (2002) 926.
- [46] P. Walden, Bull. Acad. Imper. Sci. 8 (1914) 405.
- [47] J. S. Wilkes, J.A. Levisky, R.A. Wilson and C. L. Hussey, Inorg. Chem. 21 (1982) 1263.
- [48] A. A. Fannin, D. A. Floreani, L. A. King, J.S. Landers, B. J. Piersma, D. J. Stech, R. L. Vaughn, J. S. Wilkes and J. L. Williams, J. Phys. Chem. 88 (1984) 2614.
- [49] S. E. Fry and N. J. Pienta, J. Am. Chem. Soc. 107 (1986) 6399.
- [50] J.A. Boon, J.A. Levisky, J.L. Pflug and J.S. Wilkes, J. Org. Chem. 51 (1986) 480.
- [51] J. Fuller, R. T. Carlin, H. C. De Long and D. Haworth, J. Chem. Soc., Chem. Commun. 3 (1994) 299.
- [52] J. D. Pandey and A. Yasmin, Proc. Ind. Acad. Sci. 109 (1997) 289.
- [53] J. D. Pandey, Y. Akhtar and A. K. Sharma, Ind. J. Chem. 37 (1998) 1094.
- [54] J. I. Kim, J. Phys. Chem. 82 (1978) 191.
- [55] W. Kemp, Organic spectroscopy, 3rd (ELBS) Ed., Macmillan Press: Hampshire: U.K. (1993).
- [56] J. J. Lagowski, The Chemistry of Non-Aqueous Solvents, Academic, New York, (1966).
- [57] B. E. Conway and R. G. Barradas, Chemical Physics of Ionic Solutions, Wiley: New York (1966).
- [58] D. T. Richens, The Chemistry of Aqua Ions; Wile: New York (1997).
- [59] K. Ibuki and M. Nakahara, J. Phys. Chem. 94 (1990) 8370.
- [60] A. Henni, J. H. Jonathan, T. Paitoon and C. Amit, J. Chem. Eng. Data 48 (2003) 1062.
- [61] J. Burgess, Metal Ions in Solutions; Ellis Horwood: New York (1978).

- [62] H. S. Harned and B. B. Owen, *The Physical Chemistry of Electrolytic Solutions*, Reinhold Publishing Corporation: New York (1958).
- [63] J. S. Muishead-Gould and K. J. Laidler, *Chemical Physics of Ionic Solutions*, Wiley: New York (1966).
- [64] J. F. Coetzee and C. D. Ritchie, *Solute-Solvent Interactions*, Marcel Dekker: New York (1969).
- [65] R. G. Bates, *J. Electroanal. Chem. Interfac. Electrochem.* 29 (1971) 1.
- [66] G. S. Kell, C. M. Daries and J. Jarynski, *Water and Aqueous Solutions, Structure, Thermodynamics and Transport process*, Wiley: New York (1972).
- [67] E. S. Amis and J. F. Hinton, *Solvent effects on Chemical Phenomena*, Academic: New York (1973).
- [68] A. K. Covington, T. Dickinson, *Physical Chemistry of Organic Solvent Systems*, Plenum Press: New York (1973).
- [69] J. E. Gordon, *The Organic Chemistry of Electrolyte Solutions*, Wiley-Interscience: New York (1975).
- [70] F. Franks, *Physico-Chemical processes in Mixed Aqueous Solvents*, Heinemann: London (1967).
- [71] F. Franks, *Water—A Comprehensive Treatise*, Plenum Press: New York (1973).
- [72] V. Gutmann, *Electrochim. Acta.* 21 (1967) 661.
- [73] U. Mayer and V. Gutmann, *Adv. Inorg. Chem. Radiochem.* 17 (1975) 189.
- [74] R. G. Pearson, *Hard and Soft Acids and Bases*, Strondsburgh: (1973).
- [75] G. R. Behbehani, M. Dillon, J. Symth and W. E. Waghorne, *J. Sol. Chem.* 31 (2002) 811.
- [76] C. Guha, J. M. Chakraborty, S. Karanjai and B. Das, *J. Phys. Chem. B* 107 (2003) 12814.
- [77] P. L. Jones and J. F. Pethica, *Proc. Royal Soc. Lond. A* 256 (1960) 454.
- [78] I. Prigogine and S. Garikian, *Physica.* 16 (1950) 239.
- [79] I. Prigogine and A. Belleman, *J. Chem. Phys.* 21 (1953) 561.
- [80] A. J. Treszczanowicz and G. C. Benson, *Fluid Phase Equilib.* 23 (1985) 117.
- [81] Wen-Lu Weng, *J. Chem. Eng. Data* 45 (2002) 606.
- [82] P. S. Nikam and S. J. Kharat, *J. Chem. Eng. Data* 50 (2005) 455.

- [83] R. P. Rastogi, J. Nath and J. Mishra, *J. Phys. Chem.* 71 (1966) 1277.
- [84] K. S. Pitzer and G. Mayora, *J. Phys. Chem.* 77 (1973) 2300.
- [85] D. Cook and H. C. L-Higgins, *Proc. Royal. Soc. A*209 (1951) 28.
- [86] J. S. Rowlinson, *Liquid and Liquid Mixtures*, Scientific Publications: London (1959).
- [87] J. S. Rowlinson, *The theory of regular Solutions*, *Proc. Royal. Soc. Lond. A.* 214 (1952) 192.
- [88] J. L. Lebowitz and J. S. Rowlinson, *J. Chem. Phys.* 41 (1964) 133.
- [89] J. A. Barker and D.J. Henderson, *J. Chem. Phys.* 47 (1967) 4714.
- [90] P. J. Flory, R. A. Orwoll and A. Vrij, *J. Am. Chem. Soc.* 86 (1964) 3507.
- [91] P. J. Flory and A. Abe, *J. Am. Chem. Soc.* 86 (1964) 3563.
- [92] P. J. Flory, *J. Am. Chem. Soc.* 87 (1965) 1833.
- [93] D. Patterson and G. Delmas, *Discuss. Faraday Soc.* 49 (1970) 98.
- [94] A. Heintz, *Ber. Bunsenges. J. Phys.* 89 (1985) 172.
- [95] H. Funke, *J. Pure. Appl. Chem.* 61 (1989) 1429.
- [96] A. Heintz and D. Papaioannou, *Thermochimica Acta.* 310 (1998) 69.
- [97] A. Heintz, P. K. Naicker, S. P. Verevkin, R. Pfestrof and B. Bunsenges, *J. Phys. Chem.* 102 (1998) 953.
- [98] S. Villa, N. Riesco, I. Garcia de la Fuente, J. A. Gonzalz and J. C. Cobos, *Fluid Phase Equilib.* 216 (2004) 123.
- [99] S. L. Oswal, *Thermochim. Acta.* 425 (2005) 59.
- [100] A. Pineiro, A. Amigo, R. Bravo and P. Brocos, *Fluid Phase Equilib.* 173 (2000) 211.
- [101] A. Pineiro, *Fluid Phase Equilib.* 216 (2004) 245.
- [102] M. Gepert and B. Stachowska, *J. Sol. Chem.* 35 (2006) 425.
- [103] H. S. Harned and B. B. Owen, *The Physical Chemistry of Electrolyte Solutions*, Reinhold Publishing Corporation: New York (1943).
- [104] C. Tanford, *Hydrophobic Effect: Formation of Micelles and Biological Membranes*, Wiley-Interscience: New York (1980).
- [105] E. Vikingstad, *Aggregation Process in Solutions*, Elsevier: Amsterdam (1983).

- [106] J. E. Desnoyers, M. Arel, H. Perron and C. Jolicoenn, *J. Phys. Chem.* 73 (1969) 3346.
- [107] A. K. Covington and T. Dickinson, *Physical Chemistry of Organic Solvent Systems*, Plenum Press: New York (1973).
- [108] D. K. Hazra and B. Das, *J. Chem. Eng. Data* 36 (1991) 403.
- [109] D. O. Masson, *Phil. Mag.* 8 (1929) 218.
- [110] O. Redlich and D. M. Meyer, *Chem. Rev.* 64 (1964) 221.
- [111] B. B. Owen and S. R. Brinkley, *J. Ann. N. Y. Acad. Sci.* 51 (1949) 753.
- [112] F. J. Millero, *Water and Aqueous Solutions: Structure, Thermodynamics and Transport Processes*, Wiley- Interscience: New York (1972).
- [113] R. Gopal and M. A. Siddiqi, *J. Phys. Chem.* 73 (1969) 3390.
- [114] J. Padova and I. Abrahamer, *J. Phys. Chem.* 71 (1967) 2112.
- [115] R. Gopal, D. K. Agarwal and R. Kumar, *Bull. Chem. Soc. Jpn.* 46 (1973) 1973.
- [116] R. Gopal and P. P. Rastogi, *Z. Phys. Chem. (N.F.)* 69 (1970) 1.
- [117] B. Das and D. K. Hazra, *J. Chem. Eng. Data* 36 (1991) 403.
- [118] L. G. Hepler, *Can. J. Chem.* 47 (1969) 4613.
- [119] L. G. Hepler, J. M. Stokes and R. H. Stokes, *Trans. Faraday Soc.* 61 (1965) 20.
- [120] F. H. Spedding, M. J. Pikal and B. O. Ayres, *J. Phys. Chem.* 70 (1966) 2440.
- [121] L. A. Dunn, *Trans. Faraday Soc.* 64 (1968) 2951.
- [122] R. Pogue and G. Atkinson, *J. Chem. Eng. Data* 33 (1988) 370.
- [123] B. E. Conway, R. E. Verral and J. E. Desnoyers, *Trans. Faraday Soc.* 62 (1966) 2738.
- [124] K. Uosaki, Y. Koudo and N. Tokura, *Bull. Chem. Soc. Jpn.* 45 (1972) 871.
- [125] B. S. Krumgalz, *J. Chem. Soc. Faraday Trans. I* 76 (1980) 1887.
- [126] A. W. Quin, D. F. Hoffmann and P. Munk, *J. Chem. Eng. Data* 37 (1992) 55.
- [127] Z. Atik, *J. Sol. Chem.* 33 (2004) 1447.
- [128] R. H. Stokes and R. Mills, *Viscosity of Electrolytes and Related Properties*, Pergamon: Great Britain (1965).
- [129] F. Vaslow, *Water and Aqueous Solutions*, Wiley- Interscience: New York (1972).
- [130] E. N. Da and C. Andrade, *Phil. Mag.* 17 (1934) 698.

- [131] J. Frankel, Kinetic Theory of Liquids, Dover Publications: New York (1955).
- [132] R. Furth, Proc. Camb. Phil. Soc. 37 (1941) 281.
- [133] R. Furth, Proc. Camb. Phil. Soc. 37 (1941) 252.
- [134] R. H. Ewell and H. Eyring, J. Chem. Phys. 5 (1937) 726.
- [135] F. C. Auluck, S. C. De and D. S. Kothari, Proc. Natl. Inst. Sci. 10 (1944) 397.
- [136] R. Eisenschitz, Proc. Roy. Soc. 215 (1952) 29.
- [137] J. E. Lennard-Jones and A. F. Devonshire, Proc. Roy. Soc. A 163 (1937) 53.
- [138] J. E. Lennard-Jones and A. F. Devonshire, Proc. Roy. Soc. A 165 (1938) 1.
- [139] J. A. Pople, Proc. Roy. Soc. A 215 (1952) 67.
- [140] R. Eisenchitz, Proc. Phys. Soc. A 62 (1949) 41.
- [141] J. G. Kirkwood, J. Chem. Phys. 14 (1946) 180.
- [142] J. G. Kirkwood, Theory of Liquids, Science Publishers: New York (1968).
- [143] J. E. Mayer and E. Montroll, J. Chem. Phys. 9 (1941) 2.
- [144] J. E. Mayer, J. Chem. Phys. 15 (1947) 187.
- [145] M. Born and H. S. Green, Proc. Roy. Soc. A 188 (1946) 10.
- [146] M. Born and H. S. Green, Proc. Roy. Soc. A 190 (1947) 455.
- [147] J. G. Kirkwood, F. P. Buff and M. S. Green, J. Chem. Phys. 17 (1949) 988.
- [148] J. G. Kirkwood, J. Chem. Phys. 3 (1935) 300.
- [149] J. G. Kirkwood, J. Chem. Phys. 7 (1939) 919.
- [150] J. G. Kirkwood and Z. W. Salsburg, Faraday Soc. Discuss. 15 (1953) 28.
- [151] J. G. Kirkwood and E. M. Boggs, J. Chem. Phys. 10 (1942) 394.
- [152] J. G. Kirkwood, E. K. Maun and B. J. Alder, J. Chem. Phys. 18 (1950) 1040.
- [153] J. G. Kirkwood, V. A. Lewinson and B. J. Alder, J. Chem. Phys. 20 (1952) 929.
- [154] R. W. Zwanzig, J.G. Kirkwood, K. F. Stripp and I. Oppenheim, J. Chem. Phys. 21 (1953) 2050.
- [155] S. A. Rice and P. Gray, The Statistical Mechanics of Simple Liquids. An introduction to the theory of equilibrium and Non-equilibrium Phenomena, Interscience Publishers: New York (1965).
- [156] S. A. Rice, The Kinetic Theory of Dense Fluids, Colloquium Lecturers in Pure and Applied Science, No. 9 Mobil Oil Corp. Research Lab., Dallas: Texas (1964).

- [157] S. A. Rice and A. R. Allnatt, *J. Chem. Phys.* 34 (1961) 2144.
- [158] A. R. Allnatt and S. A. Rice, *J. Chem. Phys.* 34 (1961) 2156.
- [159] H. C. Longuet-Higgins and J. P. Valleeu, *Mol. Phys.* 1 (1958) 284.
- [160] H. T. Davis, S. A. Rice and J. V. Sengers, *J. Chem. Phys.* 35 (1961) 2210.
- [161] H. T. Davis and K. D. Luks, *J. Phys. Chem.* 69 (1965) 869.
- [162] J. O. Hirschfelder, C. F. Curtis and R. B. Bird, *Molecular Theory of Gases and Liquids*, John Wiley and Sons: New York (1954), reprinted with notes added (1964).
- [163] J. D. Rogers and F. G. Brickwedde, *Physica*. 32 (1966) 1001.
- [164] J. P. Boon and G. Thomaes, *Physica*. 29 (1963) 208.
- [165] J. P. Boon and G. Thomaes, *Physica*. 28 (1962) 1074.
- [166] J. P. Boon and G. Thomaes, *Physica*. 29 (1963) 123.
- [167] J. P. Boon, J. C. Legros and G. Thomaes, *Physica*. 33 (1967) 547.
- [168] T.H. Holleman and J. Hijmans, *Physica* 28 (1962) 604.
- [169] H. Eyring, *J. Chem. Phys.* 4 (1936) 283.
- [170] H. Eyring and J. O. Hirschfelder, *J. Phys. Chem.* 41 (1937) 249.
- [171] J. F. Kincaid, H. Eyring and A. E. Stearn, *Chem. Rev.* 28 (1941) 301.
- [172] H. Eyring, T. Ree and N. Hirai, *Proc. Natl. Acad. Sci.* 44 (1958) 683.
- [173] E. J. Fuller, T. Ree and H. Eyring, *Proc. Natl. Acad. Sci.* 45 (1959) 1594.
- [174] C. M. Carlson and H. Eyring, *Proc. Natl. Acad. Sci.* 46 (1960) 333.
- [175] T. R. Thomson, H. Eyring and T. Ree, *Proc. Natl. Acad. Sci.* 46 (1960) 336.
- [176] J. Walter and H. Eyring, *J. Chem. Phys.* 9 (1941) 393.
- [177] T. Ree and H. Eyring, *Ind. Eng. Chem.* 50 (1958) 1036.
- [178] C. M. Carlson, H. Eyring and T. Ree, *Proc. Natl. Acad. Sci.* 46 (1960) 649.
- [179] H. Eyring and T. Ree, *Proc. Natl. Acad. Sci.* 47 (1961) 526.
- [180] H. Eyring and M.S. John, *Significant Liquid Structures*, John Willey & Sons: New York (1969).
- [181] Gruneisen, *Wiss, Abhandl, Physik-tech. Reich-austatt.* 4 (1905) 239.
- [182] G. Jones and M. Dole, *J. Am. Chem. Soc.* 51 (1929) 2950.
- [183] P. Debye, E. Hückel, *Z. Phys. Chem.* 24 (1923) 185.
- [184] H. Falkenhagen, M. Dole, *Phys. Z.* 30 (1929) 611.

- [185] H. Falkenhagen, E.L. Vernon, *Phys. Z.* 33 (1932) 140.
- [186] H. Falkenhagen and E. L. Vernon, *Phil. Mag.* 14 (1932) 537.
- [187] M. Kaminsky, *Discuss Faraday Soc.* 24 (1957) 171.
- [188] D. Feakins, D. J. Freemantle and K. G. Lawrence, *J. Chem. Soc. Faraday Trans. I* 70 (1974) 795.
- [189] J. Crudden, G. M. Delancy, D. Feakins, P.J. O'Relly, W. E. Waghorne and K. G. Lawrence, *J. Chem. Soc. Faraday Trans I.* 82 (1986) 2195.
- [190] A. K. Covington and T. Dickinson, *Physical Chemistry of Organic Solvent Systems*, Plenum Press: New York (1973).
- [191] H. S. Harned and B. B. Owen, *The Physical Chemistry of Electrolytic Solutions*, Reinhold Publishing Corporation: New York (1958).
- [192] M. Kaminsky, *Z. Phys. Chem.* 12 (1957) 206.
- [193] J. Desnoyers and G. Perron, *J. Sol. Chem.* 1 (1972) 199.
- [194] R. J. M. Bicknell, K. G. Lawrence and D. Feakins, *J. Chem. Soc. Faraday I* 76 (1980) 637.
- [195] R. L. Kay, T. Vituccio, C. Zawoyski and D. F. Evans, *J. Phys. Chem.* 70 (1966) 2336.
- [196] N. P. Yao and D. N. Bennion, *J. Phys. Chem.* 75 (1971) 1727.
- [197] M. Kaminsky, *Discussions Faraday Soc.* 24 (1957) 171.
- [198] D. Feakins and K. G. Lawrence, *J. Chem. Soc. A* (1966) 212.
- [199] V. Vand, *J. Phys. Chem.* 52 (1948) 277.
- [200] D. G. Thomas, *J. Colloid Sci.* 20 (1965) 267.
- [201] S. P. Moulik, *J. Ind. Chem. Soc.* 49 (1972) 483.
- [202] D. England and G. Pilling, *J. Phys. Chem.* 76 (1972) 1902.
- [203] D. E. Goldsack and R. C. Franchetto, *Can. J. Chem.* 55 (1977) 1062.
- [204] D. E. Goldsack and R. C. Franchetto, *Can. J. Chem.* 56 (1978) 1442.
- [205] C. A. Angell, *J. Phys. Chem.* 70 (1966) 2793.
- [206] C. A. Angell, *J. Chem. Phys.* 46 (1967) 4673.
- [207] K. R. Chowdhury and D. K. Majumdar, *Electrochim. Acta* 28 (1983) 23.
- [208] K. R. Chowdhury and D. K. Majumdar, *Electrochim. Acta.* 28 (1983) 597.

- [209] K. R. Chowdhury and D. K. Majumdar, *Electrochim. Acta* 29 (1984) 1371.
- [210] P. P. Rastogi, *Bull. Chem. Soc. Japan* 43 (1970) 2442.
- [211] R. Gopal and P. P. Rostogi, *Z. Phys. Chem. (N.F.)* 69 (1970) 1.
- [212] C. M. Criss, M. J. Mostroiani, *J. Phys. Chem.* 75 (1971) 2532.
- [213] K. Tamaski, Y. Ohara and Y. Isomura, *Bull. Chem. Soc. Japan* 46 (1973) 951.
- [214] P. P. Deluca and T. V. Rabagay, *J. Phys. Chem.* 79 (1975) 2493.
- [215] B. N. Prasad, N. P. Singh, M. M. Singh, *Ind. J. Chem.* 14 (1976) 322.
- [216] B. N. Prasad, M. M. Agarwal, *Ind. J. Chem.* 14 (1976) 343.
- [217] R. T. M. Bicknell, K. G. Lawrence, M. A. Scelay, D. Feakins and L. Werblan, *J. Chem. Soc. Faraday I* 72 (1976) 307.
- [218] J. M. Mcdowall, N. Martinus and C. A. Vincent, *J. Chem. Soc. Faraday I* 72 (1976) 654.
- [219] A. Sacco, G. Petrella and M. Castagnola, *J. Phys. Chem.* 80 (1976) 749.
- [220] R. L. Blokhra, Y. P. Segal, *Ind. J. Chem.* 15A (1977) 36.
- [221] N. C. Das and P. B. Das, *Ind. J. Chem.*, 15^a (1977) 826.
- [222] A. Sacco, G. Petrella, M. Della Monica and M. Castagnola, *J. Chem. Soc. Faraday I* 73 (1977) 1936.
- [223] P. K. Mandal, B. K. Seal and A. S. Basu, *Z. Phys. Chem.* 87 (1974) 295.
- [224] J. I. Kim, *J. Phys. Chem.* 82 (1978) 191.
- [225] S. K. Vijaylakshamna, *Indian J. Chem.* 17A (1979) 511.
- [226] A. Sacco, G. Petrella and M. D. Monica, *J. Chem. Soc. Faraday I* 75 (1979) 2325.
- [227] P. T. Thomson, M. Durbana, J. L. Turner and R. H. Wood, *J. Sol. Chem.* 9 (1980) 955.
- [228] K. Kurotaki and S. Kawamura, *J. Chem. Soc. Faraday I* 77 (1981) 217.
- [229] N. Martinus and C. A. Vincent, *J. Chem. Soc. Faraday Trans I* 77 (1981) 141.
- [230] A. Sacco, A. D. Giglio and A. D. Atti, *J. Chem. Soc. Faraday I*, 77 (1981) 2693.
- [231] D. S. Gill and A. N. Sharma, *J. Chem. Soc. Faraday I* 78 (1982) 475.
- [232] A. Sacco, G. Petrella, A. D. Atti and M. Castagnolo, *J. Chem. Soc. Faraday I* 78 (1982) 1507.
- [233] A. Sacco, A. D. Giglio, A. D. Atti and M. Castagnolo, *J. Chem. Soc. Faraday I* 79 (1983) 431.

- [234] K. G. Lawrence and A. Sacco, *J. Chem. Soc. Faraday I* 79 (1983) 615.
- [235] K. Miyajima, M. Sawada and M. Nakagaki, *Bull. Chem. Soc. Japan* 56 (1983) 827.
- [236] J. Doenech and S. Rivera, *J. Chem. Soc. Faraday I* 80 (1984) 1249.
- [237] D. Dasgupta, S. Das and D. K. Hazra, *Bull. Chem. Soc. Japan* 62 (1989) 1246.
- [238] S. Taniewska-Osinska and M. Jozwaik, *J. Chem. Soc. Faraday Trans I* 85 (1989) 2141.
- [239] D. Nandi and D. K. Hazra, *J. Chem. Soc. Faraday Trans I* 85 (1989) 4227.
- [240] I. Ibulci and M. Nakahara, *J. Phys. Chem.* 94 (1990) 8370-8373.
- [241] W.M. Cox and J. H. Wolfenden, *Proc. Roy. Soc. London* 145 (1934) 475.
- [242] R.W. Gurney, *Ionic Processes in Solution*, Mc Graw Hill: New York (1953).
- [243] E.R. Nightingale Jr. *J. Phys. Chem.* 63 (1959) 1381.
- [244] A. Einstein, *Ann. Phys.* 19 (1906) 289.
- [245] G.S. Benson and A.R. Gordon, *J. Chem. Phys.* 13 (1945) 473.
- [246] D. F. T. Tuan and R. M. Fuoss, *J. Phys. Chem.* 67 (1963) 1343.
- [247] C. H. Springer, J. F. Coetzee and R. L. Key, *J. Phys. Chem.* 73 (1969) 471.
- [248] G. Petrella and A. Sacco, *J. Chem. Soc. Faraday Trans. I* 74 (1978) 2070.
- [249] B.S. Krumgalz, *J. Chem. Soc. Faraday I* 76 (1980) 1275.
- [250] B.S. Krumgalz, *Russ. J. Phys. Chem.* 46 (1972) 858.
- [251] B.S. Krumgalz, *Russ. J. Phys. Chem.* 47 (1973) 956.
- [252] B.S. Krumgalz, *Russ. J. Phys. Chem.* 48 (1974) 1163.
- [253] B.S. Krumgalz, *Russ. J. Phys. Chem.* 45 (1971) 1448.
- [254] H. D. B. Jenkins and M. S. F. Pritchett, *J. Chem. Soc. Faraday I* 80 (1984) 721.
- [255] K. Fajan, *Naturwissenschaften* 9 (1921) 729.
- [256] D. F. C. Morris, *Struct. Bonding* 6 (1969) 157.
- [257] R. W. Gurney, *Ionic Processes in Solutions*, Doves:New York (1962).
- [258] H. S. Frank and W. Y. Wen, *Disc. Farad. Soc.* 24 (1957) 133-140.
- [259] Z. Asmus, *Naturforsch.* 4 (1949) 589.
- [260] M. H. Abraham, J. Liszi and E. Papp, *J. Chem. Soc. Faraday I* 78 (1982) 197.
- [261] M. H. Abraham, J. Liszi and L. Meszaros, *J. Chem. Phys.* 70 (1979) 2491.
- [262] M. H. Abraham and J. Liszi, *J. Chem. Soc. Faraday I* 76 (1980) 1219.

- [263] S. Glasstone, K.J. Laidler and H. Eyring, *The Theory of Rate Process*, McGraw Hill: New York (1941).
- [264] E. R. Nightingale and R. F. Benck, *J. Phys. Chem.* 63 (1959) 1777.
- [265] D. Feakins, D. J. Freemantle and K. G. Lawrence, *J. Chem. Soc. Faraday I* 70 (1974) 795.
- [266] R. Sinha, *J. Phys. Chem.* 44 (1940) 25.
- [267] V. Vand, *Viscosity of solutions and suspensions. I. Theory*, *J. Phys. Chem.* 52 (1948) 277.
- [268] D. G. Thomas, *J. Colloid Sci.* 20 (1965) 267.
- [269] S. P. Moulik, *J. Phys. Chem.* 72 (1968) 4682.
- [270] S. P. Moulik, *Electrochim. Acta* 17 (1972) 1491.
- [271] S. P. Moulik, *J. Indian Chem. Soc.* 49 (1972) 483.
- [272] R. J. Fort and W. R. Moore, *Trans. Faraday Soc.* 62 (1966) 1112.
- [273] G. R. Naidu and P. R. Naidu, *Ind. J. Chem.* 22A (1983) 324.
- [274] O. Redlich and A. T. Kister, *Ind. Eng. Chem.* 40 (1948) 345.
- [275] L. Pikkarainen, *J. Chem. Eng. Data* 28 (1983) 344-347.
- [276] L. Pikkarainen, *J. Chem. Eng. Data* 28 (1983) 381-383.
- [277] L. S. Manjeshwar and T. Aminabhavi, *J. Chem. Eng. Data* 33 (1988) 184.
- [278] K. P. Rao and K. S. Reddy, *J. Chem. Eng. Data* 33 (1988) 130.
- [279] S. Glasstone, K. J. Laidler and H. Eyring, *The Theory of Rate Process*, McGraw Hill: New York (1941).
- [280] D. S. Gill, T. S. Kaur, H. Kaur, I. M. Joshi and J. Singh, *J. Chem. Soc. Faraday Trans.* 89 (1993) 1737.
- [281] J. G. Mathieson and B. E. Conway, *J. Sol. Chem.* 3 (1974) 455-477.
- [282] S. Bhowmik and R. K. Mohanty, *Ind. J. Chem.* 25A (1986) 416.
- [283] M. V. Kaulgud and K. S. Mohan Rao, *Ind. J. Chem.* 27A (1988) 12.
- [284] K. J. Patil, A. B. Wazalwar and G. R. Mehta, *Ind. J. Chem.* 27A (1988) 799.
- [285] M. Iqbal and R. E. Verrall, *Can. J. Chem.* 67 (1989) 727-735.
- [286] M. Kikuchi, M. Sakurai and K. Nitta, *J. Chem. Eng. Data* 41 (1996) 1439.
- [287] B. E. Conway and R. E. Verral, *J. Phys. Chem.* 70 (1966) 3952.
- [288] K. Gekko and H. Noguchi, *J. Phys. Chem.* 83 (1979) 2706.

- [289] W. L. Masterson, *J. Chem. Phys.* 22 (1954) 1830.
- [290] L. G. Hepler, *Can. J. Chem.* 47 (1969) 4613.
- [291] M. V. Kaulgud and K. J. Patil, *J. Phys. Chem.* 80 (1976) 138.
- [292] K. J. Patil, G. R. Mehta and R. K. Chandewar, *Ind. J. Chem.* 25A (1986) 1147.
- [293] C. Lafuente, B. Ginar, A. Villares, I. Gascon and P. Cea, *Int. J. Thermophys.* 25 (2004) 1735.
- [294] G. Douheret, A. Pal and M. I. Davis, *J. Chem. Thermodyn.* 22 (1990) 99.
- [295] I. Gascon, S. Martin, P. Cea, M. C. Lopez and F. M. Royo, *J. Sol. Chem.* 31 (2002) 905.
- [296] R. Mehra and M. Pancholi, *J. Ind. Chem. Soc.* 82 (2005) 791.
- [297] S. L. Oswal and K. D. Prajapati, *J. Chem. Eng. Data.* 43 (1998) 367.
- [298] K. Hsu-Chen and T. Chein-Hsium, *J. Chem. Eng. Data* 50 (2005) 608-615.
- [299] D. W. Marquardt, *J. Soc. Ind. Appl. Math.* 11 (1963) 431.
- [300] L. Onsager, *Z. Phys. Chem.*, 1927, 28, 277.
- [301] R. M. Fuoss, *Rev. Pure Appl. Chem.* 18 (1968) 125.
- [302] E. Pitts, *Proc. Roy. Soc.*, 217A (1953) 43.
- [303] R. M. Fuoss, L. Onsager, *J. Phys. Chem.* 61 (1957) 668.
- [304] R. M. Fuoss, *Chemical Physics of Ionic Solutions*, Wiley: New York (1966).
- [305] E. Pitts, R. E. Tabor and J. Daly, *Trans. Faraday Soc.* 65 (1969) 849.
- [306] R. M. Fuoss and K. L. Hsia, *Proc. Natl. Acad. Sci.* 57 (1967) 1550.
- [307] R. M. Fuoss and K. L. Hsia, *J. Am. Chem. Soc.* 90 (1968) 3055.
- [308] R. Fernandez-Prini and J. E. Prue, *Z. Phys. Chem.* 228 (1965) 373.
- [309] R. Fernandez-Prini, *J.E. Prue. Z. Phys. Chem.* 228 (1965) 473.
- [310] D. F. Evans and R. L. Kay, *J. Phys. Chem.* 70 (1966) 366.
- [311] D. F. Arrington and E. Griswold, *J. Phys. Chem.* 74 (1970) 123.
- [312] R. M. Fuoss and C. A. Kraus, *J. Am. Chem. Soc.* 55 (1933) 476.
- [313] T. Shedlovsky, *J. Franklin, Instt.* 225 (1938) 739.
- [314] J. C. Justice, *J. Chem. Phys.* 65 (1968) 353.
- [315] J. C. Justice, R. Bury and C. Treiner, *J. Chem. Phys.* 65 (1968) 1708.

- [316] R. M. Fuoss and F. Accascina, *Electrolytic Conductance*, Wiley: New York (1959).
- [317] N. K. Bjerrum and Dan. Vidensk. Selek. Mat. Fys. Medd. 7 (1926) 9.
- [318] M. Tissier and G. Douheret, *J. Soln. Chem.* 7 (1978) 87.
- [319] R. Fernandez-Prini, *Trans. Faraday Soc.* 62 (1966) 1257.
- [320] R. M. Fuoss and L. Onsager, *J. Phys. Chem.* 66 (1962) 1722.
- [321] R. M. Fuoss and L. Onsager, *J. Phys. Chem.* 67 (1963) 621.
- [322] R. M. Fuoss, *J. Phys. Chem.* 79 (1975) 525.
- [323] P. C. Carman and D. P. Laurie, *J. Sol. Chem.* 5 (1976) 457.
- [324] R. M. Fuoss, *J. Phys. Chem.* 81 (1977) 1829.
- [325] R. M. Fuoss, *Proc. Nat. Acad. Sci.* 75 (1978) 16.
- [326] R. M. Fuoss, *J. Phys. Chem.* 82 (1978) 2427.
- [327] W. H. Lee and R. J. Wheaton, *J. Chem. Soc. Faraday II* 74 (1978) 743.
- [328] W. H. Lee and R. J. Wheaton, *J. Chem. Soc. Faraday Trans. II* 74 (1978) 1456.
- [329] W. H. Lee and R. J. Wheaton, *J. Chem. Soc. Faraday Trans. I* 75 (1979) 1128.
- [330] W. H. Lee and R. J. Wheaton, *J. Chem. Soc. Faraday Trans. II* (1978) 1456.
- [331] A. D. Pethybridge and S. S. Taba, *J. Chem. Soc. Faraday I* 76 (1980) 368.
- [332] M. Bester-Rogac, R. Neueder and J. Barthel, *J. Solution Chem.* 28 (1999) 1071.
- [333] H. S. Harned and B. B. Owen, *The Physical Chemistry of Electrolytic Solutions*, Reinhold Publishing Corporation: New York (1964).
- [334] E. Balaguruswami, *Numerical Methods*, Tata McGraw-Hill Publishing Company: New Delhi (2007).
- [335] M. N. Roy, B. Sinha and V. K. Dakua, *Pak. J. Sci. Ind. Res.* 49 (2006) 153.
- [336] B. S. Krumgalz, *J. Chem. Soc. Faraday I* 79 (1983) 571-587.
- [337] B. S. Krumgalz, *J. Chem. Soc. Faraday I* 81 (1985) 241-243.
- [338] P. Walden, H. Ulich, D. Bush, *Z. Phys. Chem.* 123 (1926) 429.
- [339] R. M. Fuoss and E. Hirsch, *J. Am. Chem. Soc.* 82 (1960) 1018.
- [340] S. Takezawa, Y. Kondo and N. Tokura, *J. Phys. Chem.* 77 (1973) 2133.
- [341] D. S. Gill, *J. Chem. Soc. Faraday I* 77 (1981) 751.
- [342] D. S. Gill, N. Kumari and M. S. Chauhan, *J. Chem. Soc. Farada Trans I* 81 (1985) 687.

- [343] M. A. Coplan and R. M. Fuoss, *J. Phys. Chem.* (1964) 1177.
- [344] J. F. Coetzee and G. P. Cunningham, *J. Am. Chem. Soc.* 87 (1965) 2529.
- [345] R. H. Stokes and R. A. Robinson, *Trans. Faraday Soc.* 53 (1957) 301.
- [346] M. Born, *Z. Phys. Chem.* 1 (1920) 221.
- [347] R. H. Boyd, *J. Chem. Phys.* 35 (1961) 1281.
- [348] R. Zwanzig, *J. Chem. Phys.* 38 (1963) 1603.
- [349] E. J. Passeron, *J. Phys. Chem.* 68 (1964) 2728.
- [350] P. Walden, *Z. Phys. Chem.* 55 (1906) 207.
- [351] P. Walden, *Z. Phys. Chem.* 78 (1912) 257.
- [352] R. A. Robinson, R.H. Stokes, *Electrolyte Solutions*, Butterworths: London (1959).
- [353] R. Gopal and M. M. Hussain, *J. Ind. Chem. Soc.* 40 (1963) 981.
- [354] L. G. Longworth, *J. Phys. Chem.* 67 (1963) 689.
- [355] M. Della Monica, U. Lamauna and L. Seutatore, *J. Phys. Chem.* 72 (1968) 2124.
- [356] S. Broersma, *J. Chem. Phys.* 28 (1958) 1158.
- [357] D. G. Miller, *J. Phys. Chem.* 64 (1960) 1598.
- [358] G. J. Hills, *Chemical Physics of Ionic Solutions*, Wiley: New York (1966).
- [359] R. H. Stokes and I. A. Weeks, *Conductances of electrolytes in solutions of the sucrose polymer Ficoll*, *Australian J. Chem.* 17 (1964) 304.
- [360] R. H. Stokes, *The Structure of Electrolytic Solutions*, Wiley: New York (1959).
- [361] D. S. Gill, *J. Chem. Soc. Faraday I* 77 (1981) 751.
- [362] R. Zwanzig, *J. Chem. Phys.* 52 (1970) 3625.
- [363] H. S. Franks, *Chemical Physics of Ionic Solutions*, Wiley; New York (1966).
- [364] G. Atkinson and S. K. Kor, *J. Phys. Chem.* 69 (1965) 128.
- [365] R. L. Kay, G. P. Cunningham and D.F. Evans, *Hydrogen bonded Solvent Systems*, Taylor and Francis: London (1968).
- [366] R. L. Kay, B. J. Hales and G. P. Cunningham, *J. Phys. Chem.* 71 (1967) 3925.
- [367] R. L. Kay, C. Zawoyski and D. F. Evans, *J. Phys. Chem.* 69 (1965) 4208.
- [368] D. F. Evans and J. L. Broadwater, *J. Phys. Chem.* 72 (1968) 1037.

- [369] M. Spiro, *Physical Chemistry of Organic Solvent Systems*, Plenum Press: New York (1973).
- [370] R. Fernandez-Prini and G. Atkinson, *J. Phys. Chem.* 75 (1971) 239.
- [371] L. Bahadur and M. V. Ramanamurti, *J. Chem. Soc. Faraday I* 76 (1980) 1409.
- [372] L. Bahadur and M. V. Ramanamurti, *J. Electrochem. Soc.* 128 (1981) 339.
- [373] L. Bahadur and M. V. Ramanamurti, *Can. J. Chem.* 62 (1984) 1051.
- [374] J. L. Broadwater and R. L. Kay, *J. Phys. Chem.* 74 (1970) 3802.
- [375] S. Das and D. K. Hazra, *Indian J. Chem.* 274 (1988) 1073.
- [376] S. Das, D.K. Hazra, *J. Ind. Chem. Soc. LXV* (1988) 100.
- [377] R. L. Kay and J. L. Broadwater, *Electrochim. Acta* 16 (1971) 667.
- [378] R. L. Kay and J. L. Broadwater, *J. Sol. Chem.* 5 (1976) 57.
- [379] A. D. Aprano and R. M. Fuoss, *J. Phys. Chem.* 67 (1963) 1704.
- [380] P. Hemmes, *J. Phys. Chem.* 78 (1974) 907.
- [381] J. Hubbard and L. Onsager, *Ind. J. Chem. Phys.* 67 (1977) 4850.
- [382] N. Islam, M. R. Islam, M. Ahmed, *Z. Phys. Chem.* 262 (1981) 129.
- [383] D. S. Gill, A. N. Sharma and H. Schneider, *J. Chem. Soc. Faraday I* 78 (1982) 465.
- [384] Kablukov, Hydrogen chloride in ether and in benzene, *Z. 336hysic. Chem.* 4 (1889) 430.
- [385] Plotnikov, Complexes in ether, *Z. 336hysic. Chem.* 67 (1906) 502
- [386] Walden, *Z. 336hysic. Chem.* 147 (1930) 1.
- [387] R. M. Fuoss and F. Accascina, *Electrolytic Conductance*, Interscience: New York (1959).
- [388] R. M. Fuoss and C. A. Kraus, *J. Am. Chem. Soc.* 55 (1933) 2387.
- [389] R. M. Fuoss and E. Hirsch, *J. Am. Chem. Soc.* 82 (1960) 1013.
- [390] A. Sinha and M. N. Roy, *Phys. Chem. Liq.* 45 (2007) 67.
- [391] M. Delsignore, H. Farber and S. Petrucci, *J. Phys. Chem.* 89 (1985) 4968.
- [392] C. J. Cramer and D. G. Truhlar, *J. Am. Chem. Soc.* 113 (1991) 8305.
- [393] D. J. Giesen, J. W. Stores, C. J. Cramer and D. G. Truhlar, *J. Am. Chem. Soc.* 117 (1995) 1057.
- [394] C. J. Cramer and D. G. Truhlar, *J. Org. Chem.* 61 (1996) 8720.
- [395] C. J. Cramer and D. G. Truhlar, *Erratum.* 101 (1999) 309.

- [396] G. D. Hawkins, C. J. Cramer and D. G. Truhlar, *J. Phys. Chem. B* 101 (1997) 7147.
- [397] G. D. Hawkins, C. J. Cramer and D. G. Truhlar, *J. Phys. Chem. B* 102 (1998) 3257.
- [398] A. Gil-Villegas, A. Galindo, P. J. Whitehead, S. J. Mills, G. Jackson and A. N. Burgess, *J. Chem. Phys.* 106 (1997) 4168.
- [399] A. Galindo, L. A. Davies, A. Gil-Villegas and G. Jackson, *Mol. Phys.* 93 (1998) 241.
- [400] M. Roses, C. Rafols, J. Ortega and E. Bosch, *J. Chem. Soc. Perkin Trans. 2* (1995) 1607.
- [401] O. Bernard, W. Kunz, P. Turq and L. Blum, *J. Phys. Chem.* 96 (1992) 3833.
- [402] S. Durand-Vidal, P. Turq and O. Bernard, *J. Phys. Chem.* 100 (1996) 17345.
- [403] H. L. Bianchi, I. Dujovne and R. Fernandez-Prini, *J. Sol. Chem.* 29 (2000) 237.
- [404] A. Chandra and B. Bagchi, *J. Phys. Chem. B* 104 (2000) 9067.
- [405] Y.Y. Fialkov, G.N. Fenerly, *Russ. Inorg. Chem.* 9 (1964) 1205.
- [406] Y.Y. Fialkov, *Russ. J. Phys. Chem* 41 (1967) 398.
- [407] A. Ali and M. Tariq, *Chem. Eng. Comm.* 195 (2007) 43,
- [408] S. C. Bhatia, R. Bhatia and G. P. Dubuey, *J. Mol. Liq.* 145 (2009) 88.
- [409] S. L. Oswal, P.P. Palsanwala, *Acoust. Lett.* 13 (1989) 66.
- [410] J. D. Pandey, P. Jain and V. Vyas, *Can. J. Chem.* 72 (1994) 2486.
- [411] W. Heller, *J. Phys. Chem.* 69 (1965) 1123.
- [412] V. Minkin, O. Osipov and Y. Zhdanov, *Dipole Moments in Organic Chemistry*, Plenum Press: New York (1970).
- [413] O. Redlich and A. Kister, *Ind. Eng. Chem.* 40 (1948) 345.
- [414] J. F. Comesaña, J. J. Otero, E. Camesella and A. Correa, *J. Chem. Eng. Data* 46 (2001) 1153.

REFERENCES OF CHAPTER-III

- [1] N. Saha and B. Das, *J. Chem. Eng. Data.* 42 (1997) 227.
- [2] M. G. Prolongo, R. M. Masegosa, I. H. Fuentes and A. Horta, *J. Phys. Chem.* 88 (1984) 2163.

- [3] D. D. Perrin and W. L. F. Armarego, *Purification of Laboratory Chemicals*, 3rd Ed., Pergamon Press: Oxford, England (1988).
- [4] M. N. Roy, D. Nandi and D. K. Hazra, *J. Indian Chem. Soc.* 70 (1993) 123.
- [5] M. N. Roy, R. Dey and A. Jha, *J. Chem. Eng. Data* 46 (2001) 1327.
- [6] A. Sinha and M. N. Roy, *Phys. Chem. Liq.* 44 (2006) 303.
- [7] C. Redlich, W. S. Beckett, J. Sparer, K. W. Barwick, C. A. Riely, H. Miller, S. L. Sigal, S. L. Shalat and M. R. Cullen, *Annals of Internal Medicine* 108 (1988) 680.
- [8] Clayden, *Organic Chemistry*. Oxford: Oxford University Press (2001).
- [9] S. Zen and E. Kaji, *Org. Synth.* 6 (1988) 503.
- [10] B. Winter, R. Weber, P. M. Schmidt and I. V. Hertel, *J. Phys. Chem. B* 108 (2004) 14558.
- [11] H. Bergersen, R. R. T. Marinho, W. Pokapanich, A. Lindblad, O. Björneholm, L. J. Sæthre and G. Öhrwall, *Phys. Condens. Matter* 19 (2007) 326101.
- [12] X. Li, X. Xu, C. Zhou, *Chem. Commun.* 48 (2012) 12240.
- [13] Z. J. Liu, J. Zhang, S. L. Chen, E. Shi, Y. Xu and X. B. Wan, *Angew. Chem., Int. Ed.*, 51 (2012) 3231.
- [14] D. Nolan, R. Darcy and B. J. Ravoo, *Langmuir* 19 (2003) 4469.
- [15] T. Welton, *Chem. Rev.* 99 (1999) 2071.
- [16] H. M. Zerth, N. M. Leonard and R. S. Mohan, *Org. Lett.* 5 (2003) 55.
- [17] J. Dupont, R. F. de Souza and P. A. Z. Suarez, *Chem. Rev.* 102 (2002) 3667-3692.
- [18] R. G. Weiss, *Tetrahedron* 44 (1988) 3413.
- [19] H. Jervis, M. E. Raimondi, R. Raja, T. Maschmeyer, J. M. Seddon, D. W. Bruce, *Chem. Commun.* 5 (1999) 2031.
- [20] B. M. Quinn, Z. Ding, R. Moulton and A. J. Bard, *Langmuir* 18 (2002) 1734.
- [21] C. Lagrost, D. Carrie, M. Vaultier and P. Hapiot, *J. Phys. Chem. A* 107 (2003) 745.
- [22] S. Carda-Broch, A. Berthod and D. W. Armstrong, *Anal. Bioanal. Chem.* 375 (2003) 191.
- [23] P. Wang, S. M. Zakeeruddin, P. Comte, I. Exnar and M. Graätzel, *J. Am. Chem. Soc.* 125 (2003) 1166.
- [24] J. E. Jr. Lind, J. J. Zwolenik and R. M. Fuoss, *J. Am. Chem. Soc.* 81 (1959) 1557.
- [25] M. N. Roy, A. Banerjee and R. K. Das, *J. Chem. Thermodyn.* 41 (2009) 1187.

- [26] B. Das and N. Saha, *J. Chem. Eng. Data* 45 (2000) 353.
- [27] I. M. Abdulagatov and N. D. Azizov, *Fluid Phase Equilib.* 240 (2006) 204.
- [28] *Refractometry: Theory, Electronic document*, www2.ups.edu/faculty/hanson/labtechniques/.../theory.htm. accessed January 21, 2010.

REFERENCES OF CHAPTER-IV

- [1] C. G. Janz, R. P. T. Tomkins, *Non-aqueous Electrolytes Handbook*, Vol. 2, Academic Press: New York (1973).
- [2] D. Aurbach, *Non-aqueous Electrochemistry*, Marcel Dekker, Inc: New York (1999).
- [3] J. A. Krom, J. T. Petty, A. Streitwieser, *J. Am. Chem. Soc.* 115 (1993) 8024.
- [4] D. Das, B. Das, D. K. Hazra, *J. Solution Chem.* 31 (2002) 425.
- [5] C. Guha, J. M. Chakraborty, S. Karanjai, B. Das, *Phys. Chem. B*, 107 (2003) 12814.
- [6] D. Das, B. Das, D. K. Hazra, *J. Solution Chem.* 32 (2003) 77.
- [7] M. N. Roy, D. Nandi, D. K. Hazra, *J. Indian Chem. Soc.* 70 (1993) 123.
- [8] M. N. Roy, B. Sinha, V. K. Dakua, A. Sinha, *Pak. J. Sci. Ind. Res.* 49 (2006) 153.
- [9] B. Das, N. Saha, *J. Chem. Eng. Data* 45 (2000) 2.
- [10] M. N. Roy, P. Pradhan, R. K. Das, P. G. Guha, B. Sinha, *J. Chem. Eng. Data* 53 (2008) 1417.
- [11] R. Chanda, M. N. Roy, *Fluid Phase Equilib.* 269 (2008) 134.
- [12] Z. Chen, M. Hojo, *J. Phys. Chem. B* 101 (1997) 10896.
- [13] D. Parvatalu, A.K. Srivastava, *J. Chem. Eng. Data* 48 (2003) 608.
- [14] F. J. Millero, In *Structure and Transport Process in Water and Aqueous Solutions*; Horne, R. A., Ed.; Wiley: New York (1972).
- [15] D. D. Perrin, W. L. F. Armarego, *Purification of laboratory chemicals*, 3rd ed.; Pergamon Press: Oxford (1988).
- [16] P. Rohdewald, M. Moldner, *J. Phys. Chem.* 77 (1973) 373.
- [17] J. E. Lind Jr., J. J. Zwolenik, R. M. Fuoss, *J. Am. Chem. Soc.* 81 (1959) 1557.
- [18] R. M. Fuoss, C. A. Kraus, *J. Am. Chem. Soc.* 55 (1933) 2387.
- [19] Y. Harada, M. Salamon, S. Petrucci, *J. Phys. Chem.* 89 (1985) 2006.

- [20] B. S. Krumgalz, *J. Chem. Soc. Faraday. Trans I*, 79 (1983) 571.
- [21] M. Delsignore, H. Farber, *J. Phys. Chem.* 89 (1985) 4968.
- [22] E. Hirsch, R.M. Fuoss, *J. Am. Chem. Soc.* 82 (1960) 1013.
- [23] D. Nandi, S. Das, D.K. Hazra, *Ind. J. Chem. A* 27 (1988) 574.
- [24] R. M. Fuoss, *J. Phys. Chem.*, 82 (1978) 2427.
- [25] B. Per, *Acta Chem. Scand.* 31(A) (1977) 869.
- [26] D. S. Gill, M. S. Chauhan, *Z. Phys. Chem. NF. Z. Phys. Chem. NF.* 140 (1984) 139.
- [27] J. Barthel, M. B. Rogac, R. Neueder, *J. Solution Chem.* 28 (1999) 1071.
- [28] M. N. Roy, B. Sinha, V. K. Dakua, *J. Chem. Eng. Data* 51 (2006) 590.
- [29] D. O. Masson, *Philos. Mag.* 8 (1929) 218.
- [30] G. Jones, M. Dole, *J. Am. Chem. Soc.* 51 (1929) 2950.
- [31] F. J. Millero, A. Lo Surdo, C. Shin, *J. Phys. Chem.* 82 (1978) 784.

REFERENCES OF CHAPTER-V

- [1] C. G. Janz, R. P. T. Tomkins. *Non-aqueous Electrolytes Handbook*. Vol. 2, Academic Press: New York (1973).
- [2] D. Aurbach. *Non-aqueous Electrochemistry*. Marcel Dekker, Inc: New York (1999).
- [3] J. A. Krom, J. T. Petty, A. Streitwieser. *J. Am. Chem. Soc.* 115 (1993) 8024.
- [4] A. K. Covington, T. Dickinson. *Physical Chemistry of Organic Solvent Systems*. Plenum: New York (1973).
- [5] A. P. Abbott, D. J. Schiffrin, *J. Chem. Soc. Faraday Trans. I.* 86 (1990) 1453.
- [6] M. N. Roy, D. Nandi, D. K. Hazra, *J. Indian Chem. Soc.* 70 (1993) 123.
- [7] M. Solomon, M.C. Uchiyama. *J. Sol. Chem.* 16 (1987) 21.
- [8] F. J. Millero. In *Structure and Transport Process in Water and Aqueous Solutions*. Horne, R. A., Ed.; Wiley: New York (1972).
- [9] D. D. Perrin, W.L.F. Armarego. *Purification of laboratory chemicals*, 3rd ed. Pergamon Press: Oxford (1988).
- [10] C. Zhao, P. Ma, J. Li, *J. Chem. Thermodyn.* 37 (2005) 37.

- [11] J. E. Lind Jr., J.J. Zwolenik, R.M. Fuoss, *J. Am. Chem. Soc.* 81 (1959) 1557.
- [12] http://www.chemicalbook.com/ChemicalProductProperty_EN_CB6854698.htm
[cited 2013 Sep 12].
- [13] <http://www.microkat.gr/msds/o-toluidine.htm> [cited 2013 Sep 12].
- [14] http://www.rafoeg.de/20,Dokumentenarchiv/20,Daten/dielectric_chart.pdf
[cited 2013 Sep 12].
- [15] S. Singh, B. P. S. Sethi, R. C. Katyal, V. K. Rattan, *J. Chem. Eng. Data.* 49 (2004) 1373-1375.
- [16] O. Ciocirlan, O. Iulian, *J. Serb. Chem. Soc.* 74 (3) (2009) 317-329.
- [17] http://www.chemicalbook.com/ChemicalProductProperty_EN_CB1854572.htm
[cited 2013
- [18] <http://www.microkat.gr/msds/2-nitrotoluene.htm> [cited 2013 Sep 12].
- [19] R.M. Fuoss, C.A. Kraus, *J. Am. Chem. Soc.* 55 (1933) 2387.
- [20] Y. Harada, M. Salamon, S. Petrucci, *J. Phys. Chem.* 89 (1985) 2006.
- [21] B. S. Krungalz, *J. Chem. Soc. Faraday Trans.* 79 (1983) 571.
- [22] M. Delsignore, H. Farber, S. Petrucci, *J. Phys. Chem.* 89 (1985) 4968.
- [23] E. Hirsch, R.M. Fuoss, *J. Am. Chem. Soc.* 82 (1960) 1013.
- [24] M. N. Roy, R. Chanda, A. Bhattacharjee, *Fluid Phase Equilib.* 280 (2009) 76.
- [25] M. N. Roy, A. Sinha, *J. Phy. Chem. Liq.* 45 (2007) 67.
- [26] M. N. Roy, R. Chanda, *Fluid Phase Equilib.* 269 (2008) 134.
- [27] R. M. Fuoss, *J. Phys. Chem.* 82 (1978) 2427.
- [28] B. Per, *Acta Chem. Scand.* 31(A) (1977) 869.
- [29] R. Dewan, M. N. Roy, 54 (2012) 28.
- [30] D. S. Gill, M. S. Chauhan, *Z. Phys. Chem. NF.* 140 (1984) 139.
- [31] J. Barthel, M. B. Rogac, R. Neueder, *J. Solution Chem.* 28 (1999) 1071.
- [32] S. R. C. Hughes, D. H. Price. *Inorg. Phys. Theor. A* (1966) 1993.
- [33] M. N. Roy, B. Sinha, V. K. Dakua, *J. Chem. Eng. Data.* 51 (2006) 590.
- [34] D.O. Masson, *Philos. Mag.* 8 (1929) 218.
- [35] G. Jones, M. Dole, *J. Am Chem. Soc.* 51 (1929) 2950.
- [36] B. Sinha, P. K. Roy, D. K. Sarkar, D. Brahman, *J. Chem. Thermodyn.* 42 (2010) 380.

- [37] F.J. Millero, A. Lo Surdo, C. Shin, *J. Phys. Chem.* 82 (1978) 784.
[38] M. N. Roy, D. Ekka, I. Banik, A. Majumdar, *Thermochemica Acta* 547 (2012) 89.

REFERENCES OF CHAPTER-VI

- [1] J. L. Anderson, J. Ding, T. Welton, D. W. Armstrong, *J. Am. Chem. Soc.* 124 (2002) 14247.
[2] S. Pandey, *Anal. Chim. Acta.* 556 (2006) 38.
[3] T. Welton, *Chem. Rev.* 99 (1999) 2071.
[4] P. Bonhote, A. P. Dias, N. Papageorgiou, K. Kalyanasundaram, M. Graätzel, *Inorg. Chem.* 35 (1996) 1168.
[5] C. D. Tran, S. H. P. Lacerda, *Anal. Chem.* 74 (2002) 5337.
[6] K. Zhuo, Y. Chen, J. Chen, G. Bai, J. Wang, *Phys. Chem. Chem. Phys.* 13 (2011) 14542.
[7] B. Datta, S. Barman, M. N. Roy, *J. Mol. Liq.* 214 (2016) 264.
[8] A. Bhattacharjee, M. N. Roy, *Phys. Chem. Chem. Phys.* 12 (2010) 14534.
[9] D. Ekka, M. N. Roy, *J. Phys. Chem. B* 116 (2012) 11687.
[10] J. E. Lind Jr., J.J. Zwolenik, R.M. Fuoss, *J. Am. Chem. Soc.* 81 (1959) 1557.
[11] M. N. Roy, T. Ray, M. C. Roy, B. Datta, *RSC Adv.* 4 (2014) 62244.
[12] L. Yu, Y. Zhu, X.G. Hu, X. H. Pang, M. W. Zhao, *Fluid Phase Equilib.* 252 (2007) 28.
[13] A. Pal, H. Kumar, R. Maan, H. K. Sharma, S. Sharma, *J. Chem. Thermodyn.* 91 (2015) 146.
[14] R. M. Fuoss, *J. Phy. Chem.* 77 (1980) 34.
[15] P. Beronius, *Acta Chem. Scand.* 31(A) (1977) 869.
[16] R. Dewan, M. N. Roy, *J. Chem. Thermodyn.* 54 (2012) 28.
[17] D. S. Gill, M. S. Chauhan, *Z. Phys.* 140 (1984) 139.
[18] H. Shekaari, Y. Mansoorib, A. Kazempour, *Electrochimica Acta* 67 (2012) 104.
[19] J. Barthel, M. B. Rogac, R. Neueder, *J. Soln. Chem.* 28 (1999) 1071.
[20] H. Shekaari, A. Kazempour, *Electrochimica Acta* 80 (2012) 196.
[21] D. O. Masson, *Phil. Magaz.* 8 (1929) 218.
[22] B. Datta and M. N. Roy, *Phys. Chem. Liq.* 53 (2015) 574.

- [23] R. Dewan, B. Datta, M. C. Roy, M. N. Roy, *Fluid Phase Equilib.* 358 (2013) 233.
- [24] H. Shekaari, A. Kazempour, Z. Ghasedi-Khajeh, *Fluid Phase Equilib.* 316 (2012) 102.
- [25] H. Shekaari, A. Kazempour, *Fluid Phase Equilib.* 309 (2011) 1.
- [26] P. K. Banipal, T. S. Banipal, J. C. Ahluwalia, B. S. Lark, *J. Chem. Thermodyn.* 34 (2002) 1825.
- [27] H. Kumar, I. Behal, M. Singla, *J. Chem. Thermodyn.* 95 (2016) 1.
- [28] A. Pal, N. Chauhan, *Ind. J. Chem.* 48(A) (2009) 1069.
- [29] R. W. Gurney, *Ionic Processes in Solution*, McGraw Hill, New York (1953).
- [30] A. K. Covington and T. Dickinson, *Physical chemistry of organic solvent systems*, Plenum, New York (1973).
- [31] K. B. Belibagli, E. Agranci, *J. Solution Chem.* 19 (1990) 867.
- [32] M. N. Roy, R. Chanda, R. K. Das, D. Ekka, *J. Chem. Eng. Data.* 56 (2011) 3285.
- [33] L. G. Helper, *Canad. J. Chem.* 47 (1969) 4613.
- [34] N. Dey, B. K. Saikia, I. Haque, *Canad. J. Chem.* 58 (1980) 1512.
- [35] H. Shekaari, A. Kazempourb, M. Khoshalhan, *Phys. Chem. Chem. Phys.* 17 (2015) 2179.
- [36] G. Jones, M. Dole, *J. Am. Chem. Soc.* 51 (1929) 2950.
- [37] F. J. Millero, *Chem. Rev.* 71 (1971) 147.
- [38] A. Roy, S. Saha, M. N. Roy, *Fluid Phase Equilib.* 425 (2016) 252.
- [39] I. Banik, M. N. Roy, *J. Mol. Liq.* 169 (2012) 8.
- [40] A. Ali, S. Hyder, S. Sabir, D. Chand, A. K. Nain, *J. Chem. Thermodyn.* 38 (2006) 136.
- [41] T. Ray, M. N. Roy, *RSC Adv.* 5 (2015) 89431.
- [42] R. C. Remsing, I. D. Petrik, Z. Liuc, G. Moyna, *Phys. Chem. Chem. Phys.* 12 (2010) 14827.
- [43] L. Jia, C. M. Pedersen, Y. Qiao, T. Deng, P. Zuo, W. Ge, Z. Qin, X. Hou, Y. Wang, *Phys. Chem. Chem. Phys.* 17 (2015) 23173.
- [44] B. A. Marekha, O. N. Kalugin, M. Briac, A. Idrissi, *Phys. Chem. Chem. Phys.* 17 (2015) 23183.

[45] M. N. Roy, A. Roy, S. Saha, Carbohydrate Polymers. 151 (2016) 458.

REFERENCES OF CHAPTER-VII

- [1] T. Welton, Chemical Review, 99 (1999) 2071.
- [2] M. J. Earle, K. R. Seddon, Pure Appl. Chem. 72 (2000) 1391.
- [3] J. Dupont, R. F. de Souza, P. A. Z. Suarez, Chem. Rev. 102 (2002) 3667.
- [4] N. V. Plechkova, K. R. Seddon, Chem. Soc. Rev. 37 (2008) 123.
- [5] F. Endres, S. El Abedin Zein, Phys. Chem. Chem. Phys. 8 (2006) 2101.
- [6] P. Wang, S. M. Zakeeruddin, J. E. Moser, M. Graätzel, J. Phys. Chem. B, 107 (2003) 13280.
- [7] D. Das, B. Das, D. K. Hazra, J. Sol. Chem. 31 (2002) 425.
- [8] C. Guha, J. M. Chakraborty, S. Karanjai, B. Das J. Phys. Chem. B, 107 (2003) 12814.
- [9] D. Das, B. Das, D. K. Hazra, J. Sol. Chem. 32 (2003) 77.
- [10] M. N. Roy, D. Nandi, D. K. Hazra, J Ind. Chem. Soc. 70 (1993) 123.
- [11] O. Popvyeh, R. P. T. Tomkins Nonaqueous Solution Chemistry, Chapter 4; Wiley-Interscience: New York (1981).
- [12] A. J. Matheson Molecular Acoustics; Wiley-Interscience: London (1971).
- [13] J. M. McDowall, C.A. Vincent, Viscosity behavior of some simple electrolytes in formamide solution, J. Chem. Soc. Farad. Trans. 1 (1974) 1862.
- [14] M. R. J. Deck, K. J. Bird, A. J. Parker, Aust. J. Chem. 28 (1975) 955-963.
- [15] M. N. Roy, B. Sinha, R. Dey, A. Sinha, Int. J. Therm. 26 (2005) 1549.
- [16] M. N. Roy, R. Dewan, P. K. Roy, D. Biswas J. Chem. Eng. Data 55 (2010) 3617.
- [17] M. N. Roy, A. Bhattacharjee, P. Chakraborti, Therm. Acta 507 (2010) 135.
- [18] C. Zhao, P. Ma, J. Li, J. Chem. Thermodyn. 37 (2005) 37.
- [19] A. Bhattacharjee, M. N. Roy, Phys. Chem. Chem. Phys. 12 (2010) 14534.
- [20] E. B. Freyer, J. D. Hubbard, D. H. Andrews, J. Am. Chem. Soc. 51 (1929) 759.
- [21] O. Kiyohara, K. Arakawa, Bul. Chem. Soc. Jap. 43 (1970) 3037.
- [22] O. Kiyohara, J. P. E. Grolier, and G. C. Benson, Can J. Chem. Ed. 52 (1974) 2287.
- [23] N. M. Murthy, S. V. Subrahmanyam, Bul. Chem. Soc. Jap. 50 (1977) 2589.
- [24] A. Sinha, A. Bhattacharjee and M. N. Roy, J. Disper. Sci. Tech. 30 (2009) 1003.
- [25] B. Per, Acta Chem. Scand. 31 (1977) 869.
- [26] S. Gill and M. S. Chauhan, Z. Phys. Chemie NF. 140 (1984) 139.
- [27] J. Barthel, M. B. Rogac and R. Neueder, J. Sol. Chem. 28 (1999) 1071.

- [28] J. M. Chakraborty and B. Das, *Z. Phys. Chemie NF.* 218 (2004) 219.
- [29] R. M. Fuoss and E. Hirsch, *J. Am. Chem. Soc.* 82 (1960) 1013.
- [30] D. Ekka, M.N. Roy, *J. Phys. Chem. B*, 116 (2012) 11687.
- [31] D.O. Masson, *Phil. Mag.* 8 (1929) 218.
- [32] M. N. Roy, D. Ekka, R. Dewan, *Acta Chimi. Slov.* 58 (2011) 792.
- [33] G. Jones, M. Dole, *J. Am. Chem. Soc.* 51 (1929) 2950.
- [34] F. J. Millero, Molal volumes of electrolytes, *Chem. Rev.* 71 (1971) 147.
- [35] F. J. Millero, A. Losurdo, C. Shin, *J. Phys. Chem.* 82 (1978) 784.
- [36] M. Born, E. Wolf, *Principles of Optics: Electromagnetic Theory of Propagation, Interference and Diffraction of Light*, 7th edn, Cambridge University Press, London, (1999).
- [37] M. Deetlefs, K. Seddon, M. Shara, *Phys. Chem. Chem. Phys.* 8 (2006) 642.
- [38] M. K. Praharaj, A. Satapathy, P. Mishra, S. Mishra, *J. Chem. Pharma. Res.* 5 (2013) 49.
- [39] H. N. So'limo, A. M. Cases, A. C. Go'mez Marigliano, C. M. Bonatti, *J. Chem. Eng. Data* 46 (2001) 712.
- [40] T. T. Nguyen, *Clays and Clay Minerals.* 34 (1986) 521.
- [41] K. Sreekanth, D. Sravana Kumar, M. Kondaiah, D. Krishna Rao, *J. Chem. Pharma. Res.* 3 (2011) 29.

REFERENCES OF CHAPTER-VIII

- [35] J. Szejtli, *Chem. Rev.* 98 (1998) 1743.
- [36] K. A. Connors, *Chem. Rev.* 97 (1997) 1325.
- [37] E. Pinho, M. Grootveld, G. Soarse, M. Henriques, *Carbohydrate Polymers.* 101 (2014) 121.
- [38] B. Wei, *Carbohydrate Polymers.* 134 (2015) 398.
- [39] G. Yu, B. Hua, C. Han, *Org. Lett.* 16 (2014) 2486.
- [40] H. Li, D. Chen, Y. Sun, Y. B. Zheng, L. Tan, P. S. Weiss, Y. Yang, *J. Am. Chem. Soc.* 135 (2013) 1570.
- [41] T. Welton, *Chem. Rev.* 99 (1999) 2071.
- [42] B. Winter, R. Weber, P. M. Schmidt, I. V. Hertel, *J. Phys. Chem. B* 108 (2004) 14558.

- [43] H. Bergersen, R. R. T. Marinho, W. Pokapanich, A. Lindblad, O. Björneholm, L. J. Sæthre, G. Öhrwall, *Phys.: Condens. Matter* 19 (2007) 326101.
- [44] X. Li, X. Xu, C. Zhou, *Chem. Commun.* 48 (2012) 12240.
- [45] Z. J. Liu, J. Zhang, S. L. Chen, E. Shi, Y. Xu and X. B. Wan, *Angew. Chem. Int. Ed.* 51 (2012) 3231.
- [46] M. Uyanik, H. Okamoto, T. Yasui and K. Ishihara, *Science*. 328 (2010) 1376.
- [47] V. Sindelar, M.A. Cejas, F.M. Raymo, W. Chen, S.E. Parker, A.E. Kaifer, *Chem. Eur. J.* 11 (2005) 7054.
- [48] T. Wang, M. D. Wang, C. Ding, J. Fu, *Chem. Commun.* 50 (2014) 12469.
- [49] M.N. Roy, D. Ekka, S. Saha, M.C. Roy, *RSC Adv.* 4 (2014) 42383.
- [50] M.N. Roy, A. Roy, S. Saha, *Carbohydrate Polymers*. 151 (2016) 458.
- [51] S. Saha, T. Ray, S. Basak, M. N. Roy, *New J. Chem.* 40 (2016) 651.
- [52] Y. Gao, Z. Li, J. Du, B. Han, G. Li, W. Hou, D. Shen, L. Zheng, G. Zhang, *Chem. Eur. J.* 11 (2005) 5875 .
- [53] Á. Piñeiro, X. Banquy, S. Pérez-Casas, E. Tovar, A. Garcia, A. Villa, A. Amigo, A. E. Mark, M. Costas, *J. Phys. Chem. B.* 111 (2007) 4383.
- [54] Y. Gao, X. Zhao, B. Dong, L. Zheng, N. Li, S. Zhang, *J. Phys. Chem. B.* 110 (2006) 8576.
- [55] M. N. Roy, S. Saha, S. Barman, D. Ekka, *RSC Adv.* 6 (2016) 8881.
- [56] A. Apelblat, E. Manzurola, Z. Orekhova, J. Soln. *Chem.* 36 (2007) 891.
- [57] D. Ekka and M. N. Roy, *RSC Adv.* 4 (2014) 19831.
- [58] D. O. Masson, *Phil. Mag.* 8 (1929) 218.
- [59] A. Roy, S. Saha, M.N. Roy, *Fluid Phase Equilib.* 425 (2016) 252.
- [60] G. Jones, D. Dole, *J. Am. Chem. Soc.* 51 (1929) 2950.
- [61] J. S. Negi, S. Singh, *Carbohydrate Polymers* 92 (2013) 1835.
- [62] W. Zhang, X. Gong, Y. Cai, C. Zhang, X. Yu, J. Fan, G. Diao, *Carbohydrate Polymers* 95 (2013) 366.
- [63] S. Milovanovic, D. Markovic, K. Aksentijevic, D. B. Stojanovic, J. Ivanovic, I. Zizovic, *Carbohydrate Polymers*. 147 (2016) 344.
- [64] M. Shamsipur, G. Khayatian, *J. Inclusion Phenom.* 39 (2001) 109.
- [65] S. Barman, M. N. Roy, *RSC Adv.* 6 (2016) 76381.

[66] D. P. Shoemaker, C. W. Garland, McGraw-Hill: New York. (1967) 131.

REFERENCES OF CHAPTER-IX

- [1] M. L. Bender and M. Komiyama, in Cyclodextrin Chemistry, Springer-Verlag, New York (1978).
- [2] J. Szejtli and T. Osa, vol. 3, Elsevier, Oxford (1996).
- [3] J. Szejtli, Chem. Rev. 98 (1998) 1743.
- [4] A. E. Kaifer, Acc. Chem. Res. 32 (1999) 62-71.
- [5] N. S. Krishnaveni, K. Surendra, M. A. Reddy, Y. V. D. Nageswar, K. R. J. Rao, Org. Chem. (2003) 2018.
- [6] M. Wei and A. E. Tonelli, Macromolecules 34 (2001) 4061.
- [7] J. Li, X. Li, Zhou, Z. X. Ni, K. W. Leong, Macromolecules 34 (2001) 7236.
- [8] K. Yoshida, T. Shimomura, K. Ito, R. Hayakawa, Langmuir 15 (1999) 910.
- [9] H. Okumura, Y. Kawaguchi, A. Harada, Macromolecules 34 (2001) 6338.
- [10] P. Lo Nostro, I. Santoni, M. Bonini, P. Baglioni, Langmuir 19 (2003) 2313.
- [11] H. Jiao, S. H. Goh, S. Valiyaveetil, Macromolecules 35 (2002) 1980.
- [12] J. Li, X. Ni, Z. Zhou, K. W. Leong, J. Am. Chem. Soc. 125 (2003) 1788.
- [13] C. C. Rusa, C. Luca, A. E. Tonelli, Macromolecules 34 (2001) 1318.
- [14] J. Li and D. Yan, Macromolecules 34 (2001) 1542.
- [15] M. Ceccato, P. Lo Nostro, P. Baglioni, Langmuir 13 (1997) 2436.
- [16] P. Lo Nostro, J. R. Lopes, C. Cardelli, Langmuir 17 (2001) 4610.
- [17] P. Ferreira, I. S. Goncalves, M. Pillinger, J. Rocha, P. Santos, Organometallics 19 (2000) 1455.
- [18] J. Liu, J. Alvarez, W. Ong, E. Roman, A. E. Kaifer, Langmuir 17 (2001) 6762.
- [19] F. M. Menger and M. J. Sherrod, J. Am. Chem. Soc. 110 (1988) 8606.
- [20] J. Boger, D. G. Brenner, J. R. Knowles, J. Am. Chem. Soc. 101 (1979) 7630.
- [21] D. Nolan, R. Darcy, B. J. Ravoo, Langmuir 19 (2003) 4469.
- [22] T. Welton, Chem. Rev. 99 (1999) 2071.
- [23] H. M. Zerth, N. M. Leonard, R. S. Mohan, Org. Lett. 5 (2003) 55.

- [24] J. Dupont, R. F. de Souza, P. A. Z. Suarez, *Chem. Rev.* 102 (2002) 3667.
- [25] R. G. Weiss, *Tetrahedron* 44 (1988) 3413.
- [26] H. Jervis, M. E. Raimondi, R. Raja, T. Maschmeyer, J. M. Seddon, D. W Bruce, *Chem. Commun.* 5 (1999) 2031.
- [27] A. J. Carmichael, C. Hardacre, J. D. Holbrey, M. Nieuwenhuyzen, K. R. Seddon, *Mol. Phys.* 99 (2001) 795.
- [28] G. Law and P. R. Watson, *Langmuir* 17 (2001) 6138.
- [29] J. L. Anderson, R. Ding, A. Ellern, D. W. Armstrong, *J. Am. Chem. Soc.* 127 (2005) 593.
- [30] A. Beyaz, W. S. Oh, V. P. Reddy, *Colloids Surf. B.* 35 (2004) 119.
- [31] L. Li, J. Groenewold, S. J. Picken, *Chem Mater.* 17 (2005) 250.
- [32] J. Bowers, C. P. Butts, P. J. Martin, *Langmuir* 20 (2004) 2191.
- [33] J. E. Lind, J. J. Zwolenik, R. M. Fuoss, *J. Am. Chem. Soc.* 81(7) (1959) 1557.
- [34] S. D. Qi, S. Y. Cui, X. G. Chen, Z. D. Hu, *J. Chromatogr. A.* 1059 (2004) 191.
- [35] C. D. Tran and S. D. Lacerda, *Anal. Chem.*, 74 (2002) 5337.
- [36] G. Law and P. R. Watson, *Langmuir* 17 (2001) 6138.
- [37] J. Szejtli, *Chem Rev.* 98 (1998) 1743.
- [38] I. N. Topchieva, A. E. Tonelli, I. G. Panova, E. V. Matuchina, F. A. Kalashnikov,; V. I. Gerasimov, C. C. Rusa, M. Rusa, M. A. Hunt, *Langmuir* 20 (2004) 9036.
- [39] M. N. Roy, M. C. Roy, K. Roy, *RSC Adv.* 5 (2015) 56717.

REFERENCES OF CHAPTER-X

- [1] V. E. Dickinson, M. E. Williams, S. M. Hendrickson, H. Masui R. W. Murray, *J. Am. Chem. Soc.* 121 (1999) 613.
- [2] J. L. Anderson, J. Ding, T. Welton, D. W. Armstrong, *J. Am. Chem. Soc.* 124 (2002), 14247.
- [3] S. Pandey, *Anal. Chim. Acta.* 556 (2006) 38.
- [4] P. Lozano, T. De Diego, D. Carrie, M. Vaultier J. L. Iborra, *J. Mol. Catal. B* 21 (2003) 9.

- [5] J. A. Laszlo, D. L. Compton, *Biotechnol. Bioeng.* 75 (2001) 181.
- [6] B. M. Quinn, Z. Ding, R. Moulton, A. J. Bard, *Langmuir* 18 (2002) 1734.
- [7] C. Lagrost, D. Carrie, M. Vaultier, P. Hapiot, *J. Phys. Chem. A* 107 (2003) 745.
- [8] S. Carda-Broch, A. Berthod, D. W. Armstrong, *Anal. Bioanal. Chem.* 375 (2003) 191.
- [9] P. Wang, S. M. Zakeeruddin, P. Comte, I. Exnar, M. Graätzel, *J. Am. Chem. Soc.* 125 (2003) 1166.
- [10] T. Welton, *Chem. Rev* 99 (1999) 2071.
- [11] P. Bonhote, A. P. Dias, N. Papageorgiou, K. Kalyanasundaram, M. Graätzel, *Inorg. Chem.* 35 (1996) 1168.
- [12] C. D. Tran, S. H. P. Lacerda, *Anal. Chem.* 74 (2002) 5337.
- [13] K. Fumino, P. Stange, V. Fossog, R. Hempelmann, R. Ludwig, *Angew. Chem. Int. Ed.* 52 (2013) 12439.
- [14] R. Dewan, B. Datta, M. C. Roy, M. N. Roy, *Fluid Phase Equilib.* 358 (2013) 233.
- [15] A. Bhattacharjee, M. N. Roy, *Phys. Chem. Chem. Phys.* 12 (2010) 14534.
- [16] D. Ekka, M. N. Roy, *J. Phys. Chem. B* 116 (2012) 11687.
- [17] M. G. Freire, C. M. S. S. Neves, P. J. Carvalho, R. L. Gardas, A. M. Freire, I. M. Marrucho, L. M. N. B. F. Santos, J. A. P. Coutinho, *J. Phys. Chem. B* 111 (2007) 13082.
- [18] J. E. Lind Jr., J. J. Zwolenik, R. M. Fuoss, *J. Am. Chem. Soc.* 81 (1959) 1557.
- [19] D. Ekka, M. N. Roy, *RSC Adv.* 4 (2014) 19831.
- [20] O. Borodin, W. A. Henderson, E. T. Fox, M. Berman, M. Gobet, S. Greenbaum, *J. Phys. Chem. B* 117 (2013) 10581.
- [21] R. M. Fuoss, *J. Phys. Chem.* 82 (1978) 2427.
- [22] P. Beronius, *Acta Chem. Scand.* 31 (1977) 869.
- [23] D. S. Gill, M. S. Chauhan, *Z. Phys. Chem. NF* 140 (1984) 139.
- [24] J. Barthel, M. B. Rogac, R. Neueder, *J. Sol. Chem.* 28 (1999) 1071.
- [25] A. Sinha, A. Bhattacharjee, M. N. Roy, *J. Disp. Sc. and Techn.* 30 (2009) 1003.
- [26] R. Dewan, M. N. Roy, *J. Chem. Thermodyn.* 54 (2012) 28.

- [27] S. Glasstone. *An Introduction to Electrochemistry*, Van Nostrand Company, New York, (1965) 45.
- [28] M. Petrowsky, R. Frech, *J. Phys. Chem. B* 112 (2008) 8285.
- [29] T. Sigvartsen, B. Gestblom, E. Noreland, J. Songstad, *J. Acta Chem. Scand.* 43 (1989) 103.
- [30] F. M. Gray, *Solid State Ionics* 40 (1990) 637.
- [31] R. M. Fuoss, C. A. Kraus, *J. Am. Chem. Soc.* 55 (1933) 2387.
- [32] Y. Harada, M. Salamon, S. Petrucci, *J. Phys. Chem.* 89 (1985) 2006.
- [33] B. S. Krumgalz, *J. Chem. Soc.* 79 (1983) 571.
- [34] M. N. Roy, T. Ray, M. C. Roy, B. Datta, *RSC Adv.* 4 (2014) 62244.
- [35] Z. Chen, M. Hojo, *J. Phys. Chem. B* 101 (1997) 10896.
- [36] M. Delsignore, H. Farber and S. Petrucci, *J. Phys. Chem.* 89 (1985) 4968.
- [37] M. N. Roy, R. Chanda and A. Bhattacharjee, *Fluid Phase Equilib.* 280 (2009) 76.
- [38] D. O. Masson, *Philosophical Magazine* 8 (1929) 218.
- [39] B. Datta, M. N. Roy, *Phys. Chem. Liq.* 53 (2015) 574.
- [40] T. Ray, M. N. Roy, *RSC Adv.* 5 (2015) 89431.
- [41] L. G. Helper, *Can. J. Chem.* 47 (1969) 4613.
- [42] M. N. Roy, V. K. Dakua, B. Sinha, *Int. J. Thermophys.* 28 (2007) 1275.
- [43] G. Jones, M. Dole, *J. Am. Chem. Soc.* 51 (1929) 2950.
- [44] F. J. Millero, *Chem. Rev.* 71 (1971) 147.
- [45] B. M. Sato, C. T. Martins, O. A. El Seoud, *New J. Chem.* 36 (2012) 2353.
- [46] R. Yamdagni, P. Kebarle, *J. Am. Chem. Soc.* 36 (1972) 2940.
- [47] J. M. Andanson, A. Baiker *J. Phys. Chem. C* 117 (2013) 12210.

The logo for the index is a stylized, symmetrical emblem. It features a central black hexagon with the word "INDEX" written in white, serif, all-caps font. This hexagon is surrounded by a complex, multi-pointed star-like border made of black lines, with some points extending further outwards. The entire logo is centered at the top of the page.

INDEX

A

Acetonitrile, 122, 159, 286
Activity coefficient, 93, 98
Apparent molal isentropic compressibility, 88
Apparent molal volume, 60
Association constant, 93, 163, 289
 α -cyclodextrin, 137, 253, 271

B

1-butyl-4-methylpyridinium hexafluorophosphate, 135, 286
1-Butyl-1-methylpyrrolidinium bromide, 134, 234
1-butyl-1-methylpyrrolidinium chloride, 136, 199
Biological processes, 139, 199, 211
Biomolecules, 139, 199, 211
Bjerrum's critical distance, 94
Bjerrum distance, 164, 186
Bjerrum parameter, 98, 99
Boltzmann constant, 69, 164
 β -cyclodextrin, 138, 253, 271

C

Cell model, 57

Conductance, 45, 91
Conductimetric method, 91
Conductance parameters, 94
Covalent bonding, 48
Crystal lattice, 34
Crystallographic radii, 84, 110, 115, 163, 185, 203, 289

D

1,3-Dioxolane, 127, 182
D(-)Fructose, 139, 199
D(+)-Galactose, 139, 199
Debye relaxation time, 105
Debye-Hückel theory, 71
Density, 58
Designer solvent, 41
Diethyl carbonate (DEC), 124, 160,
Dipole-dipole forces, 47
Dipole-dipole interaction, 47
Dipole-induced dipole forces, 47

E

Electric dipoles, 54
Electrochemistry, 38, 54
Electrolytes, 36, 109, 113, 117
Electroplating, 36

Electrostatic forces, 34, 35, 104
Electrostriction, 59, 298
Enthalpy, 53, 205
Entropy, 53, 205
Extended Jones-Dole equation, 72
Excess molar volumes, 58

F

Falkenhagen-Vernon equation, 73
First-generation ionic liquids, 41
Fluidity, 74
Food technology, 139
Formamide, 127, 234
Free volume, 57
FTIR spectroscopy, 117, 234, 254, 288
Fuel cells, 37
Fuoss conductance equation (1978), 98, 163, 185, 235, 289
Fuoss-Hsia conductance equation, 94
Fuoss-Kraus equation, 83, 161, 183,
Fuoss-Onsager equation, 92

G

Gibbs energy, 59, 165, 237, 229, 290
Green chemistry, 43
Green processing, 41
Green solvents, 41

H

Host-guest inclusion complex, 26, 253, 271
Hydration number, 102
Hydrodynamic radius, 105
Hydrogen bonding, 30, 47, 112, 120, 246, 208, 209
Hydrophobic interactions, 41, 262
Hydrophobic cavity, 253

I

Inclusion complexes, 26, 253, 254, 271, 272
Intermediate dipole-dipole forces, 47
Intermolecular forces, 46
Intermolecular interaction, 57, 66
Interactions in solution systems, 51
Ion-association, 108
Ion-dipole force, 50
Ionic fluids, 39
Ionic liquids, 36, 199, 233, 285
Ionic mobility, 46
Ionic solids, 33, 159, 181, 253
Ion-ion interactions, 52, 56
Ion-pair formation, 107, 163
Ion-solvation, 46, 159, 283
Ion-solvent interaction, 44, 166, 240, 297
Isentropic compressibilities, 88

J

Jones-dole equation, 72, 167, 188, 299

K

Kohlrausch's equation, 91

Kohlrausch's law, 100

L

Landon dispersion interactions, 47

Lattice energy, 46

Lee-wheaton conductance equation, 98

Limiting apparent molar expansibilities, 63

Limiting apparent molar isentropic compressibility, 89

Limiting apparent molar volumes, 166, 187, 296

Limiting molar conductance, 164, 185, 295

Lithium perchlorate, 131, 160

Lithium hexafluoroarsenate, 132, 160

Lithium iodide, 130, 160

Lithium-ion batteries, 37

Lorentz-lorenz relation, 241

M

Mass measurements, 143

Masson equation, 62, 166, 187, 239, 296

Melting point, 36

Molar refraction, 114, 234

Molecular interaction, 45

N

2-Nitrotoluene, 125, 182

N,N-Dimethylacetamide, 130, 234

N,N-Dimethylformamide, 128, 234

N-Dodecyl N,N-dimethyl-3-ammonio-1-propanesulfonate, 134, 271

NMR measurement, 119, 155, 199, 255

Non-aqueous electrolyte solution, 65

Non-electrolytes, 55, 113

O

Onsager coefficient, 109

Organic ionic liquids, 39

Owen-brinkley equation, 62

o-Toluidine, 124, 182

o-Xylene, 123, 182

P

Partial molar volumes, 56

Pharmaceutical, 37

Physicochemical properties, 44

Pitt's equation, 92

Pitzer equation, 62

Polarization, 107

Preferential solvation models, 112

R

Redlich-meyer equation, 62

Reference electrolyte, 77

Refractive index, 53, 115, 235

Relative permittivity, 39, 159, 186,
233

Room temperature ionic liquid, 39

S

Second-generation ionic liquids, 42

Shedlovsky's equation, 93

Solute-solute interactions, 59

Solute-solvent interactions, 59

Solution chemistry, 45

Solvation number, 85

Solute-cosolute interactions, 210

Stoke's radii, 84

Structure-breaker, 210

Structure-maker, 210

Surface Tension, 116, 154, 257, 274

Surface active ionic liquid, 271

T

Ternary association, 110

Ternary solution, 116

Tetrabutylammonium Iodide, 133,
253

Tetrahyptylammonium Iodide, 132,
181

Tetrahydrofuran, 126, 234

Thermodynamic properties, 45

Thomas equation, 85

Transfer volumes, 207, 208

Transport properties, 56, 88

Triple-ion formation, 108, 109, 161,
183, 289

U

Ultrasonic speed, 53, 149, 242

V

Variable viscosity, 37

Viscosity A-coefficient, 167, 188,
211, 240, 299

Viscosity B-coefficient, 167, 188, 211,
240, 299

Viscosity measurement, 148, 167,
188, 211, 240, 299

Volatile organic compounds, 41

W

Walden product, 103

Walden rule, 104

Water distiller, 156

Water, 121

Z

Zwanzig's theory 106

APPENDIX: A

LIST OF PUBLICATIONS

1. 'Ionic interplay of lithium salts in binary mixtures of acetonitrile and diethyl carbonate probed by physicochemical approach'



Fluid Phase Equilibria 358 (2013) 233–240

(Included in the Thesis)

2. 'Essential foundation of triple-ion and ion-pair formation of tetraheptylammonium iodide (Hept₄NI) salt in organic solvents investigated by physicochemical approach'



Phys.Chem.Liq. 53 (2015) 574–586

(Included in the Thesis)

3. 'A study of NMR, density, viscosity and conductance vis-à-vis interactions of 1-butyl-1-methylpyrrolidinium chloride with oligosaccharides in aqueous environments'

Communicated (Included in the Thesis)

4. 'Exploration of Miscellaneous Interfaces of a Green Liquid in Diverse Solvent Systems by the Process of Physicochemical Contrivances'



I. J. Adv. Chem. Sci. 2(4)(2014) 253-263

(Included in the Thesis)

5. 'Inclusion complexation of tetrabutylammonium iodide by cyclodextrins'



(Accepted) J. Chem. Sci.

(Included in the Thesis)

6. 'Self assembly inclusion of ionic liquid into hollow cylinder oligosaccharides'



J. Mol. Liq. 214 (2016) 264-269.

(Included in the Thesis)

7. 'Physicochemical Study of Solution Behavior of Ionic Liquid Prevalent in Diverse Solvent Systems at Different Temperatures'



Chem. Phys. Lett. 665 (2016) 85-94.

(Included in the Thesis)

8. 'Study of ion-pair and triple-ion origination of an ionic liquid ([bmmim][BF₄]) predominant in solvent systems'



RSC Adv.4 (2014) 62244-62254.

9. 'Insertion behavior of imidazolium and pyrrolidinium based ionic liquids into α and β -cyclodextrins: mechanism and factors leading to host-guest inclusion complexes†'



RSC Adv. 6 (2016) 100016-100027.

APPENDIX-B

LIST OF SEMINARS/ SYMPOSIUMS/ CONFERENCES ATTENDED

1. **Science Academies' Lecture Workshop on Modern Trends in Chemistry and Chemistry Education**, November 22-23, 2012, organized by the Department of Chemistry, University of North Bengal, Darjeeling-734-013, West Bengal.
2. **Workshop on Intellectual Property and Innovation Management in Knowledge Era**, organized by National Research Development Corporation (NRDC), New Delhi, and University of North Bengal (NBU), Siliguri, on 12th February, 2013, at University of North Bengal, Siliguri, West Bengal.
3. **National Seminar on Frontiers in Chemistry-2013**, held at the Department of Chemistry, University of North Bengal, on February 28th, 2013, Sponsored by University Grants Commission, New Delhi, and organized by Department of Chemistry, University of North Bengal.
4. **Workshop on Diversities and Frontiers in Chemistry (State University Network)**, held at the Department of Chemistry, University of North Bengal during August 07-08, 2013 and organized by Department of Chemistry, Jadavpur University, Kolkata & Department of Chemistry, University of North Bengal, Siliguri.
5. **International Seminar on 5th Asian Conference on Colloid and Interface Science**, held at Department of chemistry, University of North Bengal, Darjeeling during November 20-23, 2013 and organized by the Asian Society for Colloid and Surface Science and Department of Chemistry, University of North Bengal, Darjeeling, India.
6. **National Seminar on Frontiers in Chemistry-2014**, held at the Department of Chemistry, University of North Bengal, on March 11-12, 2014, Sponsored by University Grants Commission, New Delhi, and organized by Department of Chemistry, University of North Bengal.
7. **Scientific Training Programme**, held at North Bengal Science Centre, March 13-19, 2014, organized by North Bengal Science Centre (National Council of Science Museums, Ministry of Culture Govt. of India).

8. **One-day Seminar on Chemistry In Commemoration of the 153rd Birth Anniversary of Acharya Prafulla Chandra Ray**, held at Department of chemistry, University of North Bengal, Darjeeling during September 12, 2014, organized by The Chemical Research Society of India NBU Local Chapter in collaboration with Department of Chemistry, University of North Bengal.
9. **Science Academies' Lecture Workshop on "Spectroscopy of Emerging Materials"**, held at the Department of Chemistry, University of North Bengal, on November 26-27, 2014, organized by Department of Chemistry, University of North Bengal.
10. **National Seminar on Frontiers in Chemistry-2015**, held at the Department of Chemistry, University of North Bengal, on February 17-18, 2015, Sponsored by University Grants Commission, New Delhi, and organized by Department of Chemistry, University of North Bengal.
11. **"Recent Trends on Chemistry and Biology Interface"**, held at Department of chemistry, University of North Bengal, Darjeeling during September 12, 2014, organized by The Chemical Research Society of India NBU Local and Department of Chemistry, University of North Bengal.
12. **Science Academies' Lecture Workshop on "Recent Developments on the Theoretical and Experimental Aspects of Advanced Materials"**, held at the Department of Chemistry, University of North Bengal, on September 18-19, 2015, organized by Department of Chemistry, University of North Bengal.
13. **19th CRSI National Symposium in Chemistry**, held at University of North Bengal July 14-16, 2016, organized by Department of Chemistry, University of North Bengal.
14. **20th CRSI National Symposium in Chemistry**, held at Gauhati University February 03-05, 2017, organized by Department of Chemistry, Gauhati University.
15. **Recent Trends in Chemistry (RTC-2017)**, held at Sikkim Manipal Institute of Technology, February 03-05, 2017, organized by Department of Chemistry, Sikkim Manipal Institute of Technology.